Author:
Reyes Prieto, Nidia Mariel

Title:
Circadian gene expression of tryptophan hydroxylase 2 in the Dorsal and Median Raphe nuclei is altered by dysregulated glucocorticoid rhythms

“Circadian gene expression of tryptophan hydroxylase 2 in the Dorsal and Median Raphe nuclei is altered by dysregulated glucocorticoid rhythms”

Nidia Mariel Reyes Prieto

A dissertation submitted to the University of Bristol in accordance with the requirements for award of the degree of Doctor of Philosophy to the Faculty of Health Sciences

September 2018

Word count: 80,013

Abstract

Stress-related psychiatric disorders have been characterized by dysregulated rhythms of the hypothalamic-pituitary-adrenal axis (HPA axis) and a dysfunctional serotonergic system. However, the molecular mechanism of this relationship is not entirely described. This thesis has explored the link between an altered HPA axis circadian rhythm and the effect on tryptophan hydroxylase 2 *(tph2)* mRNA expression, the rate-limiting enzyme in the biosynthesis of serotonin. Three different experimental conditions were used in this study: 1) normal control conditions, 2) administration of the long-acting synthetic glucocorticoid methylprednisolone (MPL), and 3) constant light exposure for five weeks (LL). To evaluate the effects of these models, Radioimmunoassays (RIA) were used to assess plasma corticosterone (CORT) levels, and in situ hybridization histochemistry (ISHH) was used to measure *tph2* mRNA in six different regions (interfascicular part DRI, caudal part DRC, ventral part DRV, dorsal part DRD, ventrolateral part/ventrolateral periaqueductal grey part DRVL/VLPAG and medium raphe nucleus MnR) of the Raphe Complex over a 24-hour period within 5 different time points (3 am, 9 am, 3pm, 6 pm, 9 pm). Relative to controls, the MPL model suppressed CORT, while the LL model displayed a hyperactive CORT secretion. Linear Mixed Model analyses showed that *tph2* mRNA expression changed in the DRD, DRV, DRVL/VLPAG and in the MnR nucleus. The MPL induced a bi-phasic rhythm in expression with the loss of the nadir at 9 am and the peak at 6 pm whereas the LL treatment triggered high-levels of expression at 3 am and 9 pm with a flat expression between 9 am and 6 pm. This altered expression of *tph2* mRNA was specific to the caudal levels of each area, with exception of the DRD. Measurements from each rostro-caudal bregma level showed precise changes which might be indicating a specific neuroanatomical functionality of each region of the Raphe Complex.

Acknowledgements

In correspondence to the help, not only financial, but superior in experience, innovation, training and professionalism from the Mexican government through the National Council of Science and Technology (CONACyT), I thank my country very much for the opportunity and support granted. An additional thanks for the financial support from the Neuroendocrinology Charitable Trust which allowed me to dedicate my entire time to this PhD.

I want to thank Professor Stafford who with credulity chose me to be a part of their team and has been a good mentor. To Becky for her interest in my research, whose guide based on the confidence of my knowledge set the course to achieve a joint goal in favour of science. And to Jamie who in a rational and assertive manner landed my rumbling ideas.

To all the members of the Lightman group, for their time and shared expertise. A special mention to Yvonne for her patience, dedication and time devoted to the experiments of this project and to Fran for her pertinent comments and the precision of her knowledge which enlarged the level of this research.

A special thanks to Dr Chris Lowry, worldwide expert in the area, who invited me to his lab and shared with me all the tools and knowledge to develop this project. A big thanks to James Hazell who guided me step by step in the Linear Mixed Model Analysis.

I also extend my appreciations to the reviewers who will invest their time in the revision of this thesis, whose knowledge and experience will extend the results of all the work of this PhD.

In the personal field, I firstly thank my parents who undoubtedly have taught me by their example that with discipline and perseverance great things can be achieved in the personal and academic field. I enjoy very much having their scientific virtues, without them, this PhD would not have been possible. To my mother, who has accompanied me every day along this path called life, who has raised me in times

of weakness and held firmly when I needed it most, who has even sometimes defied her limits of patience but never succumbed to restlessness when it comes to giving me encouragement, skill that has not been absent during this doctorate, for her, my love, gratitude and heart. To my father, whose tenacity and perseverance devoted to the scientific research are examples of academic excellence, thanks for your example of dedication that has allowed me not to give in to the moments of scientific frustration.

To my Sister, for her technical, moral, inspiring, strengthening and complicity support, for the hours listened to on points in the void, for the advice, for the love and the best friendship that may exist between two who know each other. To her, who has always been an example to me. Thank you (and Juan) for welcoming me in your home during the writing months of this thesis and for giving me the greatest joy in the world, the best gift of all, my nephew, that only with his *petite* existence gives me an extra motivation of being.

To my brother, who has not only taught me perseverance and hard work but has showed me that whatever you do and wherever you are, care for others, be noble and smile. To him, who is the greatest example of nobility.

To all my friends, who with patience about my absence but with the insistence of their presence have make me strong every single day. For all their messages and audios which made me feel closer to home. For them, who made this time easier.

Finally, to Nirvana, the person who accompanied me all this time. For all the conversations, laughs, tears and pints we shared. To her, who had the courage to stay with me during this journey called PhD. For the borrowed dream of others that brought us together and at the end became only ours.

Author’s declaration

I declare that the work in this dissertation was carried out in accordance with the requirements of the University's Regulations and Code of Practice for Research Degree Programmes and that it has not been submitted for any other academic award. Except where indicated by specific reference in the text, the work is the candidate's own work. Work done in collaboration with, or with the assistance of, others, is indicated as such. Any views expressed in the dissertation are those of the author.

SIGNED: ..... DATE: .....

Table of contents

List of Figures

List of tables

Abbreviations

5-HIAA	5-hydroxyindoleacetic acid
5-HT	Serotonin
5-HTR	Serotonin receptor
AA	Acetic anhydride
ACTH	Adrenocorticotropic hormone
ADX	Adrenalectomy
AIC	Akaike information criterion
AVP	Arginine vasopressin peptide
AVP1BR	AVP 1B receptor
BMAL1	Brain-muscle-arntl-like protein 1
CLOCK	Circadian loco-motor output cycle kaput
CNS	Central nervous system
CORT	Corticosterone
CRH	Corticotropin-releasing hormone
CRHR1	CRH receptor 1
CRY	Cryptochromes
CTRL	Control
DBD	DNA binding domain
DNA	Deoxyribonucleic acid
DR	Dorsal Raphe Nucleus
DRC	Caudal part of the dorsal raphe
DRD	Dorsal part of the dorsal raphe
DRI	Intrafascicular part of the dorsal raphe
DRV	Ventral part of the dorsal raphe
DRVL	Ventrolateral part of the dorsal raphe
DTT	Dithlothreitol
GC	Glucocorticoids
GR	Glucocorticoid Receptor
GREs	glucocorticoid response elements

HDC	Histidine decarboxylase
HPA	Hypothalamic-pituitary-adrenal
ISHH	In situ hybridization histochemistry
LBD	Ligand binding domain
LD	Light-Dark
LL	Constant light
LMM	Linear Mixed effects Models
LSD	Least Significant Difference
MAO	Monoamine oxidase
MDD	Mayor depressive disorder
MnR	Median raphe nucleus
mPFC	Medial prefrontal cortex
MPL	Methylprednisolone
MR	Mineralocorticoid receptor
mRNA	Messenger RNA
NTD	N-terminal domain
PAH	Phenylalanine
PBS	Phosphate buffered saline
PER	Period genes
PH	Posterior hypothalamus
PTSD	Post-traumatic stress disorder
PVN	Paraventricular nucleus
RHT	Retino-hypothalamic tract
RIA	Radioimmunoassay
SCN	Suprachiasmatic nuclei
SD	Sprague-Dawley
SERT	Serotonin transporter
sGCs	Synthetic glucocorticoids
SSC	Saline sodium citrate
StAR	Steroidogenic acute regulatory
TEA	Triethanolamine

TF	Transcription factor
TH	Tyrosine hydroxylase
TM	Tuberomammillary nucleus
Tph	Tryptophan 5-hydroxylase
Tph2	Tryptophan hydroxylase protein2
VIP	Vasoactive intestinal peptide
VLPAG	Ventrolateral periaqueductal grey
VMAT	Vesicular monoamine transporter
VP	Vasopressin
VTA	Ventral tegmental area
WB	Western blotting

Chapter 1 General introduction

1.1 Introduction

1.2 The importance of rhythms

1.2.1 Rhythms

1.3 The circadian clock system in mammals

1.3.1 The SCN

1.3.2 Peripheral oscillators and rhythms

1.3.3 Molecular circadian clockwork (gene network)

1.3.4 Circadian rhythms in health and disease

1.4 The HPA axis

1.4.1 Structure, physiology and function of the HPA axis

1.4.2 Glucocorticoids

1.4.3 Glucocorticoid and Mineralocorticoid Receptors

1.4.4 Mechanism of action; ligand-receptor complex

1.4.5 Circadian and ultradian rhythms of glucocorticoids

1.4.6 Glucocorticoid rhythms in health and disease

1.5 Serotonergic systems

1.5.1 Serotonin; biosynthesis, transporters, receptors and degradation

1.5.2 Brain serotonergic system anatomy and functional correlates

1.5.3 Brain serotonergic system and circadian rhythms

1.5.4 Brain serotonergic systems in health and disease

1.6 Relating systems in health and disease

1.7 Hypothesis and Aims

1.7.1 Hypothesis

1.7.2 Aims

1.1 Introduction

Mental disorders account for 30% of the global non-fatal disease burden, with approximately 10% of the world's population affected by depression and/or anxiety (World Health Organization, 2017). It is important, therefore, to understand the fundamental mechanisms of these disorders. In neuroscience, we think about the mechanisms involved in the aetiology of these conditions in terms of natural rhythms of the neuroendocrine response system, and how changes in these rhythms may promote disease development.

Altered biological rhythms are associated with many important pathologies (Archer et. al, 2014; Bailey & Silver, 2014; Benca et. al, 2009; Kaper, Kramer, & Rotstein, 2013). For example, hypothalamic-pituitary-adrenal (HPA) axis activity has been widely considered as an element of study for mental disorders because of the altered HPA axis rhythms found in patients with these particular illnesses (Arborelius, Owens, Plotsky, & Nemeroff, 1999; Orchinik, 1998; Stamper et. al, 2015; Vincent et. al, 2013) and the strong relationship between stressful events and symptoms of psychiatric disorders (Faravelli et. al, 2012; Heim, Owens, Plotsky, & Nemeroff, 1997; Juruena, 2014).

On the other hand, alterations in the serotonergic system have also been widely associated with mental disorders. For example, an elevated serotonin turnover, a deficient 5-HT receptor system and an impairment of serotonin neurotransmission have been observed in depressed patients (Cowen, 2002; Esler et. al, 2007; Sharp & Cowen, 2011), modified genetic components in serotonin receptors (5-HTR), tryptophan hydroxylase (TPH) and the serotonin transporter (SERT) have been found in patients suffering from mental disorders (Lemonde *et al.*, 2003; Barton *et al.*, 2008; Le François *et al.*, 2008), and serotonin reuptake and/or degradation inhibitors have been shown to be an effective therapeutic treatment for mental disorders such as depression, anxiety and bipolar disorder (Owens and Nemeroff, 1998; Mcelroy *et al.*, 2006; Beyer and Cremers, 2008; Pringle *et al.*, 2013).

The work described in this thesis is concerned with understanding the connections between these two systems and their specific activity. Characterising this

connection could reveal an underlying cause of these pathologies, which could in turn benefit people suffering from mental disorders. The following introduction will describe the three basic elements considered for the development of this study.

1.2 The importance of rhythms

Behaviour and physiology, from human to cyanobacteria, display clear fluctuations across the day (24-hr period). In the early history of science, it was believed that these daily fluctuations were driven by external temporal cues (i.e. day/night, temperature, food availability, seasons). Subsequently, the concept of internal or "endogenous" rhythmicity emerged with the observation of persistent rhythmic activity in a "light-sensitive" plant maintained under constant darkness (De Mairan, 1729) and with observations that in humans, even under complete darkness for over a month, the sleep-wake cycle is kept synchronized to a nearly 24-hour period (Kleitman, 1939).

It is now known that most living organisms on earth have an endogenous rhythmicity which guarantees the proper organization of processes and adaptation to a rhythmic environment (day/night, seasons) (Moore MD, 1997; Czeisler and Gooley, 2007; Huang *et al.*, 2011). By contemplating the crucial role of this internal clock and the idea that disruption of this "endogenous rhythmic activity" could lead to disease, the understanding of how this clock works became of great importance to the scientific community several decades ago.

1.2.1 Rhythms

After the emergence of the idea of an "internal clock", researchers in this area have established many characteristics of this endogenous rhythmicity. Today it is well known that endogenous rhythmicity can occur across a large range of time domains; circannual rhythms (once a year) (Sweeney, 1987), infradian rhythms (>24 h) (Moore-Ede, 1986), circadian rhythms (nearly 24 h) and ultradian rhythms (<24 h) (Edmunds, 1988).

Circannual rhythms manifest, for example, in mating, hibernation, and flowering (Edmunds, 1988; Sveeney, 1987). Infradian rhythms are present in the oestrus cycles of some rodents and the menstrual cycle in higher primates (Moore-Ede, 1986). Examples of ultradian rhythms can be seen in growth hormone secretion (Tannenbaum and Martin, 1976) or blood circulation (Yosipovitch *et al.*, 2004). Circadian rhythms are far more prominent, with great examples in the sleep-wake cycle (Beersma and Gordijn, 2007), hormone secretion (Tsang, Barclay and Oster, 2013) and body-temperature cycle (Benstaali *et al.*, 2001). Although all these rhythms are of great relevance, for the interest of this study, we will focus only on circadian rhythms.

1.2.1.1 Circadian rhythms

Circadian (from the Latin "circa" meaning around and "diem" meaning day) rhythms have an endogenous period of approximately 24 hours. The period of this type of rhythm is closely matched to the rotation of the earth (Moore-Ede, 1986; Gachon *et al.*, 2004).

These rhythms have to meet the following specific requirements to be considered as a circadian rhythm; 1) they should persist even when they are removed from all daily temporal cues, and the maintenance of an oscillation without periodic clues from the outside response should persist for a minimum of two or more cycles (Edmunds, 1988; Silver and Kriegsfeld, 2014); 2) they should have the ability to be *entrained* (synchronized) to the outside world. Until today, the main synchronizers described are the light/dark and temperature cycles (Somers, 1999); 3) they should demonstrate temperature compensation. Although a temperature shift can reset the phase of the rhythm, when stabilized, this new temperature regime should have very little effect on the endogenous pattern (Pittendrigh and Caldarola, 1973).

1.3 The circadian clock system in mammals

Circadian rhythms exist in all organisms including, plants, animals, fungi and cyanobacteria (Edgar *et al.*, 2012). However, when it comes to research done in mammals, the idea of endogenous daily rhythms gave rise to a proposed

endogenous circadian clock system, which includes a central biological clock (Moore and Eichler, 1972a; Klein, Moore and S.M., 1991; Moore, Speh and Leak, 2002), peripheral oscillators (Zylka *et al.*, 1998; Balsalobre *et al.*, 2000; Kamphuis *et al.*, 2009) and a complete molecular clock network depending mainly on genetic mechanisms (Konopka and Benzer, 1971; Buijs and Kalsbeek, 2001; Zhang and Kay, 2010; Partch, Green and Takahashi, 2014).

The circadian clock system in mammals is autonomous and self-sustained, but it can also be entrained by external cues, which are called "zeitgebers" (Aschoff, 1965). This system involves three specific elements: 1) input pathways receiving environmental cues (zeitgebers); 2) a circadian oscillator (the generator of rhythm); and 3) output pathways which control responses (metabolic, physiological or behavioural) (Chung, Son and Kim, 2011b, 2011a; Son, Chung and Kim, 2011a).

In mammals, the circadian clock system is organized in a hierarchy, with the master clock residing in the suprachiasmatic nucleus (SCN) in the hypothalamus (Moore and Eichler, 1972a; Moore, Speh and Leak, 2002; Welsh, Takahashi and Kay, 2010), and secondary peripheral clocks in other brain regions and peripheral tissues (Ko and Takahashi, 2006; Kornmann *et al.*, 2007; Mukherjee *et al.*, 2010).

1.3.1 The SCN

In complex organisms such as mammals, a central pacemaker (biological clock) has evolved and concentrated in the central nervous system (CNS). In 1972, the "master" circadian pacemaker was found in the SCN of the anterior hypothalamus in mammals (Hendrickson, Wagoner and Cowan, 1972; Moore and Eichler, 1972a; Stephan and Zucker, 1972). After its discovery, the SCN was established as the internal timekeeper essential for the circadian timing of mammals. This nucleus presented rhythmicity even when isolated in vitro (Gillette and Prosser, 1988) or *in vivo* (Inouye and Kawamura, 1979) from the rest of the brain.

The SCN is a tear-drop shaped nucleus (Figure 1-1) which contains about 20,000 clock oscillating cells that form a highly organized and synchronized network (Klein, Moore and S.M., 1991; Welsh, Takahashi and Kay, 2010). This specialized

nucleus receives environmental information to adjust physiological and behavioural functions, such as locomotor activity, body temperature and hormonal secretion of the organism in the form of the alternating day/night cycle (Moore and Eichler, 1972a; Schibler and Sassone-Corsi, 2002; Dibner, Schibler and Albrecht, 2010).

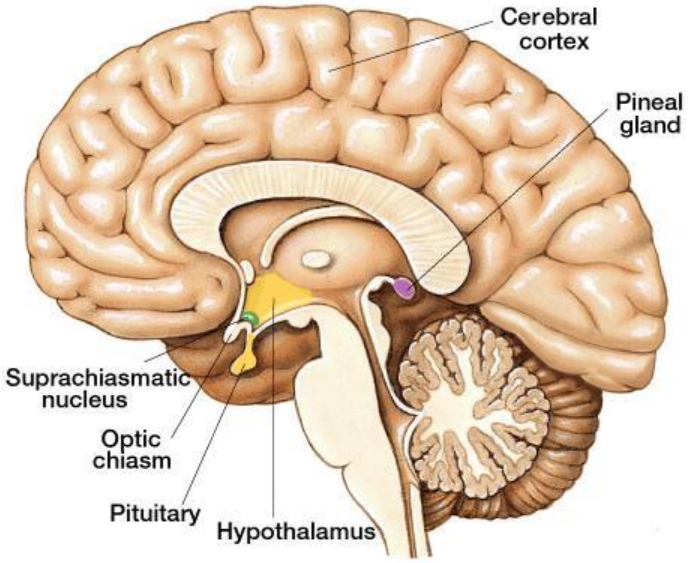

Figure 1-1: Suprachiasmatic Nucleus. The SCN is a group of brain cells located in the Hypothalamus which has been related to the control of circadian cycles of physiological and behavioural rhythms. Taken from; http://operativeneurosurgery.com/doku.phpidsuprachiasmatic.

Nowadays, after numerous studies, it has become clear that, at a molecular level, this endogenous rhythmicity in the SCN is actually generated by clock genes, forming a complex web of feedback loops (Wilsbacher and Takahashi, 1998; King and Takahashi, 2000); this will be further detailed in the following sections.

The SCN can be synchronised by both photic (Nelson and Zucker, 1981; Meijer et. al, 1999; Yamazaki et. al, 1999) and non-photic cues (Reppert and Weaver, 2002). Because of the type neurons contained in the SCN, it can be divided in 2 parts: 1) a core with vasoactive intestinal peptide (VIP) (Abrahamson and Moore, 2001); and 2) a shell with arginine vasopressin peptide (AVP) (Silver and Moore, 1998). Furthermore, all neurons in the SCN contain GABA (Moore & Speh, 1993).

There are approximately 35 different inputs to the SCN from other areas of the brain, (summarised in table 1-1) (Krout *et al.*, 2002). However, the three most important inputs to the SCN are: 1) The core of the SCN receives photic input from the retino-hypothalamic tract (RHT) (Moore and Lenn, 1972), which results in the induction of various genes (Kornhauser *et al.*, 1990) and chromatin remodelling (Crosio *et al.*, 2000); 2) non-photic input is received from projections from the intergeniculate leaflet (Hastings *et al.*, 1998); and 3) non-photic inputs from the median raphe nucleus (Meyer-Bernstein and Morin, 1996; Morin, 1999).

Table 1-1: Brain regions projecting directly to the rat SCN. Table from Krout et. al, 2002.

Amydalohippocampal zone	Lateral septum	Parastriatal N
Anterior Hth N	Laterodorsal tegmental N	Paraventricular thalamic N
Anterodorsal preoptic N	Locus coeruleus	Piriform cortex
Anteroventral periventricular Hth N	Medial amygdala	Posterior Hth N
Anteroventral preoptic N	Medial preoptic area	Precommissural N
Arcuate N	Medial preoptic N	Subfornical organ
BNST, principal N	Medial pretectal N	Subparaventricular zone
Claustrum	Median preoptic N	Tuberomammillary N
Dorsal Hth area	Median raphe N	Ventral subiculum
Dorsomedial Hth N	N incertus	Ventromedial Hth N
Infralimbic cortex	Olivary pretectal N	Zona incerta
Intergeniculate leaflet	Parabrachial N	

Moreover, the SCN also has three important projections (Watts and Swanson, 1987): 1) to the periventricular hypothalamic nuclei (Watts and Swanson, 1987; Abrahamson and Moore, 2001; Aston-Jones *et al.*, 2001); 2) to the septum and anterior paraventricular thalamus (Watts and Swanson, 1987; Moore, Speh and Leak, 2002); and 3) to the bed nucleus of stria terminalis (Watts, Swanson and Sanchez-Watts, 1987; Morin *et al.*, 1994). Additionally, a projection to the amygdala (Morin *et al.*, 1994) and to the intergeniculate leaflet (Card and Moore, 1989) has been described.

Therefore, the SCN is a very complex “central clock” which is essential for the circadian timing in mammals. Additionally, the molecular basis of how this clock works relies on genetic mechanisms and a complete circadian clockwork.

1.3.2 Peripheral oscillators and rhythms

Although the SCN is commonly known as the "master clock", many other regions in the brain and body tissue display circadian rhythms (Oishi *et al.*, 1998; McNamara *et al.*, 2001; Reick *et al.*, 2001).

The idea of the SCN as the unique time keeper changed when several studies showed that most cells in other different types of tissue had the ability to oscillate even when cultured *in vitro* (Balsalobre *et al.*, 2000; Le Minh *et al.*, 2001; Kamphuis *et al.*, 2009).

Furthermore, the idea that peripheral clocks were controlled (entrained) through hormonal and neuronal cues provided by the SCN was dismissed when different studies using food availability (Damiola *et al.*, 2000), temperature cycles (Brown *et al.*, 2002) and hormone signals (Balsalobre *et al.*, 2000) showed that rhythms in peripheral oscillators could be sustained by these conditions.

Nowadays, the idea of the SCN as a central pacemaker has changed, proposing this nucleus as the central *coordinator* of all other peripheral clocks (Dibner, Schibler and Albrecht, 2010). Moreover, both the SCN and the peripheral oscillators seem to have a very similar molecular mechanism (Kamphuis *et al.*, 2005; Liu *et al.*, 2007). This mechanism consists of two transcriptional/post-translational feedback loops involving clock genes, as described in the next section.

1.3.3 Molecular circadian clockwork (gene network)

In 1990, a study done in *Drosophila* proposed that circadian rhythms were generated by an intracellular mechanism of autoregulatory transcriptional/translational feedback loops which involved clock genes (Hardin, Hall and Rosbash, 1990). After this, a myriad of research was carried out on these "clock genes" and today, a number of essential mammalian "clock genes", necessary for the maintenance of the circadian rhythm, have been identified (Table 1-2).

Table 1-2: Main clock genes in mammals. Taken from (Cermakian and Boivin, 2003).

Gene	Characteristics of protein product	Function	Effect of mutation[b]	Links to human phenotypes
Clock	bHLH-PAS factor	Activation of clock and clock-controlled genes (with BMAL1)[c]	long period, then arrhythmic[d]	polymorphism linked with ME preference
Bmal1	bHLH-PAS factor	Activation of clock and clock-controlled genes (with CLOCK)[c]	arrhythmic	
Per1	PAS domain	Association with CRYs	short period[e]	
Per2	PAS domain	Association with CRYs	short period, then often arrhythmic[e]	mutation in one case of familial ASPS
Per3	PAS domain	Association with CRY? Output?	short period[e]	polymorphism linked with DSPS
Cry1	similar to DNA photolyases	Association with PERs and inhibition of CLOCK-BMAL1	short period[f]	
Cry2	similar to DNA photolyases	Association with PERs and inhibition of CLOCK-BMAL1	long period[f]	
CKIδ, CKIε	casein kinase	Phosphorylation of PERs, CRYs, BMAL1	short period (*CKIε*)[g]	
Rev-erbα	orphan nuclear receptor	Repression of *Bmal1 Clock* and *Cry1*) expression	short period	
Dbp	PAR bZip factor	Output; activation of *Per1*?	short period	
E4bp4	bZip factor	Output; repression of *Per1*?	(not tested)	

Abbreviations: bHLH, basic helix-loop-helix; PAS, Per-Arnt-Sim; bZip, basic leucine zipper; PAR, proline and acidic amino acid rich; *Per*, *Period*; *Cry*, *Cryptochrome*; Dbp, D-site binding protein; ME, morningness-eveningness; ASPS, advanced sleep phase syndrome; DSPS, delayed sleep phase syndrome.

[a] See main text for bibliographic references.

[b] Effect of mutation on locomotor activity rhythms in constant darkness. For the effect on molecular oscillations, refer to references cited in the text. Targeted deletion of the gene, unless otherwise indicated.

[c] Close homologs of *Clock* and *Bmal1* (*Npas2*/*Mop4* and *Bmal2*/*Mop9*, respectively), have been described, but their precise involvement in the clock has not been clarified yet.

[d] Point mutation, leading to skipping of one exon during splicing. The mutant protein has blunted transcriptional activity.

[e] *Per1* and *Per2* knock-out mice have a short period in some reports and a normal period followed by arrhythmicity in another article. Double *Per1*/*Per2* knock-outs are arrhythmic. Double *Per1*/*Per3* or *Per2*/*Per3* knock-outs have a phenotype identical to *Per1* and *Per2* knock-outs, respectively.

[f] Double *Cry1*/*Cry2* knock-outs are arrhythmic.

[g] Point mutation in hamsters, known as the *tau* mutation.

The molecular mechanism driving rhythmic gene expression consists of two positive and negative transcriptional/translational feedback loops (Figure 1-2). The core feedback loop includes two transcriptional activators, the ‘‘circadian loco-motor output cycle kaput’’ (CLOCK) and ‘‘brain-muscle-arntl-like protein 1’’ (BMAL1), and two transcriptional repressors, Period genes (PERs: PER1, PER2 and PER3) and Cryptochromes (CRYs: CRY1 and CRY2). PER and CRY are translated into their proteins which translocate from the cytoplasm to the nucleus to inhibit their own gene expression and their target genes CLOCK and BMAL1 (Gekakis *et al.*, 1998; Bunger *et al.*, 2000). The secondary loop is BMAL1 transcription being regulated by the clock-controlled nuclear receptors, retinoic acid receptor-related orphan nuclear receptors RORs and REV-ERBs. Additionally, CLOCK-BMAL1 controls the expression of REV-ERBs, and then RORs and REV-ERBs induce (RoRalpha) or repress (REV-ERBalpha/beta) BMAL1, contributing to rhythmic gene transcription and stabilizing the clockwork mechanism (Sato *et al.*, 2004; Guillaumond *et al.*, 2005).

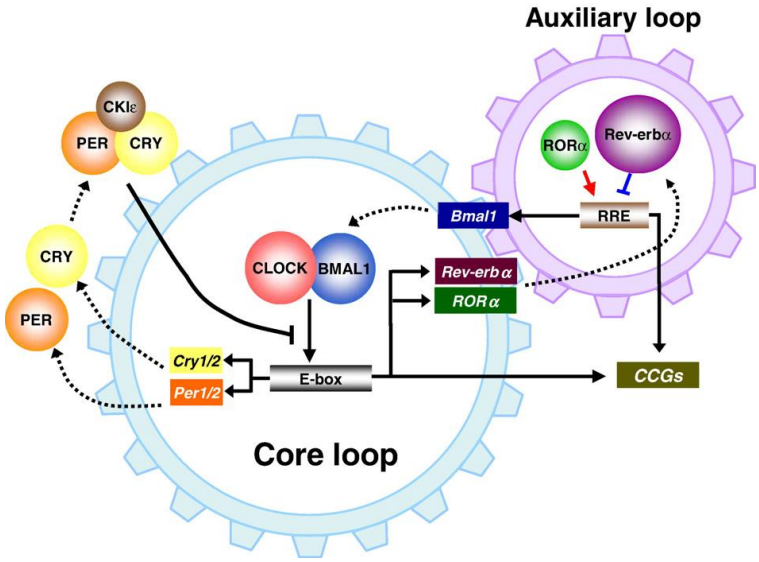

Figure 1-2: Molecular circadian clockwork. The molecular mechanisms of circadian rhythms depend of two transcriptional/translational feedback loops. CLOCK and BMAL1 induce transcription of PERs and CRYs. Then, PER and CRY repress CLOCK and BMAL1. Additionally, CLOCK and BMAL1 control transcription of ROR and REV-ERB which modulate BMAL1 levels. Taken from (Chung, Son and Kim, 2011b).

This brief description of the molecular mechanism of circadian rhythms demonstrates the complexity of the clockwork. Interestingly, this mechanism has become of great relevance when studying circadian clock-related diseases, such as sleep disorders, psychiatric disorders and metabolic disorders, which epidemiology researchers have linked to circadian abnormalities.

1.3.4 Circadian rhythms in health and disease

As described above, all organisms depend largely on the circadian system to adapt and survive effectively in a moving world. Hence, when organisms do not have a functional circadian system, their adaptation and survival is at risk, and the development of pathology becomes a common consequence (Litinski, Scheer and Shea, 2009).

A substantial area of chronobiology has studied the negative impact of a dysfunctional circadian system and its relationship with behavioural (Saper, Scammell and Lu, 2005; Krystal, Benca and Kilduff, 2013), physiological (Swaab, Fliers and Partiman, 1985; Schernhammer *et al.*, 2001), metabolic (Turek *et al.*, 2005; Garaulet and Madrid, 2010; Reiter *et al.*, 2012) and even psychiatric diseases (Desan *et al.*, 2000; Harvey, Mullin and Hinshaw, 2006; Walker and Lawrence, 2017).

One of the major endocrine circuits that has been related to circadian alterations and disorders, and which is of primary interest in our study, is the HPA axis. HPA axis activity is under circadian regulation by the SCN (Buijs and Kalsbeek, 2001). However, this circadian regulation seems to be bidirectional given the participation of glucocorticoids (GC), the endpoint of the HPA axis, in several physiological processes (Buckingham, 2006), their capacity to reset peripheral oscillators (Stratmann and Schibler, 2006), and their ability to promote accumulation of clock genes (Balsalobre *et al.*, 2000) and stimulate cyclic expression of target genes independently of the molecular circadian system (Oishi *et al.*, 2005). Therefore, the influence of the HPA axis over the circadian system, and vice versa, establishes a deep connection between abnormal rhythms of GC and the presence of pathology

(Naylor *et al.*, 2000; Liu *et al.*, 2006; Lamia, Storch and Weitz, 2008; Mukherjee *et al.*, 2010).

Of special relevance to our study too is the fact that abnormal HPA axis activity has been associated with depression and anxiety disorders (Morin, 1999; Pompili *et al.*, 2010). The bidirectional connection between GC and the circadian system seems to be of fundamental importance in this idea as it appears that GC may influence specific central functions by controlling/resetting rhythms (Lamont *et al.*, 2005; Hood *et al.*, 2010). Moreover, GCs appear to drive the accumulation of tph mRNA (rate limiting enzyme in the biosynthesis of serotonin) in the raphe nucleus (central nucleus of serotonin biosynthesis), and hence influencing the biosynthesis and neurotransmission of serotonin (Malek *et al.*, 2007), which is of major significance in the aetiology of depression and other psychiatric disorders (Murphy *et al.*, 1998; Owens and Nemeroff, 1998; Naughton, Mulrooney and Leonard, 2000a).

Thus, altered HPA axis circadian activity and malfunctioning of the serotonin system, and their relationship with depressive disorders, has been established. However, the molecular mechanisms of this association are still unknown.

1.4 The HPA axis

According to the World Health Organisation, the term stress-related disorders specifically relates to problems such as post-traumatic stress disorder (PTSD), acute stress reaction and bereavement reactions that require an exposure to a defined stressor as a precursor. There are numerous other stress-related disorders and problems such as depression, behavioural disorders, alcohol/substance use problems, self-harm/suicide, medically-unexplained somatic complaints, but these are not specifically related to stress (i.e. they may also occur in the absence of identifiable stressful life events) (World Health Organisation, 2013). But what is stress? And how does our body deal with stress?

All living organisms maintain a complex dynamic equilibrium or *homeostasis* (Cannon, 1929). This equilibrium is repetitively challenged by intrinsic or extrinsic changes, called stressors; these stressors can be physical or emotional (Chrousos

and Gold, 1992). In the 1930s, Hans Selye used the term "stress" (from physics) to define the psychological and physiological events occurring in ill patients as a consequence of prolonged adaptational responses; "Stress syndrome" (Selye, 1936).

When homeostasis is challenged by stressors with certain severity or stressors exceed a temporal threshold, the organism activates compensatory responses (Chrousos, Loriaux and Gold, 1988). The major endocrine system which relates to the compensatory responses to stress, is the HPA axis (Tsigos and Chrousos, 2002).

1.4.1 Structure, physiology and function of the HPA axis

The HPA axis is the major endocrine system which provides a rapid response against stress (Charmandari, Tsigos and Chrousos, 2005). Moreover, this system displays circadian activity and its abnormal activity and/or dysfunction of its elements are strongly associated with many pathologies (Anagnostis *et al.*, 2009; Frodl and O'Keane, 2013; Bailey and Silver, 2014; Checkley, SL and WS, 2015; Peeters *et al.*, 2015).

The HPA axis endpoint is the secretion of GC hormones (Szabó, 2014), which regulate many biological functions such as metabolism glucose (Cherrington, 1999), protein (Clarke *et al.*, 2007) and fat metabolism (Macfarlane, Forbes and Walker, 2008; Peckett, Wright and Riddell, 2011), cardiovascular functions (Carey, 2010) and immune functions (Rosenberg *et al.*, 2002).

In normal conditions, the HPA axis displays a circadian activity and an underlying ultradian rhythm (of around 60-90 minutes) of GC hormones (Deuschle, Schweiger, Weber, Gotthardt, Körner, *et al.*, 1997; Lightman *et al.*, 2000; Jamie J. Walker, Terry and Lightman, 2010; Lightman and Conway-Campbell, 2010). On top of this basal HPA rhythmicity, GC secretion increases when the organism perceives and responds to stress (Tsigos and Chrousos, 2002; Lightman, 2008; Sarabdjitsingh, Joëls and de Kloet, 2012).

The normal circadian activity of the HPA axis and the intensified stress response given by this system can be described by the following path (Figure 1-3): when the organism receives external cues (circadian information) or perceives stress, a response is initiated by afferent neural pathways from limbic, brain-stem structures and areas such as the SCN, the nucleus of the solitary tract (NTS), the posterior hypothalamus and the bed nucleus of the stria terminalis (BTS) (Engeland and Arnhold, 2005; Ulrich-Lai and Herman, 2009; Herman *et al.*, 2016), which induces the release of corticotropin-releasing hormone (CRH) and arginine vasopressin (AVP) from the parvocellular neurons of the paraventricular nucleus (PVN) of the hypothalamus (Rivier and Vale, 1983; Whitnall, Mezey and Gainer, 1985; Childs, 1992; Scott ' and Dinan, 1998). CRH and AVP are released at the level of the median eminence and, via the portal circulation, they reach the anterioir pituitrary where they bind to their receptors, the CRH receptor 1 (CRHR1) (Chalmers, Lovenberg and De Souza, 1995; Pozzoli *et al.*, 1996) and AVP 1B receptor (AVP1BR) (Antoni *et al.*, 1984; Scott and Dinan, 1998), and stimulate corticotroph cells to release adrenocorticotropic hormone (ACTH) into the circulation (Aguilera, 1994; Watts, Tanimura and Sanchez-Watts, 2004). Next, ACTH stimulates the adrenal gland to produce and secrete GC hormones (DALLMAN *et al.*, 1987; Herman *et al.*, 2003; Spiga, Waite, *et al.*, 2011) which, when released into the circulation, access target tissue, such as liver and brain, inducing metabolic effects and eliciting changes in brain function (de Kloet, 1991; De Kloet, 2004; Sarabdjitsingh, Joëls and de Kloet, 2012). Additionally, HPA axis activity, including GC production, is regulated through a feedback mechanism by which GCs inhibit ACTH release (pituitary level) and CRH and AVP release (PVN level) (Aston-Jones *et al.*, 2001)(Jones, Hillhouse and Burden, 1977; Keller-Wood and Dallman, 1984; Atkinson *et al.*, 2008; Tasker and Herman, 2011).

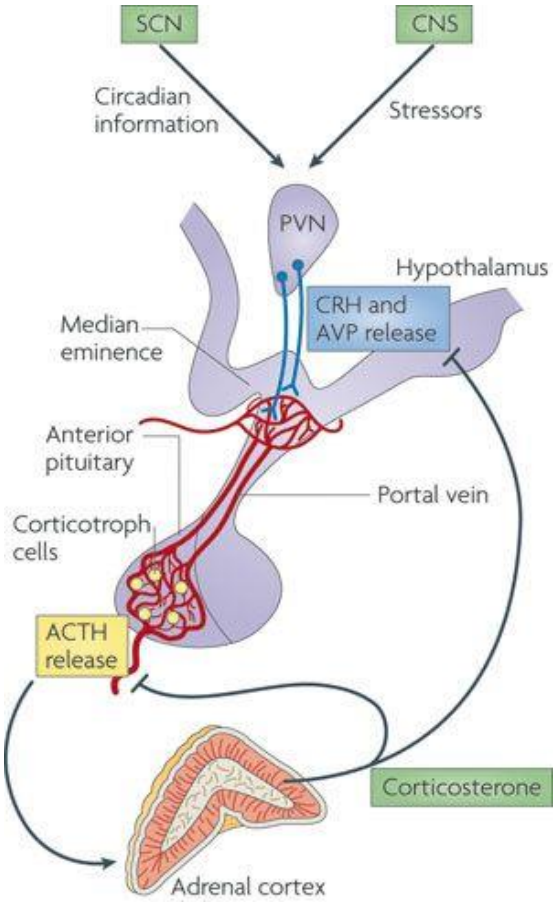

Figure 1-3: HPA axis. The hypothalamic paraventricular nucleus (PVN) responds to signals from the SCN and from stress inputs from the brainstem. The PVN projects to the median eminence and releases corticotrophin-releasing hormone (CRH) and arginine vasopressin (AVP). CRH/AVP reach the anterior pituitary which responds with the release of adrenocorticotropic hormone (ACTH). ACTH arrives at the adrenal cortex where it triggers the synthesis and secretion of glucocorticoid hormones. Reproduced with permission from Lightman and Conway-Campbell, 2010 (Lightman and Conway-Campbell, 2010).

1.4.2 Glucocorticoids

It is well established that GCs play an important role in the stress response since they are the ultimate product of the activation of the HPA axis. They are also important for many physiological processes and act as major mediators in the maintenance of the organization of the circadian timing system and the systemic homeostasis (Herbert *et al.*, 2006; Dickmeis, 2009; Dibner, Schibler and Albrecht, 2010).

1.4.2.1 Endogenous Glucocorticoids

GCs are synthesized in the adrenal cortex. The adrenal cortex consists of three zones; the zona glomerulosa, zona fasciculata and zona reticularis. GCs (cortisol in humans, corticosterone [CORT] in rodents) are synthesized in the zona fasciculata (middle zone). GC production and secretion is regulated by ACTH which has pulses occurring every 30-120 minutes and the amplitude of these pulses lead to the circadian rhythm of GCs production (Dallman et. al, 1987).

The substrate of GCs is cholesterol. When cholesterol is mobilized from the outer to the inner mitochondrial membrane by the steroidogenic acute regulatory (StAR) protein, it is converted to pregnenolone. ACTH regulation of StAR protein is the rate-limiting step in adrenal production of GCs (Wurtman and Axelrod, 1965; Arlt and Stewart, 2005; Gupta and Bhatia, 2008).

1.4.2.2 Synthetic Glucocorticoids

Synthetic glucocorticoids (sGCs) are widely used in clinic in physiological doses or as pharmacological therapies for their anti-inflammatory and immunosuppressive properties (Axelrod, 1976; Van Der Velden, 1998; Gupta and Bhatia, 2008). Nowadays, in the UK, sGCs or so called corticosteroids, are used frequently by 1% of the adult population (Van Staa *et al.*, 2001). However, the use of GCs in high doses suppresses the HPA axis activity by central suppression or adrenal gland atrophy (Krasner, 1999; Buchman, 2001; Arlt and Allolio, 2003) and can cause significant side effects such as adrenal insufficiency, diabetes, osteoporosis, and glaucoma (Schäcke, Döcke and Asadullah, 2002; Vandewalle *et al.*, 2018).

Since the use of GCs in the treatment of rheumatoid arthritis in 1949 (Hench and Kendall, 1949), a substantial amount of research in science and industry has been done to elaborate synthetic compounds with GC activity to maximize their benefits and minimize the side effects of GCs.

There are many sGCs today, and the difference between these compounds is given by structural alterations which can affect their bioavailability (absorption, half-life,

administration route, metabolism, affinity to their receptor target, concentration in target tissue) (Schäcke, Döcke and Asadullah, 2002). Whilst endogenous GCs exert their effects by binding to two nuclear receptors, the glucocorticoid receptor (GR) and mineralocorticoid receptor (MR) (discussed in detail below), modern sGCs trigger their effects by binding specifically to the GR (Chrousos, Pavlaki and Magiakou, 2000; Paragliola *et al.*, 2017).

Adverse side effects of sGCs are observed when higher doses are given over long periods of time. These side effects have been profoundly researched and described, and include effects on metabolism resulting in diabetes, increased body weight, (Huscher *et al.*, 2009), Cushing's Syndrome (Mazziotti, Gazzaruso and Giustina, 2011), bone demineralisation (Iwamoto, Takeda and Ichimura, 2002), myopathy (Waddell *et al.*, 2008), problems in cardiovascular systems (Radhakutty *et al.*, 2016), problems in gastrointestinal system (Buttgereit and Scheffold, 2002) and risk of infections (Hench and Kendall, 1949). However, the neuropsychiatric side effects, which are of particular interest for our study, have been less researched and are likely to be of great relevance since research indicates that 23% of patients using sGCs report mania during early treatment (Naber, Sand and Heigl, 1996), and shows that depression is reported in 28% of patients (Sirois, 2003) and anxiety in 60% of patients during chronic treatment (Bolanos *et al.*, 2004).

1.4.3 Glucocorticoid and Mineralocorticoid Receptors

Endogenous GCs trigger their effects by binding to two specific intracellular receptors expressed in target cells, the glucocorticoid receptor (GR) and the mineralocorticoid receptor (MR). GR and MR are nuclear receptors, which act as latent transcription factors (Mangelsdorf *et al.*, 1995). These receptors share three major characteristics; a DNA binding domain (DBD), a ligand binding domain (LBD) and a N-terminal domain (NTD) (Kumar and Thompson, 1999).

MR bind GCs with higher affinity than GR. However, GR is expressed in almost all cell types and MR is specific to epithelial cells in kidney, colon and salivary glands, and non-epithelial cells in the brain and heart (Reichardt and Schütz, 1998).

MR is activated at low concentrations of GC, whereas GR is only activated at higher concentrations (Mifsud and Reul, 2016).

Moreover, because MR is active under basal conditions it is thought to play a different role in stress in comparison to GR that functions as a response to and recovery from stress (De Kloet and Reul, 1987), MR sets the threshold for stress responsiveness (Joëls *et al.*, 2008). Additionally, both receptors act as ligand-activated transcription factors exerting both genomic and non-genomic responses, which will be discussed in the next section.

In the brain, GR is expressed in almost all types of cells and tissues in the body. GRs in the brain are found with particularly high density in the hippocampus, the medial prefrontal cortex (mPFC) and in parvocellular neurons of the PVN. It has also been found in cerebellar and olfactory cortex, thalamus and hypothalamus (J M H M Reul and De Kloet, 1985). In contrast, MR is restricted to the hippocampus, prefrontal cortex, and amygdala (Arriza *et al.*, 1988) and it has high levels of expression in kidney and adipose tissue (Edwards *et al.*, 1988)

Considering only the GR, its structure is designed by; 1) the NTD which has a transactivation domain (AF1) and has been shown to be very important for gene regulation (Hollenberg *et al.*, 1987), 2) the (DBD) which has two zinc-finger motifs that interact with specific DNA sequences known as glucocorticoid response elements (GREs) (Freedman *et al.*, 1988), and 3) the C-terminal LBD which provides a ligand-specific binding site and contains the ligand-dependent activation function 2 (AF2) (Nagpal *et al.*, 1993).

Additionally, in the interest of this study, the GR is the product of a single gene (Nr3c1), but multiple variants exist (5 variants [GR_{α}, GR_{β}, GR_{γ}, GR-A, and GR-P]. Forty distinct isoforms are generated through alternative splicing and alternate translation (Lu and Cidlowski, 2005).

Two variants, GR_{α} and GR_{β}, have had special attention given their relative abundance (Miller and Auchus, 2011). GR_{α} is expressed more than GR_{β} in healthy individuals, however a higher expression of GR_{β} compared with GR_{α} has been

correlated with glucocorticoid resistance (Honda *et al.*, 2000; Chikanza, 2002; Rhen and Cidlowski, 2005).

1.4.4 Mechanism of action; ligand-receptor complex

As described above, GCs and sGCs exert their effects by binding to GR. Additionally, GR receptor acts as a ligand-activated transcription factor. After GCs binds to GR, this ligand-receptor complex translocates to the nucleus and causes genomic and non-genomic responses. After numerous studies, genomic effects have been well described. However, non-genomic responses are still being investigated.

When GCs are absent, GR is mainly localised in the cytoplasm in a multiprotein complex containing chaperone molecules (p23, Src) (Almawi and Melemedjian, 2002), different heat shock proteins (hsp90, hsp70, hsp56 or hsp40) (Pratt *et al.*, 2006), immunophilins (Hutchison *et al.*, 1993) and kinases (MAPK) (Wikström, 2003), which stabilize and prevent its degradation. When GCs are at high levels, they bind to the GR causing it to experience a conformational change where it dissociates from the chaperone complex and translocates to the nucleus (Kitchener *et al.*, 2004). Within the nucleus, GR functions as a transcription factor, hence interacting with the DNA or other proteins, to modulate genomic responses via activating or repressing transcription of target genes (J M H M Reul and De Kloet, 1985; J. M.H.M. Reul and De Kloet, 1985; Conway-Campbell *et al.*, 2007).

1.4.4.1 Genomic effects

To modulate genomic responses (slow effects (within hours)), three main mechanisms can be described for the GC-GR complex.

1. Transactivation; the GR translocates to the nucleus where it binds to a glucocorticoid response element (GRE) (Truss and Beato, 1993) and enhances target gene expression. GRs can even bind to degenerated GRE sequences (Starick *et al.*, 2015) and GRE sequences can affect GR conformation, which in turn leads to different levels of GR affinity (Watson *et al.*, 2013).

2. Gene activation or repression: GR binds to another transcription factor (TF) and this complex binds to its "composite elements" on the DNA. Hence, this specific GR binding contains half GRE and half of another response element of another TF. Therefore, this binding can lead to gene activation or repression (Ramamoorthy and Cidlowski, 2016).
3. Transrepression; GR can also bind to a negative GRE which can lead to repression of gene transcription (Strömstedt *et al.*, 1991). Moreover, there can also be tethering of GR with another TF; GR can physically interact with another TF without having contact with DNA to influence the TF activity (Ratman *et al.*, 2013).

1.4.4.2 Non-genomic effects

It is clear that a stressful situation requires a rapid response. However, these rapid GC effects are far from clear. Researchers in this area have proposed from two to five different non-genomic mechanisms, independently of gene expression and protein synthesis, that result in the immediate action of GCs. Hypotheses suggest that: 1) GCs interact with plasma and mitochondrial membranes influencing the activity of their associated proteins (Buttgereit and Scheffold, 2002), 2) binding of GCs with the GR multiprotein complex causes disassociation of some of the complex molecules, which in turn activate other cellular processes (Pratt *et al.*, 2006), 3) there exists a protein-protein interaction between GCs and GC transporters (Haller, Mikics and Makara, 2008) and 4) non-genomic responses could be mediated by a GR variant which is membrane-bound and has already been described (Gametchu, Watson and Wu, 1993).

1.4.5 Circadian and ultradian rhythms of glucocorticoids

GCs are the archetypal example of a hormone regulated in a circadian manner by the central clock in the SCN (Abe et al, 1979; Moore and Eichler, 1972; Stephan and Zucker, 1972). The SCN regulates the GC circadian rhythm: 1) centrally by modulating CRH release into the hypophyseal portal vessels (Watts, Tanimura and Sanchez-Watts, 2004); and 2) peripherally through a neural pathway that extends from the PVN through the intermedium-lateral column of the spinal cord to the

adrenal glands (Teclemariam-mesbah *et al.*, 1999). In addition, regardless of the control of the SCN, the PVN, pituitary and adrenal cortex express circadian clock genes, which also appear to play a role in the circadian rhythm of GCs (Ishida *et al.*, 2005; Oster *et al.*, 2006).

One of the principal characteristics of GCs is that they are released in a pulsatile manner and the pulse amplitude is modulated over a 24-hour period to establish a circadian GC rhythm (Figure 1-4) (Veldhuis *et al.*, 1989; Spiga *et al.*, 2007). This rhythm exhibits remarkable plasticity and can be modified by physiological parameters such as: age and gender (Lightman *et al.*, 2000), susceptibility to disease (Windle *et al.*, 1998, 2001), early life programming (Shanks *et al.*, 2000); pathophysiological conditions in early life (Meaney *et al.*, 1989) and by chronic stress (Young, Abelson and Lightman, 2004)and constant light exposure (Waite *et al.*, 2012; Park *et al.*, 2013a).

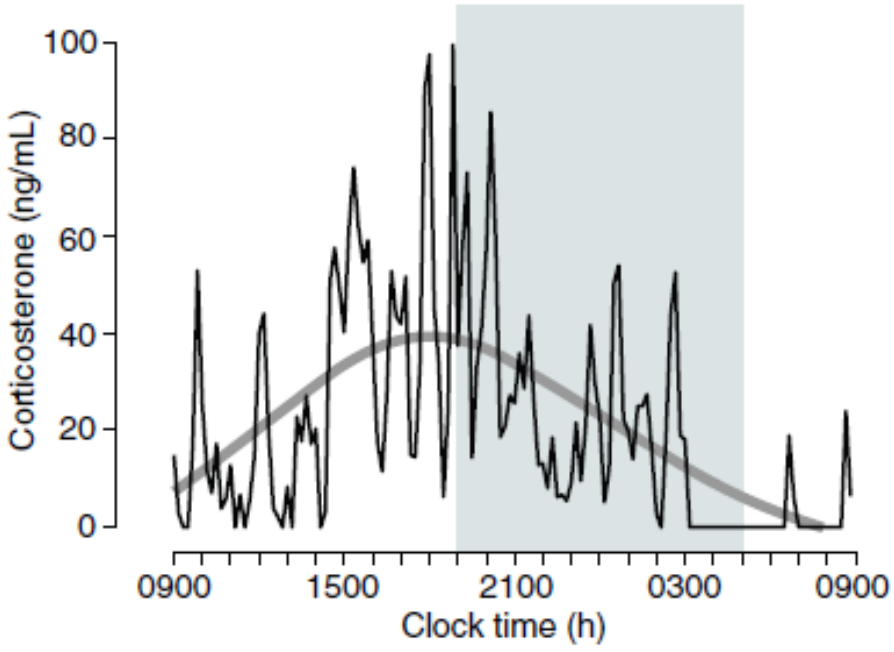

Figure 1-4: Circadian and Ultradian rhythm of plasma corticosterone. Circadian (grey line) and ultradian rhythm (black line) of corticosterone concentration in plasma of rodents in a 24 hr period. Reproduced with permission from (Spiga, Waite, et al., 2011).

However, the ultradian rhythm of GCs (Veldhuis *et al.*, 1989; Windle *et al.*, 1998) is still not fully understood, but it has been shown that it does not require input from

the SCN (Waite *et al.*, 2012). A strong hypothesis has been developed where a balance between positive feed-forward and negative feedback causes ultradian oscillations in ACTH and GC secretion (Jamie J Walker, Terry and Lightman, 2010; Park *et al.*, 2013a; F. Spiga *et al.*, 2017; Francesca Spiga *et al.*, 2017).

These rhythms in GCs are very important as it has been shown that the pulsatile secretion of GCs has an important implication in the rapid and non-rapid mediated actions of GR and MnR (de Kloet and Sarabdjitsingh, 2008) and that this pulsatility changes in disease (Windle *et al.*, 1998; Holsboer, 2000a). Therefore, these rhythms appear to set an optimal functional system which provides the organism with the appropriate neuroendocrine and behavioural responses to deal with stress, maintain homeostasis, secure adaptation and help other neuroendocrine systems maintain their circadian activity in time with other bodily processes.

1.4.6 Glucocorticoid rhythms in health and disease

Rhythms are essential structures of life. The GC rhythms have been established as fundamental characteristics for the correct functionality of the HPA axis, and hence a healthy organism. Furthermore, alterations in GC rhythms have been related to numerous pathophysiological conditions which are found in many human diseases (Young, Abelson and Lightman, 2004; Chung, Son and Kim, 2011b).

As mentioned above, dysregulation of circadian and/or ultradian GC rhythms have been reported in many diseases such as Cushing's syndrome (Van Aken *et al.*, 2005), obstructive sleep apnoea (Henley *et al.*, 2009), Parkinson's disease (Hartmann *et al.*, 1997), Huntington's disease (Aziz *et al.*, 2009), and even Alzheimer's disease (Ferrari *et al.*, 2001) . However, for the particular interest of this study, we will focus on the poorly understood relation between GC altered rhythms and psychiatric disorders, such as depression and anxiety (Pariante, Nemeroff and Miller, 1995; Daban *et al.*, 2005; Graeff, 2007). A GC-target brain region which has not been fully explored in this context is the serotonergic system within the dorsal raphe complex. This system has also been involved in regulating physiological (Ursin, 2002; Solarewicz *et al.*, 2015) and behavioural functions (Kepser & Homberg, 2015; Kiser, Steemers, Branchi, & Homberg, 2012) and it's

altered functionality has been studied in psychiatric disorders (Owens and Nemeroff, 1998; Lowry *et al.*, 2005a; Oquendo *et al.*, 2007). Moreover, a relationship between GC rhythms, serotonin and these types of condition has been established (Chaouloff, 1993; Pompili *et al.*, 2010), but not fully explained.

1.5 Serotonergic systems

Serotonin or 5-hydroxytryptamine (5-HT) is a monoamine neurotransmitter. Approximately 95% of the total body's serotonin is produced in the digestive tract (Gershon, 2004), because serotonin cannot cross the blood-brain barrier, the central and peripheral serotonergic systems are functionally separated and in this study, the focus will only be on the serotonergic system found in the central nervous system (CNS).

The brain's serotonergic system is the biggest monoaminergic system in the brain (broad projections within the brain). It is well established that brain 5-HT has a rhythmic, circadian release and is involved in several physiological and behavioural functions, including locomotor activity (Geyer, 1995), sleep (Portas, Bjorvatn and Ursin, 2000) and feeding behaviour (Voigt and Fink, 2015). Nevertheless, in this section, the discussion of brain serotonin will be focussed only on the physiological and behavioural functions of 5-HT when related to glucocorticoids and psychiatric disorders.

The vast majority of serotonin synthesis and serotonergic neurons are located in the dorsal (DR) and median raphe (MnR) nuclei situated in the brainstem (J. Abrams *et al.*, 2004; Pollak Dorocic *et al.*, 2014) therefore, these areas will be the main focus. Moreover, the neurotransmitter system formed by the raphe complex (DR and MnR) extends out to most of the CNS (Vertes, Fortin and Crane, 1999a; Waselus, Valentino and Van Bockstaele, 2011).

Alterations in the serotonergic system, including altered expression of *tph* gene, the rate-limiting enzyme for brain serotonin synthesis (Walther and Bader, 2003; Walther *et al.*, 2003; Patel, Pontrello and Burke, 2004; Zhang *et al.*, 2004), have been related to several psychiatric disorders, such as depression (Owens and

Nemeroff, 1998; Arango, Underwood and Mann, 2002; Gao *et al.*, 2012), anxiety (Lowry *et al.*, 2005a, 2008a; Ottenhof *et al.*, 2018), bipolar disorders (Mcelroy *et al.*, 2006; Oquendo *et al.*, 2007; Serretti *et al.*, 2011) among others (Naughton, Mulrooney and Leonard, 2000b; Ottenhof *et al.*, 2018). Significantly regarding this study, it has also been shown that *tph* depends on the circadian nature of circulating GC as adrenalectomy abolishes the pattern of *tph* and corticosterone administration enhances *tph2* expression in the inactive phase (Malek *et al.*, 2007; Donner, Johnson, *et al.*, 2012a).

1.5.1 Serotonin; biosynthesis, transporters, receptors and degradation

Serotonin is synthesized from the essential amino acid tryptophan. The initial and rate limiting step is the conversion of L-Tryptophan to 5-hydroxy-L-tryptophan (5-HTP) and then the second step is the conversion of 5-HTP to serotonin by L-amino acid decarboxylase as shown in Figure 1-5.

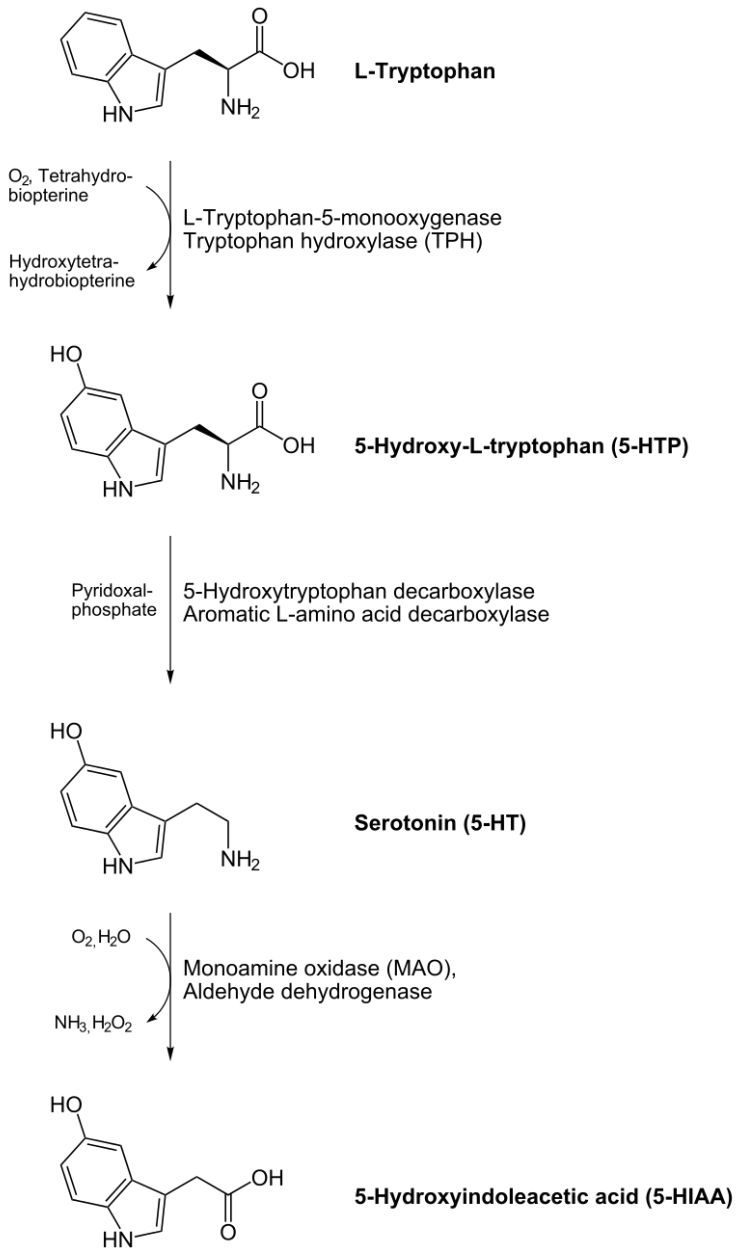

Figure 1-5: Biosynthesis of serotonin.

The rate-limiting enzyme of serotonin, i.e. the conversion of L-tryptophan to 5-HTP, is set by tryptophan 5-hydroxylase (Tph) (Fitzpatrick, 1999) which has two identified isoforms tph1 and *tph2* (López-Narváez *et al.*, 2015; Tidemand *et al.*, 2017).

1.5.1.1 Tph isoforms

The tph enzyme belongs to the aromatic amino acid hydroxylases superfamily (AAAH), which also includes phenylalanine (PAH) and tyrosine hydroxylase (TH) (Hufton, Jennings and Cotton, 1995). To date, tph-cDNAs has been cloned for rabbit (Grenett *et al.*, 1987), mouse (Stoll, Kozak and Goldman, 1990), rat (Darmon *et al.*, 1988) and human (Boularand, Darmon and Mallet, 1995).

Initial studies from Walther et al, which were evaluating the physiological effects of the loss of 5-HT using tph1 knockout mice showed that 5-HT remained unchanged in the hippocampus and frontal cortex but not in the periphery. They also found that tph1 deficient mice had no significant change in behaviour, which suggested the presence of a tph isoform (Walther and Bader, 2003). After its discovery, in post-mortem studies, Zill et. al, showed that tph2 gene is specific to the brain, whereas tph1 is responsible for the peripheral serotonergic effects (Figure 1-6) (Peter Zill *et al.*, 2004).

1.4.1.1.1 Tph1

Tph1 gene has since been identified and is mostly localized in the enterochromaffin cells of the digestive tract (Gershon and Tack, 2007). However, it is also found in small quantities in enteric neurons (Fiorica-Howells, Maroteaux and Gershon, 2000) and mast cells (Finocchiaro *et al.*, 1988). *Tph1* is also localized in the pineal gland (Patel, Pontrello and Burke, 2004; Huang *et al.*, 2008) and in the brainstem, but in this area it is expressed in a ratio of 1:15 compared to *tph2* ; the contribution of this gene on brain 5-HT is unknown (Walther *et al.*, 2003).

1.4.1.1.2 *Tph2*

The human *tph2* gene is located in chromosome 12 showing a 72% sequence homology to tph1 (Walther *et al.*, 2003). *Tph2* is primarily found in central and enteric neurons and total *tph2* mRNA is expressed 150 times more than tph1 mRNA (Yu *et al.*, 1999; Walther and Bader, 2003). Whilst *tph2 gene* can be found in frontal cortex, thalamus, hippocampus, hypothalamus and amygdala (Peter Zill *et al.*, 2004), it is mainly expressed in the raphe complex (Hamon M., Bourgom S., Artaud

F, 1981). Because *tph2* is the gene in charge of brain serotonin, this particular isoform has been implicated in the pathogenesis of many psychiatric disorders, and in the behavioural traits of these disorders (Bailly *et al.*, 1993; Moffitt *et al.*, 1998).

In the interest of this dissertation, mRNA for tph2, is expressed selectively in the brain and exists as orthologs in mice, rats and humans. Tph2 maps to synthetic regions in chromosome 7 in rats. Moreover, there are two splice variants in Tph2 of rat, but only one transcript (according to ENSEMBL), because the difference between both variants is in the 3' UTR (one is longer than the other by 276 bp) and not in the coding sequence. The two *tph2* mRNA splice variants have been found to be expressed in the rat DR and the MnR (Patel, Pontrello and Burke, 2004). $TPH2_b$ (with a short 3'-UTR) is the predominant variant in the DRN, whereas $TPH2_a$ (with a longer 3'-UTR) shows a low abundance in this nucleus (Abumaria *et al.*, 2008).

Tph2 is the major transcript of TPH protein in the raphe cells and the pattern of expression in individual raphe cells is at least as great as tph1 on pineal cells (Haycock et al., 2002). Early studies suggesting that TPH has a short functional half-life (Hasegawa et al., 1995) could imply that a high transcriptional activity is needed to maintain TPH activity, hence, tph2 expression should be somewhat stable.

Furthermore, not all tph2 mRNA synthesis seems to be made in local cell bodies as detection of tph2 mRNA in the prefrontal cortex suggests that a substantial amount of tph2 transcripts synthesized in the raphe nuclei is transported to the nerve terminal and allows local serotonin synthesis at the synapses (Perroud *et al.*, 2010; Carkaci-Salli *et al.*, 2011). Alternatively, these observations might suggest local synthesis of tph2 by another serotonergic neurons.

Moreover, rat *tph2* gene expression seems to be modulated by different environmental stressors. For example, exposing rats to a repeated forced swim test resulted in elevated *tph2* expression in the midbrain (Shishkina, Kalinina and Dygalo, 2008), while early-life experience and social defeat changed *tph2* mRNA expression in the raphe (Katherine L. Gardner *et al.*, 2009a). Moreover, over-

expression or knockdown of *tph2* in the rat brain altered anxiety-like behaviour dependant of their estrogen status (Hiroi *et al.*, 2011).

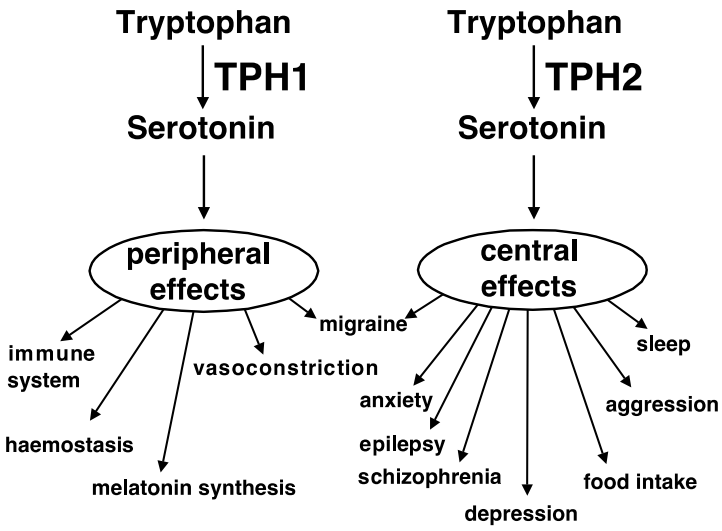

Figure 1-6: Schematic representation of tph1 and tph2 associated functions. Taken from Walther and Bader (2003).

1.5.1.2 Serotonergic transporters

Once serotonin is produced it is transported into vesicles though a vesicular monoamine transporter (VMAT). There are also two isoforms of VMAT, 1 (found in neuroendocrine cells) and 2 (neuronal) (Erickson *et al.*, 1996). Serotonin is released into the synaptic cleft where it binds to serotonin receptors, which can either be pre- or post-synaptic (Hannon and Hoyer, 2008). Serotonin reuptake transporter (SERT) is necessary to reuptake serotonin and avoid desensitising 5-HT receptors (Fuller & Wong, 1990).

1.5.1.3 Serotonergic receptors

Seven families of serotonin receptors have now been recognized (Table 1-3) (5-HT_1 to 5-HT_7). Furthermore, these receptors are not limited to the brain but those that are, are expressed in a cell-type-specific fashion (Berger, Gray and Roth, 2009).

Table 1-3: Families of 5-HT receptors.

Family	Potential	Type
5-HT$_1$	Inhibitory	G_i/G_0-protein coupled
5-HT$_2$	Excitatory	G_{q11}-protein coupled
5-HT$_3$	Excitatory	Ligand-gated Na^+/K^+ channel
5-HT$_4$	Excitatory	G_s-protein coupled
5-HT$_5$	Inhibitory	G_i/G_0-protein coupled
5-HT$_6$	Excitatory	G_s-protein coupled
5-HT$_7$	Excitatory	G_s-protein coupled

5-HT receptors can act as metabotropic or ionotropic receptors. The 5-HT$_3$ family is the only family of receptors which has been described to act in an ionotropic way (ligand-gated ion channel); these receptors are characterized by a low affinity for serotonin and rapid activation (Thompson and Lummis, 2006). The other 5-HT receptor families are metabotropic receptors which act through a G protein activation and second messenger and display high affinity for serotonin and slow activation. (Bockaert *et al.*, 2006).

The seven families of 5-HT receptors have different sub-types of receptors which have different functional properties described below;

- 5-HT$_1$ includes 1A, 1B, 1D, 1E and 1F sub-types; functional receptors include 1A, 1 B and 1D (Hoyer and Martin, 1997). The 5-HT$_{1A}$ sub-type is the most distributed serotonin receptor in the brain. These have high expression in cerebral cortex, hippocampus, septum, amygdala and raphe nucleus (el Mestikawy *et al.*, 1991), but can also be found in small quantities in other areas of the brain such as, basal ganglia and thalamus. This family of receptors is linked to anxiety (Klemenhagen *et al.*, 2006). Additionally, the 1B subtype can be found in many areas of the brain and its function depends on its location. However, in general, its function has an inhibitory

role (Jin *et al.*, 1992). The 1D has a low expression compared to 1B and can be found in the dorsal raphe nuclei, where they modulate the release of serotonin (Pullar *et al.*, 2004).

Additionally, these family of receptors, particularly 1A and 1B expressed in all, but not limited to, serotonergic neurons of the DR (Day *et al.*, 2004)(Day *et al.*, 2004). Moreover, the distribution of 5-HT1A and IB mirror expression of Tph2 with peak expression in the ventromedial DR and mid-rostral levels (Clark, McDevitt and Neumaier, 2006).

Furthermore, these types of receptors appear to be GC sensitive as several studies have shown that these receptors are negatively regulated by GC especially in the limbic system (Lanfumey *et al.*, 2008). Moreover, different research groups have shown that GC via GR and MR are involved in negative regulation of 5-HT_{1A} gene expression (Mendelson and McEwen, 1992; Meijer and de Kloet, 1994; Meijer *et al.*, 1997).

Finally, molecular data has shown the inhibitory effect of GCs on 5HT receptor gene transcription as chronic stress, hence, increased levels of CORT, have shown to reduce the activation of 5-HT receptors (Mendelson and McEwen, 1991; Laaris *et al.*, 1999; Lanfumey *et al.*, 1999). In the other hand, electrophysiological studies have demonstrated that exposure to elevated GC levels attenuated 5-HT auto receptor function in the DR in rats (Man, Young and McAllister-Williams, 2002; Fairchild, Leitch and Ingram, 2003; Judge, Ingram and Gartside, 2004).

- 5-HT_2 includes 2A, 2B and 2C. This particular family of receptors have been shown to be the main excitatory serotonin receptors (Hannon and Hoyer, 2002). The 2A subtype is expressed in central and peripheral tissue; in the brain, these receptors can be found mainly in the basal ganglia (Cook Jr. *et al.*, 1994). The 2B subtype is associated with smooth muscle and can be found in cerebellum, hypothalamus and medial part of the amygdala

(Schmuck *et al.*, 1994). The 2C subtype has a strong link to psychiatric disorders since it is a good, effective target of antidepressant action (Goodwin *et al.*, 2009).

- 5-HT_3 only has 3A and 3B. These receptors are the only ionotropic serotonin receptors. They have 5 subunits arrange around an ion channel. These receptors are excitatory and can be found in central and peripheral tissue (Gyermek, 1995).

- 5-HT_4 has 4A, 4B, 4C, 4D, 4E, 4F, 4G and 4H. The complete family is linked to adenylyl cyclase activity (Hoyer, Hannon and Martin, 2002). These receptors are found in high density in the nucleus accumbens and may be involved in memory, learning and the reward system (Reynolds *et al.*, 1995).

- 5-HT_5 includes 5A and 5B. The activity of these specific receptors is largely unknown; however, given their localization within the brain, they have been related to motor control, anxiety, depression, learning and memory consolidation (Thomas, 2006).

- 5-HT_6 has 6A and 6B. This family is located in limbic areas such as caudate and substantia nigra, but its functions are still unknown (Kohen *et al.*, 1996).

- 5-HT_7 has 7A, 7B, 7C, 7E and 7D. These are found in thalamus, hypothalamus, cerebral cortex, amygdala and dorsal raphe (Bonaventure *et al.*, 2004). These receptors have been related to depression, anxiety, cognitive disturbances, migraine and schizophrenia (Thomas and Hagan, 2004).

1.5.1.4 Serotonin degradation

After SERT reuptakes serotonin, the neurotransmitter degradation is completed mainly by monoamino oxidase which includes two isoforms; MAO_A and MAO_B,

with MAO_A being the main isoform of degradation in the brain (Shih, Wu and Chen, 2011). Serotonin gets broken up into 5-hydroxyindoleacetic acid (5-HIAA) or can be metabolized into N-methyl, N.N-dimethyl or O-methyl tryptamine to then be synthesized to melatonin (Stahl, 1998).

1.5.2 Brain serotonergic system anatomy and functional correlates

As mentioned above, the majority of brain serotonin biosynthesis and release is in the raphe complex, which comprises the dorsal raphe nucleus (DR) and the medium raphe nucleus (MnR) (Imai *et al.*, 1986); we will therefore focus on this complex.

The raphe complex is a collection of neurons which extend rostral-caudally in the brainstem in animals and humans (Taber, Brodal and Walberg, 1960), where in rats goes from -7.328 to -8.672 mm bregma (Paxinos and Watson, 2005). They contain different types of neurons with different morphologies, projections and chemical characteristics (Dahlström and K. Fuxe, 1964). However, these neurons are topographically organized according to their anatomical structure/location and their functional properties, indicating a possible connection between function and structure (cluster of neurons) (Baker, Halliday and Törk, 1990) (Figure 1-7).

Most of the afferent projections to the raphe complex originate from forebrain structures that belong to the limbic systems (Peyron *et al.*, 1997a); this will be fully discussed in the sections below.

The raphe complex can be divided into a rostral and caudal group given the neuron distribution and main projections. The rostral group has major projections to specific forebrain structures and the caudal group to *other* forebrain structures as well as a few projections to the caudal brainstem and spinal cord (Ding *et al.*, 2003). Projections from the rostral group to specific structures are different from the projections of the caudal group to other structures; hence, specificity of projections is present (Imai *et al.*, 1986; Villar *et al.*, 1988), suggesting again a link between unique function (behavioural associations) of target structures (projections of serotonergic neurons to specific forebrain structures) and specific clusters of serotonergic neurons (subregions of the raphe complex).

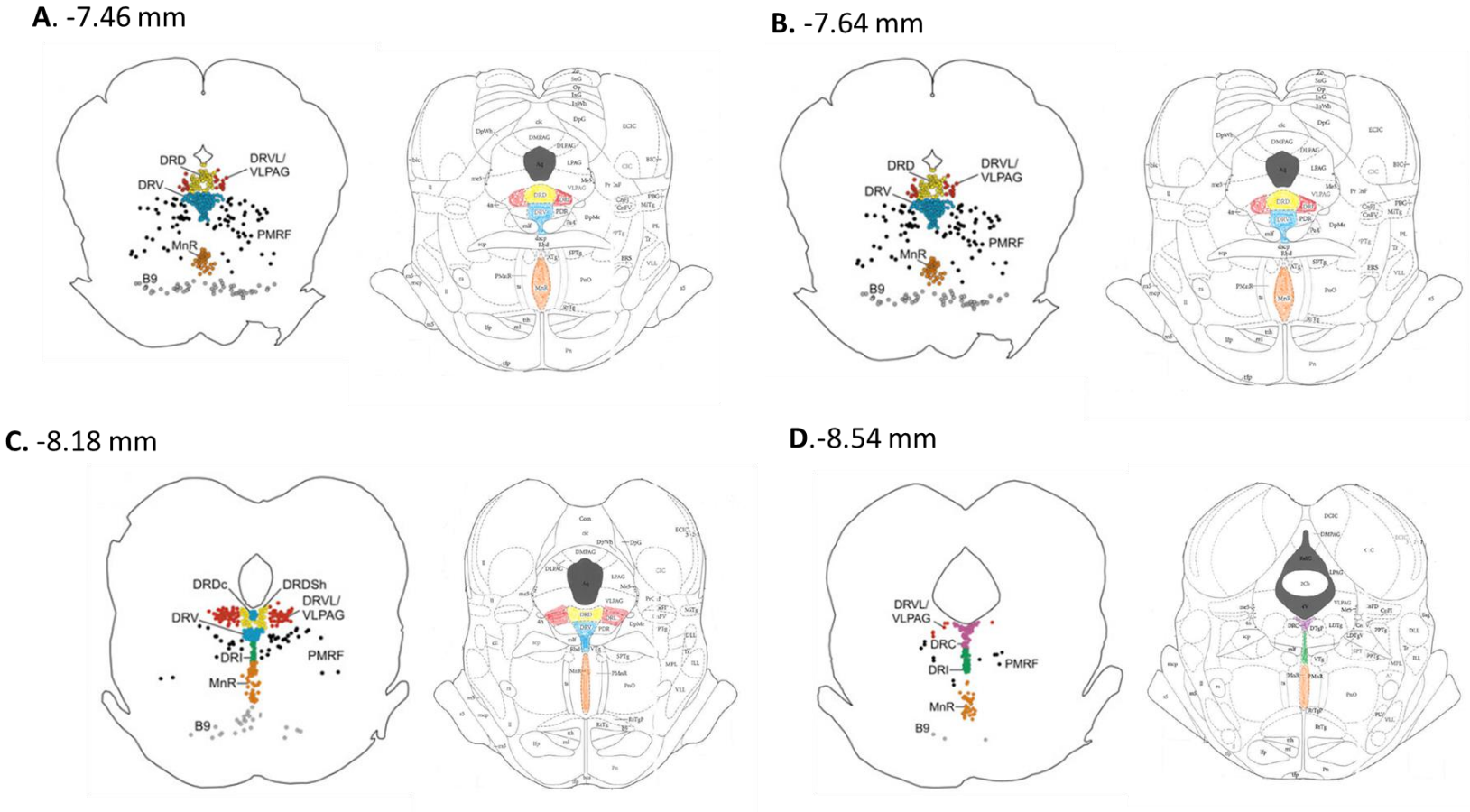

Figure 1-7: Line drawings and stereotaxic schematics of coronal sections of the rat brain. Representation of all subdivisions of the DR and MnR used for this study. Taken and modified with permission from Hale and Lowry, 2011 and The rat brain atlas from Paxinos and Watson 2005 (Paxinos and Watson, 2005; Hale and Lowry, 2011).

The functional anatomy of the DR complex has been described through different methodological techniques and by different research groups. To mention a few, studies of single unit recordings were used to investigate behavioural correlates (Fornal *et al.*, 1996; Sakai and Crochet, 2001) In vitro electrophysiology in brain slices to describe unique electrophysiologic properties (Crawford, Craige and Beck, 2010). Immunohistochemical detection of c-Fos as markers of neuronal activity (Hale *et al.*, 2010). Injections of retrograde tracers into the DR for topography of serotonergic systems (Baratta *et al.*, 2009). Microinjection of drugs into the Raphe complex to mimic behavioural outcomes (Hammack *et al.*, 2002). Microdissection techniques with liquid chromatography to describe functional topography (Evans, Heerkens and Lowry, 2009) and in situ hybridization to measure changes in gene expression (Malek, 2007; Donner, Montoya, *et al.*, 2012).

The following section corresponds to a brief summary of the findings of the anatomy and functional correlates of the Raphe complex.

1.5.2.1 Dorsal raphe (DR)

The dorsal raphe nucleus has been divided in several subregions based on the projections and function of its serotonergic neurons; these areas are the dorsal part of the dorsal raphe (DRD), the ventral part of the dorsal raphe (DRV), the intrafascicular part of the dorsal raphe (DRI), the ventro-lateral part of the dorsal raphe (DRVL/VLPAG), and the caudal part of the dorsal raphe (DRC) (Baker, Halliday and Tork, 1990) (for summary see table 1-4).

1.5.2.1.1 Dorsal Raphe nucleus, caudal part (DRC)

This area accepts afferents from medial prefrontal cortex, preoptic area, arcuate nucleus and perifornical and lateral hypothalamic areas, and midbrain and brainstem regions including the IPN, laterodorsal tegmental area, and area postrema (H. H. S. Lee *et al.*, 2003).

The DRC projects to subfornical and subcomisural organ (Lind, 1986) the ventral hippocampus, amygdala, locus coeruleus , and midline and thalamic nuclei (Imai *et al.*, 1986; Krout, Belzer and Loewy, 2002).

Hence, the DRC seems to be related to stress and anxiety circuits. Moreover, because of its common afferents to brain structures which are implicated to anxiety-related states and a specific subpopulation of serotonergic neurons, this area seems to have a special interaction with the DRD (Hale and Lowry, 2011; Hale, Shekhar and Lowry, 2012).

1.5.2.1.2 Dorsal Raphe nucleus, interfascicular part (DRI)

The DRI has not been completely detailed. However, studies have shown that the DRI receives projections from the median preoptic area, and lateral parabrachial nucleus (H. H. S. Lee *et al.*, 2003; Holstege, Mouton and Gerrits, 2003).

The DRI projects to dorsal and ventral hippocampus, medial septum, entorhinal cortex, cortical areas and barrel field cortex (Azmitia and Segal, 1978a; Köhler, Chan-Palay and Steinbusch, 1982; Waterhouse *et al.*, 1986; Kirifides *et al.*, 2001).

Therefore, the DRI may play an important role in cognitive and emotional processes and seems to have a strong interaction with DRVL/VLPAG area (Lowry *et al.*, 2007; Hale, Shekhar and Lowry, 2012).

1.5.2.1.3 Dorsal Raphe nucleus, dorsal part (DRD)

The DRD receives afferents from the lateral and ventral orbitofrontal and infralimbic cortices, central nucleus of the amygdala, BNST, and the dorsal, dorsomedial, lateral, and posterior hypothalamic nuclei (Peyron *et al.*, 1997a).

The DRD shows projections to the basolateral (Hale *et al.*, 2008) and central nuclei of the amygdala, dorsal hypothalamic area (Commons, Connolley and Valentino, 2003), nucleus accumbens, and medial prefrontal cortex (Van Bockstaele, Biswas and Pickel, 1993). Moreover, it projects to hippocampus, entorhinal cortex, septum,

locus coeruleus and prefrontal cortex (Köhler and Steinbusch, 1982a; Imai *et al.*, 1986).

The DRD seems to be important for the regulation of emotional behaviour associated with stress- and anxiety-related physiologic and behavioural responses (Commons et. al, 2003; Lowry et. al, 2008, 2005). An increase in *tph2* in the DRD has also been related to an antidepressant-like effect (Donner and Handa, 2009). However, high levels of *tph2* in the DRD were found depressed patients (H Bach-Mizrachi *et al.*, 2006).

1.5.2.1.4 Dorsal Raphe nucleus, ventral part (DRV)

The DRV shows the highest expression of *tph2* of all the DR subregions (Clark, McDevitt and Neumaier, 2006). This area receives afferents from the dorsomedial and ventromedial hypothalamus, central nucleus of the amygdala, cingulate cortex, and lateral orbital cortex (Peyron *et al.*, 1997a).

Additionally, the DRV projects to caudate putamen (Steinbusch, 1981), sensorimotor cortex, ventrolateral orbital, frontal cortex, motor cortex, visual and barrel field cortex (Waterhouse *et al.*, 1986; Coffield, Bowen and Miletic, 1992; Kirifides *et al.*, 2001).

It has been shown that the DRV plays a role in motor function and cognitive tasks (Hale and Lowry, 2011; Hale, Shekhar and Lowry, 2012).

1.5.2.1.5 Dorsal raphe nucleus, ventrolateral/ventrolateral periaqueductal grey (DRVL/VLPAG)

The DRVL/VLPAG accepts afferents from the parabrachial nucleus (H. H. S. Lee *et al.*, 2003), the solitary tract (Herbert, 1992), infralimbic cortex (Hurley *et al.*, 1991), BNTS, central amygdala (Gray and Magnuson, 1992), preoptic nucleus, median preoptic nucleus (Watts and Swanson, 1987), lateral and perifornical hypothalamic nuclei (H. H. S. Lee *et al.*, 2003) and from the retina (Fite *et al.*, 1999).

Additionally, DRVL/VLPAG projects to lateral hypothalamus (Ljubic-Thibal *et al.*, 1999), rostro-ventrolateral medulla (Bago, Marson and Dean, 2002), dorsolateral periaqueductal grey (Stezhka and Lovick, 1997), lateral geniculate body, lateral posterior nucleus of the thalamus, superior colliculus, the retina (Villar *et al.*, 1988) ventral posterior medial thalamus (Kirifides *et al.*, 2001)and parafascicular thalamic nucleus (Chen *et al.*, 1992).

DRVL/VLPAG subregions appear to be involved in the control of autonomic function and emotional behaviour. They are also involved in panic behaviours where fight-or-flight is suppressed and freezing behaviours are increased (Bandler *et al.*, 2000; K. L. Gardner *et al.*, 2009).

1.5.2.2 Median Raphe nucleus (MnR)

The median raphe nucleus (MnR) is a cluster of neurons consisting of 80% serotonergic neurons (Baker, Halliday and Törk, 1990).

The MnR is innervated by medial hypothalamic structures such as the preoptic area, the perifonical, dorsomedial and lateral hypothalamic areas and mammillary and supramammilary nuclei. It also receives projections from the medial prefrontal cortex, anterior cingulate cortex and the ventral lateral preoptic area (Vertes, Fortin and Crane, 1999). Moreover, the MnR receives projections from the DR (Tischler and Morin, 2003).

The MnR projects to the posterior hypothalamus, medial mammillary nucleus, medial supramammillary nucleus, tuberomammillary nucleus, ventrolateral dorsomedial hypothalamus and perifornical region, and anterior hypothalamic nucleus.

The MnR has been implicated in resistance, tolerance and adaptation to chronic psychosocial stress (Deakin, 1996; Graeff *et al.*, 1996). It has been implicated in ingestive behaviour (Bendotti and Samanin, 1986; Wirtshafter and Krebs, 1990) and in circadian rhythmicity given that the MnR projects directly to the SCN (Moga and Moore, 1997; Morin, 1999).

All these clusters of neurons have been shown to receive afferents from different areas and send projections to distinct forebrain areas, providing a functional correlation with behaviour. Two strong schemes have thereby been proposed; a DRC/DRD "anxiety-facilitating" system, and a DRVL/VLPAG/DRI "antidepressant-like" system (Hale, Shekhar and Lowry, 2011, 2012), which implicates an important role for the serotonergic system in psychiatric disorder.

1.5.2.3 Interactions within the Raphe Complex

As mention by experts in the area, it is important to study the fact that serotonergic neurons from specific subdivisions within the Raphe complex give rise to distributed, but related targets (Hale and Lowry, 2011). This is important because it might be the key to understand the neural functions of this areas and perhaps to develop strategies to modulate these specific neural functions.

A different approach to understand this complex system has been to study not only the related targets of serotonergic neurons but also the intra-connections within the Raphe complex. Different research groups have suggested intra-connections between the subdivisions of the Raphe complex and functional interconnections within it. Here a list of the findings;

- MnR- DR: The MnR receives projections from the DR (Tischler and Morin, 2003). Moreover, a functional interaction between the DR and MnR was shown by the fact that inhibition of the MnR prevented the increase of serotonin release in the prefrontal cortex following stimulation of the DR (Forster *et al.*, 2008) .

- The DRD-DRC; These structures have been related to an anxiety-related neuronal circuit (Lowry *et al.*, 2008b). Various anxiogenic drugs selectively increase c-Fos expression in the DRD and DRC (Abrams *et al.*, 2005). Moreover, chronic injection of estrogen-receptor-beta agonist increases tph2 expression in DRD and DRC only (Donner and Handa, 2009).

- The DRV-DRD; Both structures receive afferents from similar set of hypothalamic, limbic and cortical regions (H. S. Lee *et al.*, 2003) and injections of tracer that label fibres in the DRV also label fibres in the DRD and DRVL/VLPAG (Peyron *et al.*, 1997a).

- DRVL/VLPAG-DRV; Neurons within DRVL/VLPAG project to the DRV and selective lesions of the DRVL/VLPAG results in an increase of *tph2* gene expression in the DRV, hence DRVL.VLPAG might have an inhibitory role of the DRV (Peyron *et al.*, 1997b).

- DRVL/VLPAG-DRD; When serotonergic neurons in the DRVL/VLPAG are activated, neurons in the DRD are inactive, and when DRD neurons are active DRVL/VLPAG neurons are not, hence, a hypothesized relationship has been established, but not fully studied ((Staub, Spiga and Lowry, 2005; Hollis *et al.*, 2006; Bouwknecht *et al.*, 2007a)

- DRI-MnR; Evidence has shown that serotonergic neurons in the caudal part of the DRI are closely related to the MnR than to other subdivisions of the DR (Jacobs and Azmitia, 1992).

- DRI-DVL/VLPAG; Both subdivisions receive projections from the median preoptic (Holstege, Meiners and Tan, 1985) are and the lateral parabrachial nucleus (Saper and Loewy, 1980). Furthermore, serotonergic neurons within this subdivisions are co-activated following injections with LPS (Hollis *et al.*, 2006), after peripheral immune stimulation with *saprophytic bacterium* (Lowry *et al.*, 2007) and following exposure to warm ambient temperature (Hale et al., unpublished data).

Table 1-4; Summary of Afferent and efferent connections of all subdivisions studied from the DR complex.

Subdivision of Raphe complex	Afferents	Efferents	Functional topography
DRC	• Medial Prefrontal cortex. • Hypothalamic regions, preoptic area, arcuate nucleus, perifornical and lateral areas. • IPN, laterodorsal tegmental area and area postrema. (H. H. S. Lee *et al.*, 2003)	• Subfornical organ (Lind, 1986). • Subcommissural organ (Mikkelsen, Hay-Schmidt and Larsen, 1997). • Circumventricular organs, ependymal lining and cerebral ventricles (Simpson *et al.*, 1998). • Ventral hippocampus, amygdala • Locus coeruleus (Imai *et al.*, 1986). • Midline thalamic nuclei; paratenial, paraventricular and lateral parafascicular thalamic nuclei (Krout *et al.*, 2002).	• Stress and anxiety-related neuronal circuit (Lowry *et al.*, 2005a).
DRI	• Median preoptic area (Holstege, Meiners and Tan, 1985). • Lateral parachial nucleus (H. H. S. Lee *et al.*, 2003). • LC (Kim *et al.*, 2004).	• Dorsal and ventral hippocampus (Azmitia and Segal, 1978b; Amaral and Cowan, 1980). • Medial septum (Köhler and Steinbusch, 1982a). • Entorhinal cortex (Köhler and Steinbusch, 1982b). • Barrel field cortex (Kirifides *et al.*, 2001). • Frontal pole, dorsolateral prefrontal cortex, Medial orbital cortex, Inferior convexity and Anterior cingulate cortex (Porrino and Goldman-Rakic, 1982). • Mediodorsal thalamus (Groenewegen, 1988).	• Antidepressant like-behavioural effects (Lowry *et al.*, 2007).

DRD	• Rostral DR- Samee as mid-rostralcaudal DR. • Lateral and ventrolateral orbitoforintal and infralimbic cortices. • Central nucleus of the amygdala. • BNTS • Dorsal, dorsomedial, latera and posterior hypothalamic nuclei. (Peyron *et al.*, 1997a)	• Caudate putamen and substantia nigra, Locus coeruleus, vemtral hippocampus (Imai, Steindler and Kitai, 1986). • Subthalamic nucleus (Canteras *et al.*, 1990). • Substantia innominate (Grove, 1988). • Motor cortex (Waterhouse *et al.*, 1986). • Basolateral and central nuclei of the amygdala (Commons, Connolley and Valentino, 2003; Hale *et al.*, 2008). • Nucleus accumbens, medial prefrontal cortex and prefrontal cortex (Van Bockstaele, Biswas and Pickel, 1993). • Hippocampus and entorhinal cortex, Septum (Köhler and Steinbusch, 1982a).	• Activation of stress and anxiety related circuits(Commons, Connolley and Valentino, 2003; Lowry *et al.*, 2008c). Such as; social defeat (Gardner *et al.*, 2005), Uncontrollable stress (Amat *et al.*, 2005)and Open-field arena (restricted to the rostral part of the DRD (Bouwknecht *et al.*, 2007b).
DRV	• Dorsomedial and ventromedial hypothalamus. • Central nucleus of the amygdala. • Cingulate cortex. • Lateral and orbital cortex. (Peyron *et al.*, 1997b; H. H. S. Lee *et al.*, 2003)	• Caudate putamen (Steinbusch *et al.*, 1980). • Sensoriomotor cortex (Waterhouse *et al.*, 1986). • Ventrolateral orbital cortex (Coffield, Bowen and Miletic, 1992). • Frontal cortex (Kazakov *et al.*, 1992). • Motor cortex, Visual cortex and Barrel field cortex (Kirifides *et al.*, 2001).	• Motor function • Complex cognitive tasks (Greenwood *et al.*, 2005a)

DRVL/VLPAG	• Lateral parabrachial nucleus (H. H. S. Lee *et al.*, 2003). • Medial part of the nucleus of the solitary tract (Herbert, 1992). • Viscerosensory glossopharyngeal and vagal nerves(Herbert and Saper, 1992). • Infralimbic cortex (Hurley *et al.*, 1991) • BNTS, central amygdaloid nucleus (Gray and Magnuson, 1992). • Median preoptic nucleus (Simerly and Swanson, 1986). • Lateral and perifornical hypothalamic nuclei (Saper, Swanson and Cowan, 1979). • Retina (Kawano, Decker and Reuss, 1996a).	• Lateral hypothalamus (Ljubic-Thibal *et al.*, 1999). • Rostroventrolateral medulla (Bago, Marson and Dean, 2002). • Dorsolateral periaqueductal gray, Dorsal and ventral parts of the lateral geniculate body, Lateral posterior nucleus of the thalamus (Fite *et al.*, 1999). • Superior colliculus (Villar, Vitale and Parisi, 1987). • Retina (Waterhouse *et al.*, 1993). • Trigeminal nerve and Ventral posterior medial Thalamus (Kirifides *et al.*, 2001). • Parafascicular thalami nucleus (Chen *et al.*, 1992).	•Supressing Panic-like symptoms (Johnson *et al.*, 2005).
MnR	•Medial hypothalamic structures (preoptic area, perifornial dorsomedial and lateral hypothalamic areas, and mammillary and supramammillary nuclei). •Medial prefrontal cortex (medial angraular (frontal cortex, anterior cingulate cortex and PL). •Agranular insular cortex. •Ventral lateral preoptic area. (Vertes and Linley, 2008)	•Septohippocampla system. •Posterior hypothalamus. •Medial mammillary nucleus, Medial supramammillary nucleus and Tueromamillary nucleus. •Ventrolateral dorsomedial hypothalamus and perofornical region. •Anteriour hypothalamic nucleus •Suprachiasmatic nucleus. (Moga and Moore, 1997; Vertes and Linley, 2008)	•Implicated in inhibitory control of ingestive behaviour (Wirtshafter and Krebs, 1990). •Circadian rhythmicity (Lowry, 2002; Yamakawa and Antle, 2010). •Regulation of hippocampal theta rhythm (Vertes *et al.*, 1994). •Anxety-related behaviour (Mansur *et al.*, 2011). •Locomotor hyperactivity (Adams, Kusljic and van den Buuse, 2008).

1.5.3 Brain serotonergic system and circadian rhythms

Serotonin has its highest peak of release in periods of activity, thus correlating it to arousal and locomotor activity (Dudley, DiNardo and Glass, 1998). Furthermore, a major input to the SCN is given by serotonergic projections arising from the raphe complex. These serotonergic neurons connecting to the SCN are mainly from the MnR (Hay-Schmidt *et al.*, 2003) and secondly from the DR (Kawano, Decker and Reuss, 1996b); thus, a link between the circadian timing system and serotonin system has been established.

To my knowledge, only one other study has shown that *tph2* mRNA expression displays a circadian pattern (Malek *et al.*, 2005). However, this data was obtained under a different protocol which did not include anatomical detail (i.e. did not cover all rostro-caudal gradient and all the subdivisions of the DR and the MnR nucleus).

1.5.4 Brain serotonergic systems in health and disease

To this point, it is clear that the serotonin system is a very complicated area of study for; 1) its robust structure, 2) its circadian pattern, 3) its extensive afferents and efferents to many forebrain structures and 4) its association with many physiological and behavioural correlates. Moreover, this system has also been correlated with great significance to pathological conditions.

Psychiatric disorders such as depression and anxiety have been linked to abnormalities in serotonin neurotransmission (Domínguez-López, Howell and Gobbi, 2012). This relationship has been established at all levels of the system, from abnormalities in serotonin transporter (SERT) (Meyer, 2007), to abnormalities in 5-HT receptors (Savitz, Lucki and Drevets, 2009) and even in abnormal *tph2* mRNA expression (Jahanshahi *et al.*, 2011).

Many studies in this area have known connections between the serotonergic system and classical behavioural symptoms of the mentioned disorders. For example; lower levels of serotonin have been found in suicide victims (Mann *et al.*, 1989; Arango *et al.*, 2003), patients with anxiety and depression have been shown to have

an elevated serotonin turnover compared to healthy individuals (Esler *et al.*, 2007; Barton *et al.*, 2008), patients with panic disorders have also been shown to have reduce 5-HT_{1A} receptor binding (Neumeister, 2004), depressed suicide patients show elevated *tph2* mRNA (Helene Bach-Mizrachi et al., 2006) and tph2 knock out mice have shown an increased aggression and depression-like behaviour (Lesch *et al.*, 2012). Additionally, in recent years, several studies have establish that *tph2* variants may be genetic predictors of depression (P Zill *et al.*, 2004) as well as predictors for antidepressant treatment responsiveness (Peters *et al.*, 2004). Therefore, interventions in the 5-HT system play an important role in pharmacological therapies of mental disorders such as depression, anxiety, bipolar disorders and obsessive compulsive disorders (Andrade *et al.*, 2010).

Therefore, with all the aforementioned, a clear relationship between all levels of the serotonergic system and mental disorders is well recognised. Nevertheless, the mechanisms involved in connecting the serotonergic system to these disorders are not fully understood.

1.6 Relating systems in health and disease

When trying to uncover the underlying mechanisms of psychiatric disorders, an altered circadian rhythm of GCs and an abnormal functionality of the serotonergic system at all levels come to mind, but is there any relationship between them? Could this altered rhythm in GCs be caused by an abnormal serotonergic system, promoting psychiatric symptoms? Or is an abnormal serotonergic system caused by the altered circadian rhythms of GCs?

GCs have a circadian rhythm, which is known to be under control of the SCN (Buijs *et al.*, 1993a; Herman *et al.*, 2016). Moreover, GCs seem to influence the correct rhythmicity of the SCN and other brain functions. The serotonergic system has direct projections to the SCN; therefore, it could be mediating the daily GC rhythm in an indirect way.

Furthermore, it is known that GCs influences *tph2* mRNA accumulation in the raphe complex, contributing to its rhythmic release (Nexon *et al.*, 2009).

Additionally, GC seem to up-regulate tph2 gene expression in rats (Malek, 2007) and decrease raphe expression in mice (Clark *et al.*, 2008), suggesting a species-dependent effect of GC on tph2 gene expression.

Serotonin also plays a role in locomotor activity, arousal, sleep and feeding, all of which demonstrate a circadian activity which in turn is mediated by the SCN, which in turn is regulated also by GCs. Therefore, it is fair to say that interactions between GCs and serotonin are diverse; however, the mechanisms of these interactions are not understood.

Circadian rhythms are essential for life. These rhythms when altered can cause many pathological conditions. Psychiatric disorders have been described with important alterations in circadian rhythms of GCs and serotonin; hence, abnormal functionality of both systems appears to be related to these disorders. However, as the fundamental mechanisms are not well understood, the need to study this relationship is of great importance because a better described mechanism could elucidate potential therapeutic targets to then benefit patients with these specific disorders.

1.7 Hypothesis and Aims

Stress-related psychiatric disorders such as depression and anxiety, have a common trait, the dysregulated circadian rhythm of the HPA axis and the dysfunctional activity of the serotonergic system. The link between these two important neurobiological systems has long been suggested, but not fully understood. Hence, the main focus of my PhD was to investigate this relationship by characterizing how the HPA axis activity is related/connected to the serotonergic system's activity, to gain a better understanding of the underlying mechanisms of psychiatric disorders.

1.7.1 Hypothesis

Across the 24 hour period, there is a distinctive rhythmic variation in the expression levels of Tph2 mRNA, which encodes TPH2 the rate-limiting enzyme

in serotonin biosynthesis in the dorsal and median raphe nuclei. There is also a distinctive daily variation in circulating CORT levels, with a similar pattern to the Tph2 mRNA expression pattern. Therefore, I hypothesize the two phenomenon are related, and specifically that the changes in Tph2 mRNA expression over the 24 hour period is dependent upon the changes in circulating CORT levels. The daily variation in circulating CORT has been proposed to be important for maintaining a variety of physiological and homeostatic processes, including mood and behaviour, and is also known to become dysregulated during chronic stress, chronic illness, and during treatment with synthetic glucocorticoids, along with consequent effects on mood and affective behavioural state of the individual. I hypothesise that the documented impact on mood and behavioural is due to dysregulation of the 'normal' pattern of Tph2 mRNA expression. I therefore plan to test models that induce dysregulation of glucocorticoid secretory dynamics and assess whether the daily rhythm of Tph2 mRNA expression in the dorsal and median raphe nuclei is affected.

1.7.2 Aims

In my PhD studies, I aimed to assess the regulation of the neuroendocrine responses to altered GC rhythms and its relationship to the serotonergic system at the level of *tph2* mRNA. Therefore, the following aims were established;

Aim 1: To characterize the natural circadian rhythm of the HPA axis and the normal circadian rhythm of *tph2* mRNA expression.

a) To describe the natural circadian rhythm of CORT and the normal rhythm of *tph2* mRNA expression in all subregions of the DR (DRC, DRI, DRD, DRV, DRVL/VLPAG) and Median Raphe Nucleus (MnR) at 5 different time points across a 24-hour period.
b) To analyze the full level-by-level dataset using a Linear Mixed Model to determine where the changes occur within the rostro-caudal gradient of each DR subregion and the MnR.

Aim 2: To manipulate the HPA axis rhythm by sub-chronic administration of the long-acting sGC methylprednisolone (MPL), which is known to cause prolonged GR activation throughout the brain, characterize the resulting CORT rhythm, characterize the resulting *tph2* mRNA expression profile and compare it to its natural circadian rhythmicity.

a) To assess the effect of MPL on the rhythm of *tph2* mRNA expression profile in all the subregions of the dorsal raphe (DR; DRC, DRI, DRD, DRV, DRVL/VLPAG) and Median Raphe Nucleus (DR and MnR).
b) To analyze the full level-by-level dataset using a Linear Mixed Model to determine where the changes occur within the rostro-caudal gradient of each DR subregion and the MnR.

Aim 3: To disrupt the circadian rhythm of the HPA axis with five weeks constant light, characterize the resulting CORT rhythm, characterize the resulting *tph2* mRNA expression profile and compare it to its natural circadian rhythmicity.

a) To assess the effects of a disrupted HPA axis activity on the circadian rhythm of CORT and the rhythm of *tph2* mRNA expression profile in all the subregions of the dorsal raphe (DR; DRC, DRI, DRD, DRV, DRVL/VLPAG) and Median Raphe Nucleus (DR and MnR).
b) To analyze the full level-by-level dataset using a Linear Mixed Model to determine where the changes occur within the rostro-caudal gradient of each DR subregion and the MnR.

Chapter 2 General Methods and Materials

2.1 Animal experiments

2.2 Sample collection

2.2.1 Plasma sample collection

2.2.2 Brain and pituitary collection

2.3 Plasma sample analysis: Corticosterone radioimmunoassay (CORT RIA)

2.3.1 Diluting samples

2.3.2 Adding tracer and antibody

2.3.3 Adding charcoal solution for counting

2.4 Cryosectioning of the Dorsal and Median Raphe nuclei

2.4.1 Mounting the brain

2.4.2 Slicing of the brain and collection of brain sections

2.5 In situ hybridization histochemistry (ISHH)

2.5.1 Riboprobes

2.5.2 Transcription of sense and antisense DNA

2.5.3 Prehybridization

2.5.4 Hybridization

2.5.5 Riboprobe washing

2.5.6 ISHH solutions

2.5.7 Film exposure

2.6 Image quantification

2.6.1 Acquiring images

2.6.2 Cataloguing images by rostro-caudal level

2.6.3 Using image J

2.7 Statistical analysis

2.7.1 Statistical analyses of circulating CORT levels

2.7.2 Statistical analyses of the DR and MnR nuclei

2.1 Animal experiments

All experiments were performed using adult male Sprague-Dawley (SD) rats weighing 250-300g (Harlan Laboratories, Inc., Blackthorn, UK). All animal procedures were approved by the University of Bristol Ethical Group and were conducted in accordance with Home Office guidelines and the UK Animals (Scientific Procedures) Act, 1986.

Animals used to investigate the natural rhythm of *tph2* mRNA expression and the altered rhythm of expression after MPL treatment were given 7 days of habituation period before the start of the experiment and maintained under a 12/12 light-dark cycle (lights at 0700 h). Rats used for the third experiment arrived as p21 and were kept in specially designed chambers with 200 lux constant light (LL) over the 24-hour day for 6 weeks. All rats were housed four per cage (polycarbonate cages; 45 cm L x 25.2 cm W x 14.7 cm D) with bedding changed every two days. All animals had *ad libitum* access to food and water and were kept in an environmentally controlled, highly specialised animal facility at the University of Bristol.

All experiments were performed solely by the candidate, including animal experiments, sample collection, radio immunoassays for CORT, in situ hybridization for *tph2* mRNA and statistical analysis.

2.2 Sample collection

2.2.1 Plasma sample collection

Once rats were euthanized and decapitated, trunk bloods (approx. 10 ml) were collected and maintained in ice-cold tubes containing 75 µl of EDTA (0.5 M; pH 7.4) (the volume of EDTA was taken from other experiments from our group showing that 75 µl serves as anti-coagulant in large volumes of trunk blood, exact EDTA volume is not critical) until the experiment in the animal facility had ended. Plasma was separated by centrifugation at 4^{o}C (15 min 10000xg, Sigma 4-16KS centrifuge), and stored at -20^{o} C until radio immunoassay for CORT was performed.

2.2.2 Brain and pituitary collection

Rapidly after euthanizing and decapitation, brains and pituitaries were quickly collected. When extracting the brain, the entire brainstem and part of the spinal cord was also collected to ensure the DR and MnR would not be damaged. Brains and pituitaries were carefully frozen dorsal side down on a piece of aluminium foil that was cooled down on a flat piece of dry ice.

After the experiment in the animal facility had ended, samples were stored at -80^{o}C until cryosectioning of the DR and MnR nucleus for further in situ hybridization histochemistry (ISHH) experiments.

2.3 Plasma sample analysis: Corticosterone radioimmunoassay (CORT RIA)

Total circulating corticosterone was measured in the collected plasma samples by RIA as previously performed in our group (Walker *et al.*, 2012). All samples were diluted (1:50) in citrate buffer (pH 3.0) to denature the binding globulin. Antiserum was supplied by G Makara (Institute of Experimental Medicine, Budapest, Hungary), and ^{125}I corticosterone isotope was purchased from IZOTOP (Institute of Isotopes Co. Ltd., Budapest, Hungary) with a specific activity of ≥ 600 GBq/mg and a radioactive concentration of ≥ 3700 MBq/ml.

Each RIA included triplicates for each sample and all plasma samples were run three times in three different RIAs to prove consistency. Dilutions of 1:50 were kept exactly the same for experimental and control rats in the three assays.

2.3.1 Diluting samples

After defrosting samples, 10 µl of plasma sample in 490 µl of citrate buffer were mixed. From this diluted sample 300 µl were used to do the triplicates of each sample (100 µl for each). Samples were kept in ice-cold tubes during this step.

2.3.2 Adding tracer and antibody

After the dilution of samples, 50 µl of radiolabelled antigen (hot tracer with around 3000-4000 counts) and 50µl of antibody were added to each triplicated sample. Then, all samples were gently shaken/vortex for 10 seconds and left at -4^{o} C overnight to incubate.

Furthermore, a binding curve (standard curve with antibody and tracer) was used. Total (only radiolabelled antigen) and blank samples (citrate buffer with tracer and without antibody) and specific antigen quantity samples (QCs) were also used to assess consistency within the assays.

2.3.3 Adding charcoal solution for counting

In day 2 of the RIA, 500 µl of activated charcoal solution was added. All samples were then gently shaken/vortexed and then placed in a centrifuge (Sigma 4-16KS centrifuge, Rotor 11150-13215) for 15 minutes at 4, 000 rpm (3256 xg) to separate the unbound antigens from the bound antigens.

Straightaway after this step, the supernatant was aspirated, and the remaining antigens were measured in the pellet by the Wizard gamma counter (Perkin Elmer 2470 Automatic Gamma) with an energy range up to 1,000 keV. Quantity of antigen in each sample was then derived from the standard curve and results obtained were saved to do statistical analysis.

2.4 Cryosectioning of the Dorsal and Median Raphe nuclei

All brains were sliced in a (Leica manual) microtome at -20^{o} C with sharpened Leica blades. Brains were taken out one by one from a -80^{o} C freezer and immediately put in the cryostat chamber to stand by for 15 minutes before slicing.

2.4.1 Mounting the brain.

Following the 15 min in the -20^{o} C cryostat chamber the brain was cut using a sharp, warm (room temperature) razor blade into two pieces (Figure 2-1); forebrain and

hindbrain piece in coronal planes (at -1.000 mm and at -6.500 mm bregma)(Paxinos and Watson, 2005). Then, the forebrain piece of the brain was put back into the -80º C and the hindbrain piece of the brain (after carefully trimming off the upper part of the cerebellum) was mounted onto a sample-chuck using Tissue-Tek embedding medium. The brain was positioned in order to section from caudal to rostral.

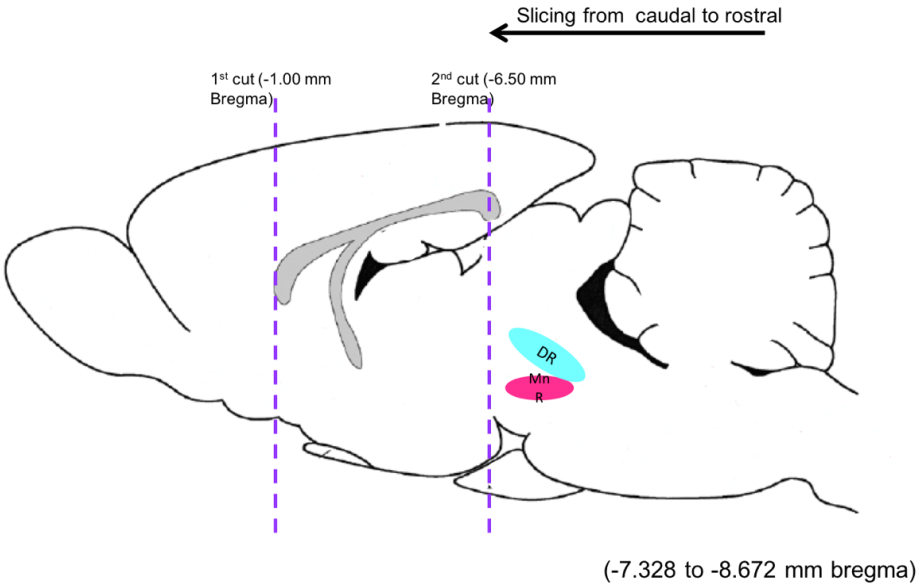

Figure 2-1: Schematic representation of the sectioning of the Dorsal and Median Raphe nuclei.

2.4.2 Slicing of the brain and collection of brain sections.

All brains were sectioned in a coronal plane at 12 µm in series of two sets (A and B) of seven slides (1-7) with nine brain sections per slide; meaning that neighbouring sections on the same slide were neuroanatomically 84 µm "apart" from each other (12 µm x 7 = 84 µm). Consequently, at the end of the collection of sections for each brain, seven different assemblages of sections would be obtained (which included the complete rostro-caudal levels of DR and MnR nuclei), this would allow us to do seven different ISHH experiments with each brain if needed.

All brain sections were collected from -7.328 to -8.672 mm bregma area which contains the DR and MnR nuclei (Paxinos and Watson, 2005). When anatomical

characteristics of level -8.756 mm bregma were reached, all consecutive sections were collected and mounted into double coated gelatine microscope slides made in our lab.

Brain section (from caudal to rostral), were collected in the following way;

1) Brain section number one (around -8.756 mm bregma) was placed onto slide one from set A (1A).
2) Brain section number two (around -8.744 mm bregma, 12 µm apart) was placed onto slide two from set A (2A).
3) Brain section number three (around -8.732 mm bregma, 12 µm apart) was placed onto slide three from set A (3A).
4) And so on, until section number 63 (around -8.000 mm bregma, 744 µm apart) was collected and placed in slide seven of set A (7A); meaning that by this point, each slide would be completed with 9 sections from different bregma levels of the DR and MnR nuclei.
5) Then, set B followed with the exact same procedure, going from brain section 64 (around -8.012 mm bregma) in slide one (1B), to section 126 (around -7.328 mm bregma) which was the 9^{th} brain section placed in slide seven from set B (7B).

Therefore, for each ISHH experiment run, two slides were used (one from each set) to have a suitable representation of the complete DR and MnR nuclei (all rostro-caudal levels) (Figure 2-2).

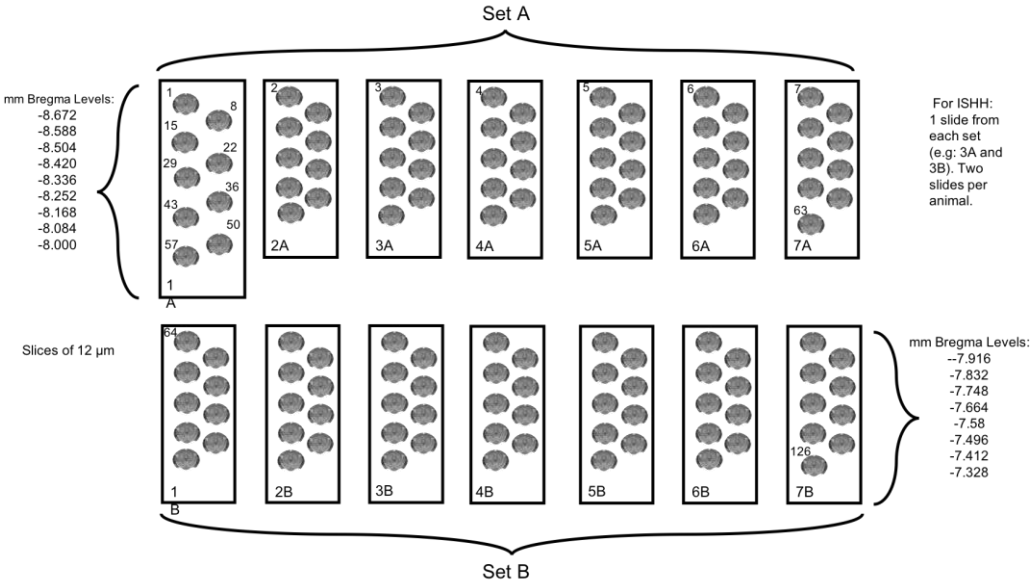

Figure 2-2: Collection of brain sections. Schematic of the seven different assemblages of the DR and MnR nuclei obtain from each animal. Each assemblage has a complete representation of the neuroanatomical extent (all rostro-caudal levels) of the DR and the MnR nuclei.

Finally, after sectioning, all slides were appropriately labelled and returned to a -80^{o} C freezer until ISHH experiments. All brains, regardless of the experiment they belonged to, were cryosectioned in the same way as explained.

2.5 In situ hybridization histochemistry (ISHH)

All ISHH were done as reported in previous studies from our collaborators and from our group (Gardner *et al.*, 2005; Donner, Johnson, *et al.*, 2012b; Waite *et al.*, 2012; Lukkes *et al.*, 2013; Donner *et al.*, 2018). This technique required a great number of optimizations to work for our specific interest. The following description includes all optimizations completed.

2.5.1 Riboprobes

As shown in Figure 2-3, ^{35}S-UTP-labelled riboprobe was directed against *tph2* mRNA and was detected using a 462 base (1552-2013) antisense riboprobe complementary to the rat cDNA encoding *tph2,* the probe contained 23 bp of encoding sequence plus 438 bp of 3' UTR (i.e. *tph2* , NCBI Reference Sequence: NC_005106.4) (K. L. Gardner *et al.*, 2009).

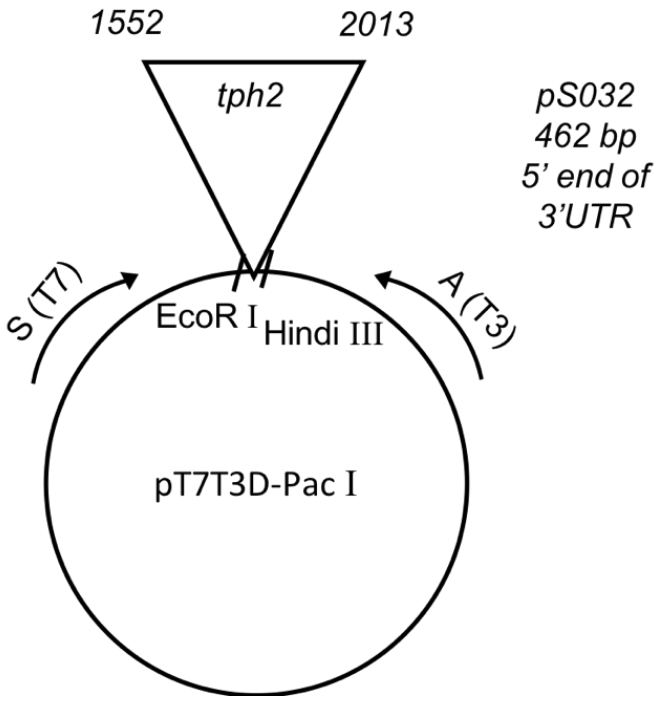

Figure 2-3: Plasmid map for tph2 riboprobe.

The riboprobe that used for the analysis picked up both variants of tph2 gene, as it was designed for a 461 pb fragment of rat tph2, containing 23 bp of coding sequence plus 438 bp of 3' UTR, which in turn is inside both variants of 3' UTR (Figure 2-4).

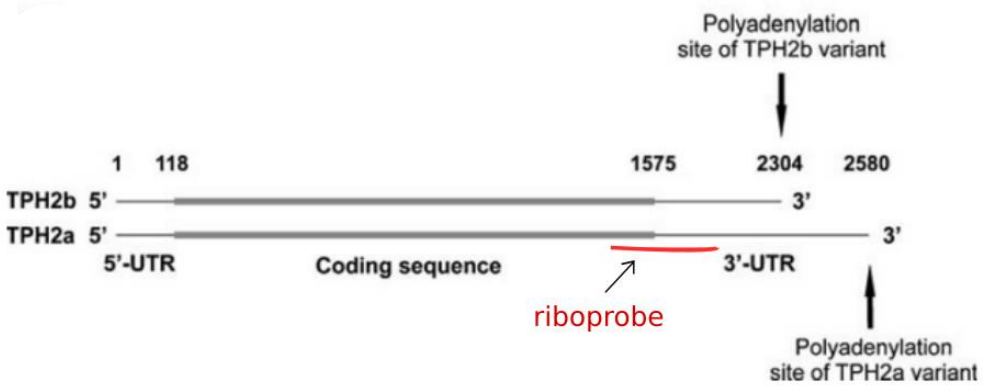

Figure 2-4: Schematic map of tph2a and tph2b splice variants, plus riboprobe construct representation. Modified from Alternative Splicing and Extensive RNA Editing of Human tph2 transcripts (Grohmann *et al.*, 2010).

Important to mention, radiolabelled oligo probes were used with no success as no specific signal was seen on films after different exposure times and high background was observed throughout the film.

2.5.1.1 Sense and antisense DNA

Two different Eppendorf tubes were used for the digestion of the sense (ISHH control) and antisense DNA. These reactions were done by adding 10 µl (approximately 4 µg) of plasmid DNA, 6 µl of sterile water, 2 µl of the appropriate reaction buffer R2 for sense (Invitrogen, Part no. Y90004, 2014) and R3 for antisense (Invitrogenm Part no. Y92500, 2014), and 2 µl of the appropriate restriction enzyme; HINDI III for sense (Invitrogen, Cat. no. 15207-012, 2014) and EcoR I for antisense (Invitrogen, Cat. no. 152020-013, 2014). The two reactions were placed in a water bath at 37^{o} C for 90 min for an optimal enzyme reaction.

2.5.1.2 Purification of the cut DNA

DNA clean-up was performed using a Min Elute Reaction Cleanup kit (Qiaqen cat no.28204) which involved 10 different steps of adding buffers, centrifuging, discarding supernatants, cleaning with ethanol and eluting the DNA to have a final volume of 10 µl of sense DNA and 10 µl of antisense DNA. These digested DNAs were stored at -20^{o}C if they were going to be used further or at 4^{o}C if the next stage of the ISHH was to follow.

2.5.1.3 Verification of well-cut DNA by gel electrophoresis

To verify if the digestion of our sense and antisense DNA was accurately done, a 1% agarose gel was done. Carefully, 0.4 g Bioline agarose in 40 ml of 1xTBE were placed in a sterile conical flask and microwaved on high power for 1 min. Once the agarose was melted and cooled down a bit 2 µl of ethidium bromide was added and well mixed. Next, the gel was poured into the gel tank (GibcoBRL 41060, Horizon 58), a comb of 8 channels was inserted and the gel was leaved to set for 20 min. The tank was flooded with 1xTBE, containing 5 µl of ethidium bromide per 100 ml.

The digested sense and antisense DNA were prepared by adding 6 µl of sterile water and 2 µl of loading buffer to 2 µl of the sense or antisense. After carefully mixing by pipetting, the 10 µl were loaded into the gel. Additionally, two samples (10 µl) of size markers were added to the gel to confirm that the DNA was the correct length. The gel tank was connected to the power supply (Hoefer PS 2A200 power pack) and left to run at 80V until the markers were about 1/3 of the way down of the gel (between 25 to 30 min).

Finally, after the gel was taken out of the tank it was placed onto clingfilm and into a GBox (Syngene). If DNA was well digested only one band would be visible in the lanes were the sense and antisense were placed, therefore the samples were then stored at -20^{o} C to continue with transcription. If other bands were found, the cutting process would be repeated.

2.5.2 Transcription of sense and antisense DNA.

To perform the synthesis of the radiolabelled probe a SP6/T7 transcription kit (version 18 Roche) was used. First, the ^{35}S- UTP (Perkin Elmer, 12.5 mCi/mL, i.e., 27750000 dpm/µg) was taken out of the freezer. UTP from the transcription kit was diluted (1:50) and MIX A (one for the sense and one for the antisense) was created with the following substances provided in the kit; 1.1 µl of ATP, 1.1 µl of CTP, 1.1 µl of GTP, 1.1 µl of the diluted UTP, 2.2 µl of 10x transcription buffer and 0.22 of 1M DTT.

In one new Eppendorf tube, 2 µl of digested DNA (sense), 6.2 µl of Mix A, .9 µl of RNase inhibitor (from kit with 40 units), 0.9 µl of sterile water, 8 µl of ^{35}S- UTP and 2 µl of T7 (RNA polymerase) were combined and carefully mixed together. Additionally, another tube was elaborated in the same way and with the same amount of substances, but antisense DNA was used instead of sense DNA and T3 (RNA polymerase instead of T7. Both reaction tubes were placed in a water bath at 37^{o} C for exactly 60 min.

While the last 10 min of the appointed hour went by, two Mix B (one for each tube) were developed with 1.5 µl of tRNA, 0.75 µl of RNase-free DNase 1 and 0.75 µl

of RNase inhibitor, to remove template DNA by reacting with the sense and antisense probes. After the 60 min were finished, 2.5 µl of Mix B were added to each tube, mixed and left to react again at 37º C for 15 min.

Afterwards, tubes were heated at 65ºC in a heating block for 5 min and quenched on ice for 2 min to denature the DNA template from the new synthesized radiolabelled RNA probe. Next, 77.5 µl of RNase free water were added to make a total of 100 µl and the clean-up of RNA followed.

2.5.2.1 Clean up of RNA

A MinElute Rneasy Cleanup kit (Qiaqen cat no. 74204) was used for this step. This procedure consisted in the adding of buffers, centrifugation and the use of ethanol to clean the radiolabelled RNA probe. At the end, 12 µl of radiolabelled probe were obtain (12 µl for each sense or anti sense probe) and the following step was to count how radioactive (cpm/µl) was the probe.

2.5.2.2 Probe counts

Counting how radioactive the probes were, allowed us to know if they were good enough to continue with further steps of the ISHH or if the transcription had to be done again. After several tests, 4,000 0000 cpm/µl were the minimum counts expected for a probe to work correctly, i.e. the signal of *tph2* mRNA was optimum and the noise (background) was minimum in all the exposure times tested.

To count, 0.5 µl of probe (sense or antisense) was diluted in 5 ml of liquid scintillation analyser (universal LSC-cocktail, Ultima gold High Flash-Point) in a polyethylene vial (Packard bioscience) tube. After well shaken tubes were counted in a beta counter (Perkin Elmer). If cpm/µl were less than expected, transcription was performed again. If it was hot enough, the probe was frozen at -80º C until hybridization step. All probes used in all the experiments of this study were used within 3 days of making.

2.5.3 Prehybridization

For this step, corresponding slides which included 32 slides per ISHH (ten for CTRL animals, ten for MPL treated animals, ten for LL treated animals and two slides for sense [control ISHH]) were taken from the -80º C freezer and placed on foil to warm up for 10 minutes before their fixation.

2.5.3.1 Fixation

Sections were fixed in 4% fresh-cold paraformaldehyde for 15 minutes. Then, they were rinsed 2 times in 1x PBS. They were acetylated in a triethanolamine (TEA)/acetic anhydride (AA) mix for 10 min. Afterwards, all slides were dehydrated through several graded alcohols; 70% ethanol for 1 minute, 80% ethanol for 1 minute, 95% ethanol for 1 minute, 100% ethanol for 1 minute, chloroform for 5 minutes, 100% ethanol for 1 minute and 95% ethanol for 1 minute. And finally, all slides were allowed to dry (around 20 minutes).

2.5.4 Hybridization

For the hybridization process each slide needed a minimum of 1,000 000 cpm/slide, therefore, depending on how hot the probe was, we used around 1.5 µl to 3.5 µl of antisense probe (35 slides) and 0.2 µl to 0.8 µl of the sense probe (3 slides) per performed ISHH. Probes were mixed separately with 2 µl of nucleic acid mix (per slide), heated to 65º C for 5 minutes and quenched on ice for 2 minutes.

Next, 1 µl of 5M DTT (per slide) and 0.5 µl of 10% SDS (per slide) were added to the probe and mixed with 120 µl of hybridization buffer (per slide). After the mix was done, 120 µl of the mix was taken to the betta counter to assure the counts (cpm/slide) were acceptable. If the counts were lower than expected the mix had to be repeated.

Once the mix had the correct amount of counts, 120 µl of mix was applied to each slide and covered with a cover slip (VWR international, Borosilicate glass; 22x60 mm). As each slide was covered, it was placed in a plastic container. After all slides

were placed correctly in the container and the container was humid enough, this was arranged in a water bath at 55° C and slides were incubated overnight.

2.5.5 Riboprobe washing

Three different water baths were used for washing (two at 50° C and one at 37° C). Five different sterilized glass containers with 1x SCC/ 50% formamide were distributed in the two 50° C water baths. Additionally, three glass containers were allocated in the 37° C water bath; one had a ribonuclease solution (250 µl RNaseA [40mg/ml] in 500 ml of RNase buffer) and the two others had only 1x SCC. Six more glass containers were set up with 1x SCC and one more with sterile water at room temperature.

The first step consisted in removing the cover slip of each slide through a wash in 1x SSC and placing it in a specialized slide holder positioned in a glass container with fresh 1x SCC at room temperature while the other slides had the cover slip removed. The sense slides were washed first to avoid contamination.

After all slides were free of their cover slip, all slides in two different holders were taken through 3 washes in fresh 1x SCC at room temperature. Then, two more washes in 1x SCC/ 50% formamide at 50° C were performed for 15 minutes each. Next, slides were only dip in 1x SCC at 37° C and taken to the next wash which consisted in 30 min under ribonuclease solution at 37° C. Afterwards, slides were again dipped in fresh 1x SSC at 37° C and immediately taken through three more washes in 1x SCC/ 50% formamide at 50° C (15 minutes each). Then, slides were given two more washes in fresh 1x SCC at room temperature and finally, slides were passed quickly through sterile water and allow to dry after this last dip. After drying, slides were ready to be exposed to an autoradiography film.

2.5.6 ISHH solutions

- **20 x SSC (saline sodium citrate):** Dissolve 175.3g of NaCL and 88.2g trisodium citrate in 800ml of distilled water. Adjust to pH 7 and make up to 1 litre. Autoclave.

- **10 x PBS (phosphate buffered saline):** Dissolve 90g NaCl, 1.65g potassium dihydrogen orthophosphate (KH2PO4) and 19.53g disodium hydrogen orthophosphate dodecahydrate (Na2HPO4:l2H2O) in 800ml distilled water. Adjust to pH 7.4. Autoclave.
- **4% formaldehyde in l x PBS:** Add 50ml 40% formaldehyde to 450ml l x PBS.
- **(TEA)/acetic anhydride (AA) mix:** Add 3.5 ml of TEA and 0.625 ml of AA in 250 ml of sterile saline.
- **Dithlothreitol (DTT):** For 1 M DTT dissolve 154.2mg/ml DTT in 0.01M sodium acetate (pH 5.2). Filter through a 0.2µm filter into a sterile container. Store as 20 µl aliquots at -20 °C.
- **10mM Tris-HCL-EDTA buffer (TE) pH 7.6:** Take 1ml of 1M Tris pH 8 and add 0.036g (1mM) EDTA. Add 80ml water, pH to 7.6, make up to 100ml and autoclave.
- **4M NaCl:** Dissolve 23.36g NaCl in 100ml water. Autoclave.
- **Hybridization Buffer (40 ml):** Store at -20°C. Use 950 µl M Tris, pH 7.4, 190 µl 0.25M EDTA, pH 8.0, 357 µl 4M NaCl, 23800 µl 50% Deionized formamide. Sigma F9037, 100ml, 9520 µl 50% Dextran Sulphate solution (50,000 MWt), 950 µl 50 X Denhardts and 1000 µl sterile water.
- **Nucleic acid Mix:** Use 250 µl single stranded salmon sperm DNA. Defrost 1ml, heat to 9^0C on heating block (to ensure single stranded). Quench on ice for 2 mins before adding, 250 µl tRNA, 500 µl sterile water. Freeze in small aliquots.
- **5 RNase buffer:** Use 25ml 1M tris pH 7.5, 25ml 0.5M EDTA pH 8.0, (ethylenediaminetetra-acetic acid, disodium salt, needs about 15g of NaOH pellets for pH 8.0) and 73.05g NaCl. Make up to 500ml and autoclave.

2.5.7 Film exposure

Different exposure times were tested in all the ISHH performed (e.g.;1 day, 2, days 3 days, 5 days, 7 days, 10 days), the *tph2* probe we used was confirmed to have an optimal exposure time in autoradiography films (Fujifilm super RX) of 3 days. A standard curve of C_{14} (carbon 14, ARC-146C, ARC Inc.) was included in each film.

Additionally, all films were developed in the automatic film processor (Kodak,) to avoid another variability source.

2.5.7.1 Set up of autoradiography films

Considering the need of consistency through this study and the high variability that can be found when assessing so many brain sections in so many slides, a scheme of exposure was developed, where in each film the three experiments (control, MPL and LL) and all the time points considered (3 am, 9 am, 3 pm, 6 pm and 9 pm) were included (Figure 2-4). This idea was to minimize variability and increase uniformity within comparisons that would be made in further analysis. Therefore, considering that for the three experiment of this study a total of 120 animals were needed (5 time points, with 8 animals/per time point), eight different ISHH to complete the n number for each time point/group from each experiment were performed.

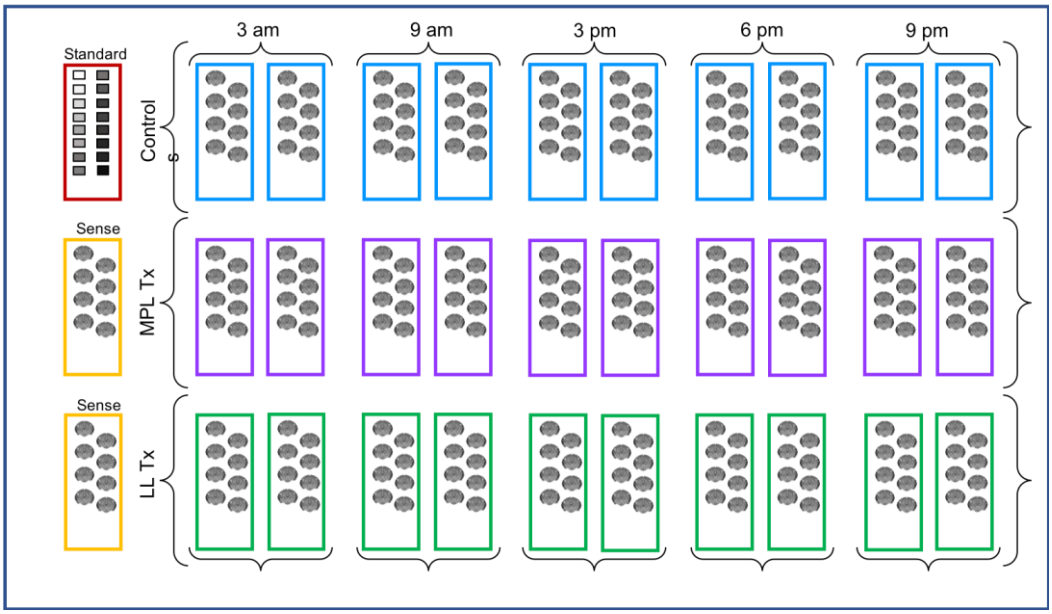

Figure 2-5: Schematic representation of autoradiography film set up for all the ISHH experiments done for this study.

2.6 Image quantification

All image analysis of ISHH were performed similarly to the method used by our collaborators (Katherine L. Gardner *et al.*, 2009a; Donner, Montoya, *et al.*, 2012; Lukkes *et al.*, 2013) and with the publicly available NIH-developed image analysis software ImageJ (https://imagej.nih.gov/ij/). However, some fluctuations were expected given the specifics of our study, .i.e, camera used to take the pictures, bregma levels considered, differences in produced atlas and calibration of each film corresponding to the C14 standard.

2.6.1 Acquiring images

All images were obtained using Scion Image version 1.63 in a power Mac 64 with a Leica MZ6 camera and the help of a light box (Wolverson) turned at all times. Additionally, a lens of 1.0 x was used with an adjusted magnification of 2.5 (Leica MOB-149). The grey scale option was chosen, and measurements of area and mean density were selected in Scion Image.

After the starting set up, to begin capturing images the "live" option was selected to visualize the correct positioning of the film. Next, the "stacks" + "capture frames" options were selected, and 16 to 18 different pictures of each brain were captured. Additionally, a montage was made out of those 16-18 pictures to produce a picture atlas of each of the brain assessed (Figure 2-5).

Fifteen different brains were exposed in each film; hence, fifteen different montages were obtained from each film (this meant 270 pictures per film for further analysis). A montage of the sense and standard curve (C_{14}) were also taken for completeness. Once all pictures were acquired for the eight ISHH films, all images were saved for image quantification analysis.

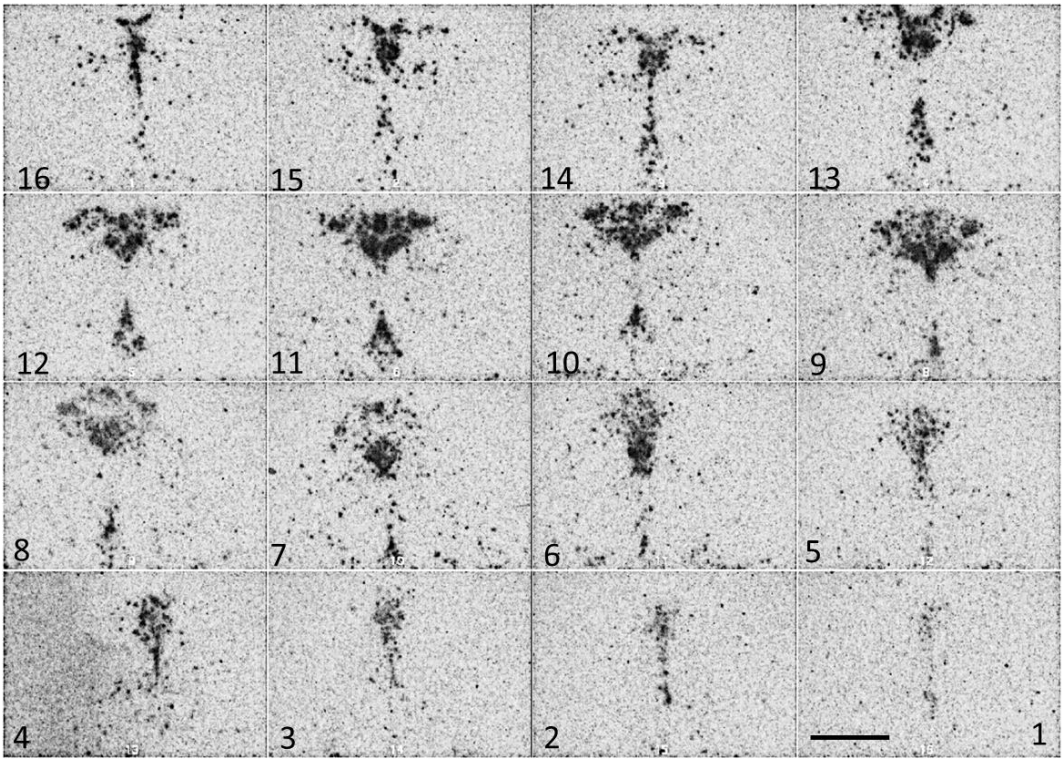

Figure 2-6: Montage of pictures taken of rat tph2 mRNA expression in the Raphe complex. Displayed (from top left to bottom right) are 17 coronal bregma levels used to measure tph2 mRNA expression in all the subregions of the DR and MnR nuclei from caudal to rostral. Scale bar 1 mm.

2.6.2 Cataloguing images by rostro-caudal level.

Before acquiring measurements of all DR and MnR nuclei images different arrangements were done for all images in the interest of uniformity for further assessment.

2.6.2.1 Analysis atlas of the DR and MnR nuclei

A rostro-caudal analysis atlas for *tph2* mRNA expression in the DR and MnR was generated by comparing the images obtained from the tissue sections with the brain atlas of Paxinos and Watson (Paxinos and Watson, 2005) and the landscape proposed by Gardner et al. (Gardner *et al.*, 2009b). Therefore, 17 different rostro-caudal levels were taken into consideration for this particular study.

Additionally, according to previous studies (Abrams *et al.*, 2004; Gardner *et al.*, 2009b) each rostro-caudal level was further divided into subregions of the DR; thus, 5 different subdivision in the DR plus the MnR nuclei where acknowledged for this study (Figure 2-6). These areas consisted of; the dorsal raphe nucleus, caudal part (DRC), –8.336 mm to –8.672 mm from bregma; dorsal raphe nucleus, interfascicular part (DRI), –8.420 mm to –8.672 mm from bregma dorsal raphe nucleus, dorsal part (DRD), –7.328 mm to –8.252 mm from bregma; dorsal raphe nucleus, ventral part (DRV), –7.328 mm to –8.204 mm from bregma; left and right dorsal raphe nucleus, ventrolateral part/ventrolateral periaqueductal grey region (left and right DRVL/VLPAG), –7.748 mm to –8.336 mm from bregma; and the median raphe nucleus (MnR), –7.496 mm to –8.672 mm from bregma.

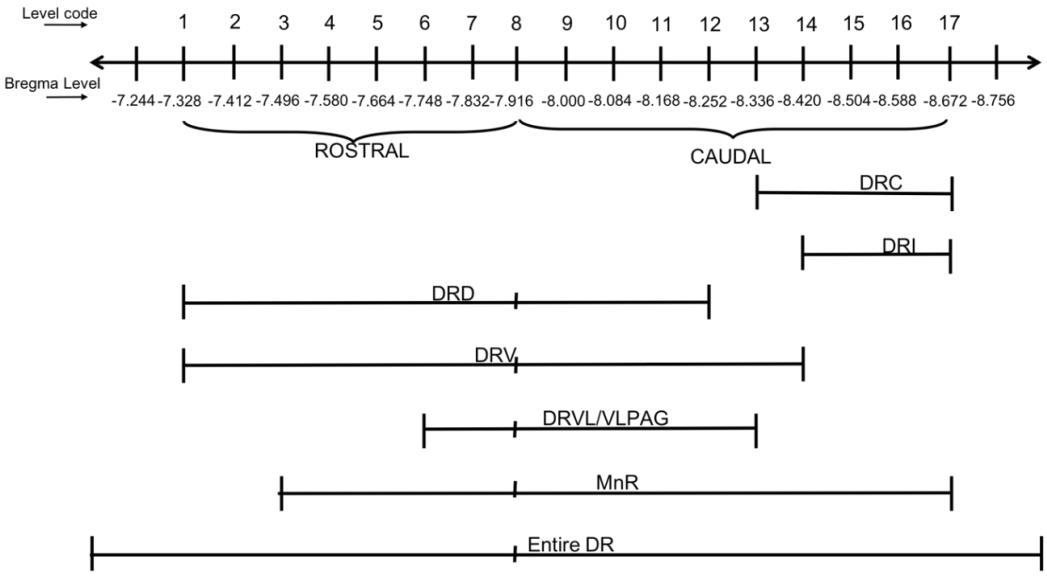

Figure 2-7: Schematic of rostro-caudal levels (including level code) DR subregions and MnR nucleus used in this study.

2.6.2.2 Rostro-Caudal level code for this study

To avoid confusion of all the possible rostro-caudal bregma levels, a level code for this study was implemented, where going from rostro level 7-328 to caudal level -8.672 mm from bregma, was coded as going from level 1 to level 17 (Table 2-1).

Table 2-1: Level code of the rostro-caudal level used in this study in comparison with mm bregma levels given by Paxinos and Watson (Paxinos and Watson, 2005).

DR and MnR Levels	
Level Code	*mm Bregma Levels*
1	-7.328
2	-7.412
3	-7.496
4	-7.580
5	-7.664
6	-7.748
7	-7.832
8	-7.916
9	-8.000
10	-8.084
11	-8.168
12	-8.252
13	-8.336
14	-8.420
15	-8.504
16	-8.588
17	-8.672

2.6.2.3 Reorganization of images

To finish cataloguing the images, after the development of the rostro-caudal analysis atlas used for this study, all images from each animal were reorganized by rostro-caudal level, i.e., all images from one animal (15-18 pictures) were studied, separated and placed in a rostro-caudal level folder independently of to which animal it belonged to, hence, 17 different rostro-caudal level folders were created, in which every single one of them included ≤ 40 images (8 per time point) of the same rostro-caudal level. This categorization would make the analysis easier by taking all the measurements of a single level for the forty animals used in each experiment, thus, the assessment of each bregma level was blinded. This categorization was done for the three different experiment.

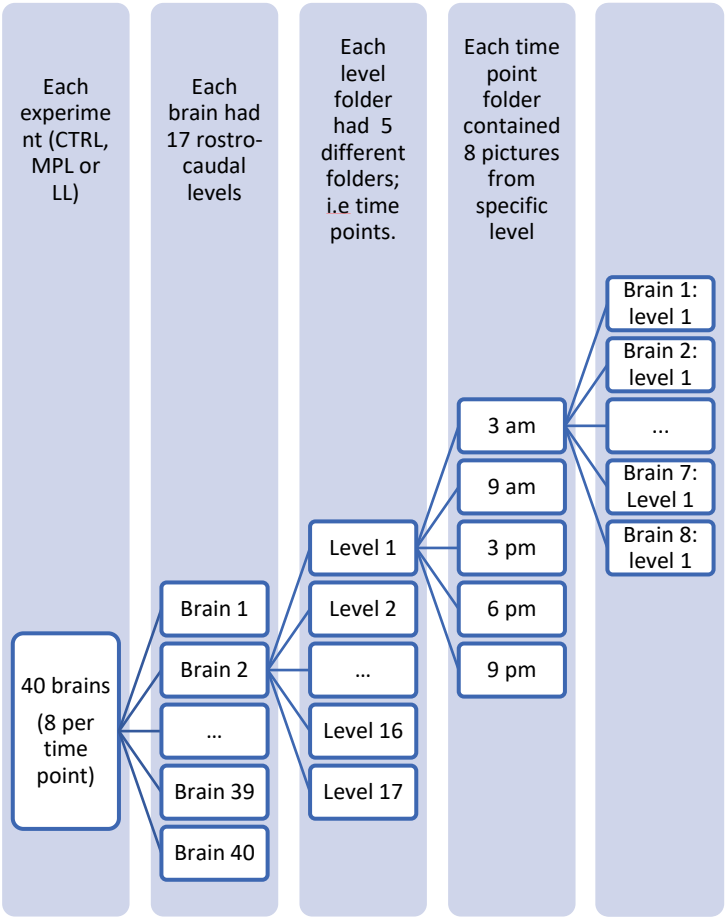

Figure 2-8: Diagram of reorganization of pictures. Level pictures of all brains went to the same 17 rostro-caudal level folders, therefore, each level folder contained 40 images.

2.6.3 Using image J

After having all the images organized by rostro-caudal level, measurements also needed to have a systematic method to keep reliability through all the 2160 images taken, therefore, different approaches were considered.

2.6.3.1 Setting the scale

When taking all the images, an extra image was taken from a ruler showing the length of one mm with the same lens and magnification used for all other images. Once Image J was open, this image of the ruler was set in the screen and with the straight-line tool, a line was drawn in that one mm shown. Then, the set scale window was opened, leaving the "distance in pixels" as it was, which showed the number of pixels in the scale bar, and in the "known distance" option, one 1 mm

was added as the “unit of length”. The “global” function was also selected, so this new scale setting would apply in every measurement taken. This setting was saved and used for all images across all experiments.

2.6.3.2 Matrix for the DR and MnR nuclei atlas

Again, to keep regularity through the different measurements of all images, matrices in the shape of the respective DR subregions and the MnR nucleus were created and overlaid with the real image. Therefore, for all images of the same rostro-caudal level, measurements were taken by the same matrix with the same area size. This matrix was done taking in consideration the rostro-caudal level analysis atlas done for this study (Figure 2-8).

With image J we created the matrix by using the “macros” and the “record” options. Once the drawn matrices where finished for each DR subregion and MnR we would click the “create” and “save as” options. Afterwards, to pull up any macro, the “plugins” + “macros” + “run” command was clicked.

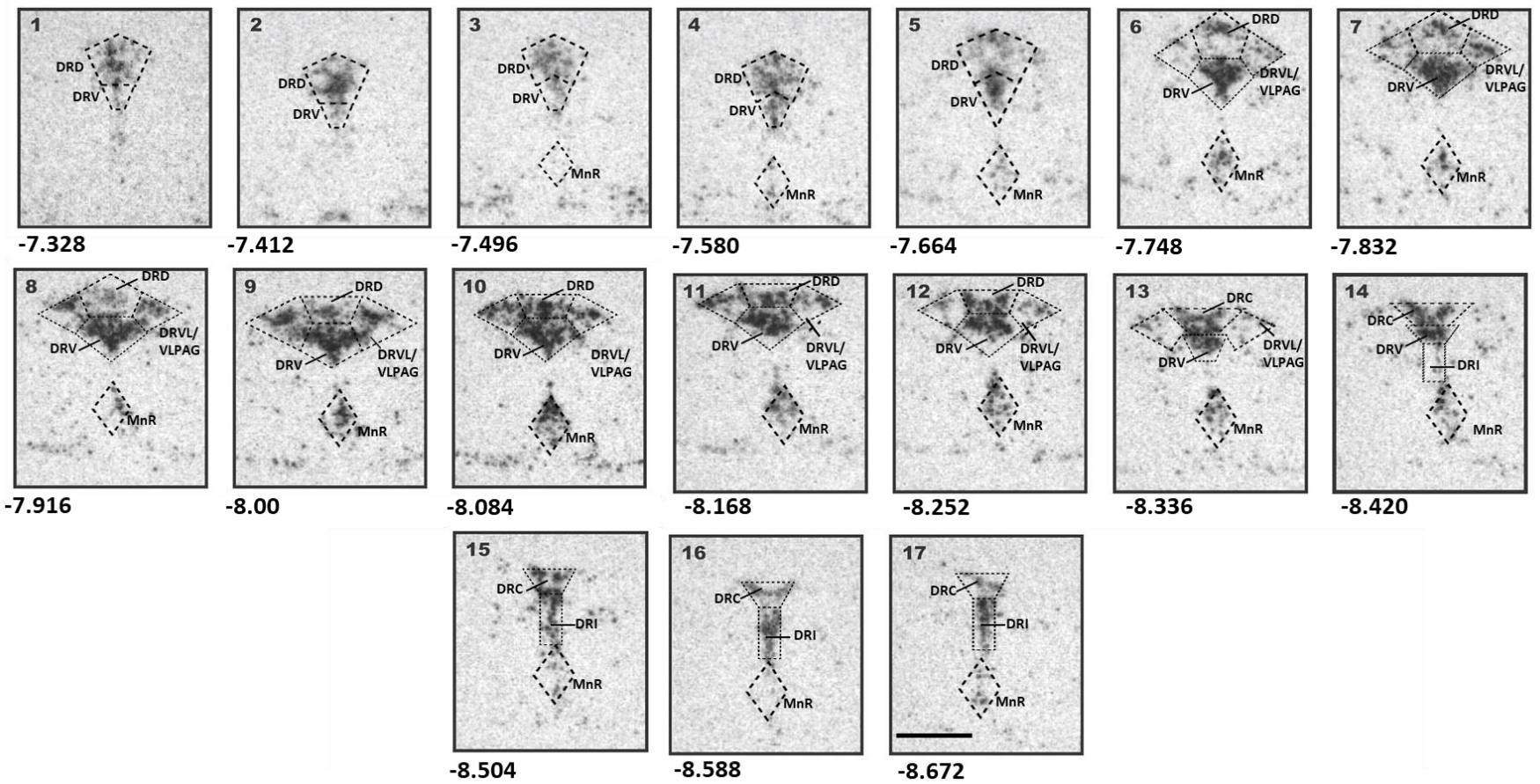

Figure 2-9: Matrix created and used for the expression of tph2 mRNA quantification at each rostro-caudal level. Displayed (from top left to bottom right) are 17 coronal bregma levels (from -7.328 to -8.672 bregma) used to measure tph2 mRNA expression in all the subregions of the Raphe complex. Scale bar 1 mm.

2.6.3.3 Units of measure and definitive measurements

For this study the unit *"grey value"* was used. Additionally, a constant threshold function was applied through the entire analysis and only the *area* (pixels) above the threshold signal would be considered. Therefore, when taking into consideration the threshold function were all pixels with a grey density below threshold were automatically excluded, and the measurements were only the area above-threshold signal given within each matrix, the ending measurement given by this specific method was *"mean grey value x mean area"*. However, because an individual background measurement was taken for each image to correct the real signal of *tph2* mRNA expression, the "mean grey value x mean area" was background-corrected, giving the ultimate unit as: *"Corrected mean grey value x mean area"* (CMGV x MA).

Additionally, as mentioned before, multiple film exposures were performed to ensure that the measurements taken were within the response range and not saturated only because of a long exposure time. All measurements were taken from films exposed for 3 days.

2.6.3.4 Acquiring measurements

After the images were organized and the matrix was finished, to begin measurements, all images from level 1 were opened in Image J. Then, the macros were pulled up to the screen and were placed over the brain region of interest by clicking "CTRL+m" a measurement would be added to a new window of Image J. Next all measurements were copied and saved in an excel file for further statistical analysis. This was done for all the rostro-caudal levels.

2.7 Statistical analysis

All statistical analyses for CORT RIAs and ISHHs were conducted using the software package IBM Statistical Package for the Social Sciences (version 24.0, SPSS Inc., Chicago, IL, USA). Additionally, Sigma Plot (Version 13.0) was used to create all graphs presented in this thesis. Statistical analyses were based on

analyses previously reported for our group and collaborators (Gardner *et al.*, 2009a; Spiga, Knight, *et al.*, 2011; Spiga, Waite, *et al.*, 2011; Donner, Johnson, *et al.*, 2012b).

2.7.1 Statistical analyses of circulating CORT levels

All data of circulating CORT was presented as MEAN ± SEM of CORT (ng/ml). Statistical analyses assessing the circadian rhythm of CORT in control, MPL treated animals or LL treated animals were done with a one-way ANOVA followed by various post hoc tests but because of the need to use a time point as control, we used the Dunnett's two-tailed test output, since all groups (time points) were compared to the 9 am time point. Statistical significance was set at $P < 0.05$.

Two-way ANOVA's were performed to compare between groups (control vs MPL treatment or control vs LL treatment). Statistical significance was set at $P < 0.05$.

Afterwards, if the two-way ANOVA's was significant, then multiple comparisons were done by a Tukey HSD test. Statistical significance was set at $P < 0.05$.

2.7.2 Statistical analyses of the DR and MnR nuclei

After obtaining all measurements of all images in Image J, values were saved and arranged in three different excel files (CTRL, MPL and LL files). All data was presented as MEAN ± SEM of *tph2* mRNA expression (CMGVxMA) for each rostro-caudal level of each DR subdivision and MnR for each rat. Statistical analysis of the DR and MnR nuclei were done in several stages.

2.7.2.1 Grubbs test

The first stage of the analysis was to identify extreme outliers in the each of the three excel files (CTRL, MPL or LL). Therefore, Grubbs' test for single outliers using two-sided $\alpha = 0.05$ (Grubbs, 1969). The percentage of outlier observations per treatment group were as follows: Control=1.3%, MPL=1.8%, LL=.89%.

2.7.2.2 Wide statistical analysis of the *tph2* mRNA expression in DR and MnR nuclei.

After removing outliers of each excel file, a wide statistical analysis was done for all data of each of the experiments (CTRL, MPL and LL) and also to compare between experiments (CTRL vs MPL and CTRL vs LL) at all time points assessed.

2.7.2.2.1 *Tph2* mRNA expression in the DR complex: overall effect of time and treatment

Thus, the second stage was collapsing all subregions and rostro-caudal level into a single Mean ± SEM value for each of the 5 different time points assessed for a given treatment (CTRL, MPL and LL, separately). Hence, the overall effect of time and treatment in *tph2* mRNA expression in the whole DR complex (DR and MnR nuclei) was assessed.

A one-way ANOVA followed by a Dunnett's two-tailed test output (all groups were compared to the 9 am group) was performed to compare the effect of time in each experiment separately (CTRL, MPL and LL). Statistical significance was set at $P < 0.05$.

Two-way ANOVA's were also performed to compare between groups (control vs MPL treatment or control vs LL treatment) and the overall effect of treatment in *tph2* mRNA expression in the whole DR complex. Statistical significance was set at $P < 0.05$.

Next, if the two-way ANOVA was significant, then multiple comparisons were done by a Tukey HSD test. Statistical significance was set at $P < 0.05$.

2.7.2.2.2 *Tph2* mRNA expression in each DR subregions and MnR nucleus; overall effect of time and treatment

Then, the third stage of the statistical analysis of *tph2* mRNA expression in the DR and MnR nuclei consisted in collapsing again all rostro-caudal levels into a single Mean ± SEM value for each of the 5 different time points assessed for a given

treatment (CTRL, MPL and LL, separately) but for these analyses we would assess the effect of time and treatment in each of the DR subregions and the MnR separately. This intended to assess the overall effect of time and treatment in *tph2* mRNA expression in each of the subregions of the DR (DRC, DRI, DRD, DRV, DRVL/VLPAG) and MnR nucleus. Moreover, because all of the subregions were divided into rostral-caudal sections, statistical analyses were performed for the whole, rostral and caudal area of each subregion separately.

One-way ANOVAs were performed to compare the effect of time in each of the subregions of the DR and MnR (whole, rostral, caudal) of all the experiments (CTRL, MPL and LL). These one-way ANOVA's were followed by a Fisher's Least Significant Difference test (LSD). Statistical significance was set at $P < 0.05$.

Two-way ANOVA's were also performed to compare between groups (control vs MPL treatment or control vs LL treatment) and the overall effect of treatment in *tph2* mRNA expression in each of the DR subregions and MnR. Statistical significance was set at $P < 0.05$.

Next, if the two-way ANOVA output was significant, then multiple comparisons were done by an LSD test. Statistical significance was set at $P < 0.05$.

2.7.2.3 Linear Mixed Models

Finally, the fourth stage of the *tph2* mRNA expression statistical analysis was performed. This analysis intended to evaluate the effects of time and treatment in all the subregions of the DR and MnR nuclei through their complete rostro-caudal extent. Therefore, because of the quantity and variability of the data (e.g. missing rostro-caudal levels, missing time points, technical outliers, statistical outliers, large amount of comparisons) these specific analyses were performed using Linear Mixed effects Models (LMM). These types of analyses are highly flexible and can accommodate a wide range of real-world data using more general covariance structures, i.e. these different covariance structures make different assumptions or no assumptions at all about the pattern of errors within subjects. Moreover, these analyses incorporate fixed and random effects and allow us to save degrees of

freedom compared to running standard linear models (for more information on LMM see appendix 1). These analyses were performed based on previous statistical methodological studies (Duricki, Soleman and Moon, 2016a, 2016b).

More specifically, these analyses modelled *tph2* mRNA expression (CMGVxMA) by experiment (CTRL, MPL or LL) or treatment (CTRL vs MPL or CTRL vs LL) in five different time point (3am, 9 am, 3 pm, 6 pm and 9 pm) within 5 different subregions of the DR (DRC, DRI, DRD, DRV, DRVL/VLPAG) plus the MnR nuclei at each rostro-caudal level (mm from bregma: −7.328, −7.412, −7.496, −7.580, −7.664, −7.748, −7.832, −7.916, −8.000, −8.084, −8.168, −8.252, −8.336, −8.420, −8.588, −8.672), hence, the need of LMMs. Additionally, some of the simple comparisons were taken back to simple ANOVAs to confirm that the LMMs were working correctly. All analyses were consistent.

2.7.2.3.1 Global methodology

Each of these analyses was run with 16 different covariate structures which included; ARMA (1,1), Compound Symmetry, Correlation Compound Symmetry, Diagonal, First-order Analytic, First-order Ante-dependence, First-order Autoregressive, First-order Factor Analytic, Heterogeneous Compound Symmetry, Heterogeneous First-order Autoregressive, Heterogeneous Toeplitz, Huynh-Feldt, Identity, Toeplitz, Unstructured, and Unstructured Correlations (for more information on covariance structures for LMM see appendix A) .

Moreover, all these models included a series of diagnostics to confirm that the assumptions made for each fitted model were not violated. These diagnostics included; descriptives, normality test, error variances and a file of analysis of predicted and residual values of the fitted model (for more information on diagnostics for LMM see appendix A).

These files were studied carefully to confirm if the assumptions of the model were not violated and the model was well fitted. If the assumptions were violated, then another covariate type was chosen. This situation never happened with any of the LMMs performed.

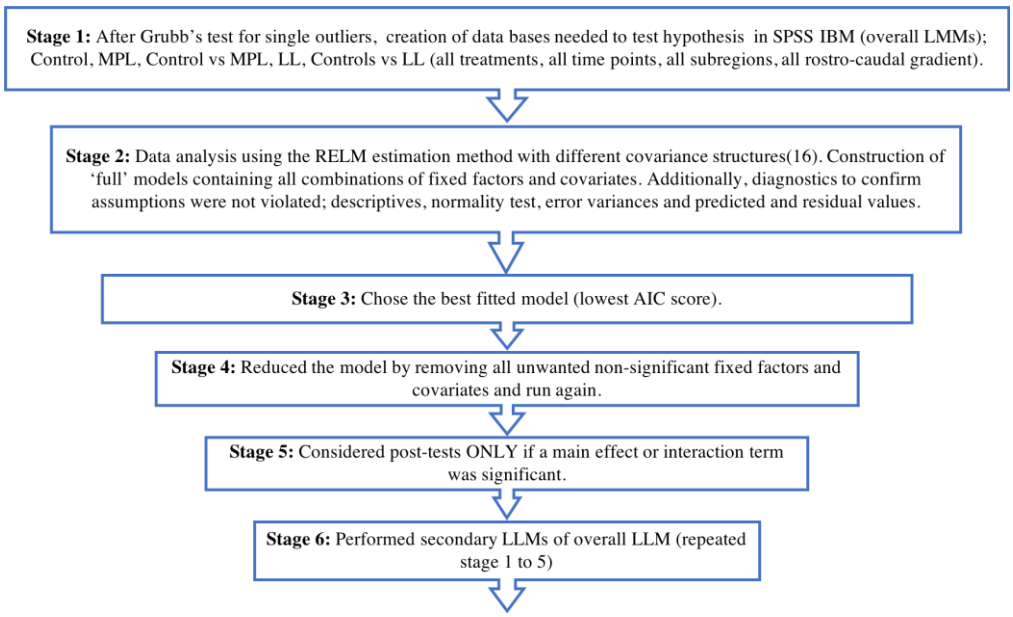

Figure 2-10: Flow chart of the LMM analysis procedure.

2.7.2.3.2 Overall Models

With these considerations, two overall models (higher level models) were run for two different conditions; 1) to assess the overall effect of time in *tph2* mRNA expression, for the CTRL, MPL and LL experiments, within each subregion of the DR and MnR nucleus throughout all their rostro-caudal extent across the 5 different time points measured and 2) to assess the effect of time and treatment, for CTRL vs MPL and CTRL vs LL comparisons, within each subregion of the DR and MnR nucleus throughout all their rostro-caudal extent across the 5 different time points measured.

As mentioned before these overall methods were run with 16 different covariates structures, therefore, to determine the best fitted model, the 16 different output models were compared with their Akaike information criterion (AIC) score and the one which had the lowest, was the best fitted model for the data. Following these overall analyses, if a main effect or interaction between a main effect and any other factor reached $p < 0.05$, secondary LMM were run for each individual subregion of the DR and the MnR nucleus (for more information on LMM see appendix A).

2.7.2.3.3 Secondary LMM models

Taken in consideration the overall models run in the previous stage, secondary models (lower level models) were run, all these models again were run with 16 different covariates structures and included all the diagnostic files.

These models intended to assess 2 different conditions; 1) the effect of time, for the CTRL, MPL and LL experiments, in each DR subregion and MnR nucleus separately, throughout all their rostro-caudal extent across the 5 different time points measured and 2) the effect of time and treatment, for CTRL vs MPL and CTRL vs LL comparisons in each DR subregion and MnR nucleus separately throughout all their rostro-caudal extent across the 5 different time points measured.

Additionally, the secondary lower level models for the second condition were done assessing each timepoint separately, thus, for example CTRL vs MPL in the DRC, at 3 am in one LMM analysis, CTRL vs MPL in the DRC at 9 am in another LMM CTRL vs MPL in the DRC at 3 pm in a third model, and so on for the 5 time points were assessed. However, these analyses only corresponded to the DRC, so the same number of LMM analysis for the DRI, DRD, DRV, DRVL/VLPAG and MnR were performed.

For the last stage of this analysis, to determine the best fitted model the covariance structures were compared to the AIC score. The model with the lowest score was the best fitted model. Following these secondary analyses, if a main effect or interaction between a main effect and any other factor reached $p < 0.05$, post hoc pairwise comparisons were made with Fisher's LSD test.

Finally, important to clarify three different conditions had to be accomplished in order to performed post hoc analyses; 1) if a main effect or interaction between a main effect and any other factor reached $p < 0.05$, 2) if both the overall and secondary LMM reach significance in interaction or a main effect and 3) if the sample sizes was not below 50% of the full sample size models (for more information on LMM see appendix A).

Chapter 3 Circadian rhythm of corticosterone and *tph2* mRNA expression in the Dorsal and Median Raphe nuclei

3.1 Introduction

3.2 Methods

3.2.1 Study design to assess the natural rhythm of CORT and *tph2* mRNA expression

3.2.2 Statistical analysis

3.3 Results

3.3.1 Circadian rhythm of circulating corticosterone

3.3.2 Circadian rhythmicity of *tph2* mRNA expression in the Raphe complex.

3.3.3 Circadian changes in *tph2* mRNA expression in subregions of the Dorsal Raphe and the MnR nucleus.

3.3.4 Circadian rhythmicity of *tph2* mRNA expression in the DR subregions and MnR nucleus; analysis across the full rostro-caudal gradient.

3.4 Discussion

3.1 Introduction

An important characteristic of GC secretion is that it has a pulsatile pattern of release from the adrenal glands, and that the pulse amplitude is modulated over a 24-hour period establishing the natural circadian rhythm of GCs (Windle *et al.*, 2001) According to previous studies, this rhythm follows a specific pattern which displays its highest peak at the onset of the active phase and its nadir at the onset of the inactive phase (Keller-Wood and Dallman, 1984).

Various studies have shown that serotonin also has a circadian rhythmic release (Barassin *et al.*, 2002). Moreover, rhythmic mRNA expression of *tph2* , the rate limiting enzyme in serotonin biosynthesis, appears to depend on the circadian pattern of circulating GC (Malek, Pévet and Raison, 2004; Donner, Montoya, *et al.*, 2012). However, the circadian pattern of *tph2* mRNA expression has not been well described in all of the subregions of the Dorsal Raphe (DR) and, even less so, in the Median Raphe (MnR) nucleus.

Therefore, and considering the above, my first results chapter is focused on confirming whether there is a circadian rhythm in the *tph2* mRNA expression profile in the DR. I also expand upon the current knowledge in the field, by performing a thorough characterization of *tph2* mRNA expression throughout the full rostro-caudal gradient of subregions of the DR and the MnR. Finally, I compare the circadian CORT profile to the pattern of *tph2* mRNA expression and discuss whether there is any type of relationship between the circadian rhythm of plasma CORT levels and the *tph2* mRNA expression profile.

3.2 Methods

3.2.1 Study design to assess the natural rhythm of CORT and *tph2* mRNA expression.

After arrival, 40 adult male SD rats (weighing between 250-300 g) were separated into five groups and housed four per cage in sound proof rooms for 7 days to habituate to the facility. All animals were maintained under a 12/12 light-dark cycle

(lights on at 0700 h) with food and water *ad libitum*. From day 3 to day 7, all animals were handled for 10 minutes at different times of day to avoid stress on the day of the experiment.

After the week of habituation, in order to collect samples, all animals were euthanized with an overdose of isoflurane (schedule 1 procedure) and decapitated with a guillotine at defined timepoints across the 24-hour cycle; 9 am, 3 pm, 6 pm, 9 pm and 3 am (n= 8 per time point). Animals were killed starting 25 minutes before the appointed hour and finishing 25 minutes past the hour. Trunk blood and whole brains were collected.

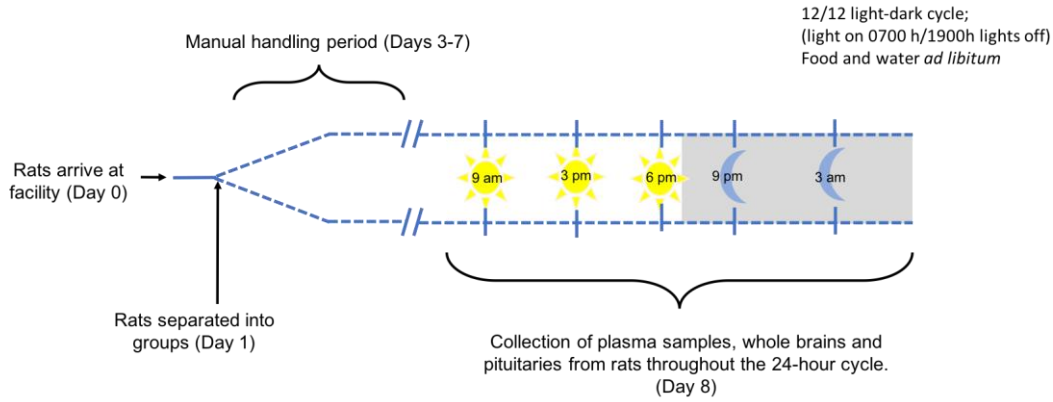

Figure 3-1: Experimental design for the assessment of the natural rhythm of CORT and tph2 mRNA expression.

3.2.2 Statistical analysis

1. One-way ANOVA was performed for the CORT data to assess the natural circadian rhythm. When an effect of time was found, Dunnet's post-test was used to compare each time point to the 9am nadir.

2. When analysing the whole Raphe complex, the same statistical tests used for the CORT analysis were used to enable a direct comparison between the rhythm of *tph2* mRNA expression and the rhythm of CORT. A one-way ANOVA with a Dunnett's (2-sided) post-test was also performed to compare each timepoint to the 9 am nadir.

3. Finally, in all the more detailed (subregional and rostro-caudal analysis) an overall and subregional LMMs were performed, followed by Fisher's Least Significant Difference (LSD) multiple comparison post-tests when a time effect was found.

3.3 Results

3.3.1 Circadian rhythm of circulating corticosterone

The levels of circulating CORT in all of our control animals resemble previous studies from our group (Atkinson *et al.*, 2008; Lightman and Conway-Campbell, 2010; Walker *et al.*, 2012). These results confirm that CORT plasma levels are following the natural circadian rhythm of adrenal CORT secretion in our control groups, with levels rising at 3pm and reaching a peak at 6pm, just prior to the onset of the dark phase (the active phase for rodents).

To analyse the data from CORT RIA in this control group (Figure 3-2), a one-way ANOVA was performed to determine if there were any differences between time points; 3 am, 9 am, 3 pm, 6 pm and 9 pm (n=8/timepoint). A significant effect of time was detected; $F_{(4, 35)} = 29.85$, $p < 0.001$, therefore further comparisons were made by a Dunnett's post hoc test which compared the mean of every group against the 9 am group. I considered the 9 am group be our control comparison group because, as seen in previous studies, it clearly has the lowest level of circulating CORT (Kitchener *et al.*, 2004; Atkinson *et al.*, 2008; Waite *et al.*, 2012). Statistically significant differences were found when comparing 9 am to 3 pm ($p<0.001$), 6 pm ($p<0.001$) and 9 pm ($p<0.05$).

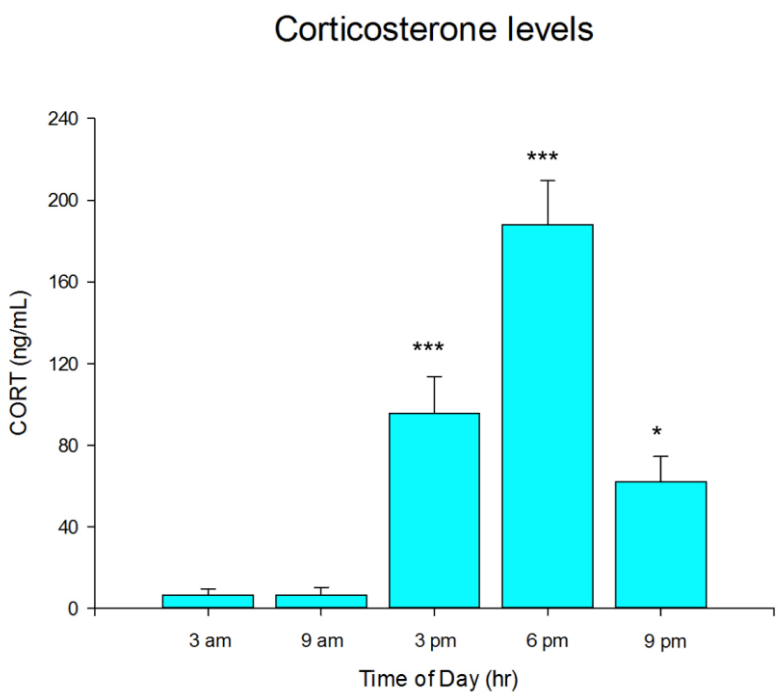

*Figure 3-2: Circadian changes in circulating CORT of control animals. CORT levels were measured in plasma obtained from trunk blood of control animals at 5 different timepoints; 3am, 9 am, 3 pm, 6 pm and 9 pm (n=8/group/timepoint). CORT levels are expressed as ng/ml. Data is presented as Mean ± SEM of CORT. One-way ANOVA was performed to assess effect of time; ($F_{(4, 35)}$ =29.85) p< 0.001. Additionally, Dunnett's (2-sided) post hoc test was performed; *** p< 0.001 at 3 pm and at 6 pm when compared to the 9 am group; *p< 0.05 at 9 pm when compared to the 9 am group.*

3.3.2 Circadian rhythmicity of *tph2* mRNA expression in the Raphe complex.

The Raphe complex contains the MnR nucleus (Brodal, Walberg and Taber, 1960) and 5 different nuclei (subregions) within the DR. These are the DRC, dorsal raphe nucleus, caudal part; DRI, dorsal raphe nucleus, interfascicular part; DRD, dorsal raphe nucleus, dorsal part; DRV, dorsal raphe nucleus, ventral part and DRVL/VLPAG, dorsal raphe nucleus, ventrolateral part/ventrolateral periaqueductal grey). These nuclei are a collection of neurons with weakly defined cytoarchitectonic limits, and the majority of these neurons are serotonergic (Dahlström and K. Fuxe, 1964).

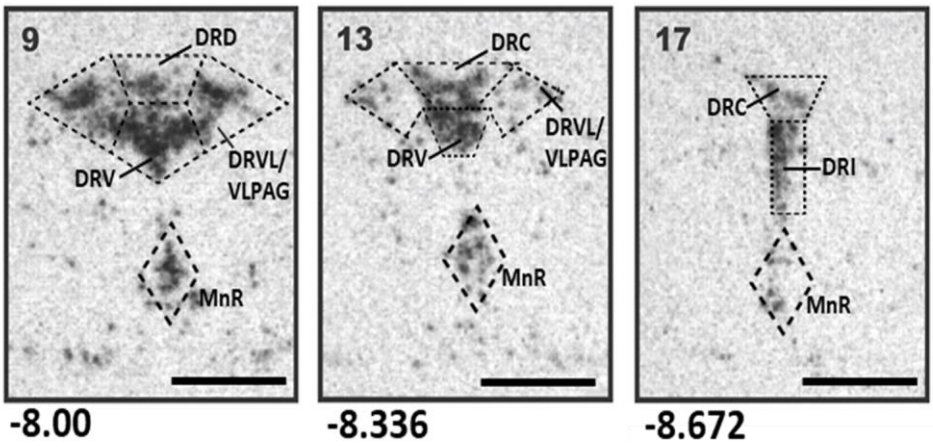

Figure 3-3: Raphe complex. Representative pictures of all DR subdivisions within three different bregma levels (-8.00, -8.336 and -8.672 bregma). Scale bar 1mm.

Although we understand and appreciate that the different nuclei within the Raphe complex are anatomically and functionally distinct (Lowry, 2002), we first wanted to very simply assess *tph2* mRNA expression in the whole Raphe complex. To do this, I averaged the *tph2* mRNA expression data of all the rostro-caudal levels of all the subregions. Interestingly, even in this 'global' analysis of the entire Raphe complex, I could detect time-dependent variation in *tph2* mRNA expression over the 24-hour period.

This analysis showed that *tph2* mRNA expression exhibited a pronounced circadian rhythm (Figure 3-3) which was confirmed as a significant effect of time by one-way ANOVA; $F_{(4, 2020)} = 29.85$, $p < 0.001$. I then performed a Dunnett's post hoc test to compare the mean of every group against the 9 am group, as it showed the lowest level of *tph2* mRNA expression. Statistically significant differences were found at 3 pm ($p<0.001$), 6 pm ($p<0.05$), 9 pm ($p<0.05$) and 3 am ($p<0.05$).

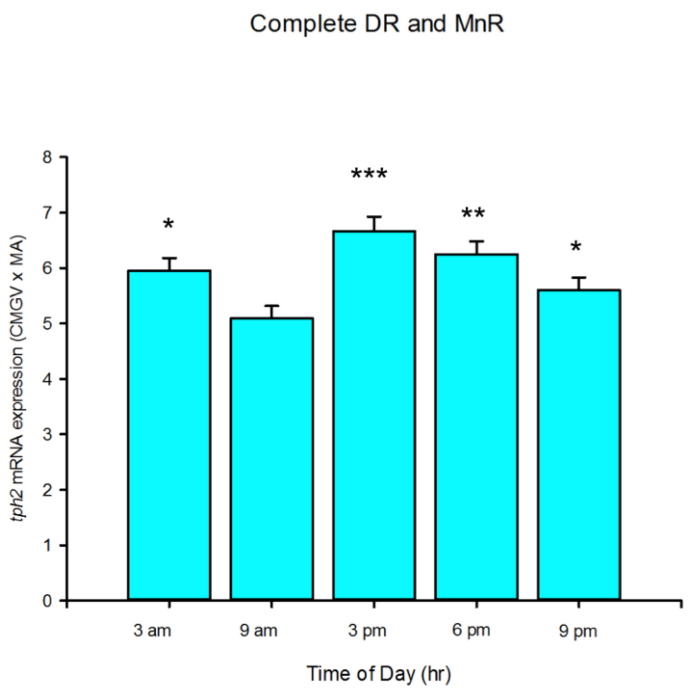

*Figure 3-4: Circadian variation in Tph2 mRNA expression in the DR and MnR complex of control animals. All measurements of tph2 mRNA expression of all levels of the DR and MnR complex were averaged for each timepoint; 3 am, 9 am, 3 pm, 6 pm and 9 pm (x axis). Tph2 mRNA quantification is expressed as Calibrated Mean Grey Value multiplied by its own Measured Area (y axis). Data points correspond to overall MEAN ± SEM of tph2 mRNA expression for each group/timepoint (n=8/group). One-way ANOVA was performed to assess effect of time; ($F_{(4, 2020)} = 5.814$) $p < 0.001$. Additionally, Dunnett's (2-sided) post hoc test was performed; *** $p < 0.001$ at 3 pm when compared to the 9 am group; ** $p < 0.01$ at 6 pm when compared to the 9 am group: *$p < 0.05$ at 3 am and 9 pm when compared to the 9 am group.*

3.3.3 Circadian changes in *tph2* mRNA expression in subregions of the Dorsal Raphe and the MnR nucleus.

As mentioned in the previous section, the Raphe complex has different anatomical and functional properties. In the last few years a large amount of research has been committed to describe and define the distinct properties of each subregion of the DR (DRC, DRI, DRD, DRV, DRVL/VLPAG) and the MnR nucleus. Following this line of research, in order to assess the overall effects of time (consistent with a circadian rhythm) on *tph2* mRNA expression in each of the subregions of the DR and the MnR nucleus, I have analysed the overall *tph2* mRNA expression across the whole rostro-caudal gradient for each subregion.

In the case of subregions that span across an extended rostro-caudal gradient, such as the DRD, DRV, DRVL/VLPAG and the MnR, further rostral and caudal analysis was performed. This was important to include in the analysis because most of the literature in this research area uses an allocation of antero-posterior division of the Raphe complex. Two different populations are recognized based on how the serotonergic clusters are distributed and also by their main projections. Two groups are well defined; the rostral group (projecting to the forebrain) and the caudal group (projecting to the brainstem) (Ding *et al.*, 2003). Furthermore, this rostral and caudal group have been shown to have different anatomical and functional properties (Jacobs and Fornal, 1991; Mitchell, Lowe and Fields, 1998; Mason, 1999; Horikawa *et al.*, 2000). Hence, we decided to use this antero-posterior division of the Raphe complex in order to assess whether there was an overall effect of time (consistent with a circadian rhythm) on *tph2* mRNA expression in the rostral group and the caudal parts of the three subregions of the DR which have this division (DRD, DRV, DRVL/VLPAG) and also in the MnR nucleus. Therefore, we analysed the overall MEAN ± SEM of *tph2* mRNA expression including either the rostral levels or the caudal levels for each subregion separately.

Interestingly, these analyses were able to detect circadian variation in *tph2* mRNA expression in some but not all of the DR subregions, as well as in the MnR nucleus, with further striking antero-posterior differences in some cases. The results for each subregion will now be described in detail in the following sections.

3.3.3.1 Dorsal Raphe nucleus, caudal part (DRC).

To assess the presence of a circadian variation in *tph2* mRNA expression throughout a 24-hour period in the DRC a one-way ANOVA was performed to determine if there was a significant effect of time.

The DRC showed a small trend for a 9 am nadir (Figure 3-5), however, no statistically significant effect of time was revealed by the one-way ANOVA; $F_{(4, 118)} = 0.948$, $p > 0.05$. Therefore, *tph2* mRNA expression within the DRC does not appear to exhibit any significant circadian variation.

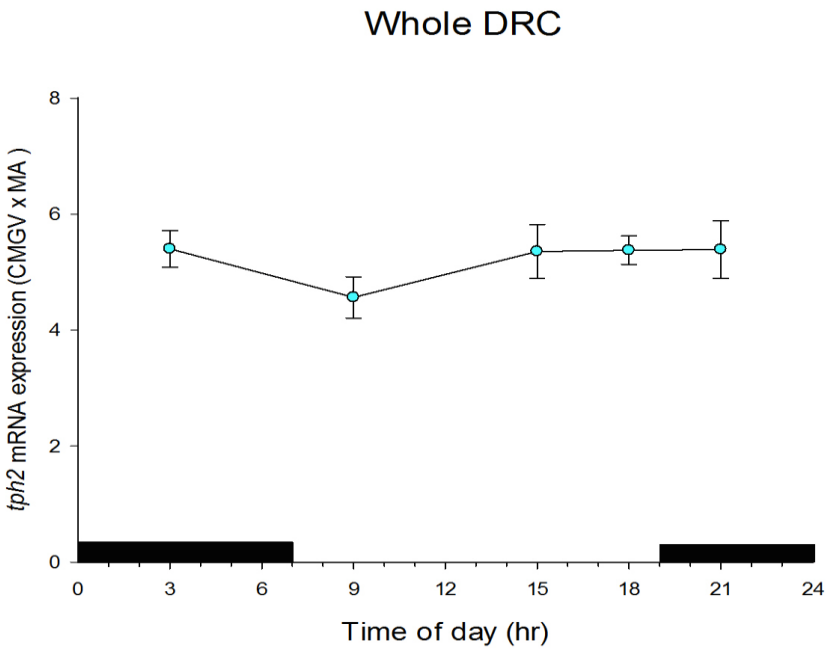

Figure 3-5: Circadian variation in tph2 mRNA expression in the DRC of control animals. Measurements of tph2 mRNA expression of the five levels of the DRC (-8.336 to -8.672 mm bregma) were averaged for each timepoint; 3 am, 9 am, 3 pm, 6 pm and 9 pm (x axis). Tph2 mRNA quantification is expressed as Calibrated Mean Grey Value multiplied by its own Measured Area (y axis). Data points correspond to overall MEAN ± SEM of tph2 mRNA expression in the DRC for each group/timepoint (n≤8/group [≤ 8 animals x 5 levels = ≤40 values]). One-way ANOVA was performed to assess effect of time; ($F_{(4, 118)}$ =0.948) p> 0.05.

3.3.3.2 Dorsal Raphe nucleus, interfascicular part (DRI).

Similar to the DRC, the one-way ANOVA was performed to assess the circadian variation of *tph2* mRNA expression over a 24-hour period in the DRI (Figure 3-5). Again, a small trend can be observed for a 9 am nadir and a peak in expression at 6 pm, however the one-way ANOVA did not detect a significant effect of time; $F_{(4,77)}$ =0.395, p> 0.05. Therefore, it appears that in the DRI there is a lack of circadian variation in *tph2* mRNA expression.

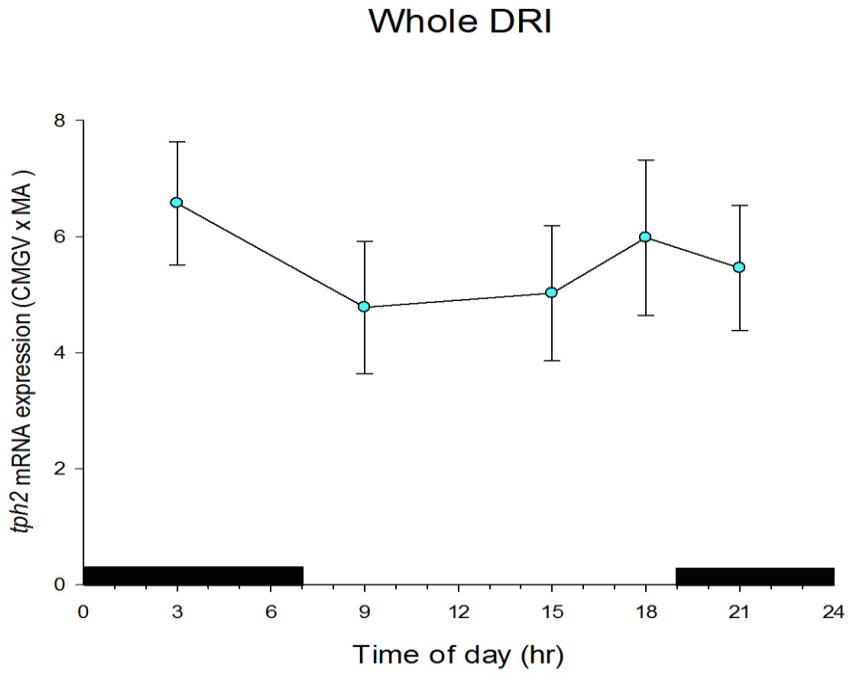

Figure 3-6: Circadian variation in tph2 mRNA expression in the DRI of control animals. Measurements of Tph2 mRNA expression of the four levels of the DRI (-8.420 to -8.672 mm bregma) were averaged for each timepoint; 3 am, 9 am, 3 pm, 6 pm and 9 pm (x axis). Tph2 mRNA quantification is expressed as Calibrated Mean Grey Value multiplied by its own Measured Area (y axis). Data points correspond to overall MEAN ± SEM of tph2 expression in the DRI for each group/timepoint (n≤ 8/group [≤ 8 animals x 4 levels = ≤32 values]). One-way ANOVA was performed to assess effect of time; ($F_{(4,77)}$ =0.395) p> 0.05.

3.3.3.3 Dorsal Raphe nucleus, dorsal part (DRD)

For the DRD, which spans rostro-caudally through levels -7.328 to -8.252 mm bregma, three separate one-way ANOVA's were performed assessing the whole, rostral and caudal DRD (Figure 3-6).

An interesting rhythm was detected in the DRD subregion. With respect to the whole DRD (Figure 3-6A), the circadian variation in *tph2* mRNA expression appeared with a well-defined nadir at 9 am and a peak in expression at 3 pm and 6 pm. A significant effect of time was detected by one-way ANOVA; ($F_{(4, 446)}$ =3.045, p< 0.01). Therefore, further multiple comparisons were made by a Fisher's LSD test and revealed that the 9 am nadir is significantly different when compared to the peak in expression at 6 pm (p<0.01) and 3 pm (p<0.01).

Moreover, the circadian pattern found in the whole DRV was also present in the rostral DRD (Figure 3-6B), however, within the rostral levels an even more profound nadir at 9 am was observed. This observation was supported by the one-way ANOVA, which revealed a significant effect of time; ($F_{(4, 299)} = 2.205$, $p < 0.05$). Additionally, Fisher's LSD post-tests detected a significant difference of the 9 am nadir when compared to *tph2* mRNA expression levels at 3 am ($p<0.05$), 3 pm ($p<0.05$) and the peak in expression at 6 pm ($p<0.01$).

Finally, when considering the caudal DRD (Figure 3-6C) no circadian variation was displayed, which was also supported by the one-way ANOVA, which revealed no significant effect of time; ($F_{(4, 180)} = 1.857$, $p > 0.05$). Therefore, it appeared that *tph2* mRNA expression within the DRD displays a circadian variation under natural conditions and that this variation is only seen in the rostral part of this area.

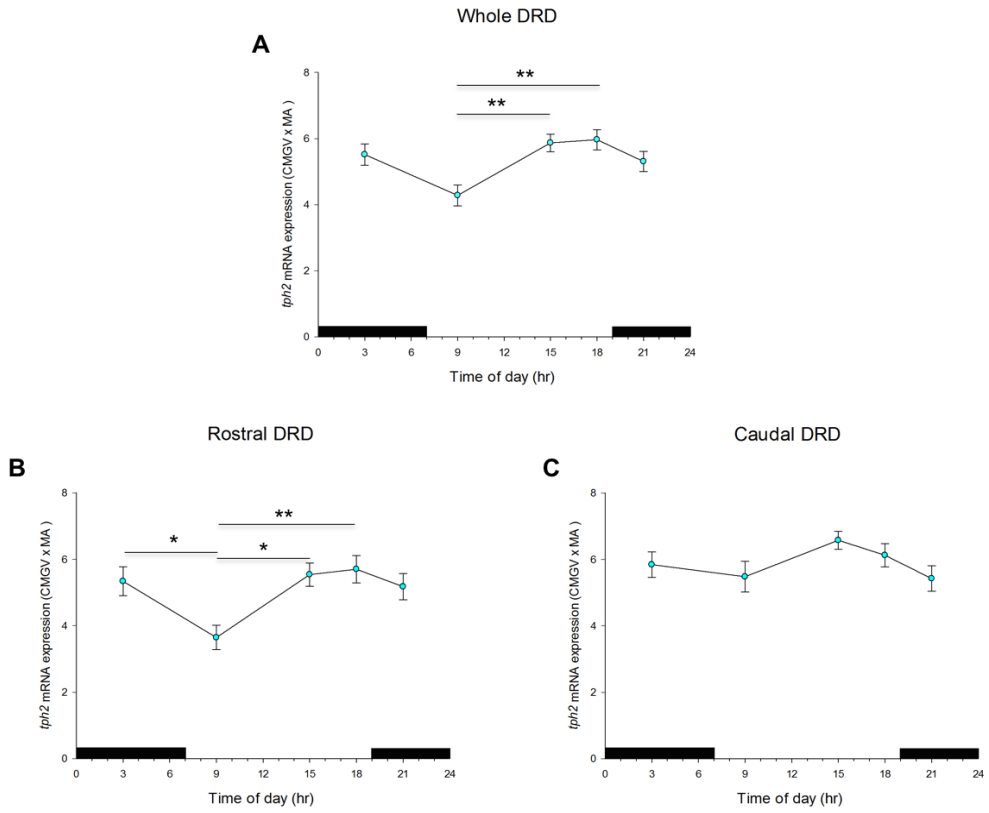

Figure 3-7: Circadian variation in tph2 mRNA expression in the DRD of control animals. For each timepoint; 3am, 9 am, 3 pm, 6 pm and 9 pm (x axis) measurements of tph2 mRNA expression (y axis) were averaged; (A) twelve levels (-7.328 to -8.252 mm bregma) for the whole DRD, (B) eight levels (-7.328 to -7.916 mm bregma) for the rostral DRD and (C) 5 levels (-7.916 to -8.252 mm bregma) for the caudal DRD. Tph2 mRNA quantification is expressed as

*Calibrated Mean Grey Value multiplied by its own Measured Area. Data points correspond to overall MEAN ± SEM of tph2 mRNA expression of the whole/rostral/caudal DRD for each group/timepoint (n≤ 8/group [≤ 8 animals x ≤12/8/5 levels = ≤96/64/40 values]). One-way ANOVAs were performed to assess effect of time : (A) ($F_{(4, 446)}$ =3.045) p< 0.01 ** p<0.01 for 9 am vs 3 pm and for 9 am vs 6 pm with Fisher's Least Significant Difference test; (B) ($F_{(4, 299)}$ =2.205) p< 0.05: **p< 0.05 for 9 am vs 6 pm, *p< 0.05 for 3am vs 9 am and for 9 am vs 3 pm with Fisher's Least Significant Difference test; (C) (F (4, 180) =1.857) p> 0.05.*

3.3.3.4 Dorsal Raphe nucleus, ventral part (DRV).

Similar to what I found in the DRD, a comparable circadian variation pattern was found within the DRV subregion. However, the circadian pattern in the DRV appears to be localised to the caudal bregma levels in the DRV, in contrast to the rostral-localised effects in the DRD (Figure 3-7).

Tph2 mRNA expression within the whole DRV (Figure 3-7A) also displayed a circadian pattern. However, in this area the peak in expression was reached at 3 pm and the nadir was maintained at 9 am. This circadian variation was detected by the one-way ANOVA, which revealed a significant effect of time; ($F_{(4, 524)}$ =2.113, p< 0.05). Furthermore, Fisher's LSD post-test showed that the peak in expression at 3 pm is statistically different from the nadir at 9 am (p<0.01) and the next low level of expression at 9 pm (p<0.05). Moreover, as mentioned before, the circadian variation in this area appears to depend primarily on the caudal levels of the area. Therefore, no circadian variation in the rostral DRV was found (Figure 3-7B) and the one-way ANOVA confirmed this observation; $F_{(4, 302)}$ =0.688, p> 0.05.

Finally, a more pronounced circadian variation pattern was observed in the caudal DRV (Figure 3-7C), which was supported by a significant effect of time in the One-way ANOVA; ($F_{(4, 256)}$ =3.700, p< 0.01). Significant differences were found when comparing the 3 pm peak to the 9 am nadir (p<0.001), and the low levels of 3 am (p<0.05) and 9 pm (p<0.05).

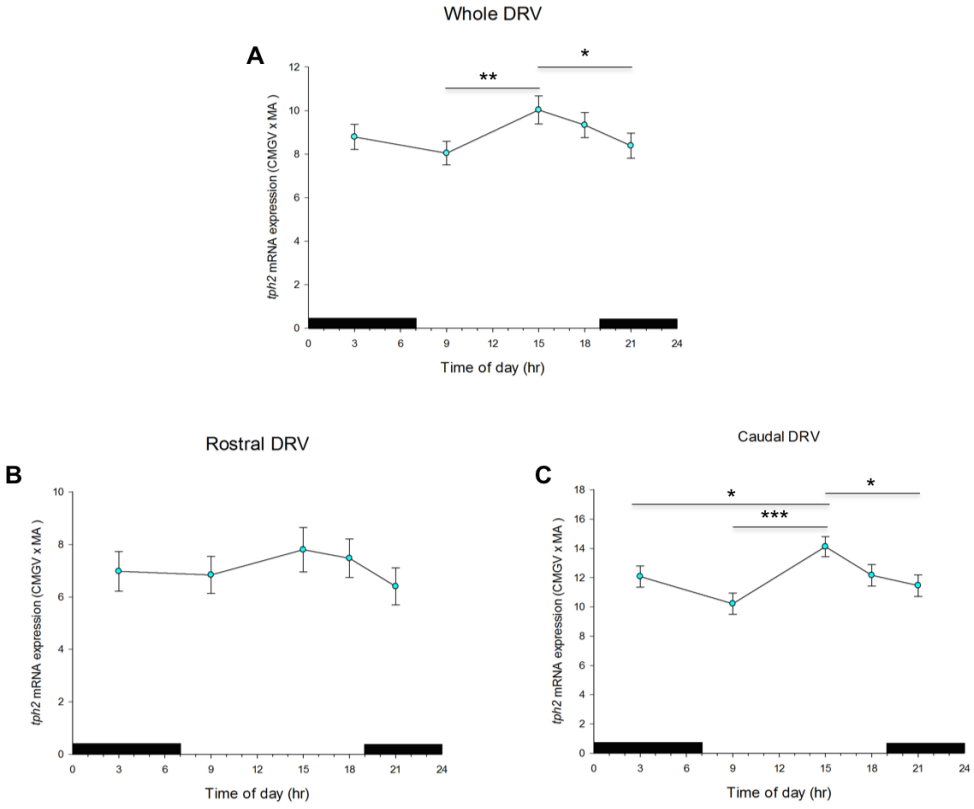

*Figure 3-8: Circadian variation in Tph2 mRNA expression profile of the DRV of control animals. For each timepoint; 3 am, 9 am, 3 pm, 6 pm and 9 pm (x axis) measurements of Tph2 mRNA expression (y axis) were averaged; (A) fourteen levels (-7.328 to -8.420 mm bregma) for the whole DRV, (B) eight levels (-7.328 to -7.916 mm bregma) and (C) seven levels (-7.916 to -8.420 mm bregma) for the caudal DRV. Tph2 mRNA quantification is expressed as Calibrated Mean Grey Value multiplied by its own Measured Area. Data points correspond to the overall MEAN ± SEM of th2 expression of the whole/rostral/caudal DRV for each group/timepoint (n≤ 8/group [≤ 8 animals x 14/8/7 levels = ≤ 112/64/56 values]). One-way ANOVAs were performed to assess effect of time ; (A) ($F_{(4, 524)}$ =2.113) p< 0.05: ** p< 0.01 for 9 am vs 3 pm and * p< 0.05 for 3pm vs 9 pm with Fisher's Least Significant Difference test; (B) ($F_{(4, 302)}$ =0.688) p> 0.05; (C) ($F_{(4, 256)}$ =3.700) p< 0.01: ***p< 0.001 for 9 am vs 3 pm, *p< 0.05 for 3am vs 3 pm and for 3 pm vs 9 pm with Fisher's Least Significant Difference test.*

3.3.3.5 Dorsal raphe nucleus, ventrolateral part/ventrolateral periaqueductal grey (DRVL/VLPAG)

The DRVL/VLPAG also displayed a strong circadian variation in *tph2* mRNA expression, which also seemed to be primarily dependent on the caudal bregma levels of the area (Figure 3-8). This circadian variation in expression was found to be very similar to the pattern found in the DRV, where the nadir is at 9 am and the peak in expression at 3 pm.

This circadian variation pattern in *tph2* mRNA expression appears to be maintained in the whole (Figure 3-8A) and caudal DRVL/VLPAG (Figure 3-8C) which were confirmed by the One-way ANOVAS; ($F_{(4, 297)}$ =2.26, $p< 0.050$) and ($F_{(4, 219)}$ =2.67, $p< 0.05$), respectively. However, no circadian variation was seen in the rostral DRVL/VLPAG (Figure 3-8B), with no effect of time detected by the one-way ANOVA; $F_{(4, 112)}$ =0.880), $p> 0.05$. Further post-tests for the whole and rostral DRVL/VLPAG revealed a significant difference ($p<0.01$) between the nadir at 9 am and the peak at 3 pm for both the whole and caudal DRVL/VLPAG. Additionally, another significant difference was found between the peak in expression at 3 pm and the low levels of *tph2* mRNA expression at 9 pm in the whole ($p<0.05$) and the caudal DRVL/VLPAG ($p<0.001$).

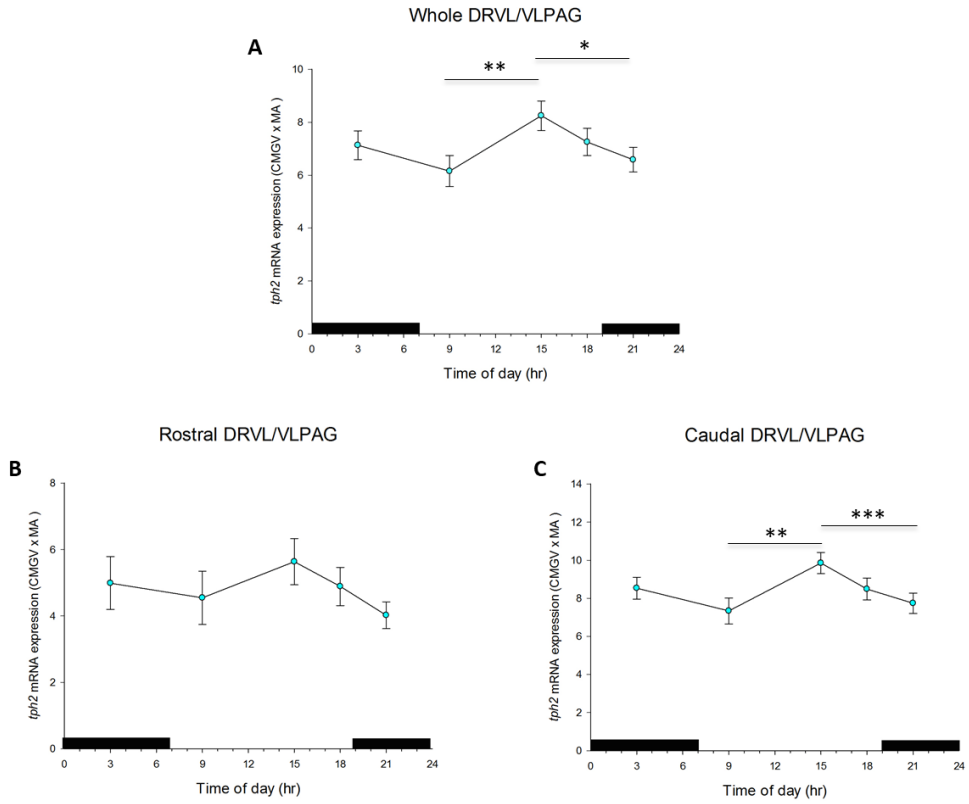

Figure 3-9: Circadian variation in Tph2 mRNA expression profile of the DRVL/VLPAG of control animals. For each timepoint; 3 am, 9 am, 3 pm, 6 pm and 9 pm (x axis) measurements of Tph2 mRNA expression (y axis) were averaged; (A) eight levels (-7.748 to -8.336 mm bregma) for the whole DRVL/VLPAG, (B) three levels (-7.748 to -7.916 mm bregma) for the rostral DRVL/VLPAG and (C) six levels (-7.916 to -8.336 mm bregma) for the caudal DRVL/VLPAG.Tph2 mRNA quantification is expressed as Calibrated Mean Grey Value multiplied by its own Measured Area. Data points correspond to the overall MEAN ± SEM of

*tph2 mRNA expression of the whole/rostral/caudal DRVL/VLPAG for each group/timepoint (n≤ 8/group [≤ 8 animals x 8/3/6 levels = ≤64/24/48 values]). One-way ANOVAs were performed to assess effect of time ; (A) ($F_{(4, 297)}$ =2.26) p< 0.050: ** p< 0.01 for 9 am vs 3 pm, *p< 0.05 for 3pm vs 9 pm with Fisher's Least Significant Difference test; (B) ($F_{(4, 112)}$ =0.880) p> 0.05; (C) ($F_{(4, 219)}$ =2.67) p< 0.05: ***p< 0.001 for 3 pm vs 9 pm, **p< 0.01 for 9 am vs 3 pm with Fisher's Least Significant Difference test.*

3.3.3.6 Median Raphe nucleus (MnR).

Comparable to the DRV and DRVL/VLPAG, the MnR shows a strong circadian variation pattern in *tph2* mRNA expression, which appears to be primarily dependent on the caudal levels of the subregion (Figure 3-9). Moreover, this pattern behaves in the same way as the other subregions mentioned before with a nadir at 9 am and a peak in expression at 3 pm.

Tph2 mRNA expression pattern in the whole (Figure 3-9A) and caudal MnR (Figure 3-9C) displayed a pronounced circadian pattern, confirmed by the significant effect of time found in the one-way ANOVAs; $F_{(4, 493)}$ =2.649, p < 0.05 and $F_{(4, 302)}$ =4.261, p< 0.01, respectively. No significant effect of time was found for the rostral MnR (Figure 3-9B); $F_{(4, 225)}$ =0.435, p> 0.05.

Further multiple comparisons in the whole MnR revealed that the peak in expression at 3 pm was statistically different from the 9 am nadir (p< 0.01) and the 9 pm (p< 0.05) low levels of expression. Additionally, because the 9am nadir shows very low levels of expression, a statistically significant difference is found when compared to 3 am (p< 0.05) and 6 pm (p< 0.05). Similar findings appeared in the caudal MnR where changes in expression levels between the peak and nadir were very robust, hence the 3 pm peak was statistically different from the 9 am nadir (p< 0.001), 6 pm (p< 0.05) and 9 pm (p< 0.01), plus an additional difference was found between the 9 am nadir and the 3 am (p< 0.05) *tph2* mRNA expression levels.

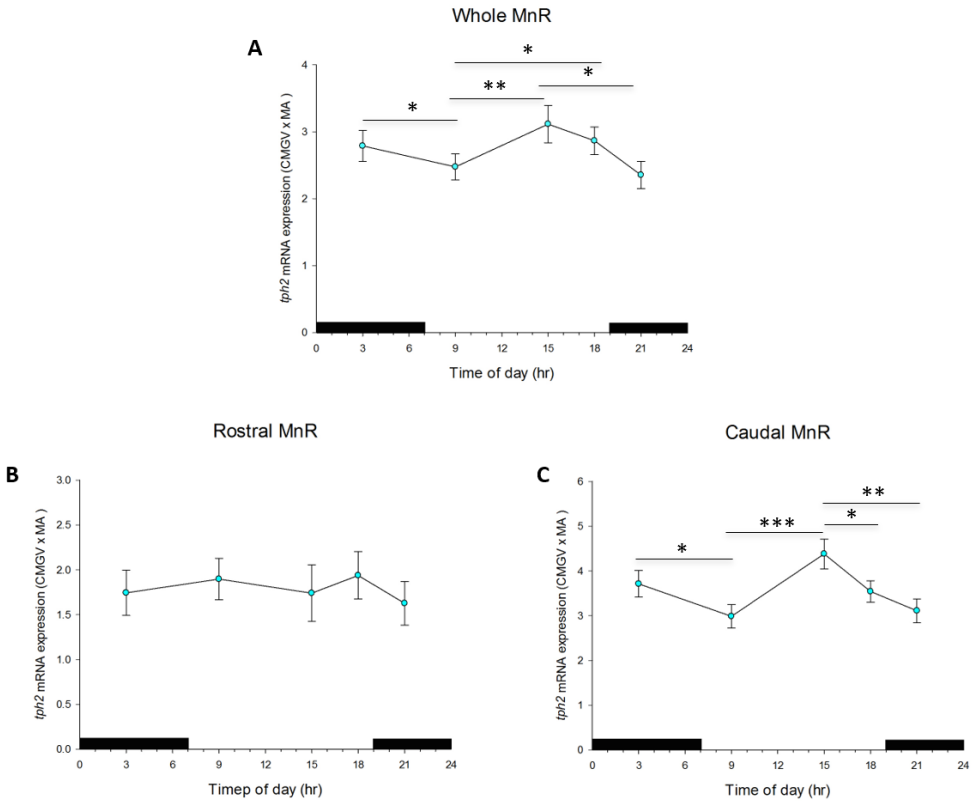

*Figure 3-10: Circadian variation in Tph2 mRNA expression profile of the whole MnR of control animals. For each timepoint; 3 am, 9 am, 3 pm, 6 pm and 9 pm (x axis) measurements of Tph2 mRNA expression (y axis) were averaged; (A) fifteen levels (-7.496 to -8.672 mm bregma) for the whole MnR, (B) six levels (-7.494 to -7.916 mm bregma) for the rostral MnR and (C) 10 levels (-7.916 to 8.672 mm bregma) for the caudal MnR. Tph2 mRNA quantification is expressed as Calibrated Mean Grey Value multiplied by its own Measured Area. Data points correspond to the overall MEAN ± SEM of tph2 mRNA expression of the whole/rostral/caudal MnR for each group/timepoint (n≤ 8/group [≤ 8 animals x 15/6/10 levels = ≤ 120/48/80 values]). One-way ANOVAs were performed to assess effect of time ; (A) ($F_{(4, 493)}$ =2.649) p < 0.05: ** p< 0.01 for 9 am vs 3 pm, *p< 0.05 for 3am vs 9 pm, for 9 am vs 6 pm and for 3 pm vs 9 pm with Fisher's Least Significant Difference test; (B) ($F_{(4, 225)}$ =0.435) p> 0.05; (C) ($F_{(4, 302)}$ =4.261) p< 0.01; ***p< 0.001 for 9 am vs 3 pm, ** p< 0.01 for 3 pm vs 9 pm, *p< 0.05 for 3 am vs 9 am and for 3 pm vs 6 pm with Fisher's Least Significant Difference test.*

3.3.4 Circadian rhythmicity of *tph2* mRNA expression in the DR subregions and MnR nucleus; analysis across the full rostro-caudal gradient.

The DR subregions and the MnR nucleus are highly specialized areas that have been revealed to have specific anatomical and functional properties (Lowry, 2002; Hornung, 2003; J. Abrams *et al.*, 2004). Nevertheless, experts in the area have

hypothesized that even throughout the rostro-caudal gradient of these particular subregions there are variations which can also have a meaningful functional output (Kirby, Rice and Valentino, 2000; Lowry *et al.*, 2000; J. Abrams *et al.*, 2004; Ruddick *et al.*, 2006; Price and Drevets, 2012), for example; the majority of serotonergic neurons show decreased firing rates during inactivity, but a small population of these neurons located in the caudal pat of the DR and MnR do not show this decline in firing rate (Peyron *et al.*, 1997a). Following this idea, and in order to assess the effects of time throughout the rostro-caudal gradient of the DR subregions and the MnR nucleus, LMM analyses were completed as described in Chapter 2 General Methods. All LMM analyses were methodically finalized, and only when significant differences in any main factor or interaction were found, Fisher's LSD post-tests followed according to previously described analyses in the Raphe (Stamper *et al.*, 2015, 2017). Finally, as data was excluded during the Grubbs analysis, results of statistical tests were deemed valid only when the remaining sample size was greater than four (half the original sample size for each timepoint at each rostro-caudal level).

Analysis of *tph2* mRNA expression using LMM analysis (Table 3-1) revealed a rostro-caudal level x time point interaction ($F_{(4,\ 247.606)} = 10.793$, p<.0. 000), a rostro-caudal level (raphe subregion) interaction ($F_{(36,\ 134.754)} = 40.036$, $p < 0.000$), a main effect of rostro-caudal level ($F_{(16,\ 111.562)} = 205.278$, $p < 0.000$), a main effect of raphe subregion ($F_{(5,\ 127.176)} = 254.618$, $p < 0.000$) and a main effect of time point ($F_{(4,\ 247.606)} = 10.793$, $p < 0.000$).

Based on this overall LMM analysis, secondary LMMs were used to determine changes over time in *tph2* mRNA expression at each rostro-caudal level of all the subregions of the DR and in the MnR nucleus separately (Table 3-1). Additionally, changes across the rostro-caudal gradient at each time point were assessed, but for simplicity, these changes are not represented in the Figures.

Table 3-1: Linear mixed model analysis results for tph2 mRNA expression in Control SD male animals.

Model	Test statistic	*p*-value
Overall analysis for Controls		
First-Order Ante-Dependence covariance structure		
Akaike's information Criterion (AIC): 7944.574		
Rostrocaudal level[1] (1-17)	$F_{(16, 111.562)} = 205.278$	.000 ***
Raphe subregion[2] (DRC, DRI, DRD, DRV,		.000 ***
DRVL/VLPAG, MnR)	$F_{(5, 127.176)} = 254.618$	
Time point[3] (3 am, 9 am, 3 pm, 6 pm, 9 pm)	$F_{(4, 247.606)} = 10.793$	.000 ***
Rostrocaudal level * Time point	$F_{(63, 140.564)} = 1.577$	.014 *
Raphe subregion * Time point	$F_{(20, 139.185)} = 1.102$	.354
Rostrocaudal level (Raphe subregion)	$F_{(36, 134.754)} = 40.036$	.000 ***
Rostrocaudal level * Time point (Raphe subregion)	$F_{(142, 185.681)} = .736$	.972
Subregional analyses		
DRC		
Unstructured covariance structure		
Akaike's Information Criterion (AIC): 416.066		
Time point (3 am, 9 am, 3 pm, 6 pm, 9 pm)	$F_{(4, 399.263)} = 1.054$	.379
Rostrocaudal level (13-17)	$F_{(4, 79.290)} = 2.541$	.046 *
Time point * Rostrocaudal level	$F_{(15, 78.086)} = 1.825$	.046 *
DRI		
Unstructured Correlations covariance structure		
Akaike's Information Criterion (AIC): 261.911		
Time point (3 am, 9 am, 3 pm, 6 pm, 9 pm)	$F_{(4, 9.629)} = 1.725$	.223
Rostrocaudal level (14-17)	$F_{(3, 4.083)} = 205.708$	.000 ***
Time point * Rostrocaudal level	$F_{(11, 5.114)} = .552$	.809
DRD		
First-Order Autoregressive covariance structure		
Akaike's Information Criterion (AIC): 1818.946		
Time point (3 am, 9 am, 3 pm, 6 pm, 9 pm)	$F_{(4, 104.957)} = 2.754$	.032*
Rostrocaudal level (1-12)	$F_{(11, 252.511)} = 28.027$	.000 ***
Time point * Rostrocaudal level	$F_{(44, 253.888)} = 1.062$	.376
DRV		
Heterogeneous First-Order Autoregressive covariance structure		

Akaike's Information Criterion (AIC): 2274.114		
Time point (3 am, 9 am, 3 pm, 6 pm, 9 pm)	$F_{(4, 78.918)}$= 3.723	.008**
Rostrocaudal level (1-14)	$F_{(13, 78.612)}$= 113.743	.000 ***
Time point * Rostrocaudal level	$F_{(52, 81.330)}$= .751	.865
DRVL/VLPAG		
First-Order Ante-Dependence covariance structure		
Akaike's Information Criterion (AIC): 1280.871		
Time point (3 am, 9 am, 3 pm, 6 pm, 9 pm)	$F_{(4, 52.840)}$ = 3.859	.008 **
Rostrocaudal level (6-13)	$F_{(7, 45.730)}$= 73.566	.000 ***
Time point * Rostrocaudal level	$F_{(28, 45.723)}$= 1.250	.247
MnR		
Unstructured covariance structure		
Akaike's Information Criterion (AIC): 1427.028		
Time point (3 am, 9 am, 3 pm, 6 pm, 9 pm)	$F_{(4, 293.819)}$= 3.081	.015 *
Rostrocaudal level (3-17)	$F_{(14, 66.643)}$= 64.654	.000 ***
Time point * Rostrocaudal level	$F_{(55, 52.645)}$= 3.463	.000 ***

Rostrocaudal levels were well-defined from bregma levels given in the atlas; where most rostral level was -7.328 mm bregma (1 according to level code) progressing to the most caudal level at –8.672 mm bregma (17 according to level code). Within this brain section 17 different and representative coronal sections of 12 µm were used to measure *tph2* mRNA of the dorsal raphe nucleus and the median raphe nucleus. 2The Raphe subregions used in this research were the following: DRC, dorsal raphe nucleus, caudal part; DRI, dorsal raphe nucleus, interfascicular part; DRD, dorsal raphe nucleus, dorsal part; DRV, dorsal raphe nucleus, ventral part and DRVL/VLPAG, dorsal raphe nucleus, ventrolateral part/ventrolateral periaqueductal grey. MnR, median raphe nucleus was also included and considered as a subregion of the Raphe complex.3 The five different time points (3 am, 9 am, 3 pm, 6 pm, 9 pm) used in this study were considered as a suitable description of the circadian rhythm of *tph2* mRNA expression. They were chosen to fit in parallel with the measured circadian rhythm of plasma CORT. *p<0.05. **p<0.01. ***p<0.001.

3.3.4.1 Dorsal Raphe nucleus (DRC)

First, and consistent with my earlier findings that total *tph2* mRNA content in the DRC was not sensitive to time of day (Figure 3-4), there was no obvious time-dependent variation detected across any rostro-caudal levels of the DRC (Figure 3-10). However, the secondary LMM analysis of the DRC (Table 3-1) did reveal a timepoint * rostro-caudal level interaction ($F_{(15, 78.086)}$= 1.825, p<0.05) and a main effect of rostro-caudal level ($F_{(4, 79.290)}$= 2.541, p <0.05). Based on detecting a significant interaction, I further interrogated the dataset with Fisher's LSD post-tests, which detected some significant differences in *tph2* mRNA expression across

rostro-caudal levels. However, every significant difference found was excluded due to the aforementioned minimum sample size criteria. Therefore, no significant differences between any of the time points were detected at any rostro-caudal level of the DRC.

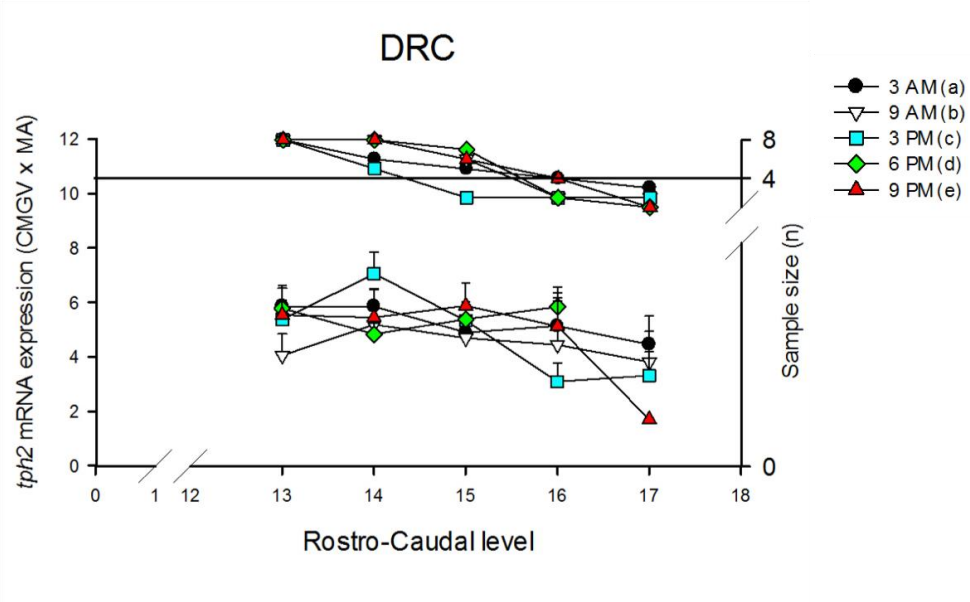

Figure 3-11: Rostro-caudal level variation of tph2 mRNA expression profile in the DRC of control animals. Tph2 mRNA expression in the DRC was measured in five different rostro-caudal levels presented in the x (-8.336 to -8.672 mm bregma). Five different timepoints; 3 am, 9 am, 3 pm, 6 pm and 9 pm are shown for each rostro-caudal level (time course). Tph2 mRNA quantification is expressed as Calibrated Mean Grey Value multiplied by its own Measured Area. Top data points are associated to the right y-axis which represent the post-Grubb's test sample size at each rostro-caudal level. Bottom data points are linked to the left y-axis which correspond to the MEAN ± SEM of tph2 mRNA expression of each group/timepoint (n≤ 8/group) at each rostro-caudal level. Fisher's Least Significant difference test showed no significant differences.

3.3.4.2 Dorsal Raphe nucleus, interfascicular part (DRI)

Again, consistent with my earlier findings that total *tph2* mRNA content in the DRI did not vary with time of day (Figure 3-5), there was no obvious time-dependent variation detected across any rostro-caudal level of the DRI (Figure 3-11). In support of this apparent lack of circadian variation within the DRI, the secondary LMM analysis revealed only a main effect of rostro-caudal level ($F_{(3,\ 4.083)}$= 205.708, p< 0.05), no main effect of time ($F_{(4,\ 9.629)}$= 1.725, p >0.05) and no interaction ($F_{(11,\ 5.114)}$= .552, p >0.05) (Table 3-1). Post-hoc tests to further

interrogate differences between time points at each rostro-caudal level of the DRI were therefore not performed.

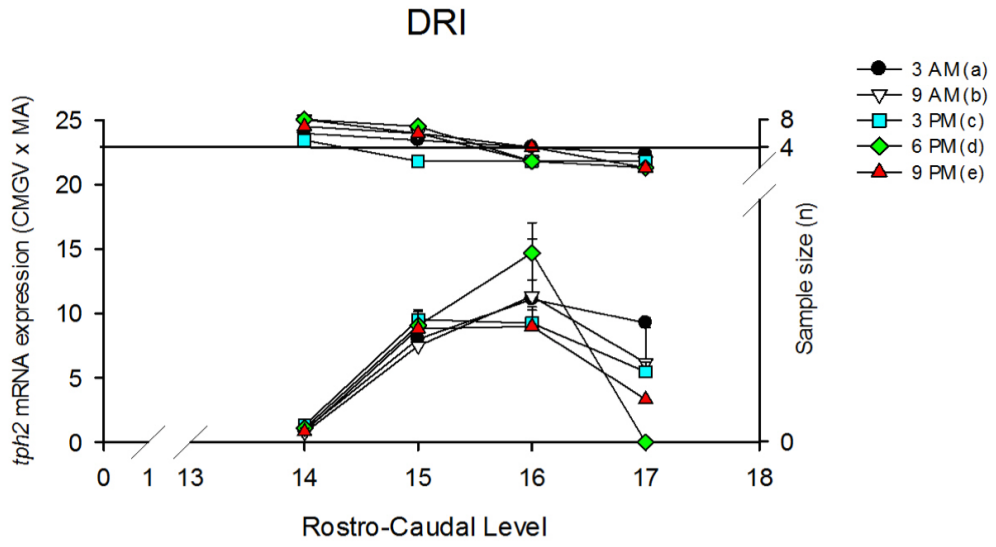

Figure 3-12: Rostro-caudal level variation of tph2 mRNA expression profile in the DRI of control animals. Tph2 mRNA expression in the DRI was measured in four different rostro-caudal levels presented in the x axis (-8.420 to -8.672 mm bregma). Five different timepoints; 3 am, 9 am, 3 pm, 6 pm and 9 pm are shown for each rostro-caudal level (time course). Tph2 mRNA quantification is expressed as Calibrated Mean Grey Value multiplied by its own Measured Area. Top data points are associated to the right y-axis which represent the post-Grubb's test sample size at each rostro-caudal level. Bottom data points are linked to the left y-axis which correspond to the MEAN ± SEM of tph2 mRNA expression for each group/timepoint (n≤8/group) at each rostro-caudal level. Fisher's Least Significant difference test showed no significant differences.

3.3.4.3 Dorsal Raphe nucleus, dorsal part (DRD).

Secondary LMM analysis within the DRD revealed a main effect of rostro-caudal level ($F_{(11, 252.511)}$= 28.027, p< 0.000) and a main effect of time ($F_{(4, 104.957)}$= 2.754, p< 0.05), however, no significant interaction was found ($F_{(44, 253.888)}$= 1.062, p> 0.05) (Table 3-1). Furthermore, post tests showed that *tph2* mRNA expression varied significantly over time at multiple rostro-caudal levels of the DRD (Figure 3-12); *tph2* mRNA expression at level 3 (-7.496 mm bregma) was increased at 9 am when compare to 6 pm; at level 4 (-7.580 mm bregma) 3 am *tph2* mRNA expression was higher when compared to 9 am, 3 pm or 9 pm; at level 6 (-7.748 mm bregma) *tph2* mRNA at 9 am was lower compared to its expression at 3 am

and; at level 8 (-7.916 mm bregma) *tph2* mRNA expression was also lower at 9 am compared to the 3 pm time point; and finally, at level 12 (-8.252 mm bregma) this low *tph2* mRNA expression at 9 am was maintained compared to 3 pm.

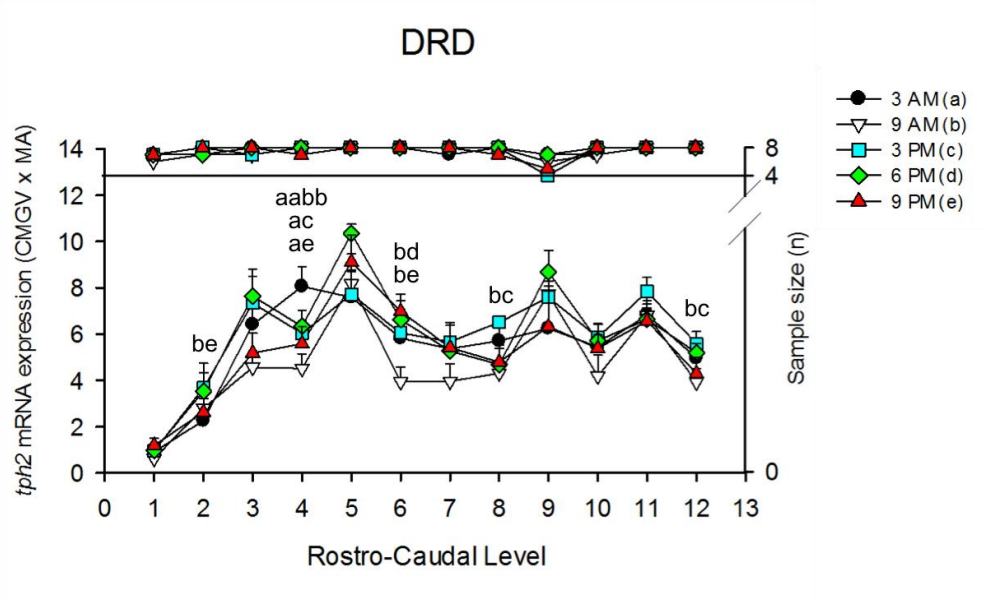

Figure 3-13: Rostro-caudal level variation of tph2 mRNA expression profile in the DRD of control animals. Tph2 mRNA expression in the DRD was measured in fourteen different rostro-caudal levels presented in the x axis (-7.328 to -8.252 mm bregma). Five different timepoints; (a) 3 am, (b) 9 am, (c) 3 pm, (d) 6 pm and (e) 9 pm are shown for each rostro-caudal level. The left y-axis shows Tph2 mRNA expression (Calibrated Mean Grey Value multiplied by its own Measured Area). Upper segmented area is associated to the right y-axis that represents the post-Grubb's test sample size at each rostro-caudal level. Fisher's Least Significant difference test results are indicated on graph and are annotated by a to e for each time point as shown in the plot key. Additionally, double letters indicate p<0.01 and simple letters for p<0.05. Here, (aabb) indicates a significant difference for 3 am vs 9 am, (ac) for 3 am vs 3 pm, (ae) for 3 am vs 9 pm, (bc) for 9 am vs 3 pm, (bd) for 9 am vs 6 pm and (be) for 9 am vs 9 pm.

3.3.4.4 Dorsal Raphe nucleus, ventral part (DRV).

Secondary LMM analysis was also performed within the DRV and it showed a main effect in rostro-caudal level ($F_{(13, 78.612)}$= 113.743, p< 0.000), a main effect of time ($F_{(4, 78.918)}$= 3.723, Figure 3-13, post tests revealed significant differences in *tph2* mRNA expression between 9 am and 3pm, across five bregma levels (-7.916, -8.084, -8.168, 8.252, -8.336 mm bregma).

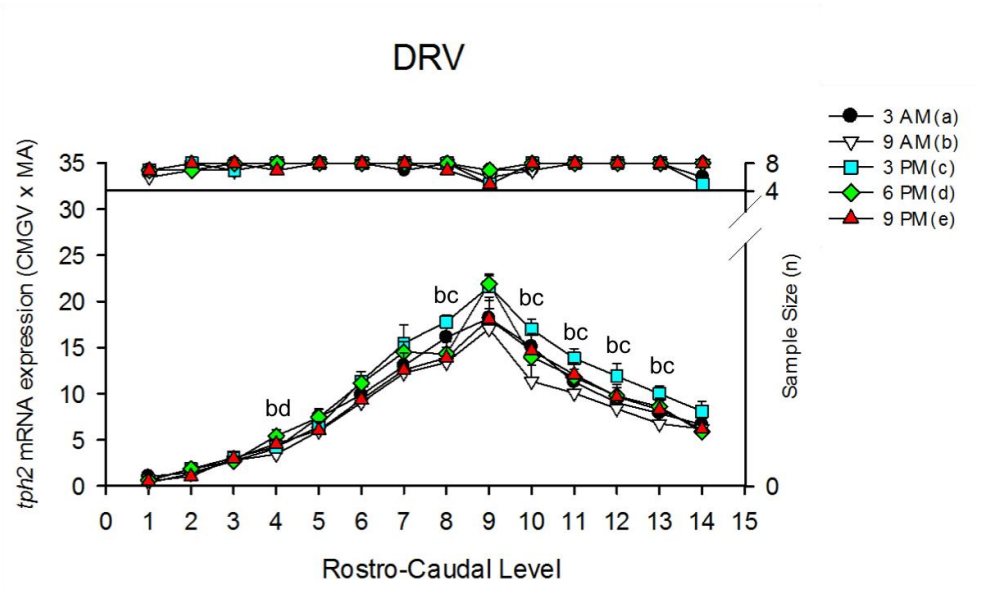

Figure 3-14: Rostro-caudal level variation of tph2 mRNA expression profile in the DRV of control animals. Tph2 mRNA expression in the DRV was measured in fourteen different rostro-caudal levels presented in the x axis (-7.328 to -8.420 mm bregma). Five different timepoints; (a) 3 am, (b) 9 am, (c) 3 pm, (d) 6 pm and (e) 9 pm are shown for each rostro-caudal level. The left y-axis shows Tph2 mRNA expression (Calibrated Mean Grey Value multiplied by its own Measured Area). Upper segmented area is associated to the right y-axis that represents the post Grubb's test sample size at each rostro-caudal level. Fisher's Least Significant difference test results are indicated on graph and are annotated by a to e for each time point as shown in the plot key. Additionally, simple letters indicate p<0.05. Here (bc) indicates a significant difference for 9 am vs 3 pm.

3.3.4.5 Dorsal Raphe nucleus, ventrolateral part/ventrolateral periaqueductal grey (DRVL/VLPAG).

Secondary LMM analysis within the DRVL/VLPAG revealed two main effects in time point ($F(4, 52.840) = 3.859$, $p<0.01$) and rostro-caudal level ($F(7, 45.730)= 73.566$, $p<0.001$), with no interaction ($F(28, 45.723)= 1.250$, $p>0.05$) (Table 3-1). Post tests revealed significant differences in *tph2* mRNA expression across six rostro-caudal levels (-7.748, -7.832, -7.916, -8.000, -8.168, 8.252) as indicated in the graph in Figure 3-14. Notably, *tph2* mRNA expression was significantly lower at 9 am than 3 pm at rostro-caudal levels 7, 11 and 12 (-7.832, -8.168, 8.252 mm bregma), and significantly lower at 9am and 3am compared to 9pm at level 6 (-7.748 mm bregma).

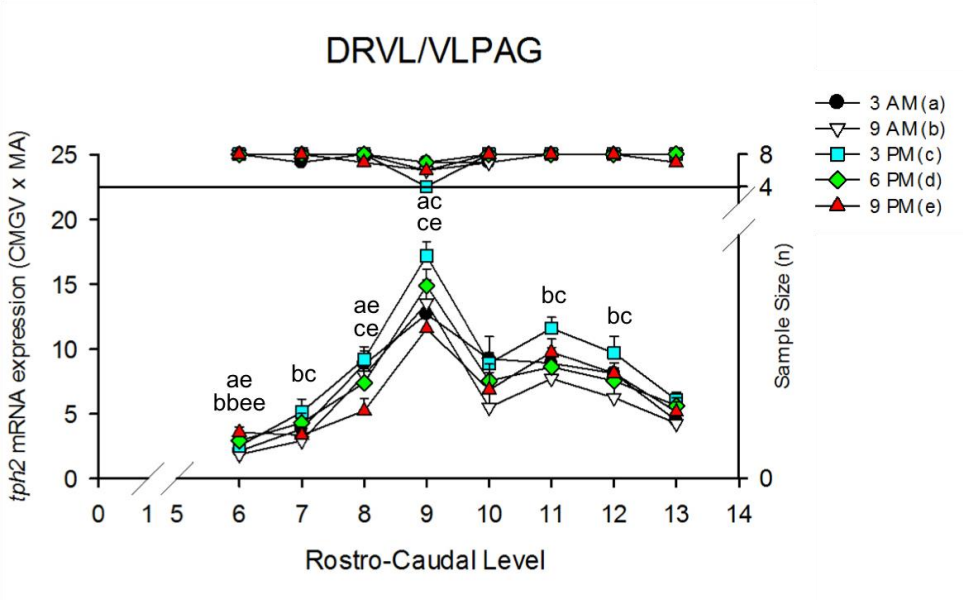

Figure 3-15; Rostro-caudal level variation of tph2 mRNA expression profile in the DRVL/VLPAG of control animals. Tph2 mRNA expression in the DRVL/VLPAG was measured in eight different rostro-caudal levels presented in the x axis (-7.748 to -8.336 mm bregma). Five different timepoints; (a) 3 am, (b) 9 am, (c) 3 pm, (d) 6 pm and (e) 9 pm are shown for each rostro-caudal level. The left y-axis shows Tph2 mRNA expression (Calibrated Mean Grey Value multiplied by its own Measured Area). Upper segmented area is associated to the right y-axis that represents the post Grubb's test sample size at each rostro-caudal level. Fisher's Least Significant difference test results are indicated on graph and are annotated by a to e for each time point as shown in the plot key. Additionally, double letters indicate p<0.01 and simple letters p<0.05. Here (bbee) indicates a significant difference for 9 am vs 9 pm, (ac) for 3 am vs 3 pm (ae) for 3 am vs 9 pm, (bc) for 9 am vs 3 pm and (ce) p< 0.05 for 3 pm vs 9 pm.

3.3.4.6 Median Raphe nucleus (MnR).

To finalize the study of the natural circadian rhythm of *tph2* mRNA expression, a Secondary LMM analysis within the MnR was performed. This analysis revealed a time point * rostro-caudal level interaction ($F_{(55,\ 52.645)}$= 3.463, p< 0.001) and two main effects in time point ($F_{(4,\ 950445,357)}$= 3.081, p< 0.05) and rostro-caudal level ($F_{(14,\ 2489.673)}$= 64.654, p< 0.001) (Table 3-1). Post tests revealed significant differences in *tph2* mRNA expression in six different rostro-caudal levels (-7.496, -8.168, -8.252, -8.336, -8.420, -8.504). Interestingly *tph2* mRNA expression appeared lower at 9 am when compared to 3pm from level 7 to level 14, but the difference was only significant at level 12 and 14. Notably, the 3 pm timepoint was significantly higher than 3 am, 9 am, 6 pm and 9 pm, albeit only at defined points from level 11 to level 15, as indicated on the graph in Figure 3-15.

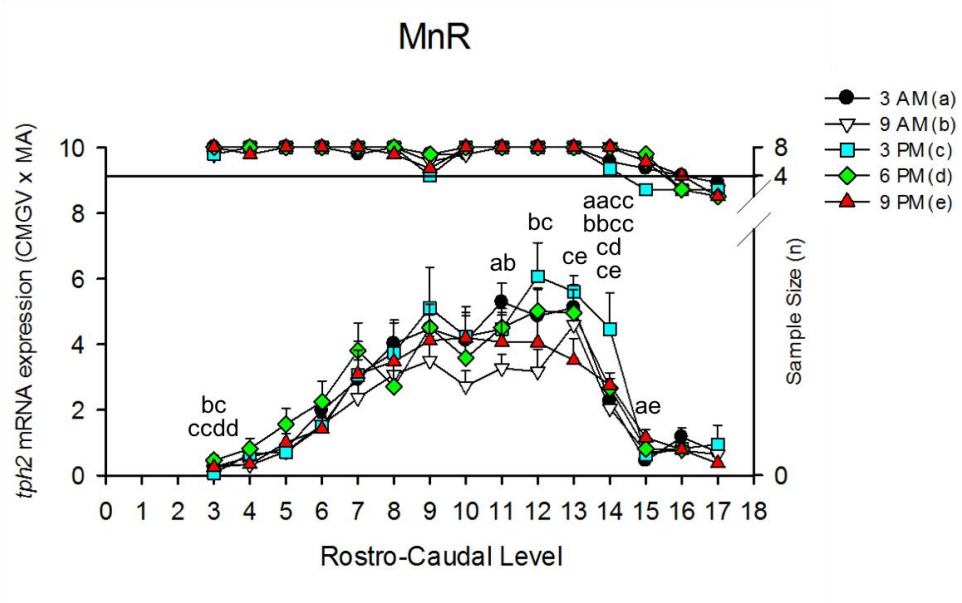

Figure 3-16: Rostro-caudal level variation of tph2 mRNA expression profile in the MnR of control animals. Tph2 mRNA expression in the MnR was measured in fifteen different rostro-caudal levels presented in the x axis (-7.496 to -8.672 mm bregma). Five different timepoints; (a) 3 am, (b) 9 am, (c) 3 pm, (d) 6 pm and (e) 9 pm are shown for each rostro-caudal level. The left y-axis shows Tph2 mRNA expression (Calibrated Mean Grey Value multiplied by its own Measured Area). Upper segmented area is associated to the right y-axis that represents the post Grubb's test sample size at each rostro-caudal level. Fisher's Least Significant difference test results are indicated on graph and are annotated by a to e for each time point as shown in the plot key. Additionally, double letters indicate p<0.01 and simple letters p<0.05. Here (aacc) indicates a significant difference for 3 am vs 3 pm, (bbcc) for 9 am vs 3 pm, (ccdd) for 3 pm vs 6 pm, (ab) for 3 am vs 9 am, (bc) for 9 am vs 3 pm, (cd) for 3 pm vs 6 pm and (ce) for 3 pm vs 9 pm.

Overall the LMM analysis of the *Tph2* mRNA expression data, level by level throughout the rostro-caudal gradient of each subdivision, was reassuringly consistent with the total *tph2* mRNA expression values for each subdivision. This data also extended the analysis to allow a more thorough appreciation of the way *tph2* mRNA expression changed over the rostro-caudal gradient and with time.

3.3.5 Summary of results

The following table is a summary of the key findings on this chapter.

Table 3-2: Table 3-3: Key findings on the circadian expression of tph2 mRNA.by subdivision of the Raphe complex and by bregma level. Differences found by statistical analysis form ANOVA's and Linear Mixed Model analysis.

	Nadir	Peak	Complete Subdivisions	LMM analysis	Figures
DR complex	9:00 AM	3:00 PM	↑ expression at 3 am, 6 pm and 9 pm when compared to nadir	NA	Figure 3-4
DRC	No significant changes				Figure 3-5 Figure 3-11
DRI	No significant changes				Figure 3-6 Figure 3-12
DRD	9:00 AM	6:00 PM	↑ expression at 3 am, 3 pm and 6 pm when compared to nadir. Specific to rostral bregma levels.	Changes at level 2, 4, 6, 8 and 12.	Figure 3-7 Figure 3-13
DRV	9:00 AM	3:00 PM	↓ expression at 3 am, 9 am and 9 pm when compared to peak. Specific to caudal bregma levels.	Changes at level 4, 8 and from 10 to 13. All changes were comparing nadir to peak.	Figure 3-8 Figure 3-14
DRVL/VLPAG	9:00 AM	3:00 PM	↓ expression at 9 am and 9 pm when compared to peak. Specific to caudal bregma levels.	Changes detected from level 6 to level 12 with exception of level 10. Most changes here comparing nadir to peak.	Figure 3-9 Figure 3-15
MnR	9:00 AM	3:00 PM	↓ expression at 9 am, 6 pm and 9 pm when compared to peak. Specific to caudal bregma levels.	Changes at level 3 and from 11 to 15. Most changes were comparing 9 am to 3 pm or 9 pm.	Figure 3-10 Figure 3-16

3.4 Discussion

According to the results described in this chapter we have determined that CORT levels in this control group (Figure 3-2) entirely correspond to the natural circadian rhythm of circulating CORT as shown in previous studies. Consequently, I can conclude with reasonable confidence that the control group used in my studies, represents "true" basal (non-stressed) experimental conditions given that levels of circulating CORT at each time studied were consistent with other previous studies from the Lightman group and others (Windle *et al.*, 1998; Spiga, Waite, *et al.*, 2011; Waite *et al.*, 2012; Park *et al.*, 2013).

Regarding the average *tph2* mRNA expression across the whole Raphe complex (Figure 3-4), the data showed a significant circadian variation in *tph2* mRNA expression, with the lowest levels of expression at 9 am, which matches to the nadir of circulating CORT. The highest level of *tph2* mRNA expression occurs at 3 pm, which coincides with the initial rise in circulating CORT. This finding is consistent with a rapid induction of *tph2* mRNA in line with rising CORT levels. The levels of *tph2* mRNA remain significantly elevated at 6 pm, relative to 9 am nadir levels, then decrease to baseline over the time course.

Considering the mean *tph2* mRNA expression in the DR subregions and the MnR nucleus we can confirm the presence of a circadian variation in the DRD (Figure 3-7), DRV(Figure 3-8), DRVL/VLPAG (Figure 3-9) and MnR (Figure 3-10) which appears to be specific of the caudal part for each area with the exclusion of the DRD which seems to be specific of the rostral part. In all of the areas with the presence of a circadian variation, the lowest point of *tph2* mRNA expression matches the nadir of circulating CORT levels at 9 am. Interestingly, in the DRV, DRVL/VLPAG and MnR the highest peak of expression is at 3 pm, moreover, in these areas the increase in *tph2* mRNA is quite transient with levels decreasing back to baseline by 9 pm. The exception to this again is the DRD where a prolonged elevation of *tph2* mRNA is evident from 3 pm to 9 pm, decreasing again from 9 pm onwards. No significant differences were found in DRC (Figure 3-5) or DRI (Figure 3-6).

Considering the rostral-caudal gradient of each of the subregions of the DR and the MnR nucleus, overall analyses showed that *tph2* mRNA expression profile changes across this gradient in all of the areas of the Raphe complex (Figure 3-11 to 3-16). This finding is consisted to previous studies (Malek et al., 2004; 2005) and represents functionally important neuroanatomical aspects of the raphe nuclei, which will be further discussed. Additionally, the data shows a circadian variation throughout the rostral-caudal levels of the DRD (Figure 3-13), DRV (Figure 3-14), DRVL/VLPAG (Figure 3-15) and MNR (Figure 3-16), and even though these changes are only statistically significant for some levels of each area, a general trend in the data can be observed.

Finally, all this data confirms the existence of a natural variation of *tph2* mRNA expression over a 24-hour period, but how is this related to the circadian expression of CORT? Is there a relationship between circulating CORT levels and *tph2* mRNA expression levels? Can circulating CORT levels modify *tph2* mRNA expression levels in all the Raphe complex? If we modify the natural circadian activity of circulating CORT, will *tph2* mRNA expression circadian activity change too? In the following chapters, I will present data from experiment models where I have manipulated the circulating glucocorticoid levels to assess the effect on *tph2* mRNA expression.

Chapter 4 Effect of the long-acting synthetic glucocorticoid Methylprednisolone on the circadian expression profile of *tph2* mRNA expression in the Dorsal and Median Raphe nuclei.

4.1 Introduction

4.2 Methods: Experimental Design

4.2.1 Study design to assess the rhythm of CORT and *tph2* mRNA expression after methylprednisolone (MPL) treatment.

4.2.2 Statistical analysis

4.3 Results

4.3.1 Circadian rhythm of circulating Corticosterone after MPL treatment.

4.3.2 Circadian rhythmicity of *tph2* mRNA expression in the Raphe complex after MPL treatment.

4.3.3 Circadian changes in *tph2* mRNA expression in subregions of the Dorsal Raphe and the MnR nucleus after MPL treatment.

4.3.4 Circadian rhythmicity of *tph2* mRNA expression in the DR subregions and MnR nucleus; analysis across the full rostro-caudal gradient.

4.4 Discussion

4.1 Introduction

Synthetic glucocorticoids (sGCs) are widely used in clinical practice for the treatment of inflammatory and immune diseases. In fact, 1% of the adult UK population are currently being prescribed oral glucocorticoid treatment (Van Staa *et al.*, 2001). Although GCs are a strong therapeutic option because of their potent anti-inflammatory and immunosuppressant properties (Keller-Wood and Dallman, 1984; Gupta and Bhatia, 2008; Paragliola *et al.*, 2017), their long-term use has been associated with numerous side effects (Brown and Chandler, 2001). While the adverse metabolic side effects of long-term GC use have been widely researched, a current area of research, that is of and of crucial interest to this study, is the less well-understood neuropsychiatric side effects. In particular, 23% of patients report mania during early treatment (Naber, Sand and Heigl, 1996), while depression is reported by 28% of patients during chronic treatment (Sirois, 2003). Anxiety is reported in 60% of patients (Bolanos *et al.*, 2004), while suicidal ideation is less common but still reported in 17.3% of patients (Bräunig, Bleistein and Rao, 1989).

Notably for my research interests, the sGC methylprednisolone (MPL) is far more long-acting than endogenous GCs. In vivo, MPL half-life is 2 to 4 hrs (Uhl *et al.*, 2002) which is considerably longer than cortisol (half-life of 60 min) (Weitzman *et al.*, 1971) or corticosterone (half-life of 15 min) (Sainio, Lehtola and Roininen, 1988). At higher doses, MPL can gain access to the brain (Earl *et al.*, 2017; Stubbs *et al.*, 2018) by saturating the MDR efflux transporter p-glycoprotein (Meijer *et al.*, 2001). Then, MPL distributes into target cells where it binds and activates the intracellular glucocorticoid receptor (GR). Furthermore, MPL causes prolonged GR activation in cell lines (Stavreva *et al.*, 2009) and *in-vivo* (Earl *et al.*, 2017).

A relationship between altered activity of GCs and mood disorders has long been suggested. As early as 1952, Brody proposed that psychiatric disorders are an extreme response to stress (Brody, 1952). Plotsky et. al, showed that patients with depression have high levels of stress hormone (Plotsky, Owens and Nemeroff, 1998), and an abnormal pulsatility of cortisol has been described in these patients (Deuschle, Schweiger, Weber, Gotthardt, K??rner, *et al.*, 1997; Young, Carlson and

Brown, 2001). Depression and anxiety disorders also have a strong relationship with the dysfunction of serotonergic systems (Owens and Nemeroff, 1994; Lowry *et al.*, 2008c). Moreover, recent studies suggest that *tph2* may be a genetic predictor for depression or anxiety (P Zill *et al.*, 2004; Peters *et al.*, 2004; Haghighi *et al.*, 2008). *Tph2* genetic variations have also been associated with major depression (Van Den Bogaert *et al.*, 2006), further to this, *tph2* variations in regulatory regions have been shown to modulate transcriptionally and post-transcriptionally gene expression, while variations in coding regions change amino acid sequence, hence function of gene product (Knight, 2005; Wang *et al.*, 2005; Pastinen, Ge and Hudson, 2006; Chen and Miller, 2008). Finally, intronic variations may also affect mRNA splicing and gene expression (Chen and Miller, 2012).

Moreover, a relationship between GC activity and the *tph2* mRNA expression profile has been suggested. Many studies have demonstrated that the *tph2* mRNA expression profile is modulated by GCs and *tph2* expression changes after stressful events (McEwen, 1998; Brown, Henderson and Keay, 2006; Katherine L. Gardner *et al.*, 2009). Notably, the removal of circulating GCs by surgical adrenalectomy, produces a disrupted *tph2* mRNA expression profile (Clark and Russo, 1997; Malek, 2007; Donner, Montoya, *et al.*, 2012). Clearly, a lot of research has focused on the understanding of serotonergic systems and their involvement in psychiatric disorders in one part, and GCs and psychiatric disorders in the other. However, the possible association between GCs, *tph2* gene (as an important modulator of 5-HT (Brommage *et al.*, 2015), hence, of pathophysiological and pharmacological relevance) and psychiatric disorders as a common triad has not been well described.

Therefore, in this study, we have tested whether sub-chronic treatment with the long-acting sGC MPL dysregulates the circadian expression profile of *tph2* mRNA in the DR and MnR, providing a potential mechanism underlying neuropsychiatric side effects reported by patients.

The experimental model used is a sub-chronic treatment regime of four days with 1mg/mL MPL provided *ad libitum* in drinking water, which acts to effectively 1) suppress endogenous CORT, and 2) replace the endogenous circadian and ultradian

pattern of circulating CORT with the long-acting sGC MPL. The model will be used to assess the changes in the *tph2* mRNA expression profile in the complete Raphe complex, in each subregion of the DR and the MnR nucleus and throughout the extended rostro-caudal gradient of each subregion of the DR and the MnR nucleus.

4.2 Methods: Experimental Design

4.2.1 Study design to assess the rhythm of CORT and *tph2* mRNA expression after methylprednisolone (MPL) treatment.

After arrival, 40 adult male Sprague Dawley (SD) rats (weighing between 250-300 g) were separated into 5 groups and housed 4 per cage in sound proof rooms for 7 days to habituate to the facility. All animals were maintained under a 12/12 light-dark cycle (lights on at 0700 h) with food and water *ad libitum*. From day 3 to day 7, all animals were handled for 10 minutes at different times of day to avoid stress on the day of the experiment.

From day 5 to day 8, all animals were submitted to 4 days of MPL treatment in their drinking water (1g/L), a dose which was previously shown to be the minimum dose to suppress CORT secretion (Spiga, Waite, *et al.*, 2011) as well as activate GRs within the brain (Earl *et al.*, 2017). During the fourth day of treatment, all animals were euthanized with an overdose of isoflurane (schedule 1 procedure) and decapitated with a guillotine at defined time points over the 24-hour cycle; 3 am, 9 am, 3 pm, 6 pm, 9 pm (n= 8 per time point) in order to collect samples. Animals were killed starting 25 minutes before the appointed hour and finishing 25 minutes past the hour. Trunk blood and whole brains were collected.

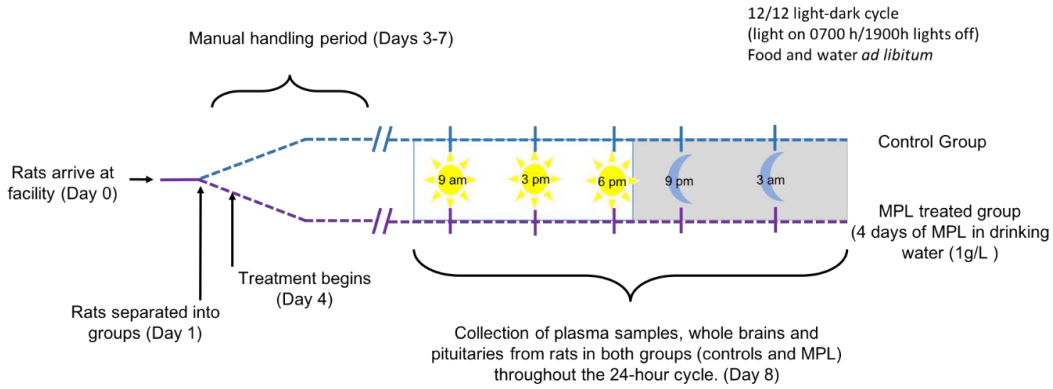

Figure 4-1: Experimental design for the assessment of the altered rhythm of CORT and tph2 mRNA expression after MPL treatment.

4.2.2 Statistical analysis

1. One-way ANOVA was performed for the CORT data to assess for an effect of time after MPL treatment. When an effect of time was found, Dunnet's post-test was used to compare each time point to the 9am nadir. Furthermore, a two-way ANOVA with a Tukey HSD post-test was performed to compare between controls and MPL treated groups.

2. When analysing the whole Raphe complex, the same statistical tests used for the CORT analysis were used to enable a direct comparison between the rhythm of *tph2* mRNA expression and the rhythm of CORT. A one-way ANOVA with a Dunnett's (2-sided) post-test was also performed, however 3 am (nadir) was here considered as the control group. Additionally, a two-way ANOVA with a Tukey HSD post-test was performed to compare between treatment groups. This fitted with previous statistical tests performed in chapter 3.

3. Finally, in all the more detailed (subregional and rostro-caudal analysis) overall and secondary LMMs were performed as in chapter 3 and 4, followed by Fisher's Least Significant Difference (LSD) multiple comparison post-tests when a time effect was found. Two different overall LLMs were performed to 1) assess the effect of time in the rostro-caudal gradient of each

subregion and 2) the effect of MPL treatment in the rostro-caudal gradient of each subregion.

4. The CTRL vs MPL comparisons made throughout this chapter were done with the data of our control groups from chapter 3. All the MPL experimental groups were independent from our control groups. This is further discussed in limitations.

4.3 Results

4.3.1 Circadian rhythm of circulating Corticosterone after MPL treatment.

The circulating CORT profile of animals after 4 days of 1g/L MPL treatment in drinking water is shown in Figure 4 -2. All time points showed particularly low levels of CORT. This dose has previously been shown to suppress CORT secretion in SD rats (Spiga, et. al, 2011) therefore the data obtained from the MPL treated group showed the treatment worked as expected.

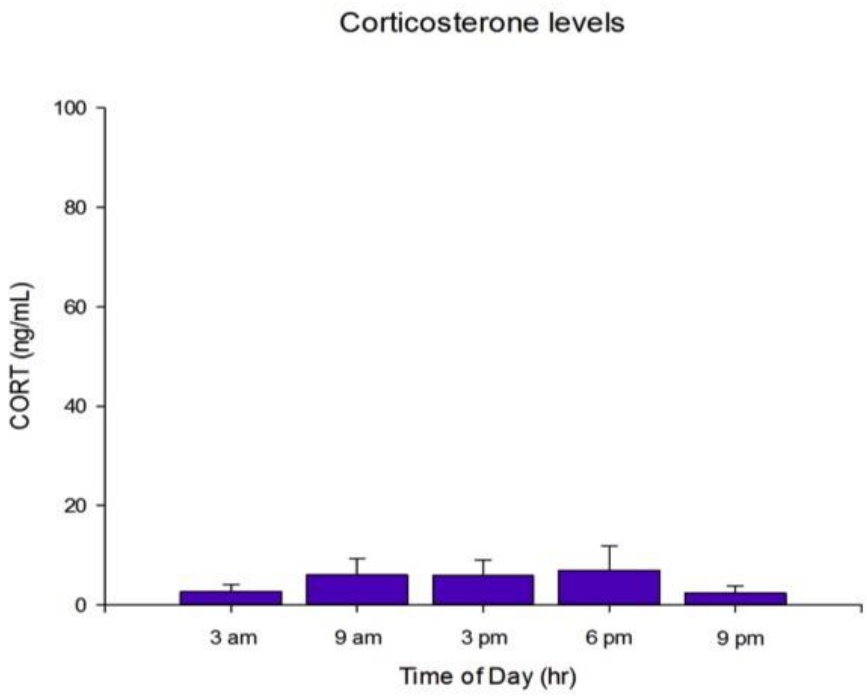

Figure 4-2: Circadian suppression of circulating CORT of MPL treated animals. CORT levels were measured in plasma obtained from trunk blood of control animals at 5 different timepoints; 3 am, 9 am, 3 pm, 6 pm and 9 pm (n=8/group/timepoint). CORT levels are expressed as ng/ml. Data is presented as Mean ± SEM of CORT. One-way ANOVA was performed to assess effect of time; $F_{(4, 35)} = 0.537$, $p > 0.05$.

A one-way ANOVA was performed to determine if there was a significant effect of time after MPL treatment. There was no statistically significant difference between groups, $F_{(4, 35)} = 0.537$, $p > 0.05$, indicating that the circadian rhythm of circulating CORT was ablated (Figure 4-2).

When comparing the control group with the MPL treated group (Figure 4 - 3), a two-way ANOVA was performed to additionally determine that there was a significant interaction between timepoint and treatment ($F_{(4, 70)} = 26.752$) $p < 0.001$, which was assessed further with a Tukey HSD test. As expected, no significant differences were found at 3 am or 9 am, which may have been expected given that endogenous CORT levels of the control animals are low during those time points. However, at the circadian CORT peak times of 3 pm, 6 pm and 9 pm, the MPL treated group had significant lower CORT levels than control animals. Again, this is consistent with adrenal CORT suppression, indicating the loss of circadian and ultradian HPA axis activity.

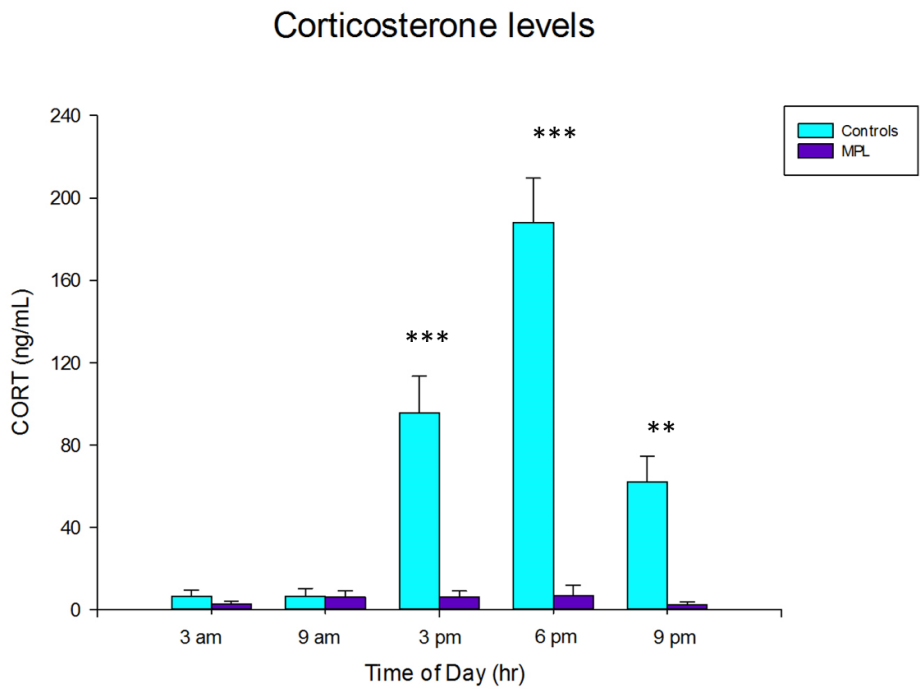

*Figure 4-3: Circadian changes in circulating CORT of Control versus MPL treated animals. CORT levels were measured in plasma obtained from trunk blood of two different groups (Control or MPL treated animals) at 5 different timepoints; 3 am, 9 am, 3 pm, 6 pm and 9 pm (n=8/group/timepoint). CORT levels are expressed as ng/ml in the y axis. Data is presented as MEAN ± SEM of CORT for each group. Two-way ANOVA was performed to assess effect of treatment; ($F_{(4, 70)}$ =26.752) p< 0.001. Additionally, a Tukey HSD test was included; *** p< 0.001 when comparing CTRL vs MPL at 3 pm and 6 pm; ** p<.01 when comparing CTRL vs MPL at 9 pm.*

4.3.2 Circadian rhythmicity of *tph2* mRNA expression in the Raphe complex after MPL treatment.

As mentioned in the introduction, this study consisted of evaluating the effect of the sGC MPL on 1) the activity pattern of *tph2* mRNA expression in all the subregions of the DR and the MnR nucleus throughout a 24-hour period and 2) the changes (if any) in this activity pattern when compared to the natural variation of expression.

First, in order to assess if there was a circadian pattern of *tph2* mRNA expression after MPL treatment, I analysed the overall averaged *tph2* mRNA expression across all rostro-caudal levels and all subregions together (Figure 4- 4). This analysis showed that *tph2* mRNA expression no longer exhibited the natural pronounced

circadian rhythm, appearing fairly 'flattened' after MPL treatment. However, there was a statistically significant effect of time of day $F_{(4, 2024)} = 5.881$, $p < 0.001$) by one-way ANOVA. Therefore, the Dunnett's post hoc test was performed to compare the mean of every group against the new observed nadir (3 am group. A significant difference was found when comparing to 9 am ($p<0.05$), 9 pm ($p<0.05$) and to the new 6 pm peak ($p<0.001$) in expression.

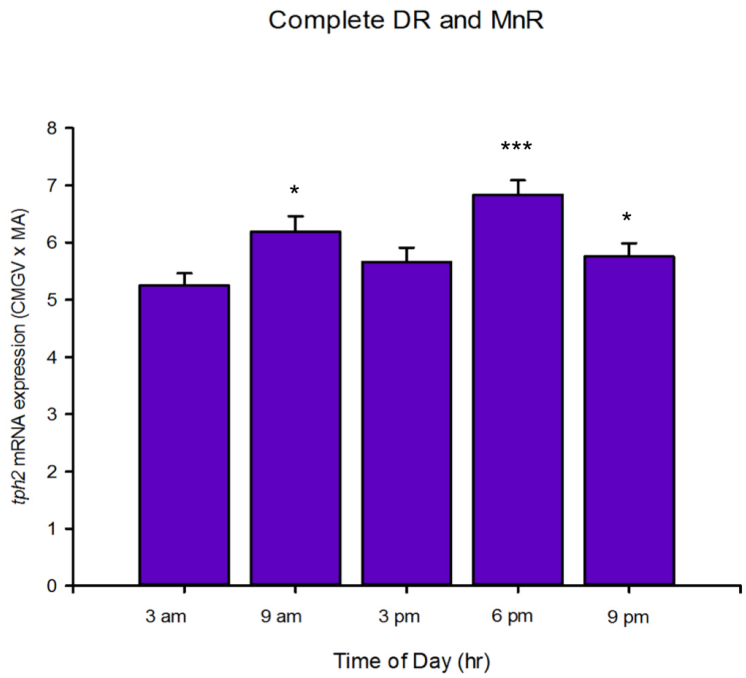

*Figure 4-4: Circadian variation in Tph2 mRNA expression in the DR and MnR complex of MPL treated animals. All measurements of tph2 mRNA expression of all levels of the DR and MnR complex were averaged for each timepoint; 3 am, 9 am, 3 pm, 6 pm and 9 pm (x axis). Tph2 mRNA quantification is expressed as Calibrated Mean Grey Value multiplied by its own Measured Area (y axis). Data points correspond to overall MEAN ± SEM of tph2 mRNA expression for each group/timepoint (n=8/group). One-way ANOVA was performed to assess effect of time; ($F_{(4, 2024)}=5.881$, $p< 0.001$). Additionally, Dunnett's (2-sided) post hoc test was performed; *** $p< 0.001$ at 6pm, *$p< 0.05$ at 9 am and *$p< 0.05$ at 9 pm when compared to the 9 am group.*

I next assessed the circadian *tph2* mRNA expression pattern after MPL treatment compared to the control dataset (Figure 4-5). This analysis showed clear modifications in the pattern of *tph2* mRNA expression after MPL treatment. Notable differences were seen after the MPL treatment, as the peak expression of *tph2* mRNA changed from 3 pm to 6 pm and the nadir from 9 am to 3 am.

The visual observations were supported by two-way ANOVA, which showed a significant interaction between timepoint and treatment reported $F_{(4, 3901)}=6.572$, $p< 0.001$. Tukey HSD test showed that the MPL group had a significant reduction in *tph2* mRNA expression at 3 am and 3 pm compared to the control group, $p< 0.05$, $p<0.01$ respectively, and a significant increase at 9 am, $p<0.01$.

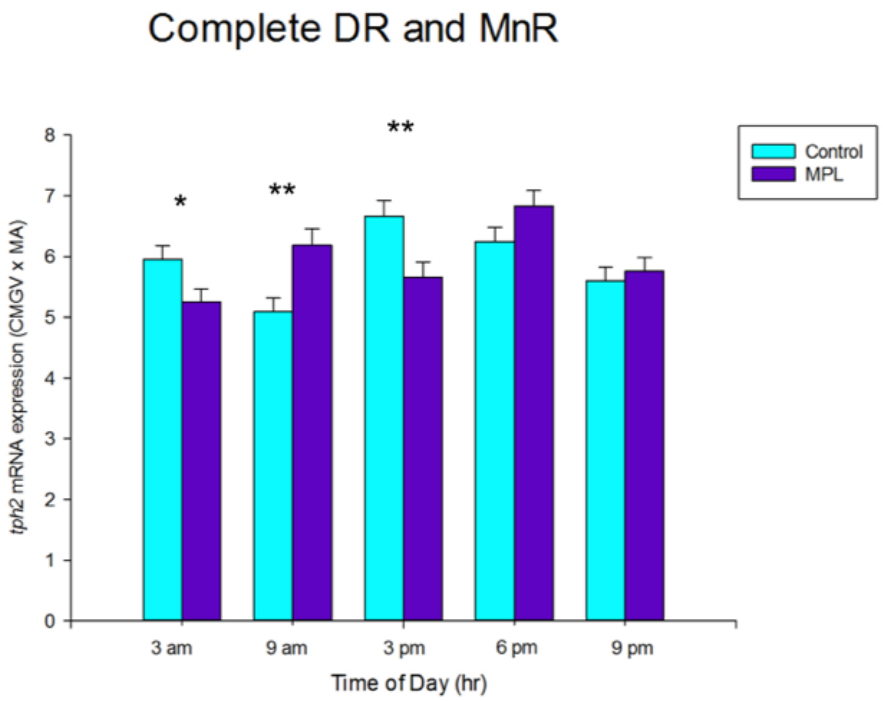

*Figure 4-5: Circadian variation in Tph2 mRNA expression in the DR and MnR complex of control vs MPL treated animals. All measurements of tph2 mRNA expression of all levels of the DR and MnR complex were averaged for each timepoint of each group; 3 am, 9 am, 3 pm, 6 pm and 9 pm (x axis). Tph2 mRNA quantification is expressed as Calibrated Mean Grey Value multiplied by its own Measured Area (y axis). Data points correspond to overall MEAN ± SEM of tph2 mRNA expression for each group/timepoint (n=8/group). A two-way ANOVA was performed to assess effect of treatment; ($F_{(4, 3901)}=6.572$, $p< 0.001$). Additionally, a Tukey HSD post hoc test was performed; **p< 0.01 at 9 am ad 3 pm when comparing CTRL vs MPL and *p< 0.05 at 3 am when comparing CTRL vs MPL.*

4.3.3 Circadian changes in *tph2* mRNA expression in subregions of the Dorsal Raphe and the MnR nucleus after MPL treatment.

As in the previous chapter, in order to assess the overall effects of time (circadian pattern) in *tph2* mRNA in each of the anatomical and functional distinct subregions

of the DR and the MnR nucleus after MPL treatment, I analysed the averaged mRNA expression across all the rostro-caudal levels for each subregion separately. I also separately evaluated the two well defined antero-posterior divisions of the Raphe complex. Thus, rostral and caudal levels were assessed for the three subregions of the DR which span rostro-caudally (DRD, DRV and DRVL/VLPAG) as well as the MnR.

Additionally, in order to describe the overall effect of MPL treatment and the changes in the circadian pattern of *tph2* mRNA expression I compared the global MEAN ± SEM of *tph2* mRNA expression from the control group (natural conditions) versus the MPL group for each of the distinct subregions of the DR and the MnR nucleus, including the two well-defined rostral and caudal groups of the DRD, DRV, DRVL/VLPAG and the MnR nucleus.

Circadian variations in *tph2* mRNA expression could be detected in some, but not all, of the DR subregions and the MnR over a 24-hour period during sub-chronic MPL treatment. These variations were predominantly localized to the caudal part of each of the subregions. Moreover, MPL treatment changed the circadian pattern of *tph2* mRNA expression, compared to controls, in many of the regions analysed.

4.3.3.1 Dorsal Raphe nucleus, caudal part (DRC).

A one-way ANOVA was performed to determine if there were any variation across the times 3 am, 9 am, 3 pm, 6 pm and 9 pm, which would indicate a circadian variation of *tph2* mRNA expression in the DRC after MPL treatment (Figure 4 - 6). Despite a trend towards a peak at 6pm and a nadir at 3am, there was no statistically significant effect of time ($F_{(4, 135)} = 1.727$) $p > 0.05$. Therefore, *tph2* mRNA expression within the DRC does not appear to display a significant circadian variation.

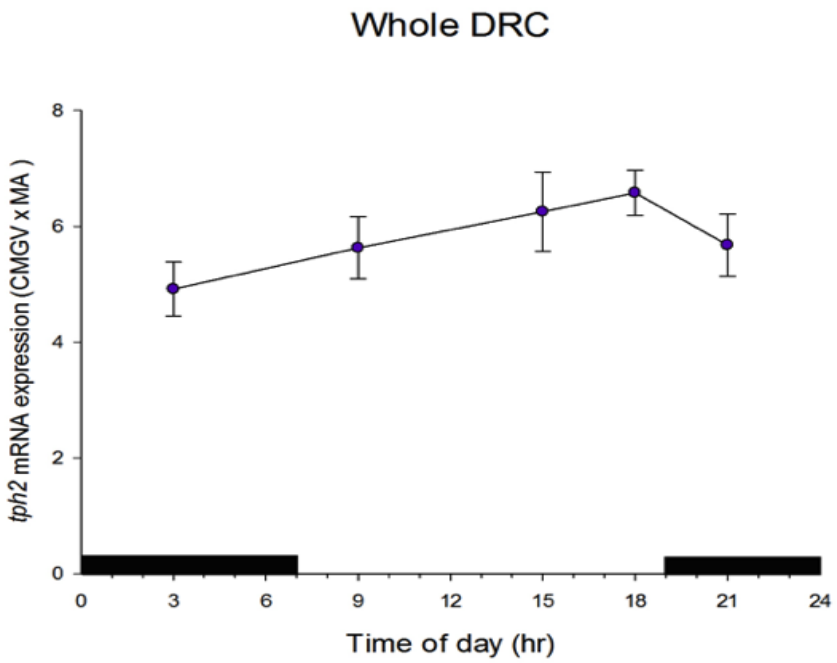

Figure 4-6: Circadian variation in tph2 mRNA expression in the DRC of MPL treated animals. Measurements of tph2 mRNA expression of the five levels of the DRC (-8.336 to -8.672 mm bregma) were averaged for each timepoint; 3 am, 9 am, 3 pm, 6 pm and 9 pm (x axis). Tph2 mRNA quantification is expressed as Calibrated Mean Grey Value multiplied by its own Measured Area (y axis). Data points correspond to overall MEAN ± SEM of tph2 mRNA expression in the DRC for each group/timepoint (n≤8/ group [≤ 8 animals x 5 levels = ≤40 values]). One-way ANOVA was performed to assess effect of time; ($F_{(4, 135)}$ =1.727) p> 0.05.

Furthermore, a two-way ANOVA was performed to determine that there was no significant interaction between timepoint and treatment in the DRC (Figure 4 - 7); ($F_{(4, 253)}$ =1.192) p> 0.05. This result might have been expected based upon the lack of circadian variation in the control group.

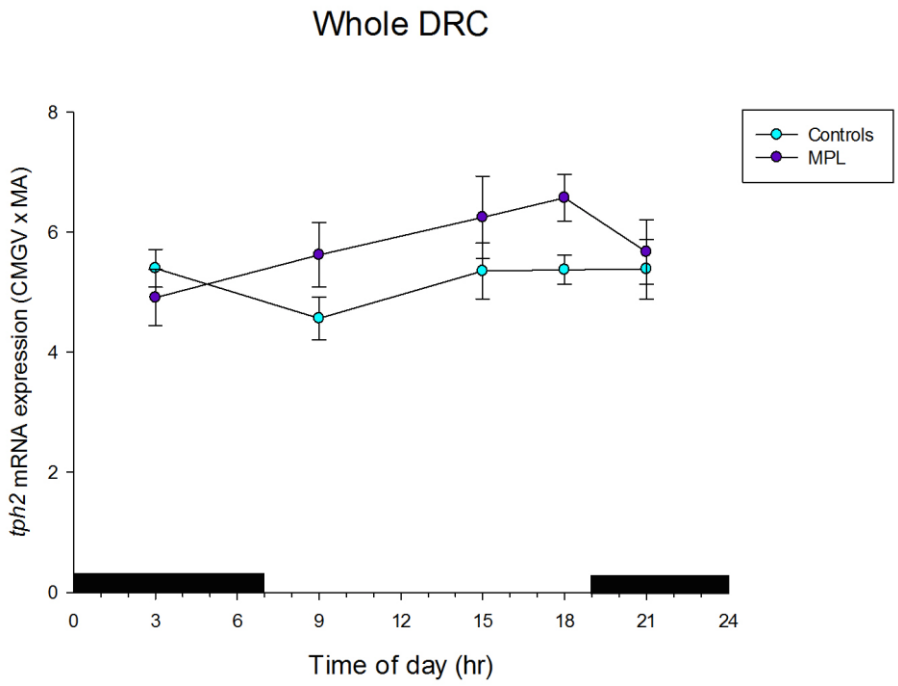

Figure 4-7: Changes in circadian variation of tph2 mRNA expression in the DRC of Control versus MPL treated animals. Measurements of tph2 mRNA expression of the five levels of the DRC (-8.336 to -8.672 mm bregma) were averaged for each timepoint; 3 am, 9 am, 3 pm, 6 pm and 9 pm (x axis) for each group separately (CTRL or MPL). Tph2 mRNA quantification is expressed as Calibrated Mean Grey Value multiplied by its own Measured Area (y axis). Data points correspond to overall MEAN ± SEM of tph2 mRNA expression in the DRC for each group/timepoint (CTRL or MPL [n≤ 8/ group [≤ 8 animals x 5 levels = ≤40 values]). Two-way ANOVA was performed to assess effect of treatment: ($F_{(4, 253)}$ =1.192) p> 0.05.

4.3.3.2 Dorsal Raphe nucleus, interfascicular part (DRI).

A one-way ANOVA was performed to determine if there were any differences between timepoints; 3 am, 9 am, 3 pm, 6 pm and 9 pm, which would indicate a circadian variation of *tph2* mRNA expression in the DRI (Figure 4 - 8). However, there was no statistically significant effect of time ($F_{(4,97)}$ =0.667) p> 0.05, indicating a lack of significant circadian variation in *tph2* mRNA expression in the DRI after MPL treatment.

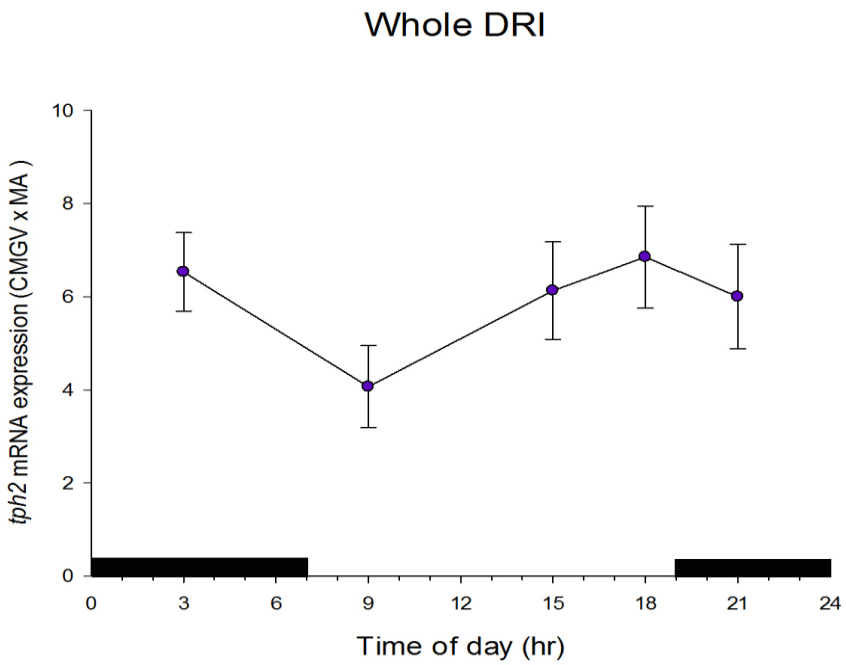

Figure 4-8: Circadian variation in tph2 mRNA expression in DRI of MPL treated animals. Measurements of tph2 mRNA expression of the four levels of the DRI (-8.420 to -8.672 mm bregma) were averaged for each timepoint; 3 am, 9 am, 3 pm, 6 pm and 9 pm (x axis). Tph2 mRNA quantification is expressed as Calibrated Mean Grey Value multiplied by its own Measured Area (y axis). Data points correspond to overall MEAN ± SEM of tph2 mRNA in the DRI for each group/timepoint (n≤8/ group [≤ 8 animals x 4 levels = ≤32 values]). One-way ANOVA was performed to assess effect of time; ($F_{(4,97)}$ =0.667) p> 0.05.

Additionally, *tph2* mRNA expression after MPL treatment behaved very similarly to the control groups throughout the 5 time points (Figure 4 - 9). A two-way ANOVA showed no significant interaction between timepoint and treatment in the DRI; ($F_{(4, 174)}$ =.162) p> 0.05. Therefore, *tph2* mRNA did not appear to exhibit a significant circadian pattern within the DRI subregion under natural conditions nor after MPL treatment.

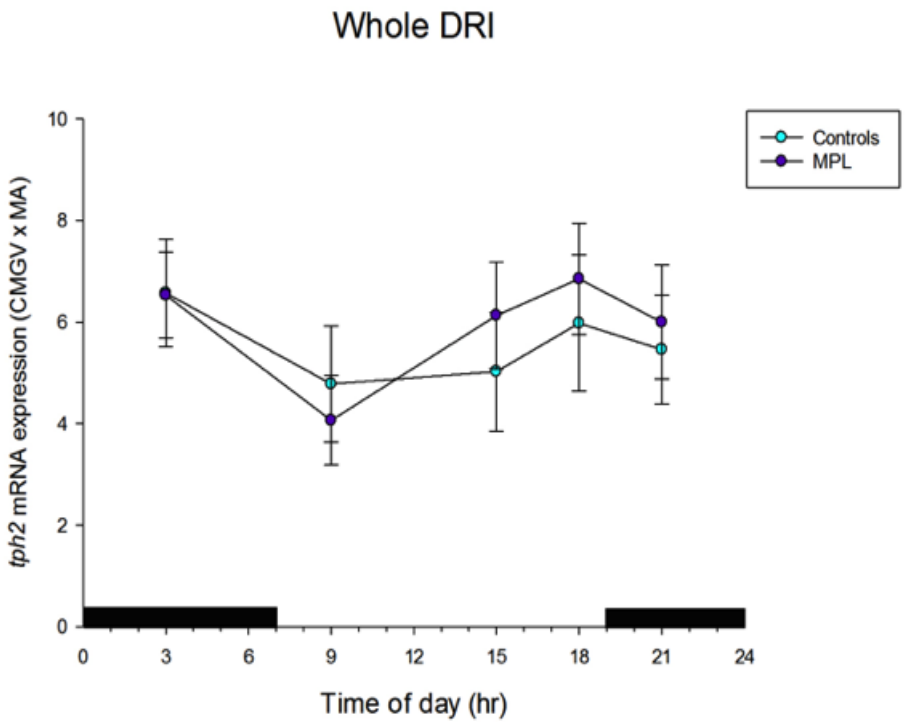

Figure 4-9: Changes in circadian variation of tph2 mRNA expression in the DRI of Control versus MPL treated animals. Measurements of Tph2 mRNA expression of the four levels of the DRI (-8.420 to -8.672 mm bregma) were averaged for each timepoint; 3 am, 9 am, 3 pm, 6 pm and 9 pm (x axis) for each group separately (CTRL or MPL). Tph2 mRNA quantification is expressed as Calibrated Mean Grey Value multiplied by its own Measured Area (y axis). Data points correspond to overall MEAN ± SEM of tph2 mRNA expression in the DRI for each group/timepoint (CTRL or MPL [n≤8/ group [≤ 8 animals x 4 levels = ≤32 values]). A Two-way ANOVA was performed to assess effect of treatment: ($F_{(4, 174)}$ =.162) p> 0.05.

4.3.3.3 Dorsal Raphe nucleus, dorsal part (DRD)

For the DRD, to determine if there is a circadian variation of *tph2* mRNA expression after MPL treatment throughout the 24-hour period, three different one-way ANOVA's were completed for the whole, rostral and caudal DRD which compared between timepoints/groups; 3 am, 9 am, 3 pm, 6 pm and 9 pm.

For the whole DRD (Figure 4 - 10A), there was a statistically significant effect of treatment; ($F_{(4, 414)}$ =3.132), p< 0.01. LSD post-tests were performed showing various statistically significant differences. The highest *tph2* mRNA expression was found at 6 pm which was significantly increased when compared to the 3 am (p< 0.01), 3 pm (p< 0.05), and 9 pm (p< 0.05) groups. Considering that 3 am had the

lowest *tph2* mRNA expression, 9 am was also significantly different from this time point, $p < 0.05$.

There was a distinct lack of circadian rhythm visible in the rostral DRD (Figure 4 -10B), and no significant effect of time detected by one-way ANOVA, $F_{(4, 272)} = 1.426$) $p > 0.05$. However, there was a robust circadian pattern in the caudal DRD (Figure 4 -10C), and a significant effect of time detected by one-way ANOVA ($F_{(4, 174)} = 3.428$), $p < 0.01$. Again, several significant differences were found with the Fishers LSD post-tests. Interestingly, exactly the same differences were found as in the whole DRI (the highest *tph2* mRNA expression was found at 6 pm) and this 6 pm time point had statistically increased *tph2* mRNA expression when compared to the 3 am ($p < 0.01$), 3 pm ($p < 0.05$), and 9 pm ($p < 0.05$). Likewise, when considering the nadir of *tph2* mRNA expression at 3 am, this was significantly different from the 9 am time point, $p < 0.05$. Therefore, it appears that *tph2* mRNA expression within the DRD displays a circadian variation after MPL treatment. Further, the variation is localised to the caudal bregma levels of this area.

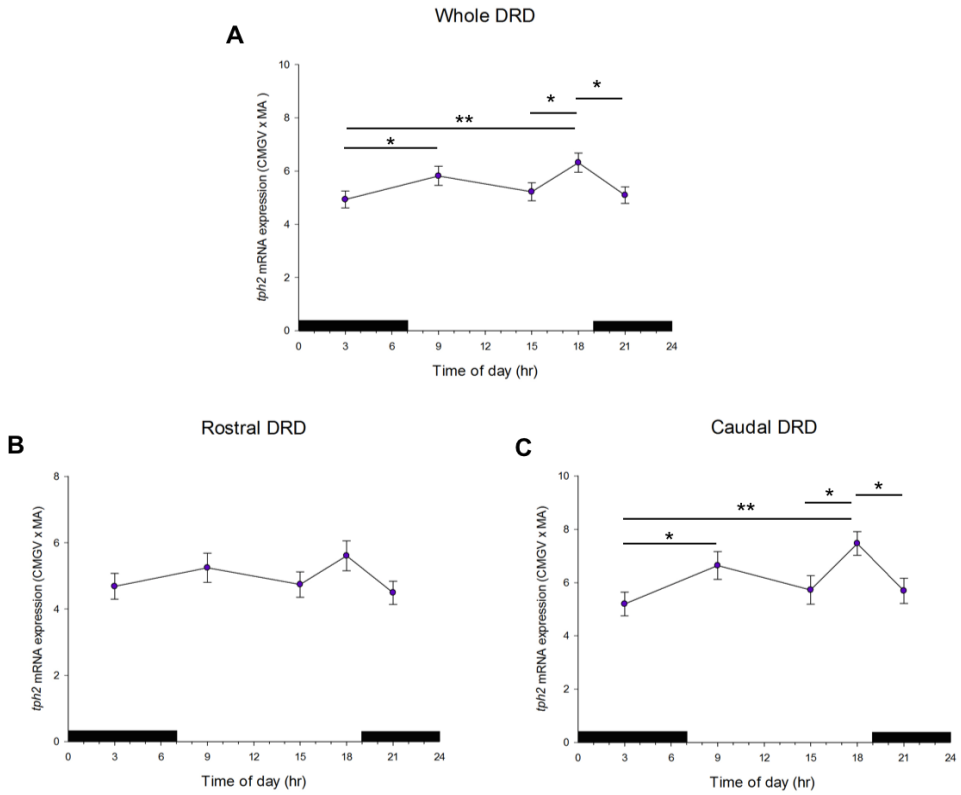

*Figure 4-10: Circadian variation in tph2 mRNA expression in the DRD of MPL treated animals. For each timepoint; 3 am, 9 am, 3 pm, 6 pm and 9 pm (x axis) measurements of tph2 mRNA expression (y axis) were averaged; (A) twelve levels (-7.328 to -8.252 mm bregma) for the whole DRD, (B) eight levels (-7.328 to -7.916 mm bregma) for the rostral DRD and (C) 5 levels (-7.916 to -8.252 mm bregma) for the caudal DRD. Tph2 mRNA quantification is expressed as Calibrated Mean Grey Value multiplied by its own Measured Area. Data points correspond to overall MEAN ± SEM of tph2 expression of the whole/rostral/caudal DRD for each group/timepoint (n≤ 8/group [≤ 8 animals x ≤ 12/8/5 levels = ≤ 96/64/40 values]). One-way ANOVAs were performed to assess effect of time: (A) ($F_{(4, 414)}$ =3.132) p< 0.01; ** p< 0.01 for 3 am vs 6 pm, * p< 0.05 for 3 am vs 9 am, for 3 pm vs 6 pm and for 6 pm vs 9 pm; (B) $F_{(4, 272)}$ =1.426) p> 0.05; (C) ($F_{(4, 174)}$ =3.428) p< 0.01; **p< 0.01 for 3 am vs 6 pm, *p< 0.05 for 3 am vs 9 am, for 3 pm vs 6 pm and for 6 pm vs 9 pm with Fisher's Least Significant Difference test.*

Next, I assessed the *tph2* mRNA expression pattern within the whole DRD compared to the control pattern (Figure 4 - 11A). The peak in expression is seen at 6pm in both controls and treated. However, the 9am nadir appears to be elevated in the MPL group. A significant interaction between timepoint and treatment was detected ($F_{(4, 860)}$ =2.799) p< 0.05, so post-tests were run. Interestingly, the only statistically significant difference was found at 9 am, where the MPL group was significantly elevated compared to the control group, p< 0.05.

Similarly, for the rostral DRD (Figure 4 - 11B) there was an elevation at 9am in the MPL group compared to controls. As a significant interaction detected ($F_{(4, 571)} = 2.236$) $p < 0.05$, post-tests were performed to show that the increased *tph2* mRNA expression in the MPL group at 9am was statistically significant, $p < 0.05$.

For the caudal DRD (Figure 4 -11C), the two-way ANOVA again showed a significant interaction; ($F_{(4, 354)} = 2.890$) $p < 0.01$. Like in the rostral DRD, a significantly higher *tph2* mRNA expression was found at 9 am in the MPL group compared to the control group, $p < 0.05$. Interestingly, there was also a significantly increased *tph2* mRNA expression at 6 pm in the MPL group compared to the control group, $p < 0.05$.

Therefore, it appears that the *tph2* mRNA expression profile within the DRD subregion is significantly altered with MPL treatment, with an increase in 9 am nadir levels throughout the whole DRD. However, the apparent MPL-dependent 'shift' in peak expression from 3pm to 6pm is localised to the caudal DRD.

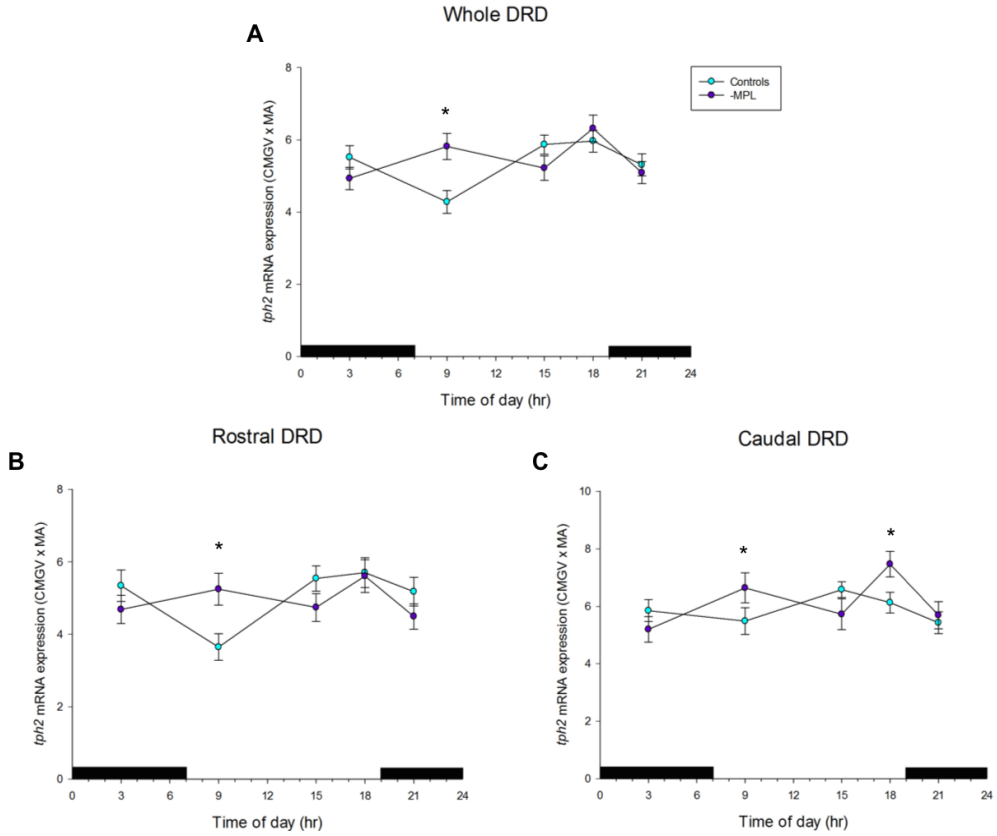

*Figure 4-11: Changes in circadian variation of tph2 mRNA expression in the DRD of Control vs MPL treated animals. For each timepoint; 3 am, 9 am, 3 pm, 6 pm and 9 pm (x axis) measurements of tph2 mRNA expression (y axis) were averaged for each group separately (CTRL or MPL); (A) twelve levels (-7.328 to -8.252 mm bregma) for the whole DRD, (B) eight levels (-7.328 to -7.916 mm bregma) for the rostral DRD and (C) 5 levels (-7.916 to -8.252 mm bregma) for the caudal DRD. Tph2 mRNA quantification is expressed as Calibrated Mean Grey Value multiplied by its own Measured Area. Data points correspond to overall MEAN ± SEM of tph2 mRNA expression of the whole/rostral/caudal DRD for each group/timepoint (CTRL vs MPL [n≤ 8/group [≤ 8 animals x ≤ 12/8/5 levels = ≤ 96/64/40 values]). Two-way ANOVAs were performed to assess effect of treatment; (A) ($F_{(4, 860)}$ =2.799) p< 0.05; * p< 0.05 when comparing CTRL vs MPL at 9 am; (B) ($F_{(4, 571)}$ =2.236) p< 0.05; * p< 0.05 when comparing CTRL vs MPL at 9 am; (C) ($F_{(4, 354)}$ =2.890) p< 0.01;*p< 0.05 when comparing CTRL vs MPL at 9 am and 6 pm with Fisher's Least Significant Difference test.*

4.3.3.4 Dorsal Raphe nucleus, ventral part (DRV).

Tph2 mRNA expression within the DRV subregion appears to exhibit very little circadian variation across the 24-hour period after MPL treatment (Figure 4-12). There was no significant effect of time detected by one-way ANOVA in the whole DRV (Figure 4-12A); ($F_{(4, 485)}$ =1.2862) p> 0.05, the rostral DRV (Figure 4-12B), ($F_{(4, 272)}$ =0.555) p> 0.05 or the caudal DRV (Figure 4-12C), $F_{(4, 244)}$ =2.178) p> 0.05.

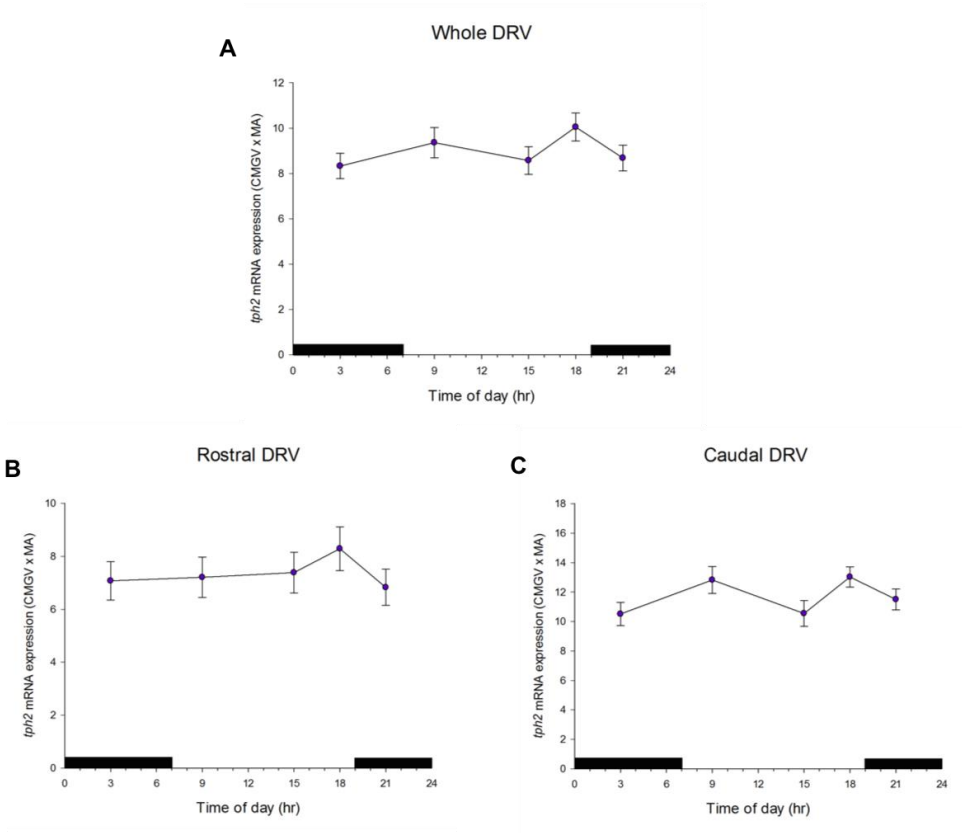

Figure 4-12: Circadian variation in tph2 mRNA expression in the DRV of MPL treated animals. For each timepoint; 3 am, 9 am, 3 pm, 6 pm and 9 pm (x axis) measurements of tph2 mRNA expression (y axis) were averaged; (A) fourteen levels (-7.328 to -8.420 mm bregma) for the whole DRV, (B) eight levels (-7.328 to -7.916 mm bregma) and (C) seven levels (-7.916 to -8.420 mm bregma) for the caudal DRV. Tph2 mRNA quantification is expressed as Calibrated Mean Grey Value multiplied by its own Measured Area. Data points correspond to the overall MEAN ± SEM of th2 expression of the whole/rostral/caudal DRV for each group/timepoint (n≤ 8/group [≤ 8 animals x 14/8/7 levels = ≤ 112/64/56 values]). One-way ANOVAs were performed to assess effect of time; (A) ($F_{(4, 485)}$ =1.2862) p> 0.05; (B) ($F_{(4, 272)}$ =0.555) p> 0.05; (C) ($F_{(4, 244)}$ =2.178) p> 0.05.

Additionally, to visualise how the modified pattern in *tph2* mRNA expression after MPL treatment compared to the control pattern, the data was plotted together (Figure 4-13). Again, the differences were more pronounced in the caudal DRV (Figure 4-13C), where it appears that the lack of circadian rhythm in the MPL group is due to elevated expression at the 9am nadir, and decreased expression at the 3pm peak. These differences are less pronounced in the whole DRV (Figure 4-13A), and minimal in the rostral DRV (Figure 4-13B).

For the whole and rostral regions of the DRV, two-way ANOVAs showed no interaction; ($F_{(4, 1009)}$ =1.635) p> 0.05 and ($F_{(4, 574)}$ =.240) p> 0.05 respectively. A

significant interaction between timepoint and treatment was found for the caudal DRV; $F_{(4, 500)} = 4.393$) $p < 0.01$ so post tests were then used to detect significant differences between MPL and control at 9 am $p<0.05$, and at 3 pm $p< 0.001$.

Thus, MPL treatment has quite profoundly changed the circadian variation in *tph2* mRNA expression profile. Furthermore, these changes seem to be specific to the caudal levels, where a convincing decrease in expression at 3 pm and an increase at 9 am results in a loss of circadian rhythmicity.

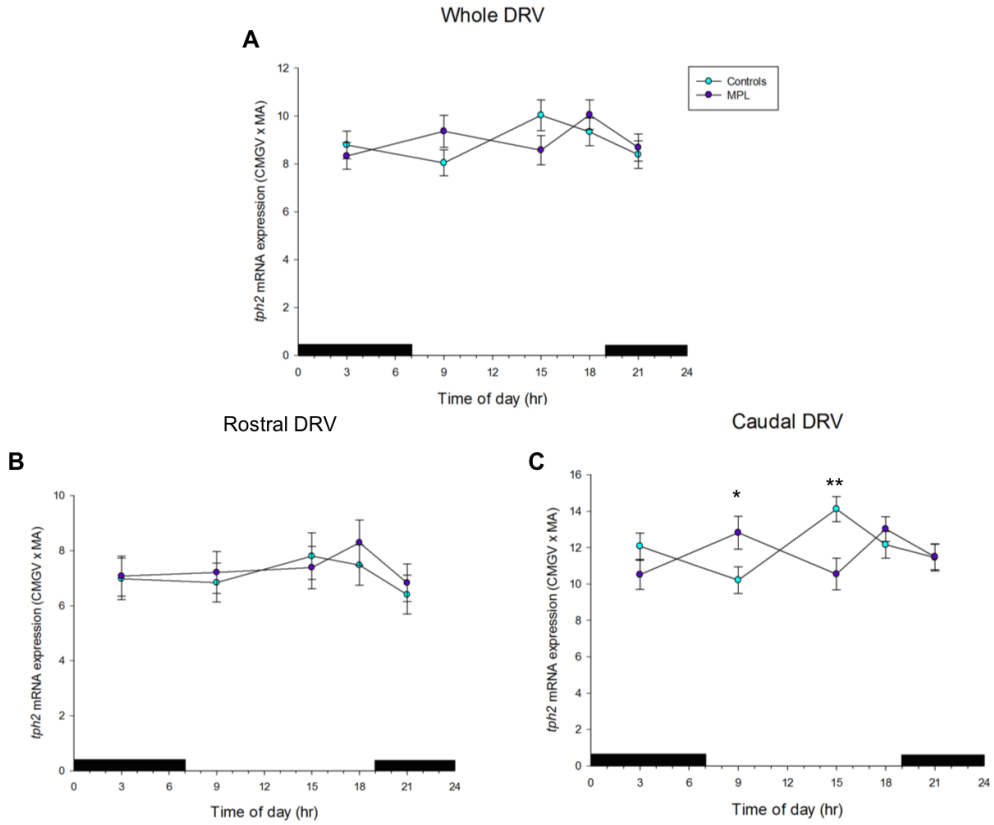

*Figure 4-13: Changes in circadian variation of tph2 mRNA expression in the DRV of Control vs MPL treated animals. For each timepoint; 3am, 9am, 3pm, 6pm and 9pm (x axis) measurements of tph2 mRNA expression (y axis) were averaged for each group separately (CTRL or MPL); (A) fourteen levels (-7.328 to -8.420 mm bregma) for the whole DRV, (B) eight levels (-7.328 to -7.916 mm bregma) and (C) seven levels (-7.916 to -8.420 mm bregma) for the caudal DRV. Tph2 mRNA quantification is expressed as Corrected Mean Grey Value multiplied by its own Measured Area (y axis). Data points correspond to the overall MEAN ± SEM of th2 expression of the whole/rostral/caudal DRV for each group/timepoint (CTRL vs MPL [n≤8/group [≤8 animals x 14/8/7 levels = ≤112/64/56 values]). Two-way ANOVAs were performed to assess effect of treatment; (A) ($F_{(4, 1009)} = 1.635$) $p> 0.05$; (B) ($F_{(4, 574)} = .240$) $p> 0.05$; (C) ($F_{(4, 500)} = 4.393$) $p< 0.01$; **$p< 0.01$ when comparing CTRL vs MPL at 3 pm and *$p<0.05$ when comparing CTRL vs MPL at 9 am with Fisher's Least Significant Difference test.*

4.3.3.5 Dorsal raphe nucleus, ventrolateral part/ventrolateral periaqueductal grey (DRVL/VLPAG)

The DRVL/VLPAG has an interesting *tph2* mRNA expression profile after MPL treatment, with a nadir at 3 am and two peaks at 9 am and 6 pm (Figure 4-14). This pattern appears to be maintained across both the rostral (Figure 4-14B) and caudal (Figure 4-14C) DRVL/VLPAG. One-way ANOVAs revealed a statistically significant effect of time for the whole DRVL/VLPAG ($F_{(4, 282)} = 2.582$) $p < 0.05$), as well as for the rostral ($F_{(4, 105)} = 2.547$) $p < 0.01$) and caudal ($F_{(4, 209)} = 4.174$) $p < 0.01$) subregions. Post tests revealed that the difference between the nadir at 3 am and the peak at 9 am was significant ($p<0.01$) in the whole, rostral and caudal DRVL/VLPAG. The difference between the nadir at 3 am and the peak at 6 pm was also found to be significant in the whole ($p<0.01$), rostral ($p<0.05$) and caudal ($p<0.01$) parts of the DRVL/VLPAG.

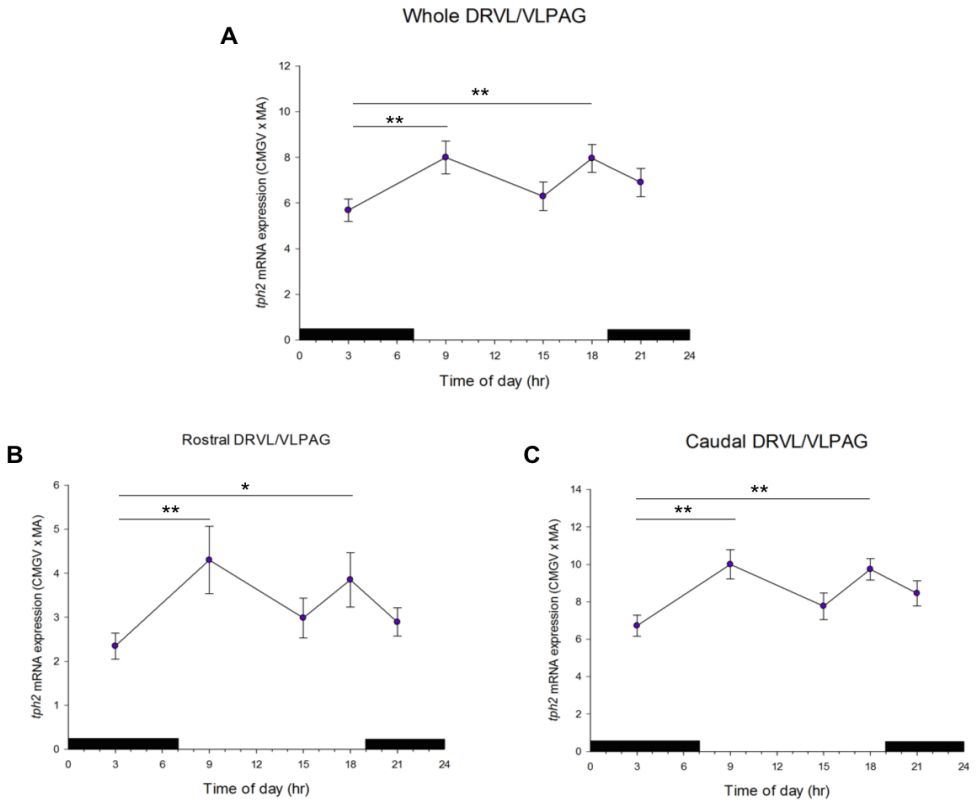

Figure 4-14: Circadian variation in tph2 mRNA expression profile in the DRVL/VLPAG of MPL treated animals. For each timepoint; 3 am, 9 am, 3 pm, 6 pm and 9 pm (x axis) measurements of Tph2 mRNA expression (y axis) were averaged; (A) eight levels (-7.748 to -

*8.336 mm bregma) for the whole DRVL/VLPAG, (B) three levels (-7.748 to -7.916 mm bregma) for the rostral DRVL/VLPAG and (C) six levels (-7.916 to -8.336 mm bregma) for the caudal DRVL/VLPAG.Tph2 mRNA quantification is expressed as Calibrated Mean Grey Value multiplied by its own Measured Area. Data points correspond to the overall MEAN ± SEM of tph2 expression of the whole/rostral/caudal DRVL/VLPAG for each group/timepoint (n≤ 8/group [≤ 8 animals x 8/3/6 levels = ≤64/24/48 values]). One-way ANOVAs were performed to assess effect of time; (A) ($F_{(4, 282)}$ =2.582) p< 0.05; **p< 0.01 for 3 am vs 9 am and for 3 am vs 6 pm; (B) ($F_{(4, 105)}$ =2.547) p< 0.01; **p< 0.01 for 3 am vs 9 am and *p< 0.05 for 3am vs 6 pm; (C) ($F_{(4, 209)}$ =4.174) p< 0.01; **p< 0.001 for 3 am vs 9 am and for 3 am vs 6 pm with Fisher's Least Significant Difference test.*

Next, I plotted the data from Figure 4 - 14 together with the control data from whole, rostral and caudal DRVL/VLPAG to assess how the pattern of DRVL/VLPAG *tph2* mRNA expression has changed after MPL treatment compared to the natural circadian rhythm (Figure 4-15).

Figure 4-15A shows how the temporal *tph2* mRNA expression pattern in the whole DRVL/VLPAG has changed from the characteristic circadian pattern in the control dataset, with nadir at 9 am and peak at 3 pm, to a dysregulated profile with nadir at 3am and peaks at 9 am and 6 pm. A significant interaction between timepoint and treatment was observed ($F_{(4, 579)}$ =3.347) p< 0.01, and post-tests show that the significant differences were found at 9 am when control levels were low and MPL treated levels were high (p< 0.05) and 3 pm when control levels were high and MPL levels were low (p< 0.05).

For the rostral DRVL/VLPAG (Figure 4 - 15B), MPL treatment resulted in a relative reduction of *tph2* mRNA across all timepoints except for the 9 am, when the control levels are at a natural nadir. The visual observation was supported by two-way ANOVA, which detected a significant interaction ($F_{(4, 217)}$ =2.890) p< 0.05. Further, post tests revealed significant differences at 3 am (p<0.01) and 3 pm (p< 0.01).

Interestingly, the caudal DRVL/VLPAG (Figure 4-15C) followed a very similar pattern to the whole DRVL/VLPAG, with a distinctive temporal dysregulation observed. Supporting the observed change with MPL treatment, a significant interaction was detected by two-way ANOVA ($F_{(4, 428)}$ =4.809) p< 0.01. Similar to the whole DRVL/VLPAG, the higher *tph2* mRNA expression for the MPL treated

group 9 am, was significantly different ($p < 0.01$). Additionally, in this caudal analysis, the small difference found at 3 am is significant ($p < 0.05$).

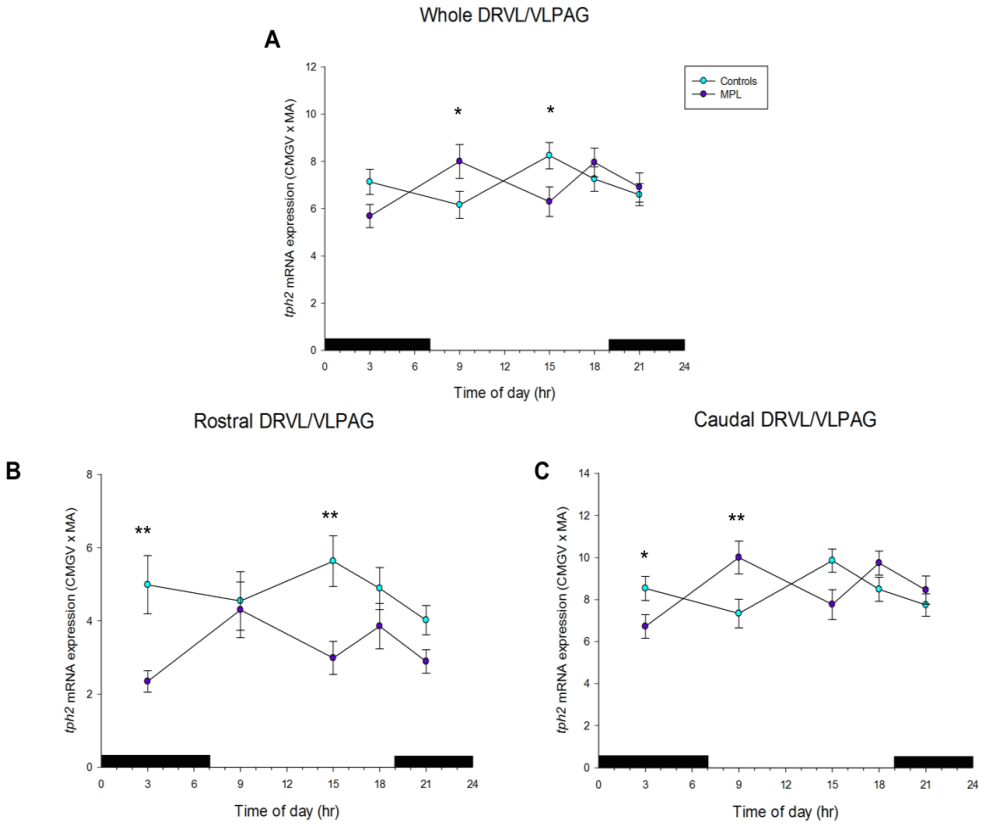

*Figure 4-15: Changes in circadian variation of tph2 mRNA expression in the DRVL/VLPAG of Control vs MPL treated animals. For each timepoint; 3am, 9am, 3pm, 6pm and 9pm (x axis) measurements of tph2 mRNA expression (y axis) were averaged for each group separately (CTRL or MPL); (A) eight levels (-7.748 to -8.336 mm bregma) for the whole DRVL/VLPAG, (B) three levels (-7.748 to -7.916 mm bregma) for the rostral DRVL/VLPAG and (C) six levels (-7.916 to -8.336 mm bregma) for the caudal DRVL/VLPAG. Tph2 mRNA quantification is expressed as Calibrated Mean Grey Value multiplied by its own Measured Area. Data points correspond to the overall MEAN ± SEM of tph2 mRNA expression of the whole/rostral/caudal DRVL/VLPAG for each group/timepoint (CTRL vs MPL [n≤ 8/group [≤ 8 animals x 8/3/6 levels = ≤64/24/48 values]).Two-way ANOVAs were performed to assess effect of treatment; (A) ($F_{(4, 579)} = 3.347$) $p < 0.01$; * $p < 0.05$ when comparing CTRL vs MPL at 9 am and 3 pm; (B) ($F_{(4, 217)} = 2.890$) $p < 0.05$; ** $p < 0.01$ when comparing CTRL vs MPL at 3 am and 3 pm; (C) ($F_{(4, 428)} = 4.809$) $p < 0.01$;**$p < 0.01$ when comparing CTRL vs MPL at 9 am and *$p < 0.05$ when comping CTRL vs MPL at 3 am with Fisher's Least Significant Difference test.*

4.3.3.6 Median Raphe nucleus (MnR).

The MnR *tph2* mRNA expression profile exhibited a strong circadian variation during MPL treatment (Figure 4 - 16). One-way ANOVAs revealed a statistically significant effect of time for the whole ($F_{(4, 492)} = 3.224$) $p < 0.05$), rostral ($F_{(4, 213)}$

=3.369) p< 0.05) and caudal ($F_{(4, 311)}$ =2.768) p< 0.05) MnR. A robust peak at 6 pm was seen in the whole MnR, where it was significantly different to the relatively flat levels at 3 am, 9 am and 3 pm as indicated in Figure 4-16A. The 6pm peak was also significantly different to 9 am and 3 pm in the rostral MnR as indicated in Figure 4-16B, and to the nadir times of 3 am and 3 pm in the caudal MnR as indicated in Figure 4-16C. Interestingly, the 9 am nadir was only seen in the rostral MnR. In the caudal MnR by contrast, the 9 am *tph2* mRNA expression was nearly as high as 6 pm.

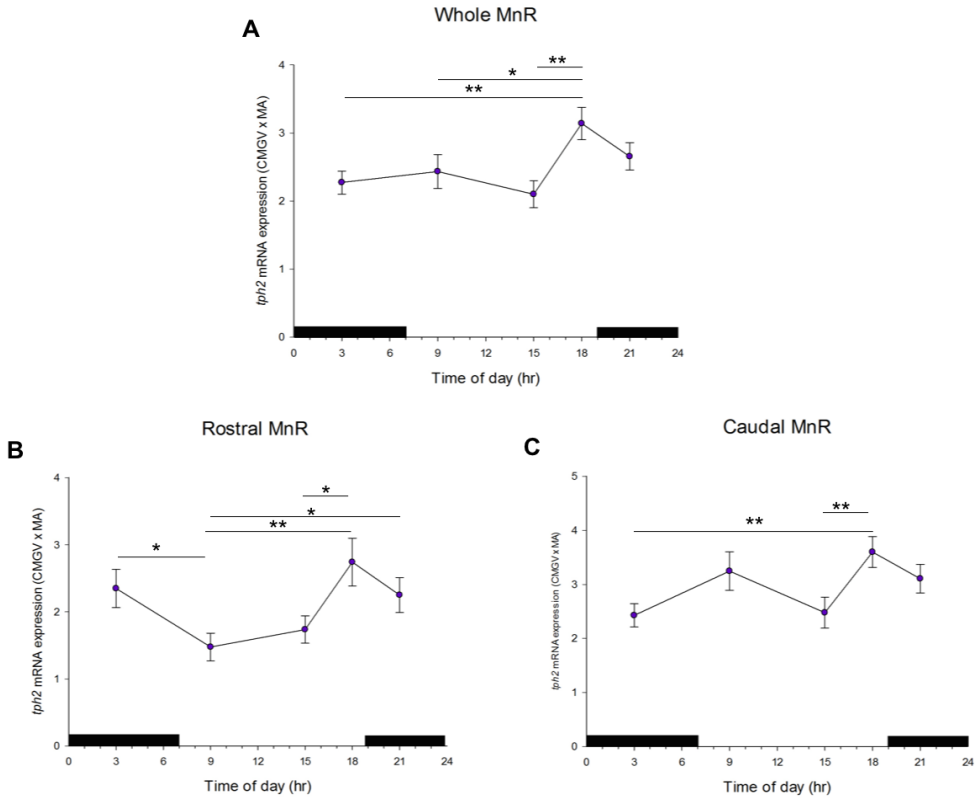

*Figure 4-16: Circadian variation in tph2 mRNA expression in the MnR of MPL treated animals. For each timepoint; 3am, 9am, 3pm, 6pm and 9pm (x axis) measurements of tph2 mRNA expression (y axis) were averaged; (A) fifteen levels (-7.496 to -8.672 mm bregma) for the whole MnR, (B) six levels (-7.494 to -7.916 mm bregma) for the rostral MnR and (C) 10 levels (-7.916 to 8.672 mm bregma) for the caudal MnR. Tph2 mRNA quantification is expressed as Calibrated Mean Grey Value multiplied by its own Measured Area. Data points correspond to the overall MEAN ± SEM of tph2 expression of the whole/rostral/caudal MnR for each group/timepoint (n≤8/group [≤ 8 animals x 15/6/10 levels = ≤120/48/80 values]). One-way ANOVAs were performed to assess effect of time; (A) ($F_{(4, 492)}$ =3.224) p< 0.05; **p< 0.01 for 3 am vs 6 pm, and for 3 pm vs 6 pm, *p< 0.05 for 9 am vs 6 pm; (B ($F_{(4, 213)}$ =3.369) p< 0.05; **p< 0.01 for 9 am vs 6 pm, *p< 0.05 for 3 am vs 9 am, for 9 am vs 9 pm and for 3 pm vs 6*

*pm; (C) ($F_{(4, 311)}$ =2.768) p< 0.05; ** p< 0.01 for 3 am vs 6 pm and for 3 pm vs 6 pm with Fisher's Least Significant Difference test.*

Then, in Figure 4-17, I assessed whether MPL treatment altered the circadian *tph2* mRNA expression profile in the whole, rostral and caudal MnR. A striking difference was seen in the whole MnR with MPL treatment, with an apparent shift in the peak expression time from 3 pm to 6 pm (Figure 4-17A). A significant interaction between treatment and time was detected by two-way ANOVA; ($F_{(4, 985)}$ =3.252) p< 0.05 and post-tests showed a significant difference with MPL treatment at 3 pm, p< 0.01. The rostral MnR (Figure 4-17B), did not show a significant effect of time ($F_{(4, 438)}$ = 0.923) p> 0.05. However, a trend of high levels of *tph2* mRNA expression after MPL Treatment can be seen at 3 am, 6 pm and 9 pm. Lastly, and very interesting, the caudal MnR (Figure 4-17C) displayed a similar, yet stronger, pattern to that observed for the whole MnR. This pattern has a contrasting temporal difference within treatment group which is supported by a significant interaction reported by two-way ANOVA; $F_{(4, 613)}$ =5.553) p< 0.01. Post test revealed that the lower levels of *tph2* mRNA expression found in the MPL groups at 3 am and 6 pm are statistically different to their corresponding control groups, p<0.01 and p<0.001, respectively.

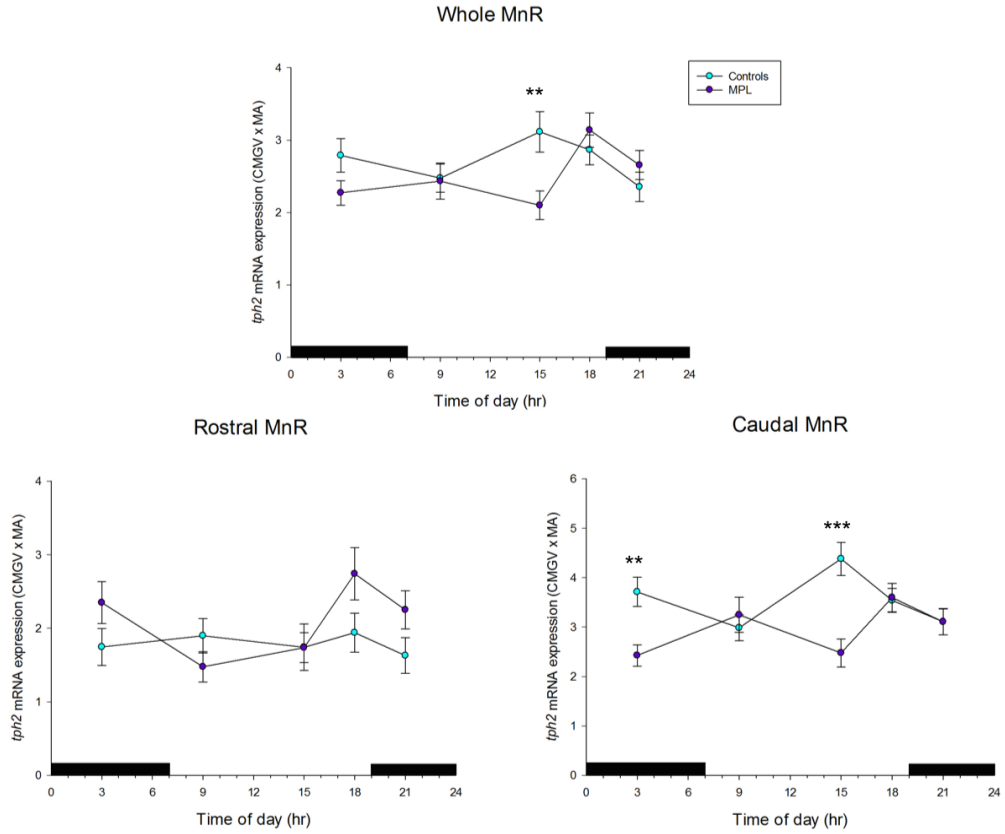

*Figure 4-17: Changes in circadian variation of tph2 mRNA expression in the MnR of Control vs MPL treated animals. For each timepoint; 3 am, 9 am, 3 pm, 6 pm and 9 pm (x axis) measurements of tph2 mRNA expression (y axis) were averaged for each group separately (CTRL or MPL; (A) fifteen levels (-7.496 to -8.672 mm bregma) for the whole MnR, (B) six levels (-7.494 to -7.916 mm bregma) for the rostral MnR and (C) 10 levels (-7.916 to 8.672 mm bregma) for the caudal MnR. Tph2 mRNA quantification is expressed as Calibrated Mean Grey Value multiplied by its own Measured Area. Data points correspond to the overall MEAN ± SEM of tph2 mRNA expression of the whole/rostral/caudal MnR for each group/timepoint (n≤ 8/group [≤ 8 animals x 15/6/10 levels = ≤ 120/48/80 values]). Two-way ANOVAs were performed to assess effect of treatment; (A) ($F_{(4, 985)} = 3.252$) $p < 0.05$; ** $p < 0.01$ when comparing CTRL vs MPL at 3 pm; (B) ($F_{(4, 438)} = 0.923$) $p > 0.05$; (C) ($F_{(4, 613)} = 5.553$) $p < 0.01$; *** $p < 0.001$ when comparing CTRL vs MPL at 3 pm, ** $p < 0.01$ when comparing CTRL vs MPL at 3 am with Fisher's Least Significant Difference test.*

4.3.4 Circadian rhythmicity of *tph2* mRNA expression in the DR subregions and MnR nucleus; analysis across the full rostro-caudal gradient.

In order to assess the effects of MPL treatment in the circadian activity of *tph2* mRNA expression throughout the rostro-caudal gradient of the DR subregions and the MnR nucleus, Linear Mixed Model (LMM) analyses were completed as

described in the methods chapter. Additionally, different LMM analysis were performed to compare the changes throughout the rostro-caudal gradient of the DR subregions and the MnR nucleus under natural conditions and after the MPL treatment.

All LMM analyses were methodically finalized and only if there were significant differences in any main factor or interaction, then, Fisher's Least Significant Difference test post hoc tests followed. All statistical tests were considered only if the sample size was above four animals (half the original sample size for each timepoint at each rostro-caudal level).

Overall, we can again see in the full rostro-caudal gradient plots (Figures 4 -18 to 4-29) that *tph2* mRNA expression levels changed in a highly characteristic manner across the anterior to posterior axis of the DR and MnR. Furthermore, in these detailed analyses, we can start to readily visualise where the time-dependent and treatment-dependent changes are localised within each subregion, if at all.

Analysis of the circadian *tph2* mRNA expression profile after MPL treatment using the LMM analysis (Table 4 - 1), revealed a rostro-caudal level * time point interaction ($F_{(63,\ 193.802)} = 1.936$, p<.0. 000), a rostro-caudal level (raphe subregion) interaction ($F_{(36,\ 217.175)} = 29.372$, p< 0.000), a main effect of rostro-caudal level ($F_{(16,\ 174.634)} = 66.544$, p < 0.000), a main effect of raphe subregion ($F_{(5,\ 116{,}289)} = 78.887$, p< 0.000) and a main effect of time point ($F_{(4,\ 147.582)} = 3.891$, p< 0.000).

Based on this first overall LMM analysis, secondary LMMs were used to determine changes in the circadian activity of *tph2* mRNA expression after MPL treatment at each rostro-caudal level of all the subregions of the DR and in the MnR nucleus separately (Table 4 - 1). Additionally, changes across the rostro-caudal gradient at each time point were assessed, but for simplicity reasons, these changes are not represented in the Figures.

Table 4-1: Linear mixed model analysis results for tph2 mRNA expression in MPL treated SD male rats

Model	Test statistic	*p*-value
Overall analysis for MPL		
Heterogeneous toeplitz covariance structure		
Akaike's Information Criterion (AIC): 8076.794		
Rostrocaudal level[1] (1-17)	$F_{(16, 174.634)} = 66.544$	.000 ***
Raphe subregion[2] (DRC, DRI, DRD, DRV, DRVL/VLPAG, MnR)	$F_{(5, 116,289)} = 78.887$	.000 ***
Time point[3] (3 am, 9 am, 3 pm, 6 pm, 9 pm)	$F_{(4, 147.582)} = 3.891$	.005 **
Rostrocaudal level * Time point	$F_{(63, 193.802)} = 1.936$	.000***
Raphe subregion * Time point	$F_{(20, 116.431)} = .349$	.996
Rostrocaudal level (Raphe subregion)	$F_{(36, 217.175)} = 29.372$	.000 ***
Rostrocaudal level * Time point (Raphe subregion)	$F_{(143, 240.602)} = .714$	.986
Subregional analyses		
DRC		
ARMA (1.1) covariance structure		
Akaike's Information Criterion (AIC): 584.683		
Time point (3 am, 9 am, 3 pm, 6 pm, 9 pm)	$F_{(4, 39.358)} = .689$	.604
Rostrocaudal level (13-17)	$F_{(4, 71.002)} = 7.420$	.000 ***
Time point * Rostrocaudal level	$F_{(16, 68.002)} = .661$	.821
DRI		
Heterogeneous Compound Symmetry covariance structure		
Akaike's Information Criterion (AIC): 387.937		
Time point (3 am, 9 am, 3 pm, 6 pm, 9 pm)	$F_{(4, 23.121)} = .706$	.596
Rostrocaudal level (14-17)	$F_{(3, 14.873)} = 64.337$	.000 ***
Time point * Rostrocaudal level	$F_{(12, 15.469)} = .848$	.608
DRD		
Unstructured covariance structure		
Akaike's Information Criterion (AIC): 1747.826		
Time point (3 am, 9 am, 3 pm, 6 pm, 9 pm)	$F_{(4, 33.913)} = 1.390$	.258
Rostrocaudal level (1-12)	$F_{(11, 29.175)} = 34.444$	.000 ***
Time point * Rostrocaudal level	$F_{(43, 31.1000)} = 1.766$	.050*
DRV		
Heterogeneous Toeplitz covariance structure		

Akaike's Information Criterion (AIC): 2203.095		
Time point (3 am, 9 am, 3 pm, 6 pm, 9 pm)	$F_{(4, 41.958)}$= 1.170	.338
Rostrocaudal level (1-14)	$F_{(13, 85.806)}$= 45.589	.000 ***
Time point * Rostrocaudal level	$F_{(51, 80.401)}$= 1.176	.254
DRVL/VLPAG		
Heterogeneous toeplitz covariance structure		
Akaike's Information Criterion (AIC): 1227.890		
Time point (3 am, 9 am, 3 pm, 6 pm, 9 pm)	$F_{(4, 23.978)}$= 1.943	.136
Rostrocaudal level (6-13)	$F_{(7, 50.969)}$= 46.764	.000 ***
Time point * Rostrocaudal level	$F_{(28, 55.769)}$= 1.642	.050 *
MnR		
Heterogeneous toeplitz covariance structure		
Akaike's Information Criterion (AIC): 1489.291		
Time point (3 am, 9 am, 3 pm, 6 pm, 9 pm)	$F_{(4, 31.202)}$= 1.429	.248
Rostrocaudal level (3-17)	$F_{(14, 59.923)}$= 18.527	.000 ***
Time point * Rostrocaudal level	$F_{(56, 61.674)}$= 1.730	.018 *

[1]Rostrocaudal levels were well-defined from bregma levels given in the atlas; where most rostral level was -7.328 mm bregma (1 according to level code) progressing to the most caudal level at –8.672 mm bregma (17 according to level code). Within this brain section 17 different and representative coronal sections of 12 µm were used to measure *tph2* mRNA of the dorsal raphe nucleus and the median raphe nucleus. [2]The Raphe subregions used in this research were the following: DRC, dorsal raphe nucleus, caudal part; DRI, dorsal raphe nucleus, interfascicular part; DRD, dorsal raphe nucleus, dorsal part; DRV, dorsal raphe nucleus, ventral part and DRVL/VLPAG, dorsal raphe nucleus, ventrolateral part/ventrolateral periaqueductal grey. MnR, median raphe nucleus was also included and considered as a subregion of the raphe complex. [3] The five different time points (3 am, 9 am, 3 pm, 6 pm, 9 pm) used in this study were considered as a suitable description of the circadian rhythm of *tph2* mRNA expression. They were chosen to fit in parallel with the measured circadian rhythm of plasma CORT after MPL treatment. *$p<0.05$. **$p<0.01$. ***$p<0.001$.

Another overall LMM analysis was performed to assess the changes in *tph2* mRNA expression profile under natural conditions and after MPL treatment (Table 4.2). The analysis revealed a treatment * timepoint interaction ($F_{(4, 409.745)}$ = 4.732, p< 0.001), a treatment * rostro-caudal level interaction ($F_{(16, 300.823)}$ = 5.733, p <0.000), a timepoint* rostro-caudal level interaction ($F_{(64, 290.087)}$ = 2.022, p< 0.000), a rostro-caudal level * raphe subregion interaction ($F_{(36, 338.936)}$ = 55.640, p< 0.000), a treatment * time point * rostro-caudal level interaction ($F_{(62, 321.711)}$ = 1.618, p<0.004) a treatment *rostro-caudal level (raphe subregion interaction) ($F_{(36, 341.576)}$ = 1.653, p < 0.013), a main effect in timepoint ($F_{(4, 356.439)}$ = 6.124, p < 0.000), a

main effect in rostro-caudal level ($F_{(16, 283.275)} = 215.876$, $p < 0.000$) and a main effect in raphe subregion ($F_{(5, 232.201)} = 302.652$, $p < 0.000$).

Based on the findings of this second overall LMM analysis, secondary LMMs were used to determine changes in the circadian activity of *tph2* mRNA expression between control animals and MPL treated animals at each rostro-caudal level of all the subregions of the DR and in the MnR nucleus separately (Table 4.2). Additionally, changes across the rostro-caudal gradient at each time point were also assessed, but for simplicity reasons, these changes are not represented in the Figures.

Table 4-2: Linear mixed model analysis results for tph2 mRNA expression in Control vs MPL treated SD male rats.

Model	**Test statistic**	***p*-value**
Overall analysis for Controls vs MPL		
First Order Ante-dependence covariance structure		
Akaike's Information Criterion (AIC): 16068.671		
Treatment[1] (CTRL vs MPL)	$F_{(1, 351.113)} = .537$	.464
Time point[2] (3 am, 9 am, 3 pm, 6 pm, 9 pm)	$F_{(4, 356.439)} = 6.124$	.000 ***
Rostrocaudal level[3] (1-17)	$F_{(16, 283.275)} = 215.876$	.000 ***
Raphe subregion[4] (DRC, DRI, DRD, DRV, DRVL/VLPAG, MnR)	$F_{(5, 232.201)} = 302.652$	.000 ***
Treatment * Time point	$F_{(4, 409.745)} = 4.732$	.001 **
Treatment * Rostrocaudal level	$F_{(16, 300.823)} = 5.733$	.000 ***
Treatment * Raphe subregion	$F_{(5, 232.913)} = .651$	.661
Time point * Rostrocaudal level	$F_{(64, 290.087)} = 2.022$	.000 ***
Time point * Raphe subregion	$F_{(20, 238.828)} = .506$	.963
Rostrocaudal level * Raphe subregion	$F_{(36, 338.936)} = 55.640$	.000 ***
Treatment * Time point * Raphe subregion	$F_{(20, 255.376)} = .597$	.913
Treatment * Time point * Rostrocaudal level	$F_{(62, 321.711)} = 1.618$	.004 **
Treatment * Rostrocaudal level (Raphe subregion)	$F_{(36, 341.576)} = 1.653$	.013 *
Time point * Rostrocaudal level (Raphe subregion)	$F_{(144, 349.080)} = 1.082$	.280
Treatment * Time point * Rostrocaudal level (Raphe subregion)	$F_{(140, 394.304)} = .863$	.847
Subregional analyses		
DRC		

First-Order Factor Analytic (Heterogeneous Diagonal Offset) covariance structure		
Akaike's Information Criterion (AIC): 1034.172		
Treatment (CTRL vs. MPL)	$F_{(1, 61.455)} = .516$	.475
Time point (3 am, 9 am, 3 pm, 6 pm, 9 pm)	$F_{(4, 60.141)} = .784$	.540
Rostrocaudal level (13-17)	$F_{(4, 25.611)} = 12.056$	.000 ***
Treatment * Timepoint	$F_{(4, 63.833)} = .852$	.498
Treatment * Rostrocaudal level	$F_{(4, 26.066)} = .995$	.428
Timepoint * Rostrocaudal level	$F_{(16, 26.414)} = .810$	.664
Treatment * Time point * Rostrocaudal level	$F_{(15, 31.158)} = .978$	.499
DRI		
Heterogeneous Compound Symmetry covariance structure		
Akaike's Information Criterion (AIC): 649.113		
Treatment (CTRL vs. MPL)	$F_{(1, 109.619)} = 2.239$	.137
Time point (3 am, 9 am, 3 pm, 6 pm, 9 pm)	$F_{(4, 105.220)} = 1.453$	.222
Rostrocaudal level (14-17)	$F_{(3, 60.618)} = 131.772$	.000 ***
Treatment * Timepoint	$F_{(4, 108.435)} = .374$	.827
Treatment * Rostrocaudal level	$F_{(3, 61.606)} = 1.572$	.205
Timepoint * Rostrocaudal level	$F_{(12, 69.887)} = 1.433$	.172
Treatment * Time point * Rostrocaudal level	$F_{(11, 72.481)} = .445$	.930
DRD		
Heterogeneous Toeplitz covariance structure		
Akaike's Information Criterion (AIC): 3464.719		
Treatment (CTRL vs. MPL)	$F_{(, 75.932)} = .239$	.626
Time point (3 am, 9 am, 3 pm, 6 pm, 9 pm)	$F_{(4, 75.890)} = 1.544$	.198
Rostrocaudal level (1-12)	$F_{(11, 160.823)} = 79.774$	.000 ***
Treatment * Timepoint	$F_{(4, 76.287)} = 2.143$	.084
Treatment * Rostrocaudal level	$F_{(11, 161.877)} = 5.716$	.000 ***
Timepoint * Rostrocaudal level	$F_{(44, 164.029)} = 1.755$	.006 **
Treatment * Time point * Rostrocaudal level	$F_{(43, 161.864)} = 1.260$	.154
DRV		
First Order Ante-Dependence covariance structure		
Akaike's Information Criterion (AIC): 4452.248		
Treatment (CTRL vs. MPL)	$F_{(1, 128.354)} = .226$	.635
Time point (3 am, 9 am, 3 pm, 6 pm, 9 pm)	$F_{(4, 127.897)} = 1.646$	.167
Rostrocaudal level (1-14)	$F_{(13, 118.533)} = 142.081$	.000 ***
Treatment * Timepoint	$F_{(4, 127.790)} = 2.715$	.033*
Treatment * Rostrocaudal level	$F_{(13, 116.938)} = 2.020$	.025*
Timepoint * Rostrocaudal level	$F_{(52, 120.436)} = 1.433$	.055
Treatment * Time point * Rostrocaudal level	$F_{(51, 117.394)} = 1.165$	.249

DRVL/VLPAG		
Heterogeneous Toeplitz covariance structure		
Akaike's Information Criterion (AIC): 2514.414		
Treatment (CTRL vs. MPL)	$F_{(1, 69.248)} = .186$	.668
Time point (3 am, 9 am, 3 pm, 6 pm, 9 pm)	$F_{(4, 69.241)} = 1.216$	.312
Rostrocaudal level (6-13)	$F_{(7, 129.116)} = 98.770$	.000 ***
Treatment * Timepoint	$F_{(4, 69.241)} = 3.003$	.024 *
Treatment * Rostrocaudal level	$F_{(7, 129.116)} = 11.427$	.000 ***
Timepoint * Rostrocaudal level	$F_{(28, 133.506)} = 1.128$	.317
Treatment * Time point * Rostrocaudal level	$F_{(28, 133.506)} = 1.523$	.060
MnR		
Unstructured covariance structure		
Akaike's Information Criterion (AIC): 2894.013		
Treatment (CTRL vs. MPL)	$F_{(1, 68.239)} = .293$	.590
Time point (3 am, 9 am, 3 pm, 6 pm, 9 pm)	$F_{(4, 68.682)} = 1.460$	.224
Rostrocaudal level (3-17)	$F_{(12, 63.075)} = 66.963$	.000 ***
Treatment * Timepoint	$F_{(4, 67.977)} = 1.570$	.192
Treatment * Rostrocaudal level	$F_{(12, 64.094)} = 3.315$	.001 **
Timepoint * Rostrocaudal level	$F_{(48, 65.953)} = 2.810$	.000 ***
Treatment * Time point * Rostrocaudal level	$F_{(47, 66.745)} = 2.425$	.000 ***

[1]Two different treatment groups (n≤40/group) were considered in this study; Controls and MPL treated SD male rats.[2]The five different time points (3 am, 9 am, 3 pm, 6 pm, 9 pm) used in this study were considered as a suitable description of the circadian rhythm of *tph2* mRNA expression. They were chosen to fit in parallel with the measured circadian rhythm of plasma CORT. [3]Rostrocaudal levels were well-defined from bregma levels given in the atlas; where most rostral level was -7.328 mm bregma (1 according to level code) progressing to the most caudal level at –8.672 mm bregma (17 according to level code). Within this brain section 17 different and representative coronal sections of 12 µm were used to measure *tph2* mRNA of the dorsal raphe nucleus and the median raphe nucleus. [4]The Raphe subregions used in this research were the following: DRC, dorsal raphe nucleus, caudal part; DRI, dorsal raphe nucleus, interfascicular part; DRD, dorsal raphe nucleus, dorsal part; DRV, dorsal raphe nucleus, ventral part and DRVL/VLPAG, dorsal raphe nucleus, ventrolateral part/ventrolateral periaqueductal grey. MnR, median raphe nucleus was also included and considered as a subregion of the Raphe complex. *$p<0.05$. **$p<0.01$. ***$p<0.001$.

4.3.4.1 Dorsal Raphe nucleus (DRC)

Secondary LMM analysis within the DRC revealed a main effect of rostro-caudal level ($F_{(4, 71.002)} = 7.420$, $p < 0.000$), but no effect of time ($F_{(4, 39.358)} = .689$, $p > 0.05$) or interaction ($F_{(16, 68.002)} = .661$, $p > 0.05$) was found (Table 4-1) (Figure 4 -18). Therefore, no circadian variation in *tph2* expression was detected in the DRC after MPL treatment, even with this full rostro-caudal gradient analysis.

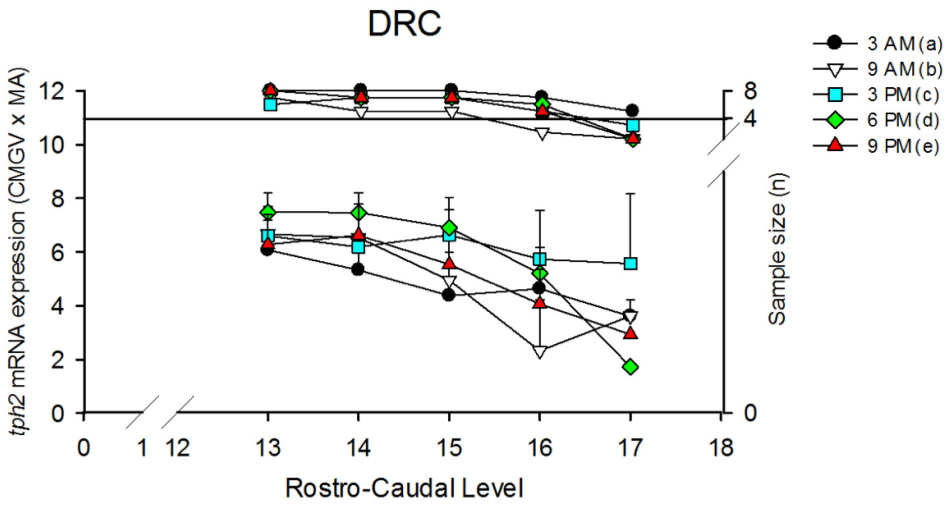

Figure 4-18: Rostro-caudal level variation of tph2 mRNA expression profile in the DRC of MPL treated animals. Tph2 mRNA expression in the DRC was measured in five different rostro-caudal levels presented in the x axis (-8.336 to -8.672 mm bregma). Five different timepoints; (a) 3 am, (b) 9 am, (c) 3 pm, (d) 6 pm and (e) 9 pm are shown for each rostro-caudal level. The left y-axis shows Tph2 mRNA expression (Calibrated Mean Grey Value multiplied by its own Measured Area). Upper segmented area is associated to the right y-axis that represents the post Grubb's test sample size at each rostro-caudal level. Fisher's Least Significant difference test were not performed.

An additional secondary LMM analysis was performed for the DRC, which evaluated the changes between control and MPL groups (Table 4-2). This analysis revealed only a significant difference in rostro-caudal level ($F_{(4, 25.611)} = 12.056$, $p < 0.000$) and no other main effect or interaction so further post tests were not performed for this region.

As shown in Figure 4-19 the DRC, appeared to have no significant changes in *tph2* mRNA expression at any timepoint or rostro-caudal level as a result of MPL treatment.

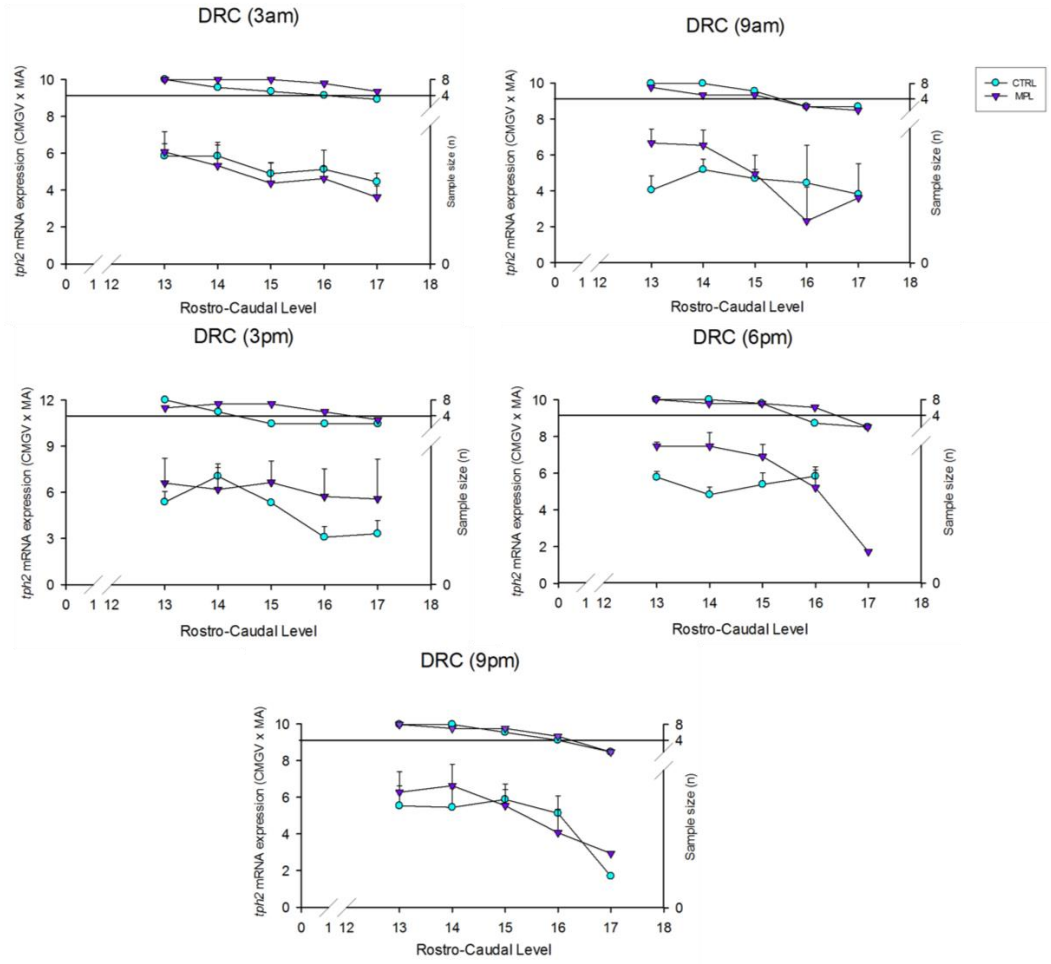

Figure 4-19: Circadian changes in tph2 mRNA expression at each rostro-caudal level in the DRC of Controls versus MPL treated animals. Tph2 mRNA expression in the DRC was measured in five different rostro-caudal levels presented in the x axis (-8.336 to -8.672 mm bregma) at five different time points; (A) 3 am, (B) 9 am, (C) 3 pm, (D) 6 pm and (E) 9 pm. Tph2 mRNA quantification is expressed as Calibrated Mean Grey Value multiplied by its own Measured Area. Top data points are associated to the right y-axis which represent the after Grubb's test sample size at each rostro-caudal level. Bottom data points are linked to the left y-axis which correspond to the MEAN ± SEM of tph2 mRNA expression for each group (CTRL or MPL [n≤8/each group]) at each of the five rostro-caudal levels of the DRC. Fisher's Least Significant Difference were not performed.

4.3.4.2 Dorsal Raphe nucleus, interfascicular part (DRI)

Secondary LMM analysis within the DRI revealed a significant main effect of rostro-caudal level ($F_{(3, 14.873)}$= 64.337, p <0.000), but no effect of time ($F_{(4, 23.121)}$= .706, $p> 0.05$) or interaction ($F_{(12, 15.469)}$= .848, $p> 0.05$) (Table 4-1). Thus, as observed in Figure 4-20, it appeared that no circadian variation in *tph2* mRNA expression in the

DRI during MPL treatment can be detected, even when examining the full rostro-caudal gradient.

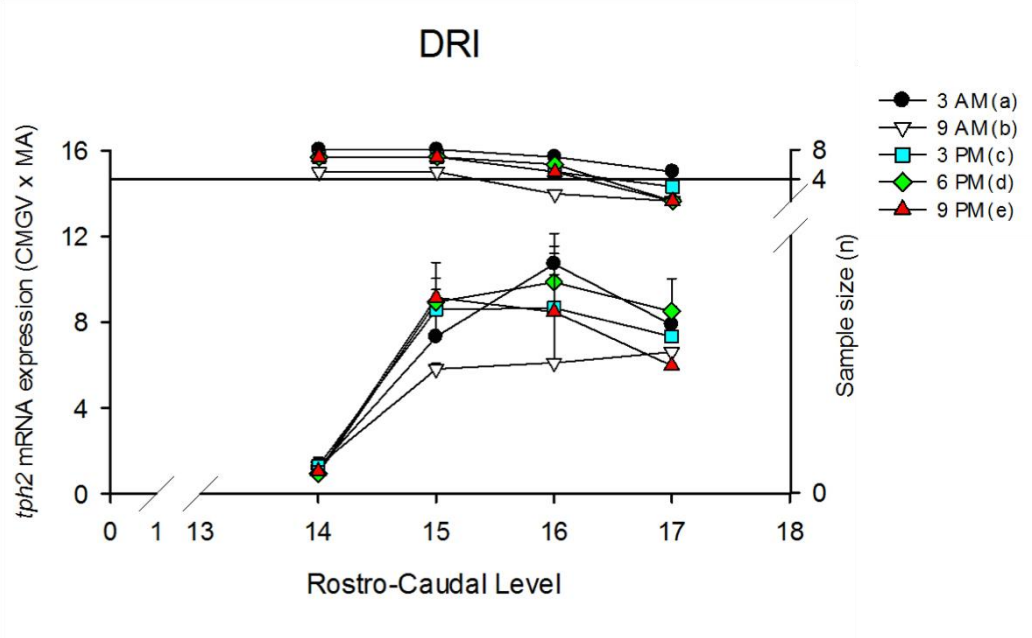

Figure 4-20: Rostro-caudal level variation of tph2 mRNA expression profile in the DRI of MPL treated animals. Tph2 mRNA expression in the DRI was measured in four different rostro-caudal levels presented in the x axis (-8.420 to -8.672 mm bregma). Five different timepoints; (a) 3 am, (b) 9 am, (c) 3 pm, (d) 6 pm and (e) 9 pm are shown for each rostro-caudal level. The left y-axis shows Tph2 mRNA expression (Calibrated Mean Grey Value multiplied by its own Measured Area). Upper segmented area is associated to the right y-axis that represents the post Grubb's test sample size at each rostro-caudal level. Fisher's Least Significant difference test were not performed.

An additional secondary LMM analysis was performed for the DRI to determine if there was any effect of MPL treatment compared to controls at any of the time points assessed. This analysis again revealed only a significant effect in rostro-caudal level ($F_{(3,\ 60.618)}$= 131.772, p< 0.000) with no other main effect or interaction (Table 4-2). Therefore, no post-tests were performed. The DRI appeared to be insensitive to change over the circadian period or with MPL treatment, even when analysed throughout the full rostro-caudal gradient, as can be observed in Figure 4-21.

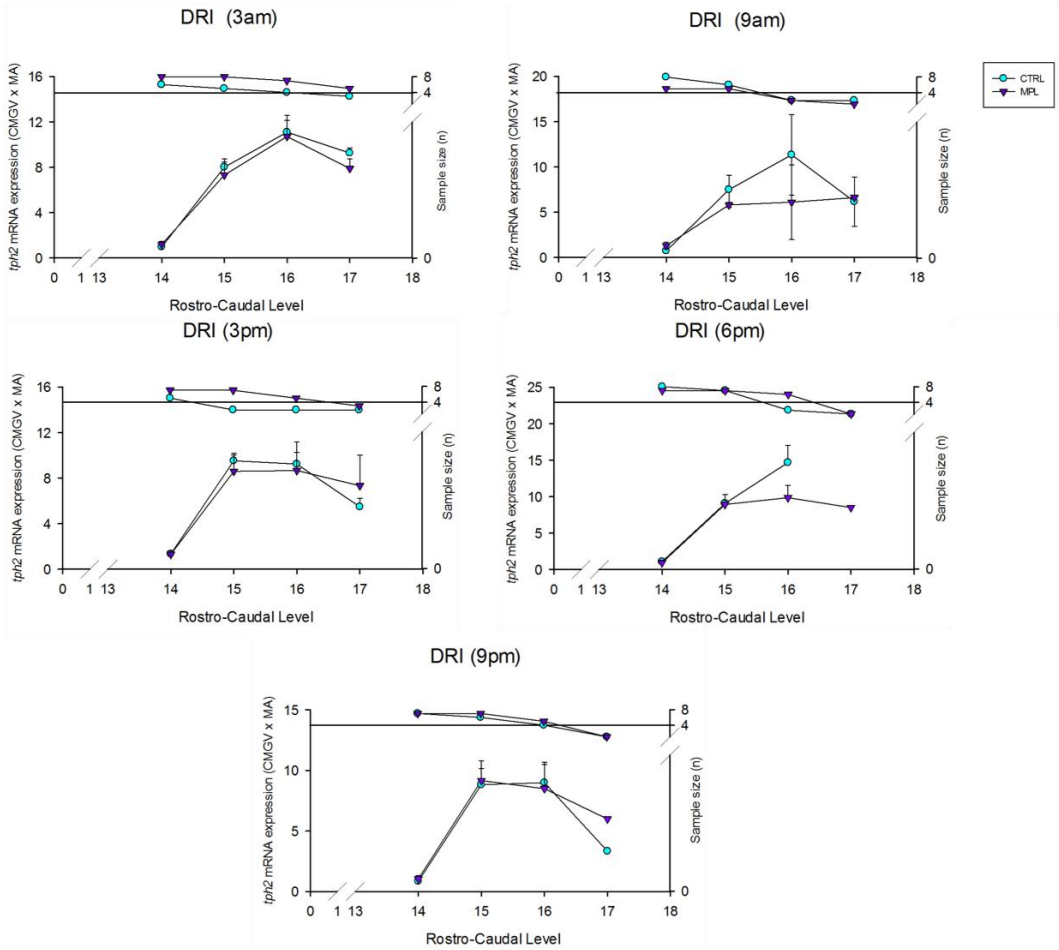

Figure 4-21: Circadian changes in tph2 mRNA expression at each rostro-caudal level in the DRI of Controls versus MPL treated animals. Tph2 mRNA expression in the DRI was measured in four different rostro-caudal levels presented in the x axis (-8.420 to -8.672mm bregma) at five different time points; (A) 3 am, (B) 9 am, (C) 3 pm, (D) 6 pm and (E) 9 pm. Tph2 mRNA quantification is expressed as Calibrated Mean Grey Value multiplied by its own Measured Area. Top data points are associated to the right y-axis which represent the after Grubb's test sample size at each rostro-caudal level. Bottom data points are linked to the left y-axis which correspond to the MEAN ± SEM of tph2 mRNA expression for each group (CTRL or MPL [n≤ 8/each group]) at each of the four rostro-caudal level of the DRI. Fisher's Least Significant Difference post hoc test were not performed.

4.3.4.3 Dorsal Raphe nucleus, dorsal part (DRD).

Secondary LMM analysis within the DRD revealed a significant main effect of rostro-caudal level ($F_{(11,\ 29.175)}$= 34.444, p<0.000) but no main effect of time ($F_{(4,\ 33.913)}$= 1.390, p>0.05). However, a significant interaction between rostro-caudal level and time was detected ($F_{(43,\ 31.1000)}$= 1.766, p= 0.050) (Table 4-1). Subsequent post tests revealed a few notable significant differences in *tph2* mRNA expression between time points, at defined rostro-caudal levels as shown in Figure 4-22.

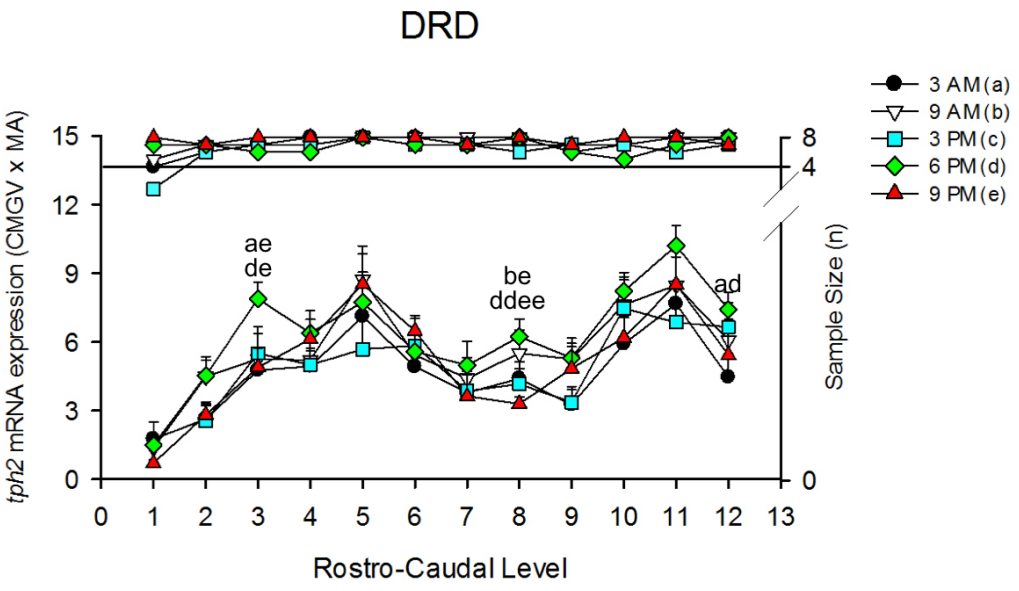

Figure 4-22: Rostro-caudal level variation of tph2 mRNA expression profile in the DRD of MPL treated animals. Tph2 mRNA expression in the DRD was measured in twelve different rostro-caudal levels presented in the x axis (-7.328 to -8.252 mm bregma). Five different timepoints; (a) 3 am, (b) 9 am, (c) 3 pm, (d) 6 pm and (e) 9 pm are shown for each rostro-caudal level. The left y-axis shows Tph2 mRNA expression (Calibrated Mean Grey Value multiplied by its own Measured Area). Upper segmented area is associated to the right y-axis that represents the post Grubb's test sample size at each rostro-caudal level. Fisher's Least Significant difference test results are indicated on graph and are annotated by a to e for each time point as shown in the plot key. Additionally, double letters indicate p<0.01 and simple letters p<0.05. Here (ddee) indicates a significant difference for 6 pm vs 9 pm, (ad) for 3 am vs 6 pm, (ae) for 3 am vs 9 pm, (be) for 9 am vs 9 pm, (de) 6 pm vs 9 pm.

A further secondary LMM analysis was performed to additionally assess the effect of MPL treatment compared to controls (Table 4-2). This analysis revealed a treatment * rostro-caudal level interaction ($F_{(11,\ 161.877)}$= 5.716, p< 0.000), a timepoint * rostro-caudal level interaction ($F_{(44,\ 164.029)}$= 1.755, p< 0.06) as well as a main effect in rostro-caudal level ($F_{(11,\ 160.823)}$ = 79.774, p< 0.000) (Table 4-2). Multiple comparisons post-tests found significant differences between MPL and controls at all time points except for 9 pm, as indicated on the graphs (Figure 4 - 23). Despite the observed increase at 9 am in the MPL treated group across nearly all levels (Figure 4 - 23B), a decrease at 3 pm with MPL across levels 3-9 (Figure 4 - 23C), and an increase with MPL at 6 pm at levels 8, 10, 11 and12 (Figure 4 - 23D), many of these changes were only significant at one or two bregma levels, as indicated on the graphs. Taken together however, these findings are fundamentally

consistent with our initial observation for the DRD (Figure 4 - 11) with an elevated nadir at the 9 am point and a loss of peak expression at the 3 pm point with MPL treatment.

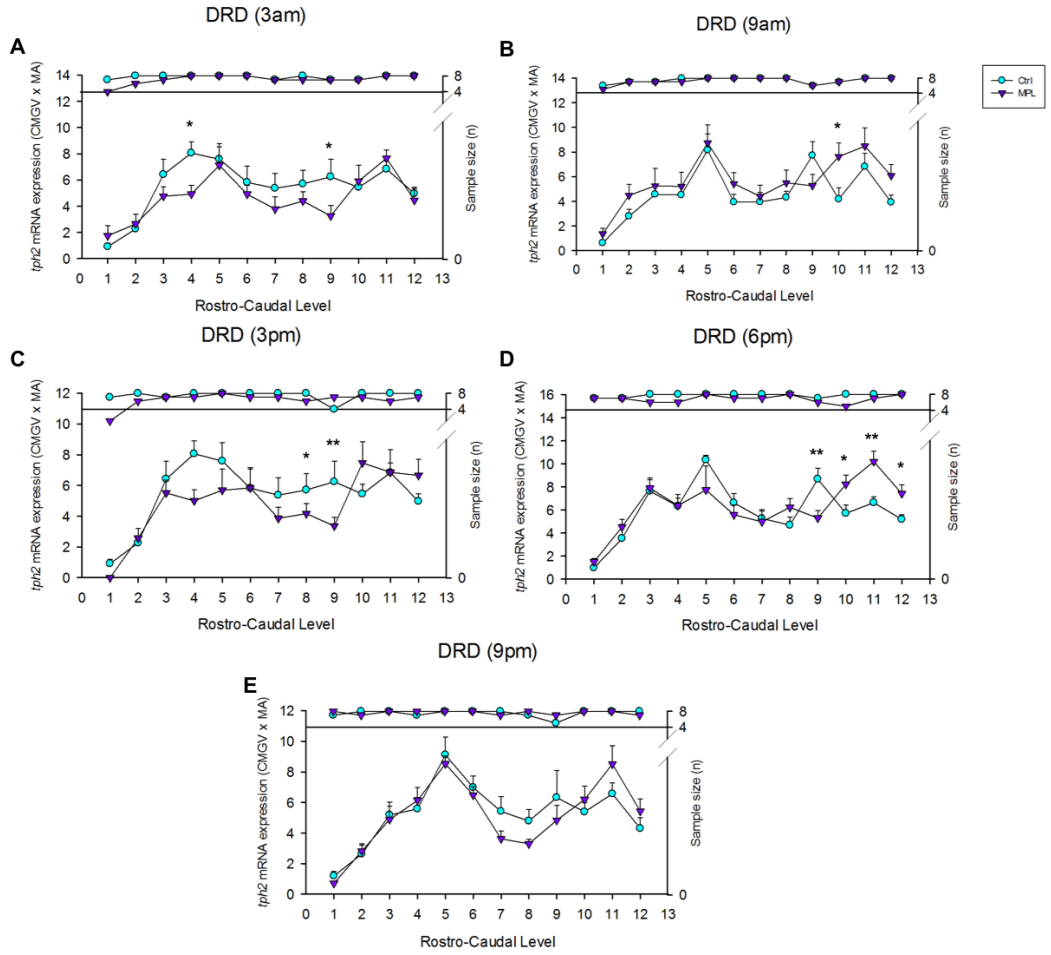

*Figure 4-23: Circadian changes in tph2 mRNA expression at each rostro-caudal level in the DRD of Controls vs MPL treated animals. Tph2 mRNA expression in the DRD was measured in twelve different rostro-caudal levels presented in the x axis (-7.328 to -8.252 mm bregma) at five different time point: (A) 3am, (B) 9 am, (C) 3 pm, (D) 6 pm and (E) 9 pm. Tph2 mRNA quantification is expressed as Calibrated Mean Grey Value multiplied by its own Measured Area. Top data points are associated to the right y-axis which represent the after Grubb's test sample size at each rostro-caudal level. Bottom data points are linked to the left y-axis which correspond to the MEAN ± SEM of tph2 mRNA expression for each group (CTRL or MPL [n≤ 8/each group]) at each of the twelve rostro-caudal level of the DRD. Fisher's Least Significant Difference post hoc test showed the following significant differences; (A) *p< 0.05 for CTRL vs MPL in level 4 and 9 at 3 am; (B) *p< 0.05 for CTRL vs MPL in level 10 at 9 am; (C) **p<0.01 for CTRL vs MPL in level 9 and *p< 0.05 in level 8 at 3 pm; (D) **p< 0.01 for CTRL vs MPL in level 9 and 11, and *p< 0.05 in level 10 and 12 at 6 pm; (E) ns at 9 pm.*

4.3.4.4 Dorsal Raphe nucleus, ventral part (DRV).

Secondary LMM analysis was also performed within the DRV and it showed only a main effect in rostro-caudal level ($F_{(13, 85.806)}$= 45.589, p< 0.000), without effect of time ($F_{(4, 41.958)}$= 1.170, p> 0.05) or interaction ($F_{(51, 80.401)}$= 1.176, p> 0.05) (Table 4 - 1). Therefore, as no circadian variation in *tph2* mRNA expression was detected, no post-tests were performed for the DRV time course data (Figure 4 - 24). Interestingly this lack of circadian variation during MPL treatment, within the full rostro-caudal gradient of the DRV, was consistent with the lack of circadian variation noted in the averaged data from the whole, rostral and caudal DRV (Figures 4 - 12,).

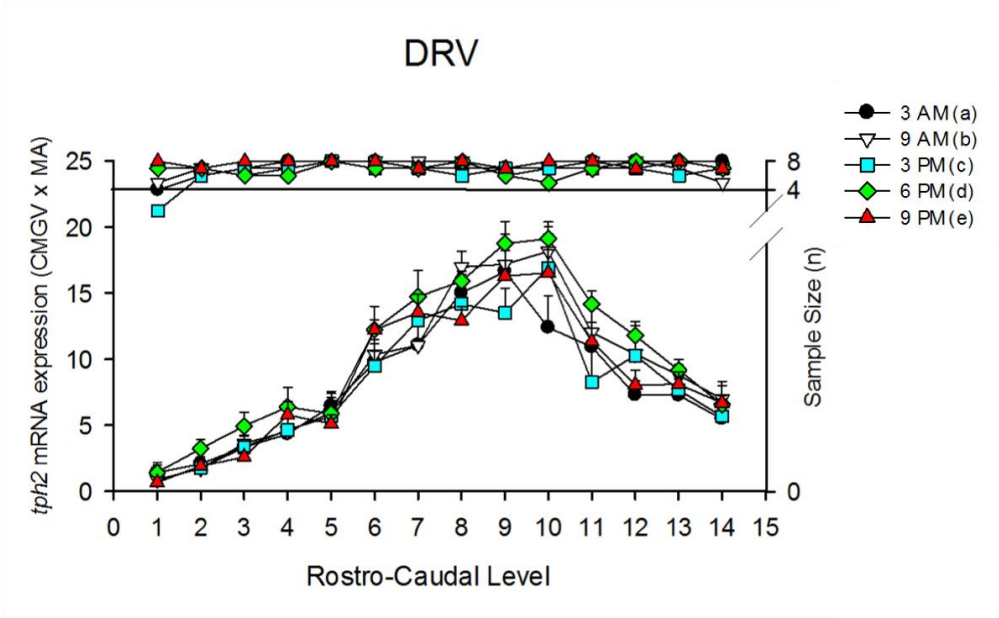

Figure 4-24: Rostro-caudal level variation of tph2 mRNA expression profile in the DRV of MPL treated animals. Tph2 mRNA expression in the DRV was measured in fourteen different rostro-caudal levels presented in the x axis (-7.328 to -8.420 mm bregma). Five different timepoints; (a) 3 am, (b) 9 am, (c) 3 pm, (d) 6 pm and (e) 9 pm are shown for each rostro-caudal level. The left y-axis shows Tph2 mRNA expression (Calibrated Mean Grey Value multiplied by its own Measured Area). Upper segmented area is associated to the right y-axis that represents the post Grubb's test sample size at each rostro-caudal level. Fisher's Least Significant difference test showed no significant differences.

An additional secondary LMM analysis was performed for the DRV to interrogate whether there was a significant effect of MPL treatment compared to controls. This analysis revealed a main effect in rostro-caudal level ($F_{(13, 118.533)}$= 142.081, p< 0.000),

a treatment * timepoint interaction ($F_{(4, 127.790)}$= 2.715, p< 0.05) and a treatment * rostro-caudal level interaction ($F_{(13, 116.938)}$= 2.020, p< 0.05) (Table 4-2). Subsequent post-tests confirmed that the differences observed (Figure 4-25) between MPL and controls at each time point were significant in at least one bregma level. Notably, a higher *tph2* mRNA expression in the MPL group was observed (Figure 4-25B) at 9 am, albeit only significant at rostro-caudal level 10 (p< 0.01). A lower *tph2* mRNA expression was observed in the MPL group at 3 pm, significantly at level 9 (p < 0.01) and level 11 (p < 0.01). A higher *tph2* mRNA expression was observed at 6pm in the MPL group, significantly at level 10 (p< 0.01). Taken together, these data are consistent with MPL treatment inducing a raised nadir in *tph2* mRNA expression in the caudal DRV at 9 am, and a loss of the 3 pm peak, also demonstrated in the mean data analysis shown in Figure 4.13.

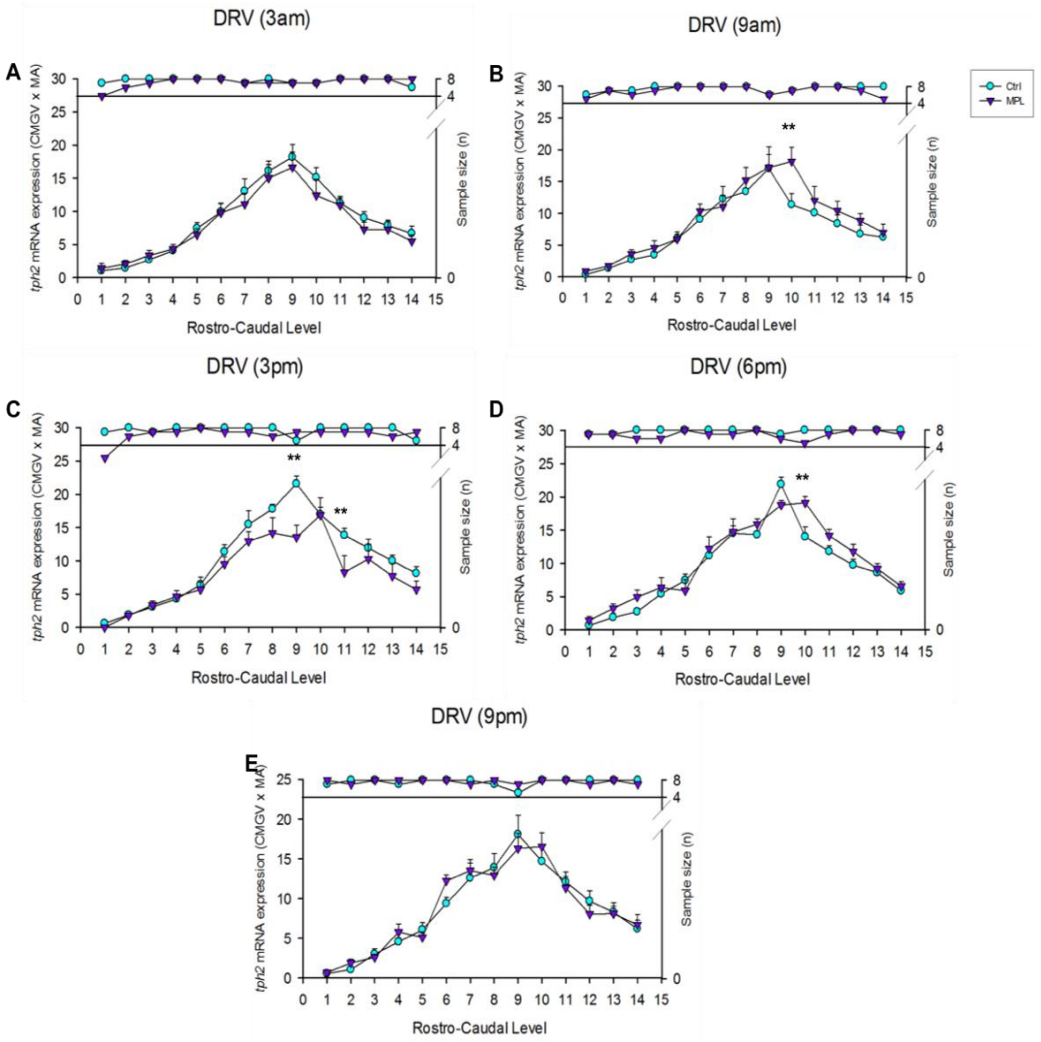

*Figure 4-25: Circadian changes in tph2 mRNA expression at each rostro-caudal level expression in the DRV of Controls vs MPL treated animals. Tph2 mRNA expression in the DRV was measured in fourteen different rostro-caudal levels presented in the x axis (-7.328 to -8.420 mm bregma) at five different time point: (A) 3 am, (B) 9 am, (C) 3 pm, (D) 6 pm and (E) 9 pm. Tph2 mRNA quantification is expressed as Calibrated Mean Value multiplied by its own Measured Area. Top data points are associated to the right y-axis which represent the after Grubb's test sample size at each rostro-caudal level. Bottom data points are linked to the left y-axis which correspond to the MEAN ± SEM of tph2 mRNA expression for each group (CTRL or MPL [n≤ 8/each group]) at each of the fourteen rostro-caudal level of the DRV. Fisher's Least Significant Difference post hoc test showed the following significant differences; (A) ns at 3 am; (B) **p< 0.01 for CTRL vs MPL in level 10 at 9 am; (C) **p< 0.01 for CTRL vs MPL in level 9 and 11 at 3 pm; (D) **p<0.01 for CTRL vs MPL in level 10 at 6 pm; (E) ns at 9 pm.*

4.3.4.5 Dorsal Raphe nucleus, ventrolateral part/ventrolateral periaqueductal grey (DRVL/VLPAG).

Secondary LMM analysis within the DRVL/VLPAG revealed a time point * rostro-caudal interaction ($F_{(28, 55.769)}$= 1.642, p< 0.050) and a main effect in rostro-caudal level ($F_{(7, 50.969)}$= 46.764, p<0.000) (Table 4-1). Fisher's LSD post tests revealed many significant differences in *tph2* mRNA expression between individual time points at each bregma level analysed, as indicated in Figure 4 - 26. Notably, 3am has the lowest expression across many of the levels assessed. Interestingly, 9 am had a higher *tph2* mRNA expression than all other timepoints across levels 8-10, although this was only significant at level 8 and level 10, as indicated in the graph. Conversely, 6pm had higher expression than all other timepoints across levels 11-13, although this was significant only at level 12 as indicated in the graph.

Therefore, a significant circadian variation in *tph2* mRNA expression was seen across the rostro-caudal gradient of the DRVL/VLPAG in the MPL treated animals, with a nadir at 3 am and a peak at 9am in the rostral levels, and a peak at 6pm in the caudal levels.

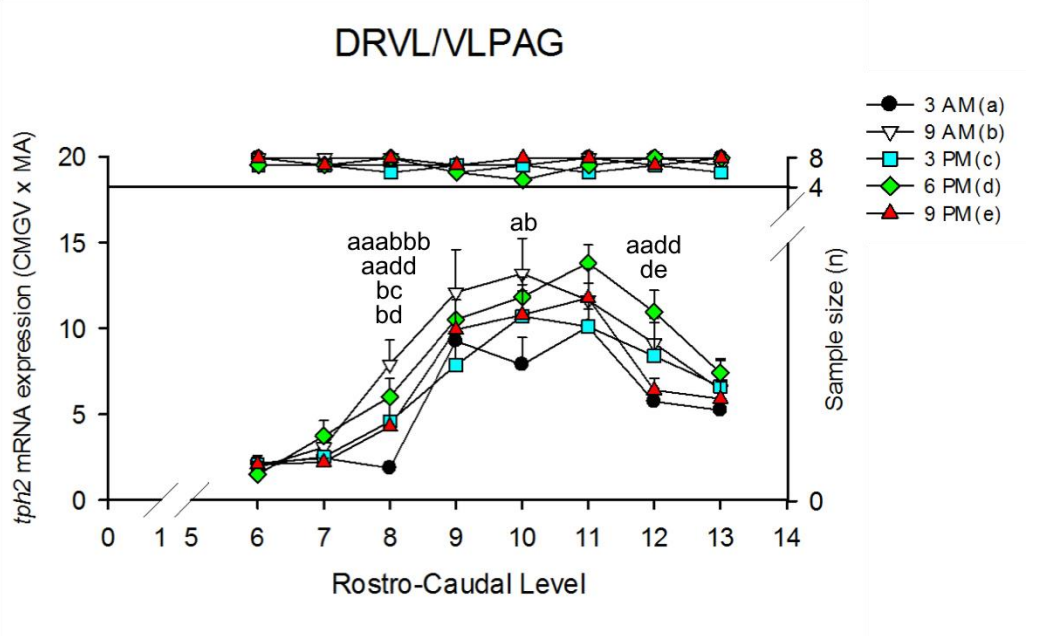

Figure 4-26: Rostro-caudal level variation of tph2 mRNA expression profile in the DRVL/VLPAG of MPL treated animals. Tph2 mRNA expression in the DRVL/VLPAG was

measured in eight different rostro-caudal levels presented in the x axis (-7.748 to -8.336 mm bregma). Five different timepoints; (a) 3 am, (b) 9 am, (c) 3 pm, (d) 6 pm and (e) 9 pm are shown for each rostro-caudal level. The left y-axis shows Tph2 mRNA expression (Calibrated Mean Grey Value multiplied by its own Measured Area). Upper segmented area is associated to the right y-axis that represents the post Grubb's test sample size at each rostro-caudal level. Fisher's Least Significant difference test results are indicated on graph and are annotated by a to e for each time point as shown in the plot key. Additionally, triple letters indicate p<0.001, double letters p<0.01 and simple letters p<0.05. Here, (aaabbb) indicates a significant difference for 3 am vs 9 am, (aadd) for 3 am vs 6 pm, (ab) for 3 am vs 9 am, (bc) for 9 am vs 3 pm, (be) for 9 am vs 9 pm, (de) for 6 pm vs 9 pm.

Additional secondary LMM analysis for DRVL/VLPAG was performed to assess for MPL treatment effects compared to controls. Analysis revealed a treatment * time point interaction ($F_{(4, 76.287)} = 2.143$, $p<0.024$), a treatment * rostro-caudal interaction ($F_{(7, 129.116)} = 11.427$, $p<0.000$) as well as the main effect in rostro-caudal level ($F_{(7, 129.116)} = 98.770$, $p< 0.000$) (Table 4 - 2). Interestingly, further Fisher's LSD tests (Figure 4 - 27) showed that changes after MPL treatment area observed across all timepoints and across the entire rostro-caudal gradient, which is consistent with data shown in the above (Figure 4-26). Additionally, a very interesting phenomenon is happening as a lower *tph2* mRNA expression was observed after MPL at 3 am and 3 pm in its rostral levels (Figure 4-27A, 4-27C) and changes in MnR caudal levels are observed at 9 am and 6 pm (Figure 4-27B, 4-27D). Although not all levels reach statistical significance, there is a strong trend in the data that follows the given observation. Moreover, this observation is consistent with the observed effect in Figure 4-15 as it strongly coincides with the low time points of expression (3 am and 3 pm) and with the peak times at 9 am and 6 pm.

Consequently, a change in the circadian variation of *tph2* mRNA expression as a result of MPL treatment can be confidently concluded here for the DRVL/VLPAG. These changes are characterised by the recurring theme of elevated *tph2* mRNA expression at 9 am, and loss of peak expression at 3 pm with MPL treatment, although there is an increased complexity as we observe how these alterations are localised within the rostro-caudal levels of the DRVL/VLPAG.

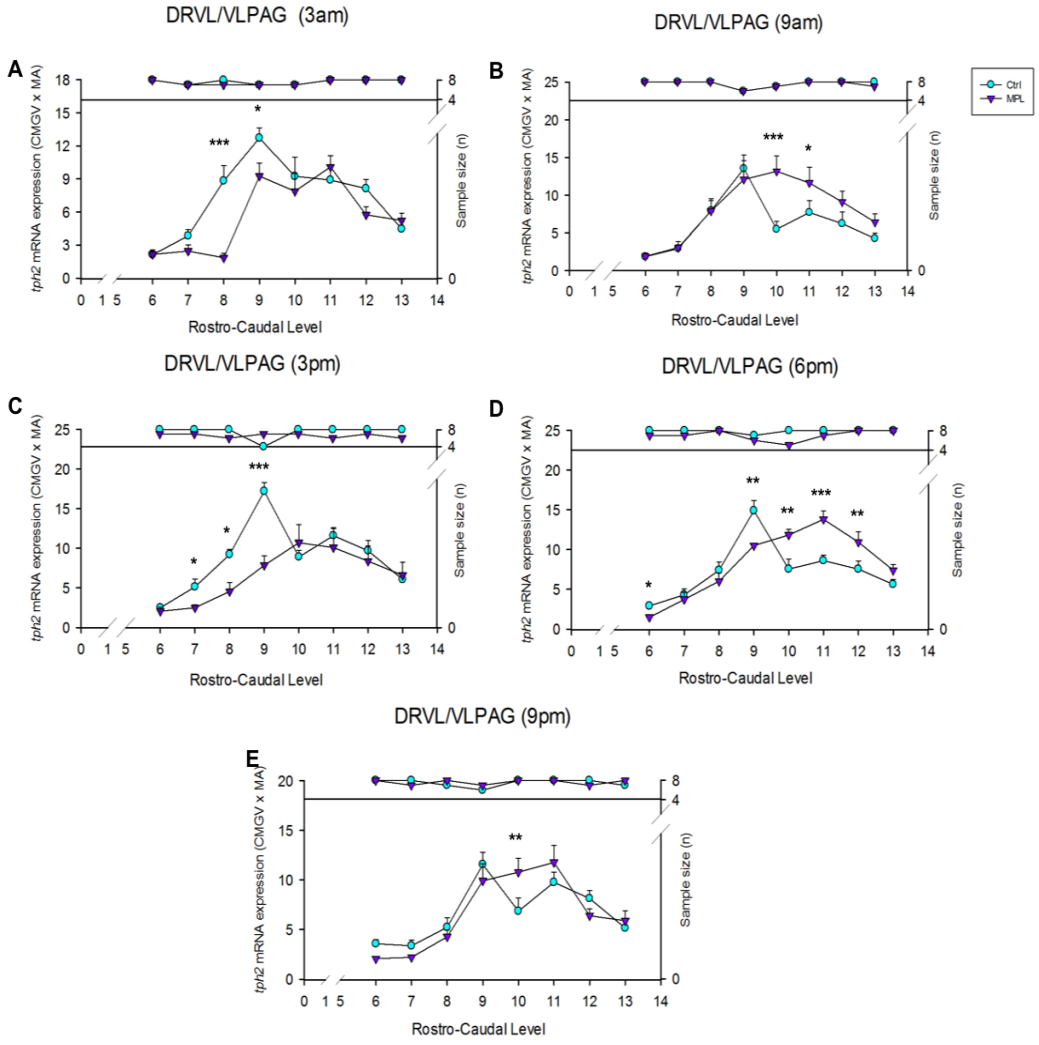

*Figure 4-27: Circadian changes in tph2 mRNA expression at each rostro-caudal level expression in the DRVL/VLPAG of Controls vs MPL treated animals. Tph2 mRNA expression in the DRVL/VLPAG was measured in eight different rostro-caudal levels presented in the x axis (-7.748 to -8.336 mm bregma) at five different time point: (A) 3am, (B) 9 am, (C) 3 pm, (D) 6 pm and (E) 9 pm. Tph2 mRNA quantification is expressed as Calibrated Mean Grey Value multiplied by its own Measured Area. Top data points are associated to the right y-axis which represent the after Grubb's test sample size at each rostro-caudal level. Bottom data points are linked to the left y-axis which correspond to the MEAN ± SEM of tph2 mRNA expression for each group (CTRL or MPL [n≤8/each group]) at each of the eight rostro-caudal level of the DRVL/VLPAG. Fisher's Least Significant Difference post hoc test showed the following significant differences; (A)***p< 0.001 for CTRL vs MPL in level 8 and *p< 0.05 in level 9 at 3 am; (B) ***p< 0.001 for CTRL vs MPL in level 10 and *p< 0.05 in level 11 at 9 am; (C) ***p< 0.001 for CTRL vs MPL in level 9 and *p< 0.05 in level 7 and 8 at 3 pm; (D) ***p< 0.001 for CTRL vs MPL in level 11, **p<0.01 in level 9, 10 and 12, and *p< 0.05 in level 6 at 6 pm; (E) **p<0.01 for CTRL vs MPL in level 10 at 9 pm.*

4.3.4.6 Median Raphe nucleus (MnR).

To complete the study of the natural circadian rhythm of *tph2* mRNA expression after MPL treatment a final secondary LMM analysis within the MnR was performed. This analysis revealed a time point * rostro-caudal level interaction ($F_{(56, 61.674)}$ = 1.730, p< 0.018) and a main effect in rostro-caudal level ($F_{(14, 59.923)}$ = 18.527, p< 0.001) (Table 4-1). Fisher's LSD post-tests revealed several significant differences in *tph2* mRNA expression between timepoints. *Tph2* mRNA expression after MPL treatment changed in five different rostro-caudal levels, as indicated in Figure 4-28. These observed changes are mainly related to the peak in expression at 6 pm and the 9 am nadir. Interestingly, this peak in expression also seemed to be different from the 3 pm point which showed low levels of expression in different levels of the MnR. Strangely, only in one single level (-8.000 mm bregma) the 3 am point was increased when compared the other time points, however, one isolated point like this is more likely to be related to a technical issue and therefore less likely to be of functional significance. Thus, a circadian variation in *tph2* mRNA expression across the rostro-caudal gradient can be clearly observed in the MnR nucleus as a result of MPL treatment.

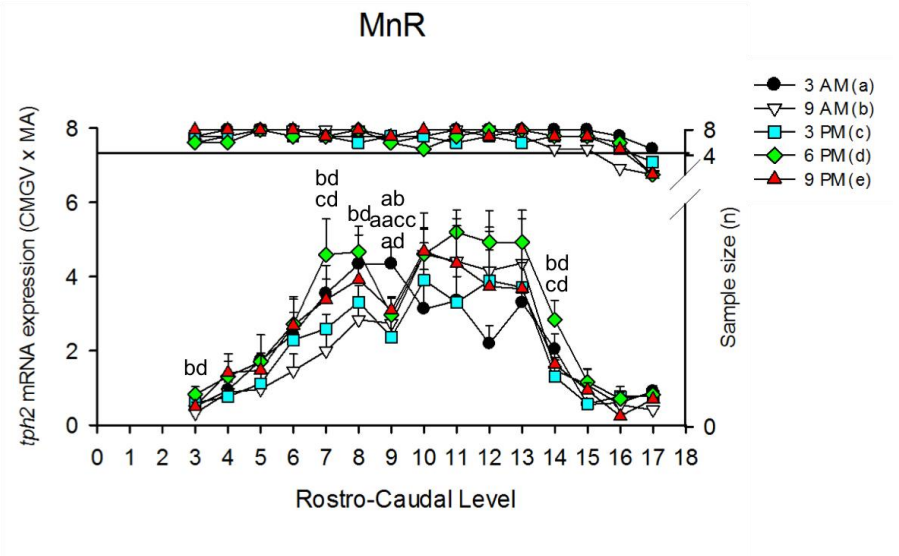

Figure 4-28: Rostro-caudal level variation of tph2 mRNA expression profile in the MnR of MPL treated animals. Tph2 mRNA expression in the MnR was measured in fifteen different rostro-caudal levels presented in the x axis (-7.496 to -8.672 mm bregma). Five different timepoints; (a) 3 am, (b) 9 am, (c) 3 pm, (d) 6 pm and (e) 9 pm are shown for each rostro-caudal level. The

left y-axis shows Tph2 mRNA expression (Calibrated Mean Grey Value multiplied by its own Measured Area). Upper segmented area is associated to the right y-axis that represents the post Grubb's test sample size at each rostro-caudal level. Fisher's Least Significant difference test results are indicated on graph and are annotated by a to e for each time point as shown in the plot key. Additionally, double letters indicate p<0.01 and simple letters p<0.05. Here (aacc) indicates a significant difference for 3 am vs 3 pm, (ab) for 3 am vs 9 am, (ad) for 3 am vs 6 pm, (bd) for 9 am vs 6 pm, (cd) for 3 pm vs 6 pm.

Lastly, to complete the study intended to assess changes in circadian activity of *tph2* mRNA expression under natural conditions and during MPL treatment, a final secondary LMM analysis for MnR was performed. These analyses revealed a treatment * rostro-caudal level interaction ($F_{(12,\ 64.094)}$= 3.315, p<0.001), a time point * rostro-caudal interaction ($F_{(48,\ 65.953)}$= 2.810, p<0.000) and a main effect in rostro-caudal level ($F_{(12,\ 63.075)}$= 66.963, p< 0.000). Multiple comparisons with Fisher's LSD post tests revealed many significant differences in *tph2* mRNA expression between MPL and controls, at all timepoints except for 9pm, and at multiple rostro-caudal levels as shown in Figure 4 - 29.

Notable effects of MPL in the MnR included: a pronounced decrease at 3am at levels 11, 12 and 13, which were all significant (p<0.05 or p<0.001 as indicated in Figure 4-29A), a pronounced elevation in *tph2* mRNA at 9am across levels 10, 11 and 12, which was significant only at level 10 (p<0.05 as indicated in Figure 4-29B); a pronounced decrease at 3pm at levels 10, 12, 13 and 14, which were all significant (p<0.05 or p<0.001 as indicated in Figure 4-29C; and an elevation at 6pm at levels 7, 8, 10, 11 and 12, significant only at level 8 (p<0.05 as indicated in Figure 4-29D. There is also a single point with a significant decrease at level 9 (Figure 4-29D), which is potentially very interesting. However, in cases like this, I cannot rule out the possibility that one isolated point that does not follow the general 'data trend' of the surrounding points may be related to a technical issue.

Overall, the full rostro-caudal dataset in the MnR revealed a highly localised and significant circadian dysregulation of *tph2* mRNA expression after MPL treatment. Interestingly, in this case, the MPL induced changes are primarily characterised by a large and significant decrease in *tph2* mRNA expression at 3pm, with an increase in expression at 6pm, relative to controls. This data is consistent with the overall averaged *tph2* mRNA analysis, shown in Figures 4-16 and Figure 4-17, which

together indicate that MPL treatment resulted in a shift in the circadian *tph2* mRNA peak from 3pm to 6pm.

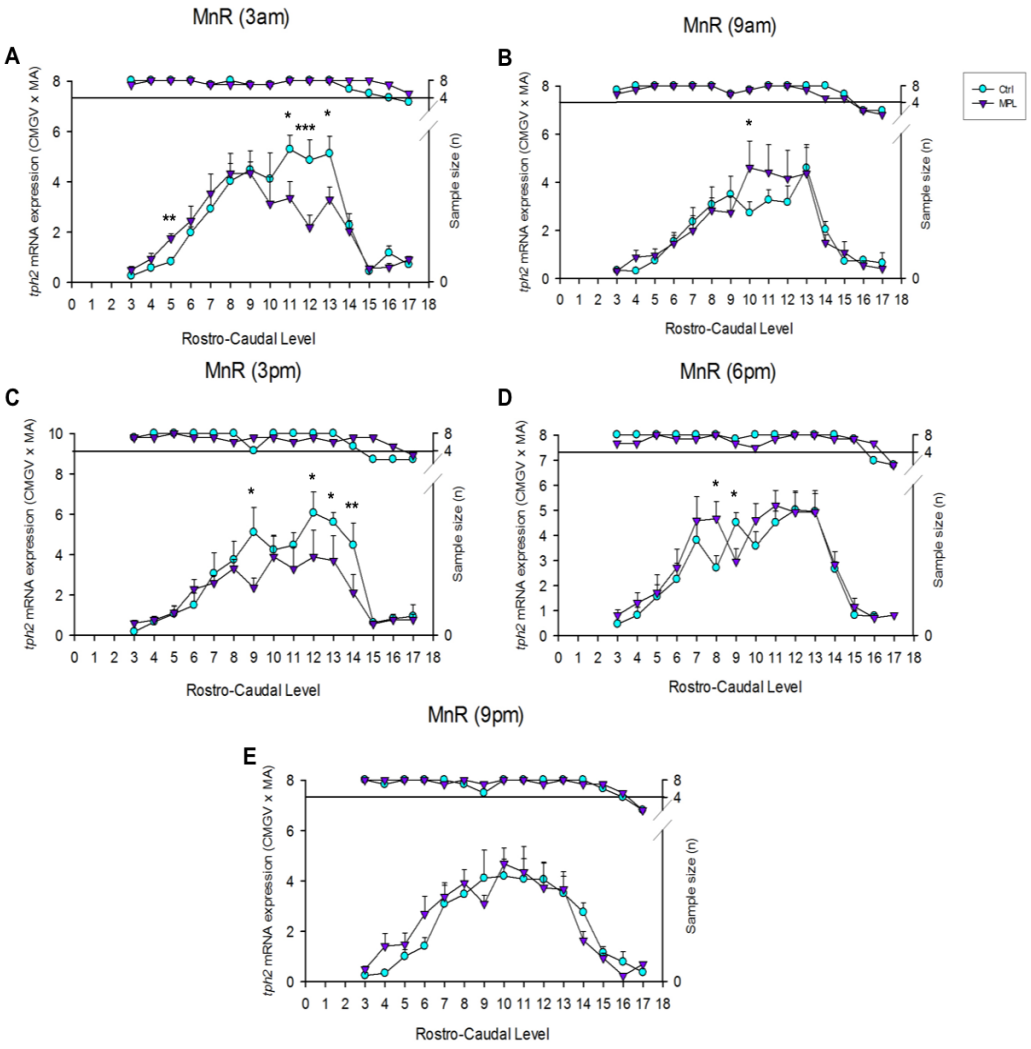

*Figure 4-29: Circadian changes in tph2 mRNA expression at each rostro-caudal level expression in the MnR of Controls vs MPL treated animals. Tph2 mRNA expression in the MnR was measured in fifteen different rostro-caudal levels presented in the x axis (-7.496 to -8.672 mm bregma) at five different time point: (A) 3am, (B) 9 am, (C) 3 pm, (D) 6 pm and (E) 9 pm. Tph2 mRNA quantification is expressed as Calibrated Mean Grey Value multiplied by its own Measured Area. Top data points are associated to the right y-axis which represent the after Grubb's test sample size at each rostro-caudal level. Bottom data points are linked to the left y-axis which correspond to the MEAN ± SEM of tph2 mRNA expression for each group (CTRL or MPL [n≤8/each group]) at each of the fifteen rostro-caudal level of the MnR. Fisher's Least Significant Difference post hoc test showed the following significant differences; (A)***p< 0.001 for CTRL vs MPL in level 12, **p<0.01 in level 5 and *p< 0.05 in level 11 and 13 at 3 am; (B) for CTRL vs MPL *p< 0.05 in level 10 at 9 am; (C) **p< 0.01 for CTRL vs MPL in level 14 and *p< 0.05 in level 9, 12 and 13 at 3 pm; (D) *p< 0.05 for CTRL vs MPL in level 9 and 9 at 6 pm; (E) ns at 9 pm.*

4.3.5 Summary of results

The following table is a summary of the key findings on this chapter.

Table 4-3: Key findings of the circadian expression of tph2 mRNA after MPL treatment. Data shown by subdivision of the Raphe complex and by bregma level. Differences found by statistical analysis form ANOVA's and Linear Mixed Model analysis.

	Nadir after MPL tx	Peak after MPL tx	Complete Subdivisions after MPL tx	LMM analysis after MPL tx	Figures
DR complex	3:00 AM	6:00 PM	↑ expression at 9 am ↓ expression at 3 am and 3 pm when compared to ctrls	NA	(Figure 4-5)
DRC	No significant changes				(Figure 4-7) (Figure 4-19)
DRI	No significant changes				(Figure 4-9) (Figure 4-21)
DRD	3:00 AM	6:00 PM	↑ expression at 9 am in rostral and caudal bregma levels and ↑ at 6 pm in caudal levels when compared to ctrls.	Changes at level 8, 9, 10, 11 when compared to Ctrls. Most differences were found at 6 pm.	(Figure 4-11) (Figure 4-23)
DRV	No differences detected		↑ expression at 9 am and ↓ expression at 3 pm only in caudal bregma levels when compared to ctrls.	Changes at level 9, 10, and 11 when compared to Ctrls.	(Figure 4-13) (Figure 4-25)
DRVL/VLPAG	3:00 AM	6:00 PM	↑ expression at 9 am and ↓ expression at 3 am and 3 pm when compared to ctrls.	Changes at level 6, 7, 8, 9, 10, 11 and 12 when compared to Ctrls. Most changes were found at 6 pm.	(Figure 4-15) (Figure 4-27)
MnR	3:00 AM/ 09:00 AM	6:00 PM	↓ expression at 3 am and 3 pm specific to caudal bregma levels when compared to ctrls.	Changes at level 5, 8, 9, 10, 12, 13 and 14 when compared to Ctrls	(Figure 4-17) (Figure 4-29)

4.4 Discussion

According to the results described in this chapter we can determine that CORT levels in our MPL group (Figure 4-2) entirely correspond to the suppressed secretion of endogenous corticosteroids as shown in previous studies from our group (Spiga et al, 2011). Moreover, with these results we can hypothesize that MPL has replaced the circadian and ultradian rhythm of circulating CORT by inducing a prolonged activation of GRs.

About, *tph2* mRNA expression in the whole Raphe complex after MPL (Figure 4-4), the data shows the presence of a flattened but significant circadian variation in *tph2* mRNA expression, with the highest expression at 6 pm and the lowest at 3 am. When compared to the pattern of activity under natural conditions, *tph2* mRNA expression after MPL treatment (Figure 4-5) seems to have changed considerably at 9 am and 3pm; the nadir of expression changed from 9 am to 3 am, while the peak of expression changed from 3 pm to 6 pm/ This change in the peak expression can be presumed as an effect of the long-acting of MPL compared to CORT and the connection between rhythms of GCs and *tph2* mRNA expression (Donner et. al, 2011; Malek et. al, 2007).

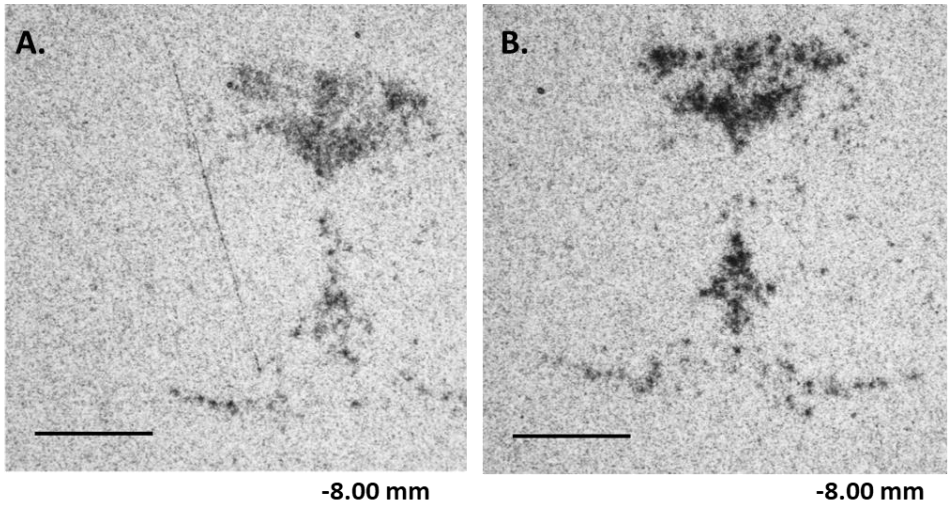

Figure 4-30 Representative image of tph2 mRNA expression of Ctrl (left) vs MPL (right). Image of bregma level 10 (-8.00 bregma level) from of a single brain section from a A) Control animal vs a single brain section of a B) LL treated animal from the 6 pm time point (peak expression after MPL tx).Scale bar 1 mm.

Regarding the assessment of the DR subregions and the MnR nucleus, there is an existent circadian rhythm in the DRD (Figure 4-10), DRVL/VLPAG (Figure 4-14) and MnR (Figure 4-16). No rhythm was found in the DRV (Figure 4-12), which was interesting as there was a circadian rhythm under in the controls. Hence, MPL treatment eliminates the circadian variation in *tph2* mRNA expression. As expected, no circadian variation was found in the DRC (Figure 4-6) or DRI (Figure 4-8), but this could be explained because no circadian variation was found under normal condition. Moreover, this circadian variation of expression after MPL treatment, in the DRD, DRVL/VLPAG and MnR did not appeared to be specific of the caudal part of each area since we also found significant differences in their rostral part. These conditions could have functional and behavioural consequences, which will be discussed further in chapter 6. Additionally, In the DRD and the MnR, the peak of *tph2* mRNA expression matches with the peak of circulating CORT, but this does not happen with the DRVL/VLPAG since the peak was at 9 am.

Continuing with the DR subregions and the MnR nucleus analysis, when compared to the natural circadian activity, as expected nothing was found for the DRC (Figure 4-7) or DRI (Figure 4-9). However, at 9 am the whole and rostral DRD (Figure 4-11) show an increase in expression, which is maintained in the caudal DRD at 9 am and 6 pm. The caudal DRV (Figure 4-13) shows an unusual change when compared to control conditions; increasing *tph2* mRNA expression at 9 am and significantly reducing it at 3 pm, when it was supposed to be high (peak of expression under natural conditions). Changes are found in the whole, rostral and caudal DRVL/VLPAG (Figure 4-15) with MPL treatment changing the peak expression from 3 pm to 9 am and the nadir of expression from 9am to 3 am. This could implicate a "inversed shifted" circadian rhythm of *tph2* mRNA. Finally, a decrease in *tph2* mRNA expression at 3 pm for the whole and caudal MnR (Figure 4-17) can be seen when compared to the natural activity pattern, but this could mean also a shifted circadian rhythm, since the peak expression has gone from 3 pm to 6 pm.

Now, bearing in mind the rostro-caudal gradient of each of the subregions of the DR and the MnR nucleus after MPL, LMM analyses showed that *tph2* mRNA expression profile changes across this gradient in all of the areas of the Raphe complex. Additionally, data shows few circadian variations throughout the rostro-caudal levels of the DRD (Figure 4-22), DRV (Figure 4-24), DRVL/VLPAG (Figure 4-26) and MNR (Figure 4-28). These changes are specific to only some levels of each area and are specific to 9 pm in the DRD, to 6 pm in the DRV, to 3 am in the DRVL/VLPAG and to 9 am and 6 pm in the MnR. These changes might have functional implications as hypothesized by others. These will be further discussed in chapter 6.

Additionally, when considering the rostro-caudal gradient and the comparison between the natural *tph2* mRNA activity and the changed pattern after MPL treatment the overall LMM analyses and secondary LMM analysis revealed that *tph2* mRNA expression profile changed across this gradient in all of the areas of the Raphe complex. Moreover, there is an effect of treatment and time point across the rostro-caudal level in the DRD (Figure 4-23), DRV (Figure 4-25), DRVL/VLPAG (Figure 4-27) and MnR (Figure 4-29); for the DRD, only the changes found in the cauda levels at 6 pm appear to be of great importance, however, changes at 3 am, 9 am and 3 pm were also found; for the DRV very precise changes were found so no assumption can be given about the effect of MPL treatment; the DRVL/VLPAG is the most interesting area since the changes found are detected across all the 24-hour period, therefore an overall effect of MPL treatment can further be discussed as a functional or behavioural implication can be assumed; for the MnR, changes can be considered at 3 am and 3 pm.

This data confirms the existence of a flattened circadian variation of *tph2* mRNA expression in a 24-hour period after MPL in 3 subregions of the DR and the MnR. Moreover, this circadian variation seems to have changed when compared to the circadian variation under natural conditions, and these changes might involve a shifted circadian rhythm. Therefore, these changes can presume a relationship between an altered HPA axis activity because of a prolonged GR activation by the long-acting of MPL and an altered *tph2* mRNA expression.

Although this data and the LMM's analysis done in this study simply describe with more precision the intricacy of the Raphe complex and the changes that *tph2* gene expression exhibit after a manipulation of the GC circadian rhythm, we can surely say that this findings could support the idea of a strong relationship between the circadian expression of *tph2* mRNA and the activity of HPA-axis. Moreover, it can contribute to the basic knowledge of why sGCs have solid neuropsychiatric side effects by proposing a novel mechanism of the connection between altered activity in the HPA axis and psychiatric disorders.

Chapter 5 Circadian changes in the rhythm of *tph2* mRNA expression in the Dorsal and Median Raphe nuclei following chronodisruption by five weeks of constant light exposure.

5.1 Introduction

5.2 Methods: Experimental design

5.2.1 Study design to assess the circadian rhythm of CORT and *tph2* mRNA expression after constant light exposure for five weeks

5.2.2 Statistical analysis

5.3 Results

5.3.1 Circadian rhythm of circulating Corticosterone after constant light (LL) treatment

5.3.2 Circadian rhythmicity of *tph2* mRNA expression in the Raphe complex after LL treatment

5.3.3 Circadian changes on *tph2* mRNA expression in subregions of the Dorsal Raphe and the MnR nucleus after LL treatment

5.3.4 Circadian rhythmicity of *tph2* mRNA expression in the DR subregions and MnR nucleus after LL treatment; analysis across the full rostro-caudal gradient.

5.4 Discussion

5.1 Introduction

Daily rhythms in behaviour and physiology are present in all organisms, including, plants, animals, fungi and cyanobacteria. These rhythmic responses are coordinated by an internal central pacemaker (biological clock) in the suprachiasmatic nucleus (SCN) of the anterior hypothalamus (Moore and Eichler, 1972a; Inouye and Kawamura, 1979; Gillette and Prosser, 1988). The SCN drives the circadian rhythmic activity of many physiological and behavioural processes (Buijs et al., 1993a, 2003).

An important characteristic of the SCN is that the ventrolateral part of this nucleus receives projections from the retina, obtaining information of the day/night (light/dark) cycle. This important information synchronises the SCN which in turn, coordinates behavioural and physiological responses to adapt and respond efficiently to the daily demands (Moore MD, 1997). Hence, light has an important contribution in synchronizing the SCN.

Since the discovery of the "internal clock" studies of the circadian biological rhythms have acquired great attention. Moreover, in recent years, many of the studies in this area of research have focused on the circadian disruption and the potential negative consequences. It has been well established that disruption of circadian rhythms is related to mood disorders, such as anxiety and depression (Kjellman *et al.*, 1985; Stetler, Dickerson and Miller, 2004; Goodman *et al.*, 2005; Germain and Kupfer, 2008; Monteleone *et al.*, 2011).

The adverse effects of disrupted circadian rhythms are most notably seen in shift workers or associated with the "jet lag" of transmeridian travel. Recent evidence has indicated that long periods of light, mixed with arousal and activity, can send unpredictable signals to the biological clock and lead to circadian disruption (Navara and Nelson, 2007), which in turn can cause fatigue, irritability, depression and anxiety (Haus and Smolensky, 2006; Gorwood *et al.*, 2007).

With respect to this, the model of constant light in rodents has been shown to cause altered circadian rhythms, and specifically the loss of the circadian CORT nadir

(Waite *et al.*, 2012). Moreover, depressive-like symptoms, anxiety and anhedonia have been well characterized in animals subjected to this model (Prendergast and Kay, 2008; Fonken *et al.*, 2010; Fonken and Nelson, 2011). Therefore, it appeared to be good experimental paradigm to study mechanisms of depression and anxiety. Important to mention is that exposure to constant light can induce a disrupted 24 hr locomotor activity (Ma *et al.*, 2007) with a significant change on the temporal distribution of activity rather than the average amount of activity or the maximum levels of activity in the 24 hr period (Cassone, 1992).

There is a strong circadian regulation of HPA axis activity, closely controlled by the SCN (Cascio, Shinsako and Dallman, 1987; Buijs *et al.*, 1993a; Buijs, 1999). Several studies have shown that lesioning the SCN in animal models results in a loss of the circadian nadir in CORT secretion (Abe, Kroning, Greer, & Critchlow, 1979; Moore & Eichler, 1972). The same loss of nadir is also observed in animals exposed to long periods of constant light (Scheving and Pauly, 1966; Honma and Hiroshige, 1978; Waite *et al.*, 2012). Importantly, despite the striking loss of circadian variation in CORT secretion, ultradian pulsatility remains intact.

Therefore, consequence of the loss of circadian nadir results in the appearance of high amplitude CORT pulses over the full 24-hour period, characteristic of a hyperactive HPA axis. Interestingly, patients with depression exhibit high levels of GCs (Plotsky, Owens and Nemeroff, 1998). Abnormal cortisol pulsatility has also been described in depressed patients (Deuschle, Schweiger, Weber, Gotthardt, *et al.*, 1997). Based upon these observations, an important HPA axis dysfunction theory has been proposed to explain the pathophysiology of depressive and anxious states (Dinan, 1994; Pariante & Lightman, 2008).

Furthermore, depression and anxiety disorders also have a well characterised and strong relationship with serotonergic systems (Owens and Nemeroff, 1994; Lowry *et al.*, 2008a). In fact, the dysfunction of serotonergic systems in depressed patients is arguably the most accepted neurochemical hypothesis (Mann *et al.*, 1989; Axelson *et al.*, 1993; Naughton, Mulrooney and Leonard, 2000; You *et al.*, 2005; Zill *et al.*, 2007). However, reports that the circadian rhythmicity of important

physiological and biochemical processes are dysregulated in depression (McClung, 2007) also deserves attention when considering the full picture.

Despite all the current knowledge outlined here, the exact mechanisms underlying the connection between depression/anxiety disorders and circadian rhythms remains uncertain. Therefore, the aim of this study was to determine whether chronic exposure to constant light, which is already well established to induce a hyperactive CORT profile due to circadian disruption of CORT secretion, could also affect the pattern of *tph2* mRNA expression, consequently suggesting a novel mechanism explaining why patients with disrupted circadian activity in the HPA axis exhibit a high vulnerability for depression and anxiety.

Thus, we assessed 1) if the pattern of circulating CORT over a 24-hour period after five weeks LL treatment was disrupted and 2) if LL treatment altered the activity of *tph2* mRNA expression profile in the complete Raphe complex, in each of the subregions of the DR and the MnR and throughout the rostro-caudal gradient of each of the subregions of the DR and the MnR nucleus and finally 3) if *tph2* mRNA expression after LL treatment was different from the natural activity pattern of *tph2* mRNA expression, demonstrating a relationship between this altered activity and the altered circulating CORT.

5.2 Methods: Experimental design

5.2.1 Study design to assess the circadian rhythm of CORT and *tph2* mRNA expression after constant light exposure for five weeks.

On day one, forty SD rats (p21) were separated into different groups and housed four per cage in environmentally controlled chambers (Waite *et al.*, 2012). These chambers had space for 4 rat cages and had controlled light (with the possibility of changing the brightness, however it was always kept in 200lux), temperature and humidity. All animals were maintained under bright constant light (200 lux) for a period of five weeks. All animals had food and water *ad libitum*. From day 30 to

day 35, all animals were handled for 10 min at different times of day to avoid stress on the day of the experiment.

At the beginning of the sixth week, in order to collect samples, all animals (now weighing 250 to 300g) were euthanized with an overdose of isoflurane (schedule 1 procedure) and decapitated with a guillotine at defined time points over the 24-hour cycle; 3 am, 9 am, 3 pm, 6 pm, 9 pm (n= 8 per time point). Animals were killed starting 20 minutes before the appointed hour and finishing 20 minutes past the hour. Trunk blood and whole brains were collected.

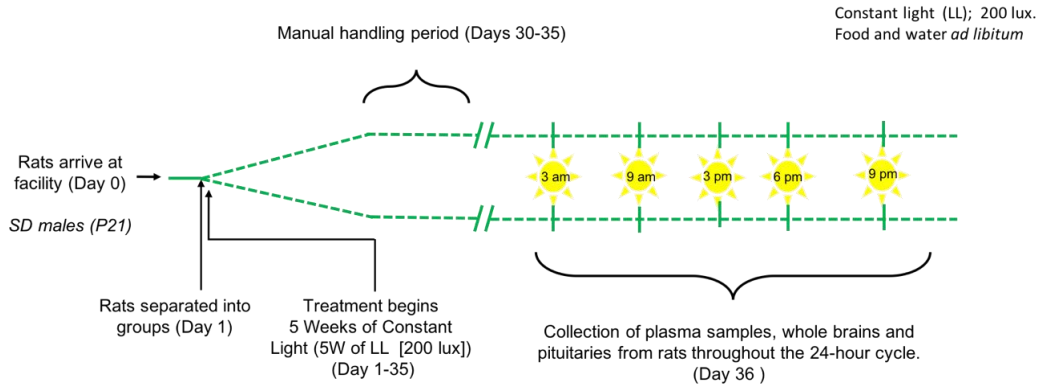

Figure 5-1: Experimental design for the assessment of the altered rhythm of CORT and tph2 mRNA expression after five weeks of constant light (LL).

5.2.2 Statistical analysis

1. One-way ANOVA was performed for the CORT data to assess for an effect of time after five weeks of LL. When an effect of time was found, Dunnet's post-test was used to compare each time point to the 9am nadir. Furthermore, a two-way ANOVA with a Tukey HSD post-test was performed to compare between controls and LL treated groups.

2. When analysing the whole Raphe complex, the same statistical tests used for the CORT analysis were used to enable a direct comparison between the rhythm of *tph2* mRNA expression and the rhythm of CORT. A one-way ANOVA with a Dunnett's (2-sided) post-test was also performed, however 3 pm (nadir) was here considered as the control group. Additionally, a two-

way ANOVA with a Tukey HSD post-test was performed to compare between treatment groups. This fitted with previous statistical tests performed in chapter 3 and 4.

3. Finally, in all the more detailed (subregional and rostro-caudal analysis) overall and secondary LMMs were performed as in chapter 3 and 4, followed by Fisher's Least Significant Difference (LSD) multiple comparison post-tests when a time effect was found. Two different overall LLMs were performed to 1) assess the effect of time in the rostro-caudal gradient of each subregion and 2) effect of treatment in the rostro-caudal gradient of each subregion.

4. The CTRL vs LL comparisons made throughout this chapter were done with the data of our control groups from chapter 3. All the LL experimental groups were independent from our control groups. This is further discussed in limitations.

5.3 Results

5.3.1 Circadian rhythm of circulating Corticosterone after constant light (LL) treatment.

Animals submitted to five weeks of LL showed high levels of circulating CORT across the 24-hour period (Figure 5-2). The results obtained suggest the loss of the normal circadian activity of CORT, which was expected as it has been shown before by several research groups (Claustrat, Valatx, Harth, *et al.*, 2008; Waite *et al.*, 2012). The results, showing the lack of a circadian nadir in CORT levels, thus confirm that the experimental paradigm used in my study successfully disrupted circadian HPA axis activity. A one-way ANOVA was performed to determine if there were any differences between time points after LL treatment, and no statistically significant difference was found; $F_{(4, 35)} = 0.875$, $p > 0.05$, supporting

the statement that there was no detectable circadian rhythm of circulating CORT remaining after five weeks of constant light exposure.

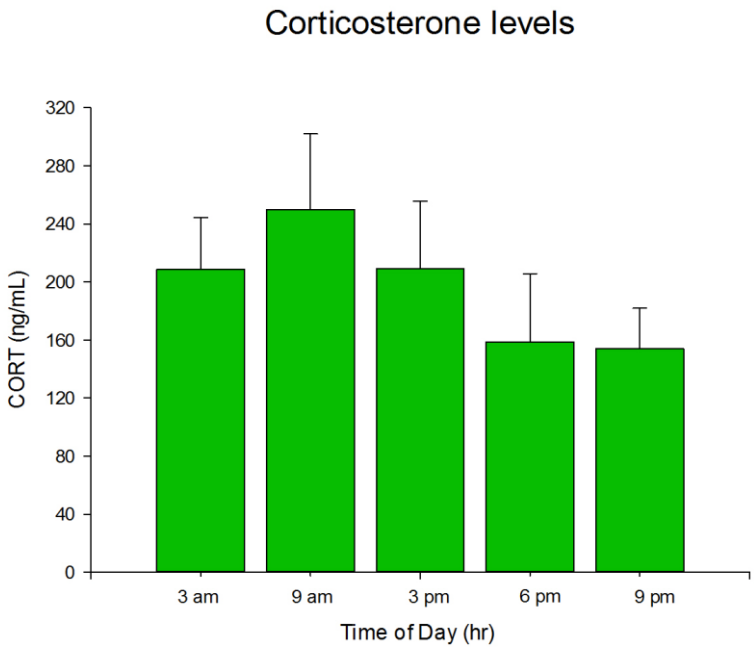

Figure 5-2: Circulating CORT of LL treated animals in a 24-hour period. CORT levels were measured in plasma obtained from trunk blood of control animals at 5 different timepoints; 3am, 9 am, 3 pm, 6 pm and 9 pm (n=8/group/timepoint). CORT levels are expressed as ng/ml. Data is presented as Mean ± SEM of CORT. One-way ANOVA was performed to assess effect of time; $F_{(4, 35)} = 0.875$, $p > 0.05$.

When comparing our control group with our LL group (Figure 5 - 3), a two-way ANOVA was performed to determine if there was a significant interaction between treatment and time; ($F_{(4, 70)} = 5.566$), $p < 0.001$. A Tukey HSD test was performed and revealed that, when CORT is at low levels in the normal circadian rhythm at 3 am and at 9 am (nadir), the LL group showed a significant increase of CORT with p values of <0.01 and p<0.001, respectively. No significant difference was found at the natural peak of CORT (6 pm), as both groups had equally high levels at this time. However, at 3 pm and 9 pm, again, high levels of CORT were found in the LL group (p<0.05) demonstrating the maintenance of high levels throughout the 24-hour period.

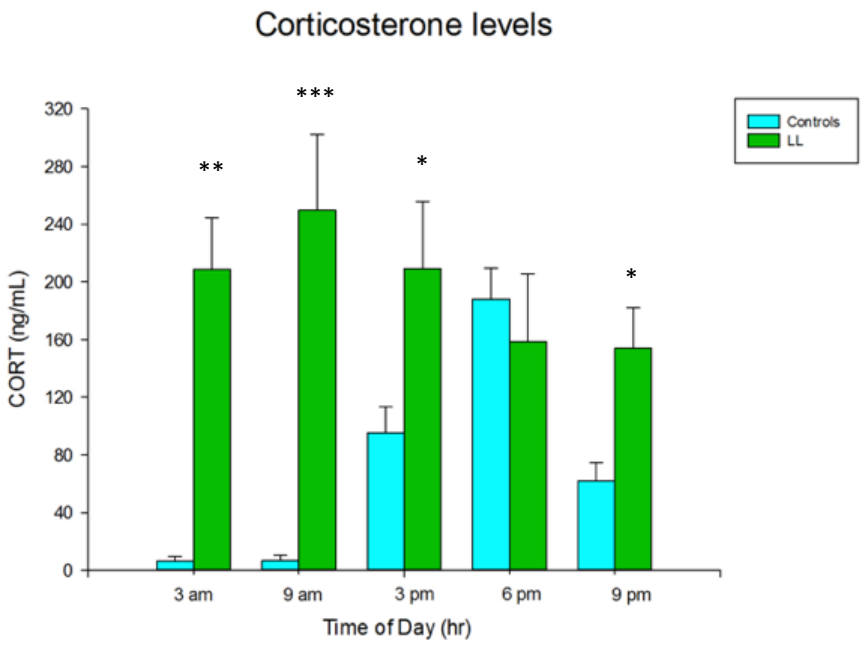

*Figure 5-3: Circadian changes in circulating CORT of Control versus LL treated animals. CORT levels were measured in plasma obtained from trunk blood of two different groups (Control or LL treated animals) at 5 different timepoints; 3am, 9 am, 3 pm, 6 pm and 9 pm (n=8/group/timepoint) presented in the x axis. CORT levels are expressed as ng/ml in the y axis. Data is presented as MEAN ± SEM of CORT for each group. Two-way ANOVA was performed to assess interaction between treatment and time; ($F_{(4, 70)} = 5.566$) $p < 0.01$. Additionally, a Tukey HSD test was included; *** $p < 0.001$ when comparing CTRL vs LL at 9 am; ** $p < 0.01$ when comparing CTRL vs LL at 3 am and * $p < 0.05$ when comparing CTRL vs LL at 3 pm and 9 pm.*

5.3.2 Circadian rhythmicity of *tph2* mRNA expression in the Raphe complex after LL treatment.

This part of the study consisted of evaluating the effect of five weeks of LL on 1) the activity of *tph2* mRNA expression in all the subregions of the DR and the MnR nucleus throughout a 24-hour period and 2) the possible changes of this activity pattern when compared to the natural variation of expression of *tph2* mRNA.

First, in order to describe the overall effect of five weeks of LL in the circadian pattern of *tph2* mRNA expression, I analysed the global averaged *tph2* mRNA expression across all rostro-caudal levels of all subregions together. This analysis indicated that the *tph2* mRNA expression profile displayed an interesting pattern of

circadian activity with a continued nadir from 9 am to 6 pm and a peak from 9 pm to 3 am (Figure 5 - 4). These changes were supported by the statistically significant effect of time found by the one-way ANOVA; ($F_{(4, 2044)} = 8.044$, $p < 0.001$). A Dunnett's post hoc test was then performed to compare the mean of every group against the 3 pm group, since it was the observed nadir for this data base. The test revealed that the high levels of expression found at 3 am and 9 pm were statistically different to 3 pm with p values of $p<0.05$ and $p< 0.01$, respectively.

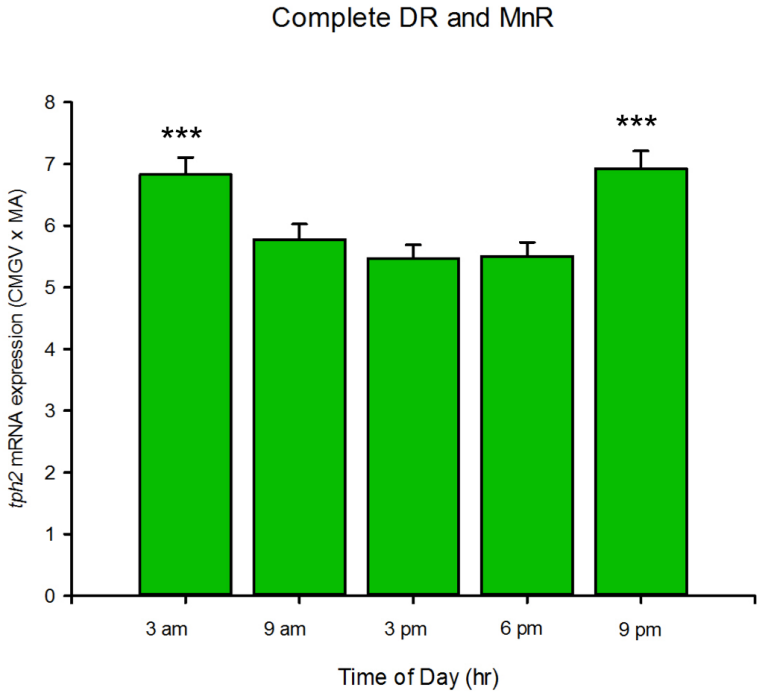

*Figure 5-4: Circadian variation in Tph2 mRNA expression in the DR and MnR complex of LL treated animals. All measurements of tph2 mRNA expression of all levels of the DR and MnR complex were averaged for each timepoint; 3 am, 9 am, 3 pm, 6 pm and 9 pm (x axis). Tph2 mRNA quantification is expressed as Calibrated Mean Grey Value multiplied by its own Measured Area (y axis). Data points correspond to overall MEAN ± SEM of tph2 mRNA expression for each group/timepoint (n=8/group). One-way ANOVA was performed to assess effect of time; ($F_{(4, 2044)} = 8.044$, $p< 0.001$). Additionally, Dunnett's (2-sided) post hoc test was performed; **p <0.01 at 9 pm when compared to the 3 pm group and *p< 0.05 at 3 am when compared to the 3 pm group.*

Next, I evaluated the *tph2* mRNA expression pattern after LL treatment compared to the control dataset (Figure 5-5). This analysis showed that across the 24-hour period, all time points assessed showed strong changes in the expression of *tph2* mRNA. Moreover, the peak expression of *tph2* mRNA expression after LL

treatment changed to 9 pm followed narrowly by the 3 am group, while the nadir occurred at 3 pm followed very closely by the 6 pm group.

These findings were supported by the significant interaction between treatment and time found by two-way ANOVA; ($F_{(4, 4004)}$ =9.966, p< 0.001). Tukey HSD test revealed that after five weeks of constant light there was a significant reduction of *tph2* mRNA expression at times when it was supposed to be high (3 pm [p<0.001] and 6 pm [p<0.05] in LL vs control comparison), and a significantly increase in expression at times when it was supposed to be low (3 am [p<0.05], 9 am [p<0.05] and 9 pm [p<0.001 in LL vs control comparison]).

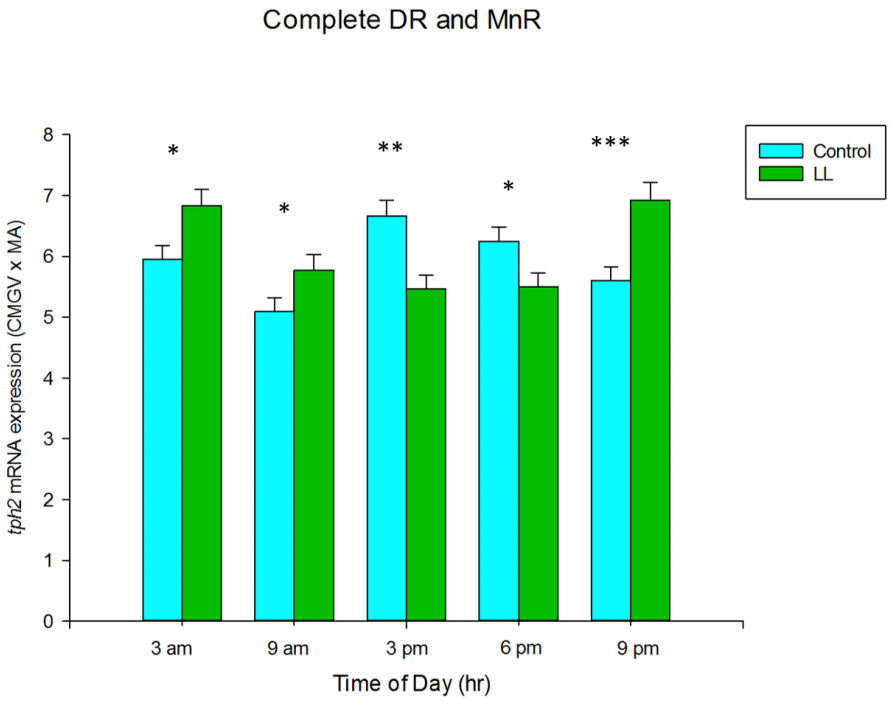

*Figure 5-5: Circadian variation in tph2 mRNA expression in the DR and MnR complex of control vs LL treated animals. All measurements of tph2 mRNA expression of all levels of the DR and MnR complex were averaged for each timepoint of each group; 3 am, 9 am, 3 pm, 6 pm and 9 pm (x axis). Tph2 mRNA quantification is expressed as Calibrated Mean Grey Value multiplied by its own Measured Area (y axis). Data points correspond to overall MEAN ± SEM of tph2 mRNA expression for each group/timepoint (n=8/group). A two-way ANOVA was performed to assess the interaction between treatment and time; ($F_{(4, 4004)}$ = 9.966, p< 0.001). Additionally, a Tukey HSD post hoc test was performed; ***p < 0.001 at 9 pm when comparing CTRL vs LL at 9 pm, **p< 0.01 at 3 pm when comparing CTRL vs LL and *p <0.05 at 3 am, 9 am and 6 pm when comparing CTRL vs LL.*

5.3.3 Circadian changes on *tph2* mRNA expression in subregions of the Dorsal Raphe and the MnR nucleus after LL treatment.

In order to assess the overall effects of time (the circadian pattern) on *tph2* mRNA expression in each of the anatomical and functional distinct subregions of the DR and the MnR nucleus after LL treatment, I analysed the averaged *tph2* mRNA expression of all the rostro-caudal levels for each subregion separately. As with the MPL analysis, I also assessed the two well defined antero-posterior division of the Raphe complex. Thus, I evaluated the rostral and caudal levels for the three subregions of the DR which extend rostro-caudally (DRD, DRV, DRVL/VLPAG) as well as the MnR.

As for the MPL study, in order to describe the overall changes in the circadian pattern of *tph2* mRNA expression after LL treatment I compared the global MEAN ± SEM of *tph2* mRNA expression from the control group (natural conditions) versus the LL group for each of the distinct subregions of the DR and the MnR nucleus, including also the antero-posterior division for the DRD, DRV, DRVL/VLPAG and the MnR nucleus.

These analyses showed circadian variations in *tph2* mRNA expression in four DR subregions and in the MnR nucleus throughout a 24-hour period after treatment. Moreover, variations were revealed after LL treatment when compared to the natural rhythm of *tph2* mRNA expression in most of the regions analysed. Again, all of these variations found seemed to be primarily localised to the caudal part of the subregions with the notable exception of the DRD.

5.3.3.1 Dorsal Raphe nucleus, caudal part (DRC).

Five weeks of LL had a strong effect on *tph2* mRNA expression in the DRC throughout the 24-hour period (Figure 5-6). This statement was supported by the significant effect of time found in the one-way ANOVA; ($F_{(49, 154)} = 4.766$) $p < .001$. Multiple comparisons with Fisher's LSD post tests showed that *tph2* mRNA expression at 9 pm was significantly different ($p < 0.01$) to the nadir expression

levels at 9 am, 3 pm and 6 pm. Moreover, 3 am also showed a high level of *tph2* mRNA expression, which was significantly different ($p<0.05$) when compared to 9 am, 3 pm and 6 pm. Interestingly, a flattened profile in of *tph2* mRNA was present from 9 am to 6 pm.

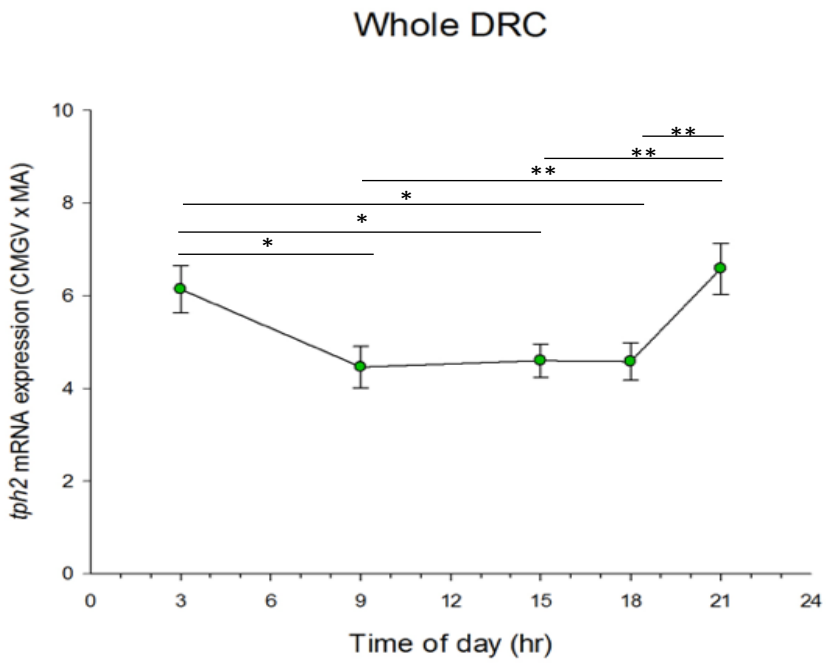

*Figure 5-6: Circadian variation in tph2 mRNA expression in the DRC of LL treated animals. Measurements of tph2 mRNA expression of the five levels of the DRC (-8.336 to -8.672 mm bregma) were averaged for each timepoint; 3 am, 9 am, 3 pm, 6 pm and 9 pm (x axis). Tph2 mRNA quantification is expressed as Calibrated Mean Grey Value multiplied by its own Measured Area (y axis). Data points correspond to overall MEAN ± SEM of tph2 mRNA expression in the DRC for each group/timepoint (n≤8/ group [≤ 8 animals x 5 levels = ≤40 values]). One-way ANOVA was performed to assess effect of time; ($F_{(4, 154)}$ =4.766) p<.001: ** p< 0.01 for 9 am vs 9 pm, 3 pm vs 9 pm and 6 pm vs 9 pm; * p< 0.05 for 3 am vs 9 am, for 3 am vs 3 pm and for 3 am vs 6 pm with Fisher's Least Significant Difference test.*

Next, a two-way ANOVA was performed to determine that there was no significant interaction between treatment and time in the DRC (Figure 5-7); ($F_{(4, 272)}$ = 2.093) p> 0.05.

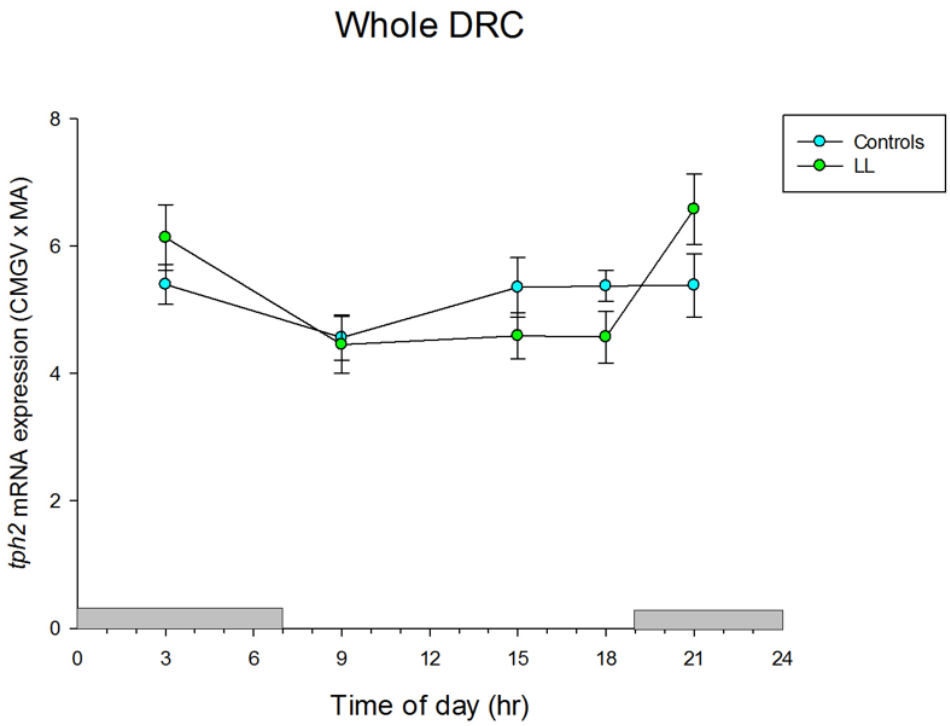

Figure 5-7: Changes in circadian variation of tph2 mRNA expression in the DRC of Control versus LL treated animals. Measurements of tph2 mRNA expression of the five levels of the DRC (-8.336 to -8.672 mm bregma) were averaged for each timepoint; 3 am, 9 am, 3 pm, 6 pm and 9 pm (x axis) for each group separately (CTRL or LL). Tph2 mRNA quantification is expressed as Calibrated Mean Grey Value multiplied by its own Measured Area (y axis). Data points correspond to overall MEAN ± SEM of tph2 mRNA expression in the DRC for each group/timepoint (CTRL or LL [n≤8/ group [≤ 8 animals x 5 levels = ≤40 values]). Two-way ANOVA was performed to assess the interaction between treatment and time: ($F_{(4, 272)} = 2.093$) $p > 0.05$.

5.3.3.2 Dorsal Raphe nucleus, interfascicular part (DRI).

Within the DRI, a one-way ANOVA showed no significant effect of time; $F_{(4,116)} = 0.663$) $p > 0.05$, demonstrating the lack of circadian rhythm in *tph2* mRNA expression in the DRI after five weeks of LL (Figure 5-8).

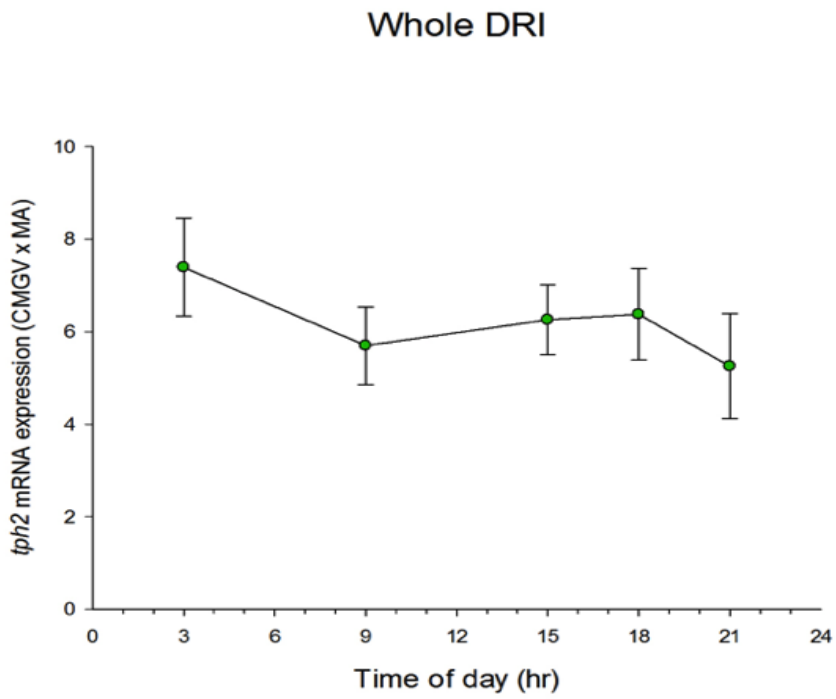

Figure 5-8: Circadian variation in tph2 mRNA expression in DRI of LL treated animals. Measurements of tph2 mRNA expression of the four levels of the DRI (-8.420 to -8.672 mm bregma) were averaged for each timepoint; 3 am, 9 am, 3 pm, 6 pm and 9 pm (x axis). Tph2 mRNA quantification is expressed as Calibrated Mean Grey Value multiplied by its own Measured Area (y axis). Data points correspond to overall MEAN ± SEM of tph2 mRNA in the DRI for each group/timepoint (n≤8/ group [≤ 8 animals x 4 levels = ≤32 values]). One-way ANOVA was performed to assess effect of time; ($F_{(4,116)}$ =0.663) p> 0.05.

Additionally, *tph2* mRNA expression after five weeks of LL behaved similarly to the control groups across the 24-hour period (Figure 5-9). The two-way ANOVA determined no interaction between treatment and time in the DRI; ($F_{(4, 193)}$ =.121) p> 0.05. Therefore, *tph2* mRNA expression didn't appear to exhibit a circadian pattern within the DRI subregion under natural conditions nor after five weeks of LL.

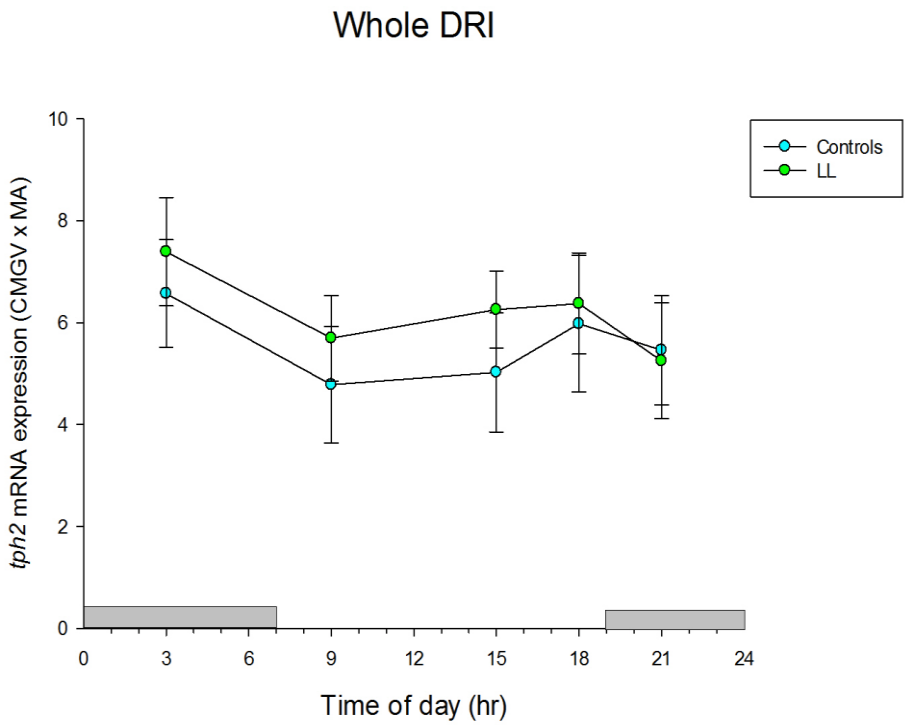

Figure 5-9: Changes in circadian variation of tph2 mRNA expression in the DRI of Control versus LL treated animals. Measurements of Tph2 mRNA expression of the four levels of the DRI (-8.420 to -8.672 mm bregma) were averaged for each timepoint; 3 am, 9 am, 3 pm, 6 pm and 9 pm (x axis) for each group separately (CTRL or LL). Tph2 mRNA quantification is expressed as Calibrated Mean Grey Value multiplied by its own Measured Area (y axis). Data points correspond to overall MEAN ± SEM of tph2 mRNA expression in the DRI for each group/timepoint (CTRL or LL [n≤8/ group [≤ 8 animals x 4 levels = ≤32 values]). A Two-way ANOVA was performed to assess interaction between treatment and time: ($F_{(4, 193)}$ =.121) p> 0.05.

5.3.3.3 Dorsal Raphe nucleus, dorsal part (DRD).

To determine if the DRD presented a circadian variation in *tph2* mRNA expression after five weeks of LL throughout the 24-hour period, one-way ANOVAs were completed for the whole, rostral and caudal DRD separately, which compared between timepoints; 3 am, 9 am, 3 pm, 6 pm and 9 pm.

For the whole DRD (Figure 5-10A) an effect of time was found; ($F_{(4, 417)}$ =4.135) p< 0.01. Hence, LSD post-tests were run and revealed that both 3 am and 9pm peak levels were significant when compared to the nadir levels of 9 am (p<0.05), 3 pm (p<0.05) and 6 pm (p<0.01).

With respect to the rostral DRD (Figure 5-10B), there was also a visible time-dependent variation over the 24 hour period, supported by a significant effect of time by one-way ANOVA; ($F_{(4, 273)} = 2.23$) $p < 0.05$. The peak expression was again seen at 3 am and 9 pm, which both had a statistically increased *tph2* mRNA expression when compared to 6 pm ($p<0.05$), although only 3 am had a statistically higher expression when compared to the 9 am group ($p<0.05$).

Finally, for the caudal DRD (Figure 5-10C), there was also a statistically significant effect of time; ($F_{(4, 178)} = 7.495$) $p < 0.001$. Similar to the whole and rostral DRD, the peak of *tph2* mRNA expression was seen at 9 pm and 3 am. The 9 pm peak was statistically increased when compared to the 9 am ($p < 0.05$), 3 pm ($p < 0.001$), and 6 pm group ($p < 0.001$). Likewise, the 3 am was statistically increased when compared to 9 am ($p < 0.05$), 3 pm ($p < 0.001$) and 6 pm ($p < 0.01$). An additional significant difference was found when comparing the low levels of expression at 3 pm with the 9 am group ($p<0.05$).

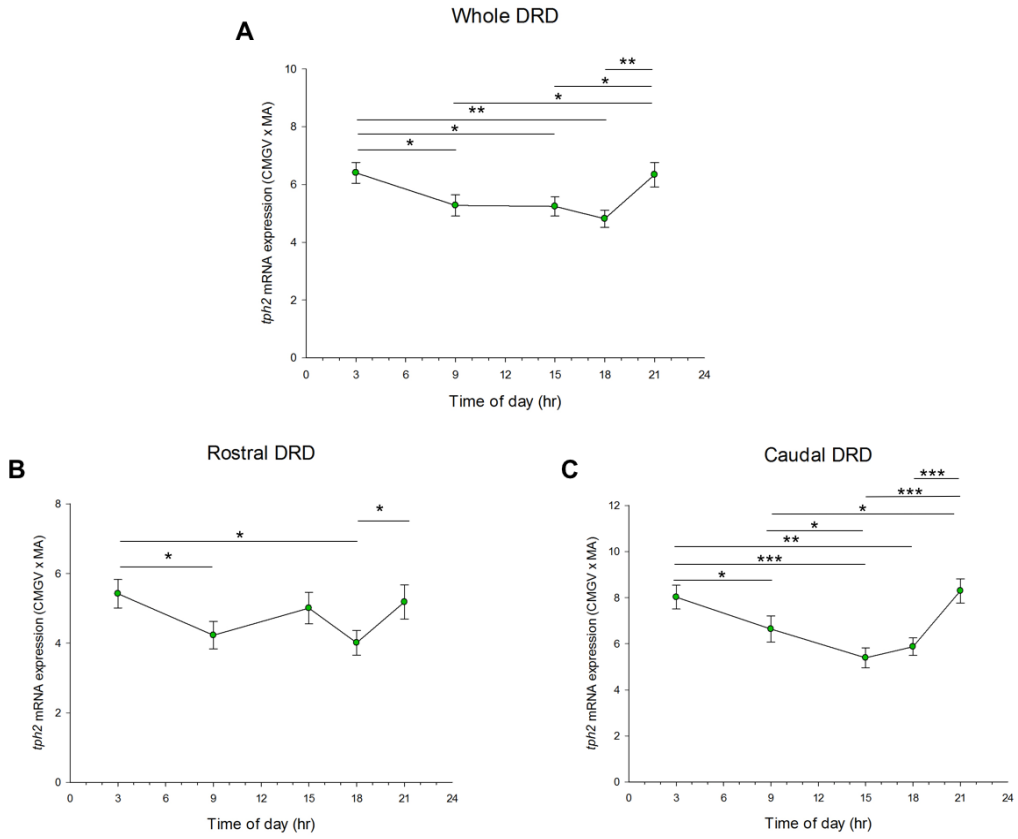

*Figure 5-10: Circadian variation in tph2 mRNA expression in the DRD of LL treated animals. For each timepoint; 3am, 9am, 3pm, 6pm and 9pm (x axis) measurements of tph2 mRNA expression (y axis) were averaged; (A) twelve levels (-7.328 to -8.252 mm bregma) for the whole DRD, (B) eight levels (-7.328 to -7.916 mm bregma) for the rostral DRD and (C) 5 levels (-7.916 to -8.252 mm bregma) for the caudal DRD. Tph2 mRNA quantification is expressed as Calibrated Mean Grey Value multiplied by its own Measured Area. Data points correspond to overall MEAN ± SEM of tph2 expression of the whole/rostral/caudal DRD for each group/timepoint (n≤8/group [≤ 8 animals x ≤12/8/5 levels = ≤96/64/40 values]). One-way ANOVAs were performed to assess effect of time: (A) ($F_{(4, 417)}$ =4.135) p< 0.01; ** p< 0.01 for 3 am vs 6 pm and for 6 pm vs 9 pm; * p< 0.05 for 3 am vs 9 am, for 3 am vs 3 pm, for 9 am vs 9 pm and for 3 pm vs 9 pm; (B) ($F_{(4, 273)}$ =2.23) p< 0.05; *p < 0.05 for 3 am vs 9 am, for 3 am vs 6 pm and for 6 pm vs 9 pm; (C) ($F_{(4, 178)}$ =7.495) p< 0.001; ***p< 0.001 for 3 am vs 3 pm, for 3 pm vs 9pm and for 6 pm vs 9 pm: **p< 0.01 for 3am vs 6 pm: *p< 0.05 for 3 am vs 9 am, for 9 am vs 3 pm and for 9 am vs 9 pm with Fisher's Least Significant Difference test.*

Next, I assessed changes between the natural circadian rhythm in *tph2* mRNA expression and the modified pattern after LL treatment in the whole DRD (Figure 5-11A). A significant interaction between treatment and time was revealed by the two-way ANOVA; ($F_{(4, 863)}$ = 4.769) p< 0.01. Thus, Fisher's LSD post-tests were run and revealed that the *tph2* mRNA expression profile after LL treatment

appeared to have changed with a significant reduction at 6 pm ($p<0.01$) and a significant increase at 3 am ($p<0.05$) and 9pm ($p<0.05$).

Interestingly, for the rostral DRD (Figure 5-11B), a marked reduction at 6 pm was observed after LL treatment. A significant interaction was found; ($F_{(4, 572)} = 2.901$) $p< 0.05$ and Fisher's LSD post-test revealed that the reduction at 6 pm was significantly different between LL and control, $p< 0.01$. LL treatment had no effect at any of the other timepoints.

With respect to the caudal DRD (Figure 5-11C), a striking contrast was observed between the LL and control groups, supported by a significant interaction in two-way ANOVA; ($F_{(4, 358)} = 7.996$) $p< 0.01$. The peak in expression of *tph2* mRNA after LL treatment was again seen at 9 pm and 3 am, both with statistically higher levels of expression, $p<0.001$ when compared to their time matched control groups. Also, a significant increase was revealed at 9 am, $p<0.05$. At 3 pm, when *tph2* mRNA expression reached its peak in control rats, the LL treated rats were at their nadir in *tph2* mRNA expression, representing a significant reduction, $p<0.05$. The highly dysregulated pattern induced by LL appeared to be a complete inversion of the control pattern in circadian *tph2* mRNA expression, with exaggerated peak levels at the 'wrong time of day'.

Therefore, it appeared that the *tph2* mRNA expression profile within the DRD subregion was significantly altered after five weeks of LL treatment, with the most striking dysregulation in the caudal DRD.

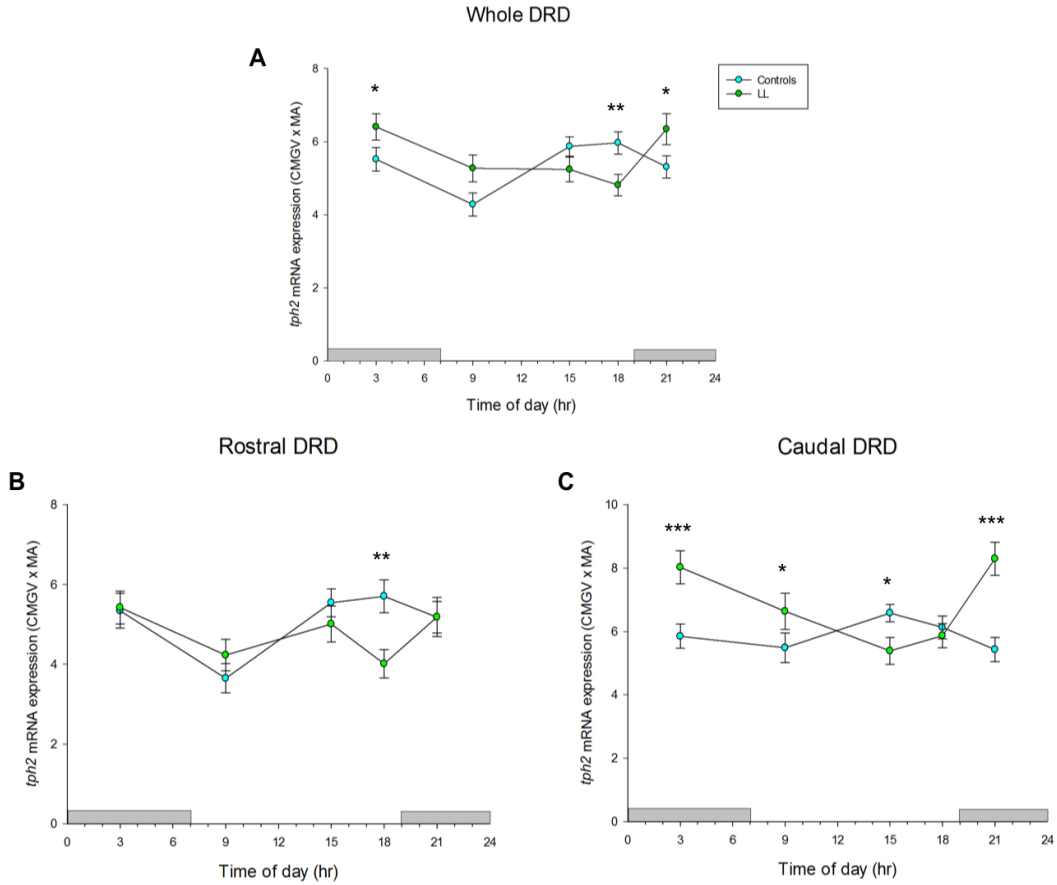

*Figure 5-11: Changes in circadian variation of tph2 mRNA expression in the DRD of Control vs LL treated animals. For each timepoint; 3am, 9am, 3pm, 6pm and 9pm (x axis) measurements of tph2 mRNA expression (y axis) were averaged for each group separately (CTRL or LL); (A) twelve levels (-7.328 to -8.252 mm bregma) for the whole DRD, (B) eight levels (-7.328 to -7.916 mm bregma) for the rostral DRD and (C) 5 levels (-7.916 to -8.252 mm bregma) for the caudal DRD. Tph2 mRNA quantification is expressed as Calibrated Mean Grey Value multiplied by its own Measured Area. Data points correspond to overall MEAN ± SEM of tph2 mRNA expression of the whole/rostral/caudal DRD for each group/timepoint (CTRL vs LL [n≤8/group [≤ 8 animals x ≤12/8/5 levels = ≤96/64/40 values]). Two-way ANOVAs were performed to assess interaction between treatment and time: (A) ($F_{(4, 863)} = 4.769$) p< 0.01; ** p< 0.01 when comparing CTRL vs LL at 6 pm; *p< 0.05 when comparing CTRL vs LL at 3 am and 9 pm; (B) ($F_{(4, 572)} = 2.901$) p< 0.05; ** p< 0.01 when comparing CTRL vs LL at 6 pm; (C) ($F_{(4, 358)} = 7.996$) p< 0.01; ***p< 0.001 when comparing CTRL vs LL at 3 am and 9 pm; *p< 0.05 when comparing CTRL vs LL at 9 am and 3 pm.*

5.3.3.4 Dorsal Raphe nucleus, ventral part (DRV).

The whole DRV subregion showed very little circadian variation after five weeks of constant light (Figure 5-12), and no significant effect of time was detected by the one-way ANOVA (Figure 5-12A); ($F_{(4, 494)} = 1.271$) p> 0.05. Similarly, there was

no significant circadian variation detected in the rostral DRV (Figure 5-12B); $F_{(4, 272)} = 0.445$) $p > 0.05$.

Fascinatingly for this area, when I took away the rostral levels a strong circadian pattern of *tph2* mRNA expression was exposed. This indicates that the circadian rhythm of *tph2* mRNA expression during constant light exposure is localised within the caudal DRV (Figure 5-12C). Accordingly, the one-way ANOVA showed a statistically significant effect of time; ($F_{(4, 256)} = 5.394$) $p < 0.001$. Similar to what was found in the caudal DRD, the peak of *tph2* mRNA expression was seen at 9 pm and 3am. Then, expression levels decreased to an apparent extended nadir between 9 am and 6 pm. Therefore, the Fisher's LSD post-tests revealed that 9 pm is statistically increased when compared to 9 am ($p<0.05$), 3 pm ($p<0.001$) and 6 pm ($p<0.01$). Similarly, at 3 am high levels were significantly higher than 9 am ($p<0.05$), 3 pm ($p<0.01$) and 6 pm ($p<0.01$).

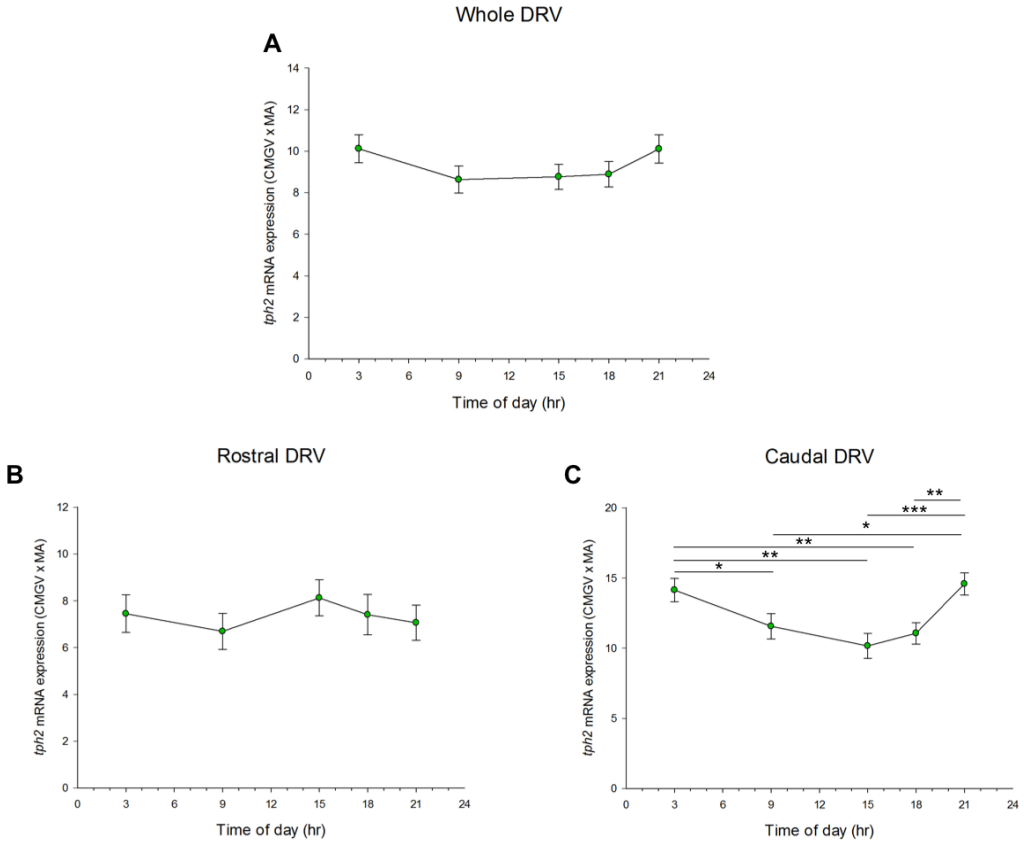

Figure 5-12: Circadian variation in tph2 mRNA expression in the DRV of LL treated animals. For each timepoint; 3 am, 9 am, 3 pm, 6 pm and 9 pm (x axis) measurements of tph2 mRNA

*expression (y axis) were averaged; (A) fourteen levels (-7.328 to -8.420 mm bregma) for the whole DRV, (B) eight levels (-7.328 to -7.916 mm bregma) and (C) seven levels (-7.916 to -8.420 mm bregma) for the caudal DRV. Tph2 mRNA quantification is expressed as Calibrated Mean Grey Value multiplied by its own Measured Area. Data points correspond to the overall MEAN ± SEM of th2 expression of the whole/rostral/caudal DRV for each group/timepoint (n≤ 8/group [≤ 8 animals x 14/8/7 levels = ≤ 112/64/56 values]). One-way ANOVAs were performed to assess effect of time; (A) ($F_{(4, 494)}$ =1.271) p> 0.05; (B) $F_{(4, 272)}$ =0.445) p> 0.05; (C) ($F_{(4, 256)}$ =5.394) p< 0.001; ***p< 0.001 for 3 pm vs 9 pm; **p< 0.01 for 3 am vs 3 pm, for 3 am vs 6 pm and for 6 pm vs 9 pm; *p< 0.05 for 3am vs 9 am and for 9 am vs 9 pm with Fisher's Least Significant Difference test.*

Then, to assess changes between the natural circadian rhythm and the altered pattern in *tph2* mRNA expression in the DRV after five weeks of LL, I plotted the data together (Figure 5-13). No interaction between treatment and time was found for either the whole DRV (Figure 5-13A); $F_{(4, 1018)}$ =2.006) p> 0.05, or the rostral DRV (Figure 5-13B); $F_{(4, 574)}$ =.055) p> 0.05. However, for the caudal DRV (Figure 5-13C), the two-way ANOVA detected a significant interaction; ($F_{(4, 512)}$ =6.479) p< 0.01. Fisher's LSD post-tests further revealed that the observed differences in the caudal DRV between the LL and control groups were both statistically significant at both 9 pm and 3 pm (p<0.01).

It therefore appeared that five weeks of constant light resulted in a fairly strong modification to the circadian rhythm of *tph2* mRNA expression in the DRV. This alteration seemed to be specific to the caudal levels of the DRV and characterised by high levels of expression at 9 pm and 3 am and decreased expression at 3 pm, resulting in a striking dysregulation of the caudal DRV *tph2* mRNA circadian rhythm that had been seen in control animals.

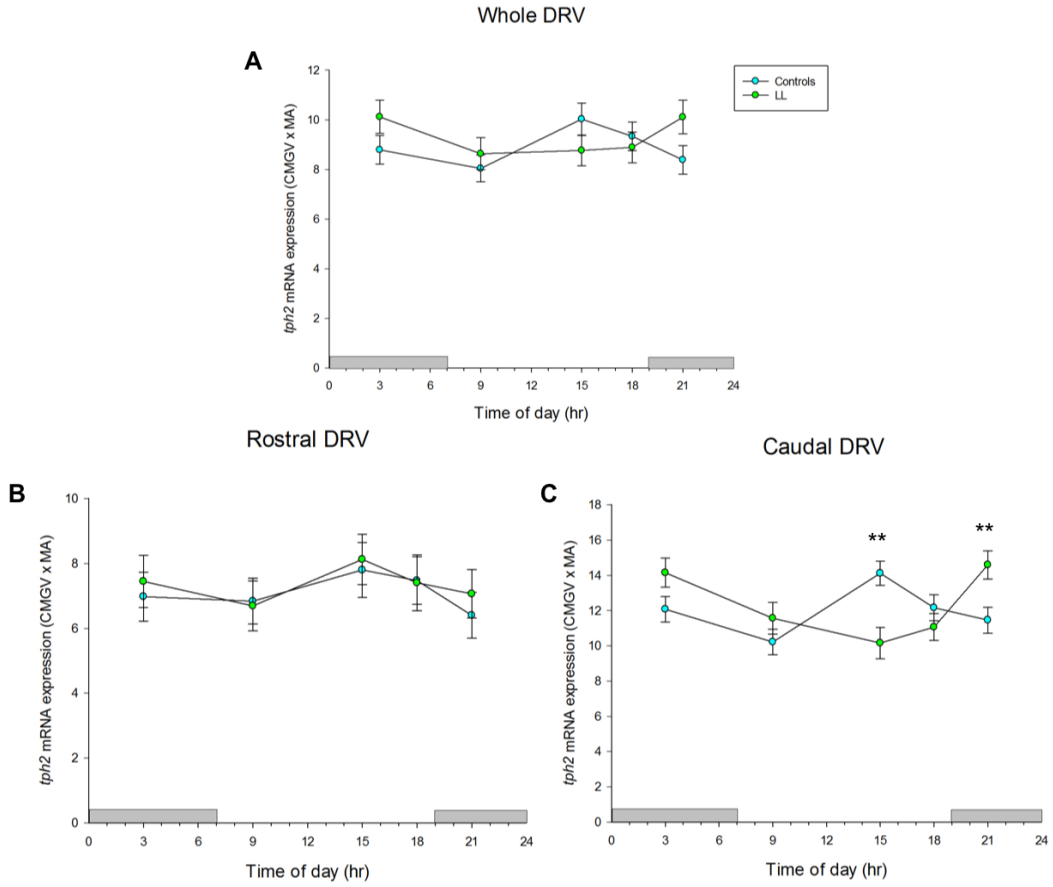

*Figure 5-13: Changes in circadian variation of tph2 mRNA expression in the DRV of Control vs LL treated animals. For each timepoint; 3am, 9am, 3pm, 6pm and 9pm (x axis) measurements of tph2 mRNA expression (y axis) were averaged for each group separately (CTRL or LL); (A) fourteen levels (-7.328 to -8.420 mm bregma) for the whole DRV, (B) eight levels (-7.328 to -7.916 mm bregma) and (C) seven levels (-7.916 to -8.420 mm bregma) for the caudal DRV. Tph2 mRNA quantification is expressed as Corrected Mean Grey Value multiplied by its own Measured Area (y axis). Data points correspond to the overall MEAN ± SEM of th2 expression of the whole/rostral/caudal DRV for each group/timepoint (CTRL vs LL [n≤ 8/group [≤ 8 animals x 14/8/7 levels = ≤ 112/64/56 values]). Two-way ANOVAs were performed to assess interaction between treatment and time ; (A) ($F_{(4, 1018)}$ =2.006) p> 0.05; (B) ($F_{(4, 574)}$ =.055) p> 0.05; (C) ($F_{(4, 512)}$ =6.479) p< 0.01; **p< .01 when comparing CTRL vs LL at 3 pm and 9 pm with Fisher's Least Significant Difference test.*

5.3.3.5 Dorsal raphe nucleus, ventrolateral part/ventrolateral periaqueductal grey (DRVL/VLPAG).

The DRVL/VLPAG subregion showed a similar circadian pattern of *tph2* mRNA expression after LL treatment to that found in the DRD and caudal DRV (Figure 5-14). Interestingly, *tph2* mRNA displayed high levels of expression at 3 am and 9 pm and low levels at 3 pm and 6 pm in the whole (Figure 5-14A) and the caudal

DRVL/VLPAG (Figure 5-14C). No circadian pattern was observed in the rostral DRVL/VLPAG (Figure 5-14B). These observations were supported by one-way ANOVA which revealed a significant effect of time for the whole ($F_{(4, 295)} = 3.976$) $p < 0.01$) and caudal DRVL/VLPAG ($F_{(4, 218)} = 4.218$) $p < 0.001$), but no effect for the rostral DRVL/VLPAG ($F_{(4, 111)} = .171$) $p > 0.05$).

Further multiple comparisons within the whole DRVL/VLPAG with Fisher's LSD post-tests showed that the peak of expression at 3 am and 9pm were both statistically increased when compared to 3 pm ($p<0.01$) and 6 pm ($p<0.01$). Comparable to the whole DRVL/VLPAG, the caudal levels of this subregion exhibited an even more pronounced rhythm in *tph2* mRNA expression over the 24-hour period. Again, *tph2* mRNA expression appeared to maintain at peak levels from 9pm to 3am, with statistical differences found between 9 pm and the lower expression times of 9 am ($p<0.05$), 3 pm ($p<0.001$) and 6 pm ($p<0.001$). Similarly, for 3 am significant differences are found when compared to 9 am ($p<0.05$), 3 pm ($p<0.001$) and 6 pm ($p<0.01$). Therefore, this circadian pattern appeared to be characterised primarily by the high expression of *tph2* mRNA at 3 am and 9 pm.

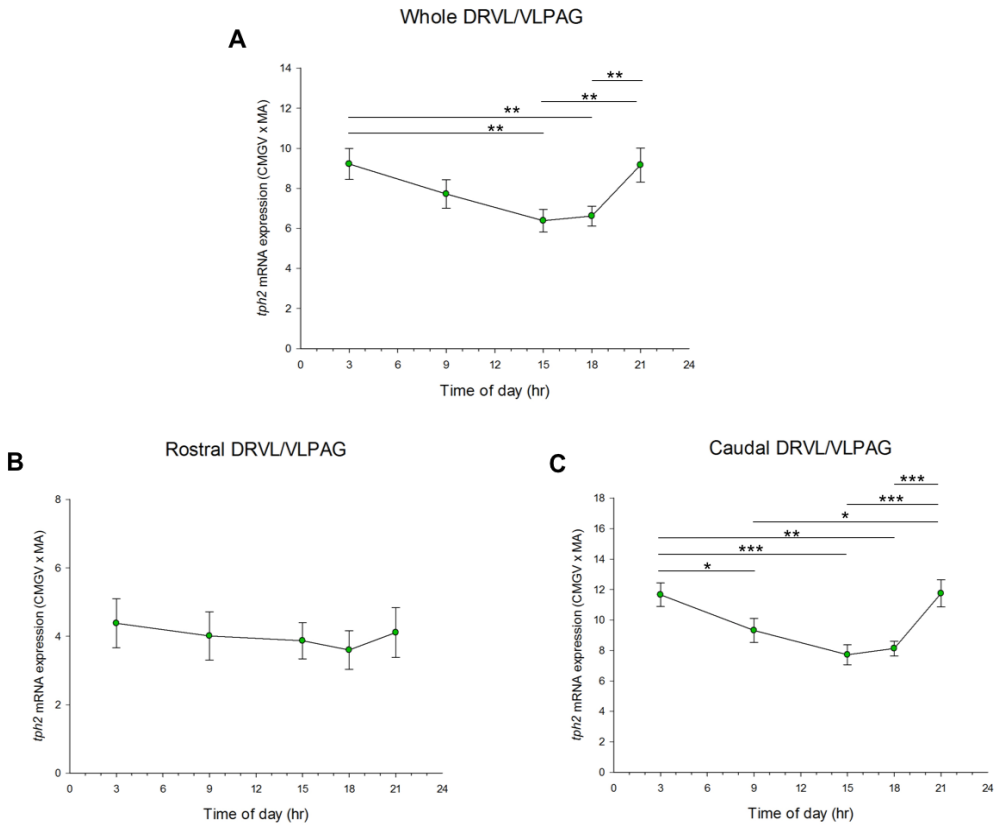

*Figure 5-14: Circadian variation in tph2 mRNA expression profile in the DRVL/VLPAG of LL treated animals. For each timepoint; 3 am, 9 am, 3 pm, 6 pm and 9 pm (x axis) measurements of Tph2 mRNA expression (y axis) were averaged; (A) eight levels (-7.748 to -8.336 mm bregma) for the whole DRVL/VLPAG, (B) three levels (-7.748 to -7.916 mm bregma) for the rostral DRVL/VLPAG and (C) six levels (-7.916 to -8.336 mm bregma) for the caudal DRVL/VLPAG.Tph2 mRNA quantification is expressed as Calibrated Mean Grey Value multiplied by its own Measured Area. Data points correspond to the overall MEAN ± SEM of tph2 expression of the whole/rostral/caudal DRVL/VLPAG for each group/timepoint (n≤ 8/group [≤ 8 animals x 8/3/6 levels = ≤64/24/48 values]). One-way ANOVAs were performed to assess effect of time; (A) ($F_{(4, 295)}$ =3.976) p< 0.01; **p< 0.01 for 3 am vs 3 pm, for 3 am vs 6 pm, for 3 pm vs 9 pm and for 6 pm vs 9 pm; (B) ($F_{(4, 111)}$ =.171) p> 0.05; (C) ($F_{(4, 218)}$ =4.218) p< 0.001; ***p< 0.001 for 3 pm vs 3 pm, for 3 pm vs 9 pm and for 6 pm vs 9 pm; **p< 0.01 for 3 am vs 6 pm; *p< 0.05 for 3am vs 9 am and for 9 am vs 9 pm with Fisher's Least Significant Difference test.*

Next, to assess changes resulting from treatment, I again plotted the data used in Figure 5-14 with the control data for the whole, rostral and caudal DRVL/VLPAG. In the whole DRVL/VLPAG (Figure 5-15A) five weeks of LL appeared to change the pattern of *tph2* mRNA expression. Again, as in the DRD and caudal DRV, the pattern appeared to be almost reversed to the one observed under normal conditions. This observation was supported by a two-way ANOVA, which revealed a

significant interaction between treatment and time; $F_{(4, 592)} = 4.905$) $p < 0.001$. Again, Fisher's LSD post-tests revealed that LL treatment triggered significantly higher levels of *tph2* mRNA expression at 3 am ($p<0.05$) and 9 pm ($p<0.01$) compared to controls, and that a significant decrease at 3 pm was detected after LL treatment ($p<0.05$).

No significant interaction; ($F_{(4, 223)} = 0.641$ $p > 0.05$ was detected in the rostral DRVL/VLPAG after five weeks of LL (Figure 5-15B). However, when I assessed only the caudal levels of the DRVL/VLPAG, the striking inverted pattern, also found in the whole DRVL/VLPAG after five weeks of LL, appeared even more pronounced (Figure 5-15C). Accordingly, a significant interaction was reported by two-way ANOVA; ($F_{(4, 437)} = 7.374$) $p < 0.001$. Post tests showed that the increased *tph2* mRNA expression found at 3 am and 9 pm in the LL group were significantly different to their time matched controls, $p < 0.001$ at 9 pm and $p < 0.01$ at 3 am. A significant increase was also detected in the LL group at 9 am ($p<0.05$). Moreover, the decrease found at 3 pm in the LL group, the nadir of this circadian dysregulated pattern, was also statistically different to the time matched control group ($p<0.05$).

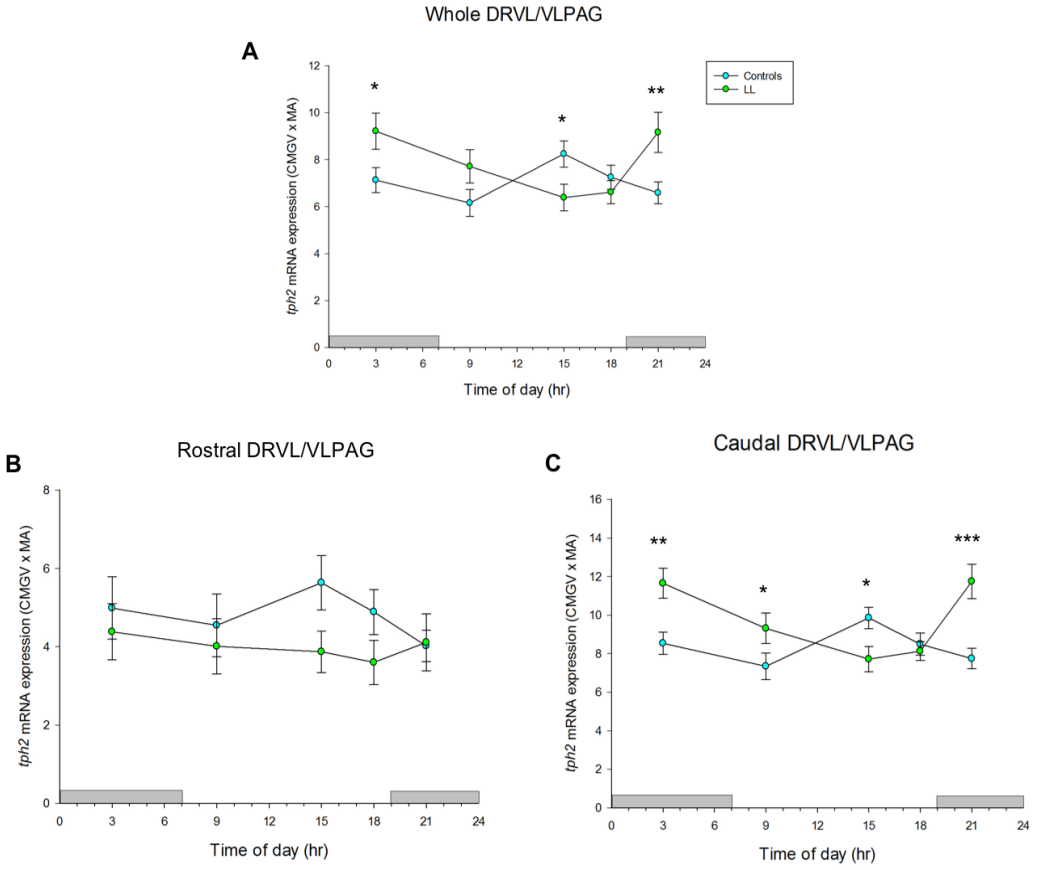

*Figure 5-15: Changes in circadian variation of tph2 mRNA expression in the DRVL/VLPAG of Control vs LL treated animals. For each timepoint; 3am, 9am, 3pm, 6pm and 9pm (x axis) measurements of tph2 mRNA expression (y axis) were averaged for each group separately (CTRL or LL); (A) eight levels (-7.748 to -8.336 mm bregma) for the whole DRVL/VLPAG, (B) three levels (-7.748 to -7.916 mm bregma) for the rostral DRVL/VLPAG and (C) six levels (-7.916 to -8.336 mm bregma) for the caudal DRVL/VLPAG. Tph2 mRNA quantification is expressed as Calibrated Mean Grey Value multiplied by its own Measured Area. Data points correspond to the overall MEAN ± SEM of tph2 mRNA expression of the whole/rostral/caudal DRVL/VLPAG for each group/timepoint (CTRL vs LL [n≤8/group [≤ 8 animals x 8/3/6 levels = ≤ 64/24/48 values]). Two-way ANOVAs were performed to assess interaction between treatment and time; (A) ($F_{(4, 592)}$ =4.905) p< 0.001; **p< 0.01 when comparing CTRL vs LL at 9 pm; * p< 0.05 when comparing CTRL vs LL at 3 am and 3 pm; (B) ($F_{(4, 223)}$ = 0.641 p> 0.05; (C) ($F_{(4, 437)}$ = 7.374) p< 0.001; *** p< 0.001 when comparing CTRL vs LL at 9 pm; ** p< 0.01 when comparing CTRL vs LL at 3 am; *p< 0.05 when comparing CTRL vs LL at 9 am and 3 pm with Fisher's Least Significant Difference test.*

5.3.3.6 Median Raphe nucleus (MnR).

To determine if the MnR showed a circadian variation in *tph2* mRNA expression after five weeks of constant light, one-way ANOVAs were completed for the whole, rostral and caudal MnR separately.

The MnR showed a fairly similar pattern to those found in the DRD, DRV and the DRVL/VLPAG, (Figure 5-16). This pattern was somewhat 'blunted' in the whole MnR (Figure 5-16A), although a significant effect of time was still found by one-way ANOVA; ($F_{(4, 523)} = 2.573$) $p < 0.05$. The observed peak in *tph2* mRNA expression at 9 pm was statistically significant when compared to 6 pm ($p<0.05$), 3 pm ($p<0.01$) and 9 am ($p<0.05$). The pattern was virtually non-existent in the rostral MnR (Figure 5-16B), the lack of circadian pattern was confirmed by one-way ANOVA with no significant effect of time; ($F_{(4, 221)} = 2.186$) $p > 0.05$. When the rostral levels were taken out, the caudal MnR exhibited a far more pronounced pattern (Figure 5-16C), and a significant effect of time was detected by one-way ANOVA; $F_{(4, 336)} = 7.409$) $p < 0.001$. Further multiple comparisons post-tests confirmed that the peak in *tph2* mRNA expression at 9 pm was statistically different from 9 am ($p<0.001$), 3 pm ($p<0.001$) and 6 pm ($p<0.001$). Additionally, high levels of *tph2* mRNA expression at 3 am also showed significant differences when compared to 9 am ($p<0.05$), 3 pm ($p<0.05$) and 6 pm ($p<0.05$).

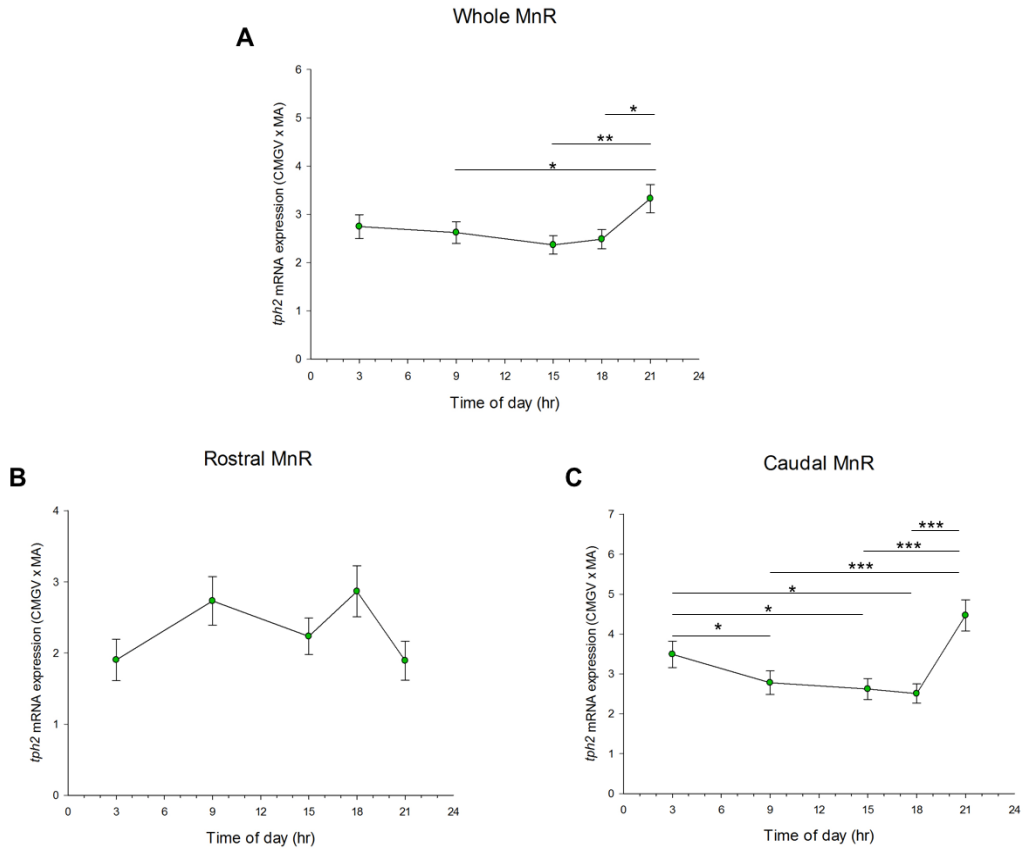

*Figure 5-16: Circadian variation in tph2 mRNA expression in the MnR of LL treated animals. For each timepoint; 3am, 9am, 3pm, 6pm and 9pm (x axis) measurements of tph2 mRNA expression (y axis) were averaged; (A) fifteen levels (-7.496 to -8.672 mm bregma) for the whole MnR, (B) six levels (-7.494 to -7.916 mm bregma) for the rostral MnR and (C) 10 levels (-7.916 to 8.672 mm bregma) for the caudal MnR. Tph2 mRNA quantification is expressed as Calibrated Mean Grey Value multiplied by its own Measured Area. Data points correspond to the overall MEAN ± SEM of tph2 expression of the whole/rostral/caudal MnR for each group/timepoint (n≤8/group [≤ 8 animals x 15/6/10 levels = ≤120/48/80 values]). One-way ANOVAs were performed to assess effect of time; (A) ($F_{(4, 523)}$ =2.573) p< 0.05; **p< 0.01 for 3 pm vs 9 pm: *p< 0.05 for 9 am vs 9 pm and for 6 pm vs 9 pm; (B) (($F_{(4, 221)}$ =2.186) p> 0.05; (C) ($F_{(4, 336)}$ =7.409) p< 0.001; ***p< 0.001 for 9 am vs 9 pm, for 3 pm vs 9 pm and for 6 pm vs 9 pm; * p< 0.05 for 3 am vs 9 am, for 3 am vs 3 pm and for 3 am vs 6 pm with Fisher's Least Significant Difference test.*

Next, I again assessed the changes between the normal circadian rhythm and the modified pattern in *tph2* mRNA expression after five weeks of LL in the whole, rostral and caudal MnR (Figure 5-17).

The whole MnR (Figure 5-17A), showed an interesting change in *tph2* mRNA expression after LL exposure, which was detected by two-way ANOVA as it revealed a significant interaction between treatment and time; ($F_{(4, 1016)}$ = 3.637) p<

0.01. Interestingly the largest differences, between LL treated rats and controls, occurred at 3 pm and 9 pm. Further multiple comparisons post-tests showed a statistically significant decrease in *tph2* mRNA expression at 3 pm after LL treatment, the time corresponding to the peak *tph2* mRNA expression of the controls. Moreover, the peak in expression changed to 9 pm after LL treatment, which was a significant increase in expression when compared to the controls.

The two-way ANOVA for the rostral MnR (Figure 5-17B) did not show a significant interaction; ($F_{(4, 446)} = 1.298$) $p > 0.05$. In contrast, for the caudal MnR (Figure 5-17C), similar findings were observed as for the whole MnR, however, these changes were more pronounced. These changes were detected by the two-way ANOVA with a significant interaction; ($F_{(4, 638)} = 7.257$) $p < 0.001$. The observed differences in the LL rats included a marked decrease in *tph2* mRNA expression at 3 pm, which was actually the peak *tph2* mRNA expression time in controls. Furthermore, the peak *tph2* mRNA expression time was shifted to 9 pm and the nadir shifted to 6 pm. The Fisher's LSD post-tests revealed these three key timepoints; 3 pm ($p<0.001$), 6 pm ($p<0.01$) and 9 pm ($p<0.01$) to be significantly different between LL and control rats. Therefore, in the caudal MnR, once again, LL treatment appeared to profoundly affect the normal circadian rhythm of *tph2* mRNA expression by increasing *tph2* mRNA expression when it would 'normally' be low (9pm) and reducing its expression when it would 'normally' be high (3 pm and 6 pm).

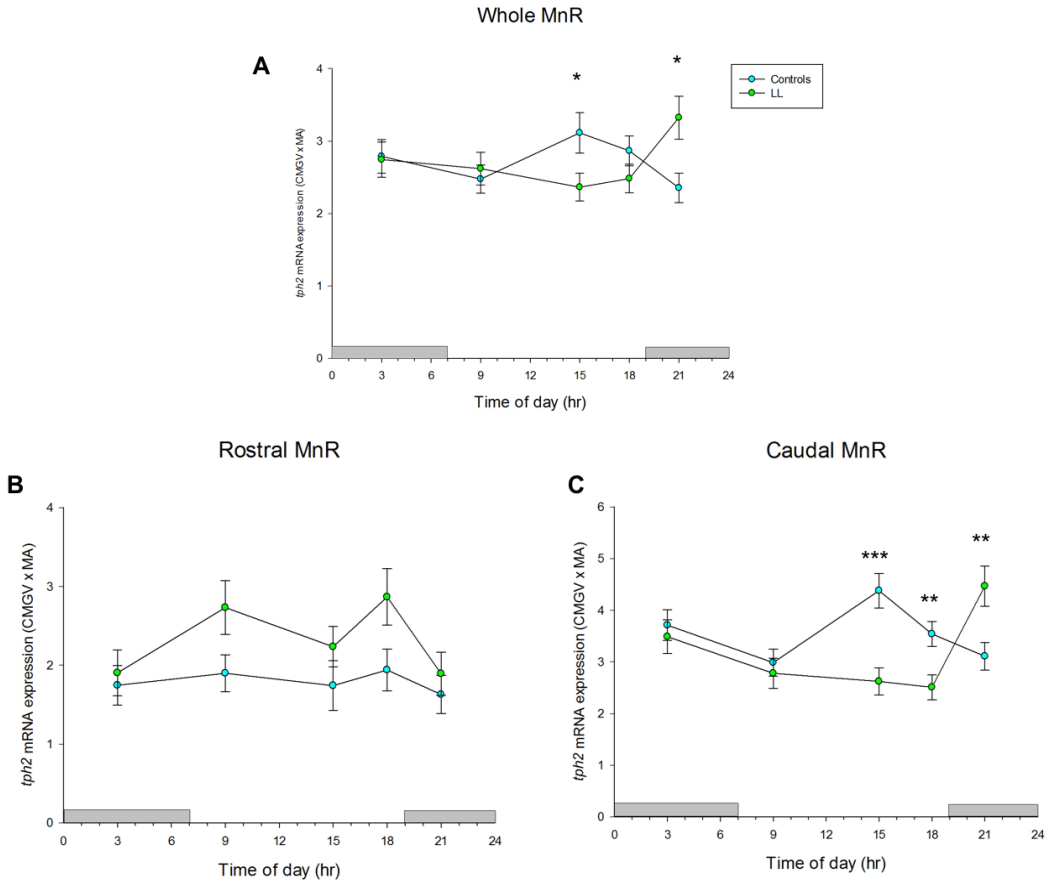

*Figure 5-17: Changes in circadian variation of tph2 mRNA expression in the MnR of Control vs LL treated animals. For each timepoint; 3am, 9am, 3pm, 6pm and 9pm (x axis) measurements of tph2 mRNA expression (y axis) were averaged for each group separately (CTRL or LL; (A) fifteen levels (-7.496 to -8.672 mm bregma) for the whole MnR, (B) six levels (-7.494 to -7.916 mm bregma) for the rostral MnR and (C) 10 levels (-7.916 to 8.672 mm bregma) for the caudal MnR. Tph2 mRNA quantification is expressed as Calibrated Mean Grey Value multiplied by its own Measured Area. Data points correspond to the overall MEAN ± SEM of tph2 mRNA expression of the whole/rostral/caudal MnR for each group/timepoint (n≤ 8/group [≤ 8 animals x 15/6/10 levels = ≤ 120/48/80 values]). Two-way ANOVAs were performed to assess interaction between treatment and time; (A) ($F_{(4, 1016)} = 3.637$) $p< 0.01$; * $p< 0.05$ when comparing CTRL vs LL at 6 pm and 9 pm; (B) ($F_{(4, 446)} = 1.298$) $p> 0.05$; (C) ($F_{(4, 638)} = 7.257$) $p< 0.001$; *** $p< 0.001$ when comparing CTRL vs LL at 3 pm; ** $p< 0.01$ when comparing CTRL vs LL at 6 pm and 9 pm with Fisher's Least Significant Difference test.*

5.3.4 Circadian rhythmicity of *tph2* mRNA expression in the DR subregions and MnR nucleus after LL treatment; analysis across the full rostro-caudal gradient.

Now, for this last section of the chapter, the goal was to assess the effects of five weeks of LL in the circadian activity of *tph2* mRNA expression throughout the

rostro-caudal gradient of the DR subregions and the MnR nucleus. To accomplish this, several Linear Mixed Model (LMM) analyses were completed as described in the general methods chapter. Furthermore, a second overall LMM analysis was used to compare the changes in *tph2* mRNA expression caused by LL treatment when compared to natural conditions throughout the rostro-caudal gradient of the DR subregions and the MnR nucleus.

As for chapter 3 and 4, all LMM analyses were finalized and only if there were significant differences in any main factor or interaction, then, Fisher's LSD post-tests followed. All statistical tests were considered only if the sample size was above four animals (half the original sample size for each timepoint at each rostro-caudal level).

In General, *tph2* mRNA expression changed throughout the rostro-caudal gradient in the all the DR subregions and MnR nucleus. Moreover, *tph2* mRNA expression also changed over time in the DRD, DRV, DRVL/VLPAG subregions and MnR nucleus (Table 5-1). Furthermore, when assessing changes in *tph2* mRNA expression under natural conditions and after LL treatment no changes were found in the DRC or DRI. Nevertheless, differences were found throughout multiple rostro-caudal levels of DRD, DRV DRVL/VLPAG and MnR at specific key time points assessed over the 24-hour period (Table 5-2).

Analysis of the circadian activity of *tph2* mRNA expression profile after LL treatment using LMM analysis revealed a rostro-caudal level * time point interaction ($F_{(64,\ 9.073)} = 3.071$, $p < .0.019$), a rostro-caudal level (raphe subregion) interaction ($F_{(36,\ 74.334)} = 36.636$, $p < 0.000$), a main effect of rostro-caudal level ($F_{(16,\ 9.292)} = 126.423$, $p < 0.000$), a main effect of raphe subregion ($F_{(5,\ 5.746)} = 102.657$, $p < 0.000$) and a main effect of time point ($F_{(4,\ 5.847)} = 8.512$, $p < 0.013$) (Table 5-1).

Based upon the significant main effects and interactions in this first overall LMM analysis, secondary LMMs were then performed to assess how *tph2* mRNA expression - over the entire rostro-caudal gradient in every subregion of the DR and the MnR changed over a 24 hour period Additionally, variations in *tph2* mRNA expression across the rostro-caudal gradient at each time point were also assessed

independently, but for simplicity reasons, these changes are not represented in the Figures.

Table 5-1: Linear mixed model analysis results for tph2 mRNA expression in LL treated SD male rats

Model	Test statistic	*p*-value
Overall analysis for LL		
Unstructured Correlations covariance structure		
Akaike's Information Criterion (AIC): 8636.898		
Rostrocaudal level[1] (1-17)	$F_{(16, 9.292)} = 126.423$	.000 ***
Raphe subregion[2] (DRC, DRI, DRD, DRV, DRVL/VLPAG, MnR)	$F_{(5, 5.746)} = 102.657$	.000 ***
Time point[3] (3 am, 9 am, 3 pm, 6 pm, 9 pm)	$F_{(4, 5.847)} = 8.512$	.013 *
Rostrocaudal level * Time point	$F_{(64, 9.073)} = 3.071$	.019 *
Raphe subregion * Time point	$F_{(20, 5.469)} = .756$	.706
Rostrocaudal level (Raphe subregion)	$F_{(36, 74.334)} = 36.636$	.000 ***
Rostrocaudal level * Time point (Raphe subregion)	$F_{(144, 24.459)} = .949$	.596
Subregional analyses		
DRC		
First-Order Ante-dependence covariance structure		
Akaike's Information Criterion (AIC): 664.394		
Time point (3 am, 9 am, 3 pm, 6 pm, 9 pm)	$F_{(4, 41.467)} = 2.201$	.086
Rostrocaudal level (13-17)	$F_{(4, 33.510)} = 5.362$	.002 **
Time point * Rostrocaudal level	$F_{(16, 33.878)} = 1.326$	.238
DRI		
Heterogeneous First-Order Autoregressive covariance structure		
Akaike's Information Criterion (AIC): 508.139		
Time point (3 am, 9 am, 3 pm, 6 pm, 9 pm)	$F_{(4, 30.737)} = 1.178$	.340
Rostrocaudal level (14-17)	$F_{(3, 31.567)} = 59.167$	.000 ***
Time point * Rostrocaudal level	$F_{(12, 32.994)} = 1.522$	.166
DRD		

Unstructured Correlations covariance structure		
Akaike's Information Criterion (AIC): 1745.481		
Time point (3 am, 9 am, 3 pm, 6 pm, 9 pm)	$F_{(4, 34.643)}$= 4.007	.009**
Rostrocaudal level (1-12)	$F_{(11,30.222)}$= 316.301	.000***
Time point * Rostrocaudal level	$F_{(44,32.025)}$= 3.360	.000***
DRV		
Heterogeneous Toeplitz covariance structure		
Akaike's Information Criterion (AIC): 2201.773		
Time point (3 am, 9 am, 3 pm, 6 pm, 9 pm)	$F_{(4, 41.987)}$= 1.911	.126
Rostrocaudal level (1-14)	$F_{(13, 66.808)}$= 48.956	.000 ***
Time point * Rostrocaudal level	$F_{(52, 69.091)}$= 1.634	.028 *
DRVL/VLPAG		
Heterogeneous Compound Symmetry covariance structure		
Akaike's Information Criterion (AIC): 1296.343		
Time point (3 am, 9 am, 3 pm, 6 pm, 9 pm)	$F_{(4, 37.547)}$= 3.984	.009 **
Rostrocaudal level (1-17)	$F_{(7, 69.588)}$= 69.599	.000 ***
Time point * Rostrocaudal level	$F_{(28, 70.977)}$= 1.787	.026 *
MnR		
Unstructured covariance structure		
Akaike's Information Criterion (AIC): 1534.533		
Time point (3 am, 9 am, 3 pm, 6 pm, 9 pm)	$F_{(4, 147.722)}$ = 1.424	.229
Rostrocaudal level (1-17)	$F_{(14, 10.452)}$= 25.909	.000 ***
Time point * Rostrocaudal level	$F_{(56, 1586.409)}$= 6.723	.000 ***

[1]Rostrocaudal levels were well-defined from bregma levels given in the atlas; where most rostral level was -7.328 mm bregma (1 according to level code) progressing to the most caudal level at –8.672 mm bregma (17 according to level code). Within this brain section 17 different and representative coronal sections of 12 µm were used to measure *tph2* mRNA of the dorsal raphe nucleus and the median raphe nucleus. [2]The Raphe subregions used in this research were the following: DRC, dorsal raphe nucleus, caudal part; DRI, dorsal raphe nucleus, interfascicular part; DRD, dorsal raphe nucleus, dorsal part; DRV, dorsal raphe nucleus, ventral part and DRVL/VLPAG, dorsal raphe nucleus, ventrolateral part/ventrolateral periaqueductal grey. MnR, median raphe nucleus was also included and considered as a subregion of the raphe complex. [3] The five different time points (3 am, 9 am, 3 pm, 6 pm, 9 pm) used in this study were considered as a suitable description of the circadian rhythm of *tph2* mRNA expression. They were chosen to fit in parallel with the measured circadian rhythm of plasma CORT after LL treatment. *$p<0.05$. **$p<0.01$. ***$p<0.001$.

A second overall LMM analysis was performed to evaluate now the effect of treatment (LL versus 'normal' LD conditions) at each time point, across all rostro-caudal levels and in all Raphe subregions. This analysis revealed a treatment * timepoint interaction ($F_{(4, 511.600)} = 13.180$, $p < 0.000$), a treatment * rostro-caudal level interaction ($F_{(16, 405.927)} = 5.132$, $p < 0.000$), a timepoint* rostro-caudal level interaction ($F_{(64, 444.210)} = 2.147$, $p < 0.000$), a rostro-caudal level * raphe subregion interaction ($F_{(36, 448.004)} = 61.503$, $p < 0.000$), a treatment * time point * rostro-caudal level interaction ($F_{(63, 455.830)} = 2.944$, $p < 0.004$) a treatment *rostro-caudal level (raphe subregion interaction) ($F_{(36, 435.701)} = 1.794$, $p < 0.004$), a main effect in rostro-caudal level ($F_{(16, 410.952)} = 235.431$, $p < 0.000$) and a main effect in raphe subregion ($F_{(5, 386.026)} = 210.632$, $p < 0.000$) (Table 5-2).

Considering all the significant main effects and interactions found in this overall LMM analysis, subregional LMMs were used to assess the effect of treatment (LL versus 'normal' LD conditions) at each time point, across the rostro-caudal gradient of each DR subregion and MnR nucleus separately (Table 5-2). Moreover, as explained previously, changes across the rostro-caudal gradient within each time point were also assessed, but for simplicity reasons, these changes are not represented in the Figures.

Table 5-2: Linear mixed model analysis results for tph2 mRNA expression in Control vs LL treated SD male rats.

Model	**Test statistic**	***p*-value**
Overall analysis for Controls vs LL		
Heterogeneous Toeplitz covariance structure		
Akaike's Information Criterion (AIC): 16595.877		
Treatment[1] (CTRL vs LL)	$F_{(1, 508.120)} = .171$	.679
Time point[2] (3 am, 9 am, 3 pm, 6 pm, 9 pm)	$F_{(4, 505.185)} = .274$	.895
Rostrocaudal level[3] (1-17)	$F_{(16, 410.952)} = 235.431$	.000 ***
Raphe subregion[4] (DRC, DRI, DRD, DRV, DRVL/VLPAG, MnR)	$F_{(5, 386.026)} = 210.632$	.000 ***
Treatment * Time point	$F_{(4, 511.600)} = 13.180$	.000 ***
Treatment * Rostrocaudal level	$F_{(16, 405.927)} = 5.132$	.000 ***
Treatment * Raphe subregion	$F_{(5, 384.611)} = 13.180$	.785

Time point * Rostrocaudal level	$F_{(64, 444.210)}$ = 2.147	.000 ***
Time point * Raphe subregion	$F_{(20, 387.148)}$ = .684	.843
Rostrocaudal level * Raphe subregion	$F_{(36, 448.004)}$ = 61.503	.000 ***
Treatment * Time point * Raphe subregion	$F_{(20, 388.360)}$ = .632	.889
Treatment * Time point * Rostrocaudal level	$F_{(63, 455.830)}$ = 2.944	.000 ***
Treatment * Rostrocaudal level (Raphe subregion)	$F_{(36, 435.701)}$ = 1.794	.004 **
Time point * Rostrocaudal level (Raphe subregion)	$F_{(144, 524.350)}$ = 1.058	.326
Treatment * Time point * Rostrocaudal level (Raphe subregion)	$F_{(141, 562.703)}$ = 1.120	.187
Subregional analyses		
DRC		
First-Order Autoregressive covariance structure		
Akaike's Information Criterion (AIC): 1113.543		
Treatment (CTRL vs LL)	$F_{(1, 106.215)}$ = .028	.867
Time point (3 am, 9 am, 3 pm, 6 pm, 9 pm)	$F_{(4, 98.741)}$ = .280	.890
Rostrocaudal level (13-17)	$F_{(4, 183.051)}$ = 4.389	.002 **
Treatment * Timepoint	$F_{(4, 97.135)}$= 1. 977	.104
Treatment * Rostrocaudal level	$F_{(4, 183.138)}$= .375	.826
Timepoint * Rostrocaudal level	$F_{(16, 180.577)}$ = 1.250	.234
Treatment * Time point * Rostrocaudal level	$F_{(15, 179.008)}$ = .629	.848
DRI		
Unstructured Correlations covariance structure		
Akaike's Information Criterion (AIC): 773.089		
Treatment (CTRL vs LL)	$F_{(1, 43.119)}$= 2.394	.129
Time point (3 am, 9 am, 3 pm, 6 pm, 9 pm)	$F_{(4, 43.157)}$= 1.872	.133
Rostrocaudal level (14-17)	$F_{(3, 33.719)}$= 133.870	.000 ***
Treatment * Timepoint	$F_{(4, 45.735)}$= .980	.428
Treatment * Rostrocaudal level	$F_{(3, 33.522)}$ = 2.246	.101
Timepoint * Rostrocaudal level	$F_{(12, 33.798)}$= 1.611	.135
Treatment * Time point * Rostrocaudal level	$F_{(11, 36.668)}$= 1.401	.214
DRD		
Heterogeneous Toeplitz covariance structure		
Akaike's Information Criterion (AIC): 3510.182		
Treatment (CTRL vs LL)	$F_{(1, 67.800)}$= .037	.848
Time point (3 am, 9 am, 3 pm, 6 pm, 9 pm)	$F_{(4, 67.790)}$= .850	.498
Rostrocaudal level (1-12)	$F_{(11, 128.787)}$= 100.357	.000 ***

Treatment * Timepoint	$F_{(4, 67.790)}$= 5.899	.000 ***
Treatment * Rostrocaudal level	$F_{(11, 128.787)}$= 5.701	.000 ***
Timepoint * Rostrocaudal level	$F_{(44, 140.805)}$= 1.395	.075
Treatment * Time point * Rostrocaudal level	$F_{(44, 140.805)}$= 1.803	.005 **
DRV		
Heterogeneous Toeplitz covariance structure		
Akaike's Information Criterion (AIC): 4430.078		
Treatment (CTRL vs LL)	$F_{(1, 87.798)}$= .031	.861
Time point (3 am, 9 am, 3 pm, 6 pm, 9 pm)	$F_{(4, 87.766)}$= .472	.756
Rostrocaudal level (1-14)	$F_{(13, 124.997)}$= 121.636	.000 ***
Treatment * Timepoint	$F_{(4, 87.766)}$= 3.109	.019 *
Treatment * Rostrocaudal level	$F_{(13, 124.997)}$= 1.424	.157
Timepoint * Rostrocaudal level	$F_{(52, 127.943)}$= 1.503	.034 *
Treatment * Time point * Rostrocaudal level	$F_{(52, 127.943)}$= 1.750	.006 **
DRVL/VLPAG		
Heterogeneous Toeplitz covariance structure		
Akaike's Information Criterion (AIC): 2602.203		
Treatment (CTRL vs LL)	$F_{(1, 76.607)}$ = 2.723	.103
Time point (3 am, 9 am, 3 pm, 6 pm, 9 pm)	$F_{(4, 76.570)}$= .985	.421
Rostrocaudal level (6-13)	$F_{(7, 114.074)}$= 116.452	.000 ***
Treatment * Timepoint	$F_{(4, 76.570)}$= 6.226	.000 ***
Treatment * Rostrocaudal level	$F_{(7, 114.074)}$= 7.358	.000 ***
Timepoint * Rostrocaudal level	$F_{(28, 114.112)}$ = 1.295	.172
Treatment * Time point * Rostrocaudal level	$F_{(28, 114.112)}$ = 1.624	.040 *
MnR		
First-Order Ante-dependence covariance structure		
Akaike's Information Criterion (AIC): 3055.346		
Treatment (CTRL vs LL)	$F_{(1, 117.985)}$= .437	.510
Time point (3 am, 9 am, 3 pm, 6 pm, 9 pm)	$F_{(4, 117.295)}$= .435	.783
Rostrocaudal level (3-17)	$F_{(13, 155.194)}$= 56.143	.000 ***
Treatment * Timepoint	$F_{(4, 118.402)}$= 2.539	.043 *
Treatment * Rostrocaudal level	$F_{(13, 152.320)}$= 4.234	.000 ***
Timepoint * Rostrocaudal level	$F_{(52, 164.365)}$= 2.772	.000 ***
Treatment * Time point * Rostrocaudal level	$F_{(51, 154.449)}$ = 3.667	.000 ***

[1]Two different treatment groups (n≤40/group) were considered in this study; Controls and LL treated SD male rats.[2]The five different time points (3 am, 9 am, 3 pm, 6 pm, 9 pm) used in this study were considered as a suitable description of the circadian rhythm of *tph2* mRNA expression. They were chosen to fit in parallel with the measured circadian rhythm of plasma CORT. [3]Rostrocaudal levels were well-defined from bregma levels given in the atlas; where most rostral level was -7.328 mm bregma (1 according to level code) progressing to the most caudal level at –8.672 mm bregma (17

according to level code). Within this brain section 17 different and representative coronal sections of 12 µm were used to measure *tph2* mRNA of the dorsal raphe nucleus and the median raphe nucleus. [4]The Raphe subregions used in this research were the following: DRC, dorsal raphe nucleus, caudal part; DRI, dorsal raphe nucleus, interfascicular part; DRD, dorsal raphe nucleus, dorsal part; DRV, dorsal raphe nucleus, ventral part and DRVL/VLPAG, dorsal raphe nucleus, ventrolateral part/ventrolateral periaqueductal grey. MnR, median raphe nucleus was also included and considered as a subregion of the Raphe complex. *$p<0.05$. **$p<0.01$. ***$p<0.001$.

5.3.4.1 Dorsal Raphe nucleus (DRC).

The secondary LMM analysis to assess the circadian variation, within the DRC revealed only a main effect in the rostro-caudal level variable ($F_{(4, 33.510)}= 5.362$, $p <0.000$) and no effect in time or interaction (Table 5-1) (Figure 5-18). Interestingly, the LMM was unable to detect a circadian variation in *tph2* mRNA expression within the rostro-caudal extent of the DRC after LL treatment, which is inconsistent with the circadian variation found in the simpler (averaged data) analysis (Figure 5-6). This unexpected finding could be based in the fact that the sample size for each rostro-caudal level was not big enough while the averaged analysis had sufficient data to be statistically significant.

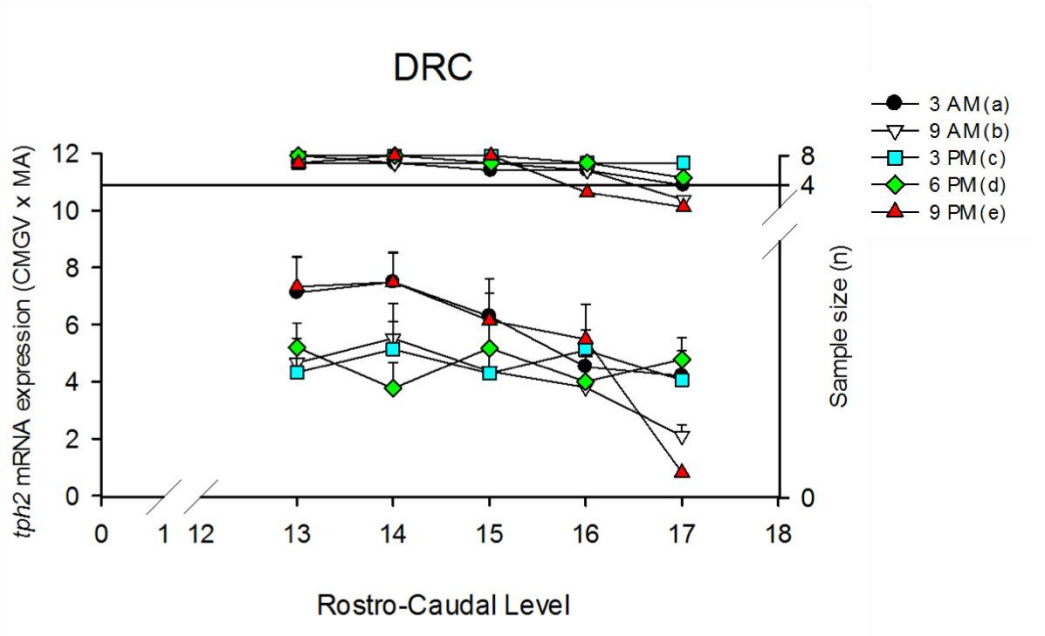

Figure 5-18: Rostro-caudal level variation of tph2 mRNA expression profile in the DRC of LL treated animals. Tph2 mRNA expression in the DRC was measured in five different rostro-caudal levels presented in the x axis (-8.336 to -8.672 mm bregma). Five different timepoints; 3 am, 9 am, 3 pm, 6 pm and 9 pm are shown for each rostro-caudal level (time course). Tph2 mRNA quantification is expressed as Calibrated Mean Grey Value multiplied by its own Measured Area. Top data points are associated to the right y-axis which represent the after

Grubb's test sample size at each rostro-caudal level. Bottom data points are linked to the left y-axis which correspond to the MEAN ± SEM of tph2 mRNA expression of each group/timepoint (n≤8/group) for each rostro-caudal level. Performed Fisher's Least Significant difference test showed the following significant differences: (ad) p< 0.05 for 3 am vs 6 pm, (ce) p< 0.05 for 3 pm vs 9 pm, (de) p< 0.05 for 6 pm vs 9 pm.

Moreover, as observed in Figure 5-19, the subregional LMM analysis to assess the circadian variation between treatment groups, revealed only a rostro-caudal level effect ($F_{(4, 183.051)}$ = 4.389, p<0.01) and no effect of treatment ($F_{(1, 508.120)}$= .171, p>0.05) or time point ($F_{(4, 505.185)}$ = .274, p>0.05), nor any other interaction (Table 5-2) within this subregion of the DRC. Therefore, no post-tests were performed.

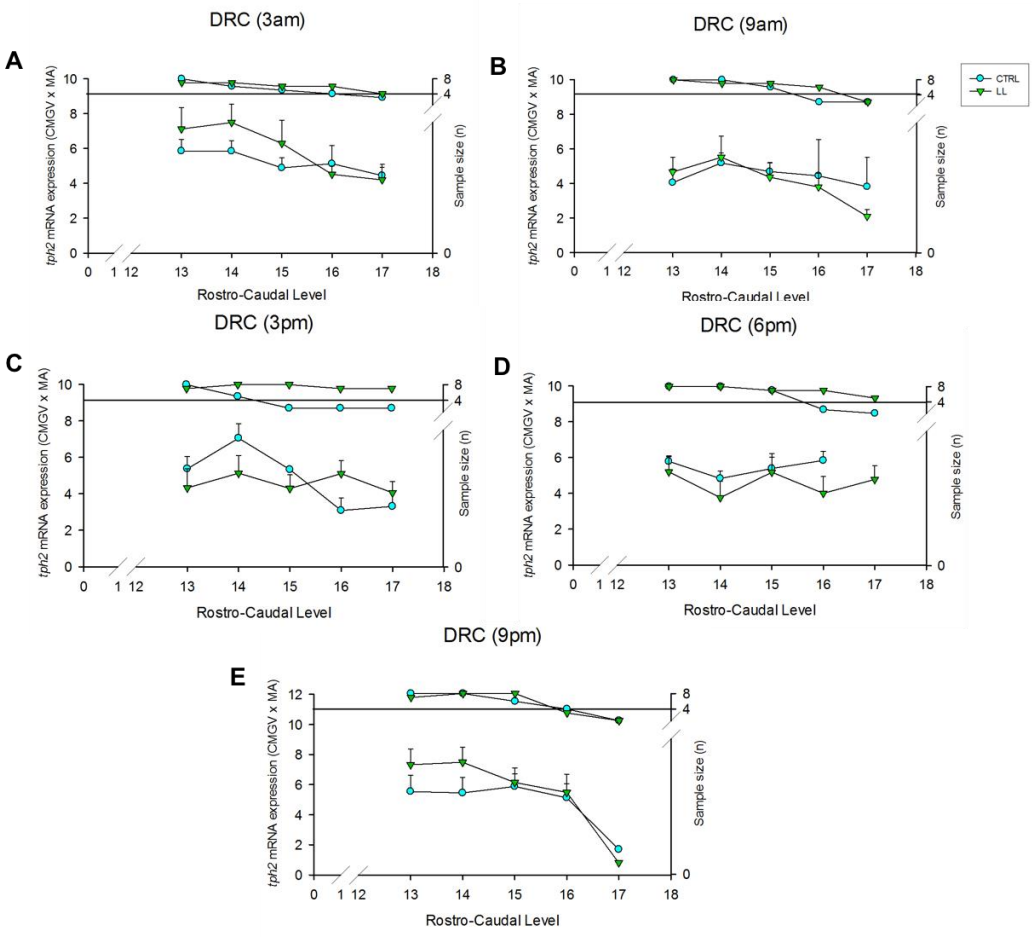

Figure 5-19: Circadian changes in tph2 mRNA expression at each rostro-caudal level in the DRC of Controls versus LL treated animals. Tph2 mRNA expression in the DRC was measured in five different rostro-caudal levels presented in the x axis (-8.336 to -8.672 mm bregma) at five different time points; (A) 3 am, (B) 9 am, (C) 3 pm, (D) 6 pm and (E) 9 pm. Tph2 mRNA quantification is expressed as Calibrated Mean Grey Value multiplied by its own Measured Area. Top data points are associated to the right y-axis which represent the after Grubb's test sample size at each rostro-caudal level. Bottom data points are linked to the left y-axis which correspond to the MEAN ± SEM of tph2 mRNA expression for each group (CTRL or LL [n≤

8/each group]) at each of the five rostro-caudal levels of the DRC. Fisher's Least Significant Difference post hoc test showed no significant differences.

Taking these LMM analyses into consideration, it seems that the DRC did not display a circadian variation within its rostro-caudal levels after five weeks of constant light. However, because even under normal conditions the DRC doesn't exhibit a circadian variation and this analysis is inconsistent to the simpler analysis, the effect shown of LL treatment in this specific DR subregion cannot be taken into consideration for interpretation.

5.3.4.2 Dorsal Raphe nucleus, interfascicular part (DRI).

Secondary LMM analysis within the DRI revealed a significant main effect of rostro-caudal level ($F_{(3,\ 31.567)}$= 59.167, p <0.000) and no effect of time or interaction (Table 5-1). Therefore, as shown in Figure 5-20, the rostro-caudal extent of the DRI does not exhibit a circadian pattern of *tph2* mRNA expression after LL treatment.

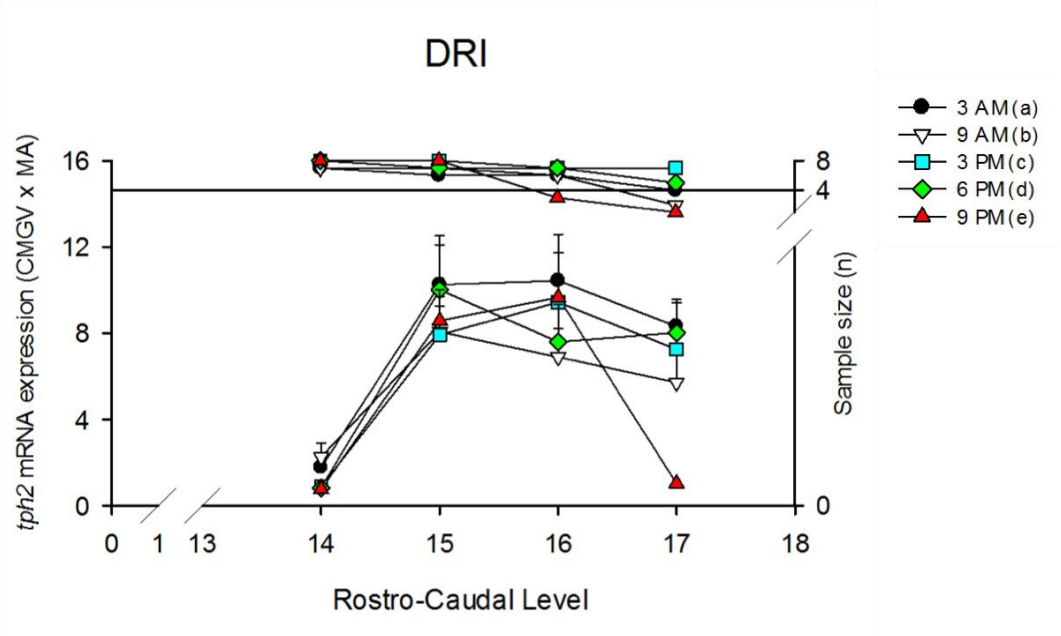

Figure 5-20: Rostro-caudal level variation of tph2 mRNA expression profile in the DRI of LL treated animals. Tph2 mRNA expression in the DRI was measured in four different rostro-caudal levels presented in the x axis (-8.420 to -8.672 mm bregma). Five different timepoints; 3 am, 9 am, 3 pm, 6 pm and 9 pm are shown for each rostro-caudal level (time course). Tph2 mRNA quantification is expressed as Calibrated Mean Grey Value multiplied by its own Measured Area. Top data points are associated to the right y-axis which represent the after

Grubb's test sample size at each rostro-caudal level. Bottom data points are linked to the left y-axis which correspond to the MEAN value ± SEM of tph2 mRNA expression for each group/timepoint (n≤ 8/group) for each rostro-caudal level. Performed Fisher's Least Significant difference test showed the following significant differences: (bc) p< 0.05 for 9 am vs 3 pm, (bd) p< 0.05 for 9 am vs 6 pm, (be) p< 0.05 for 9 am vs 9 pm.

The subregional LMM analysis assessing the pattern of circadian variation after LL treatment when compared to controls, revealed only a significant difference in rostro-caudal level ($F_{(3, 33.719)}$= 133.870, p< 0.000) (Table 5-2), therefore, no post tests were performed for this subregion (Figure 5.21).

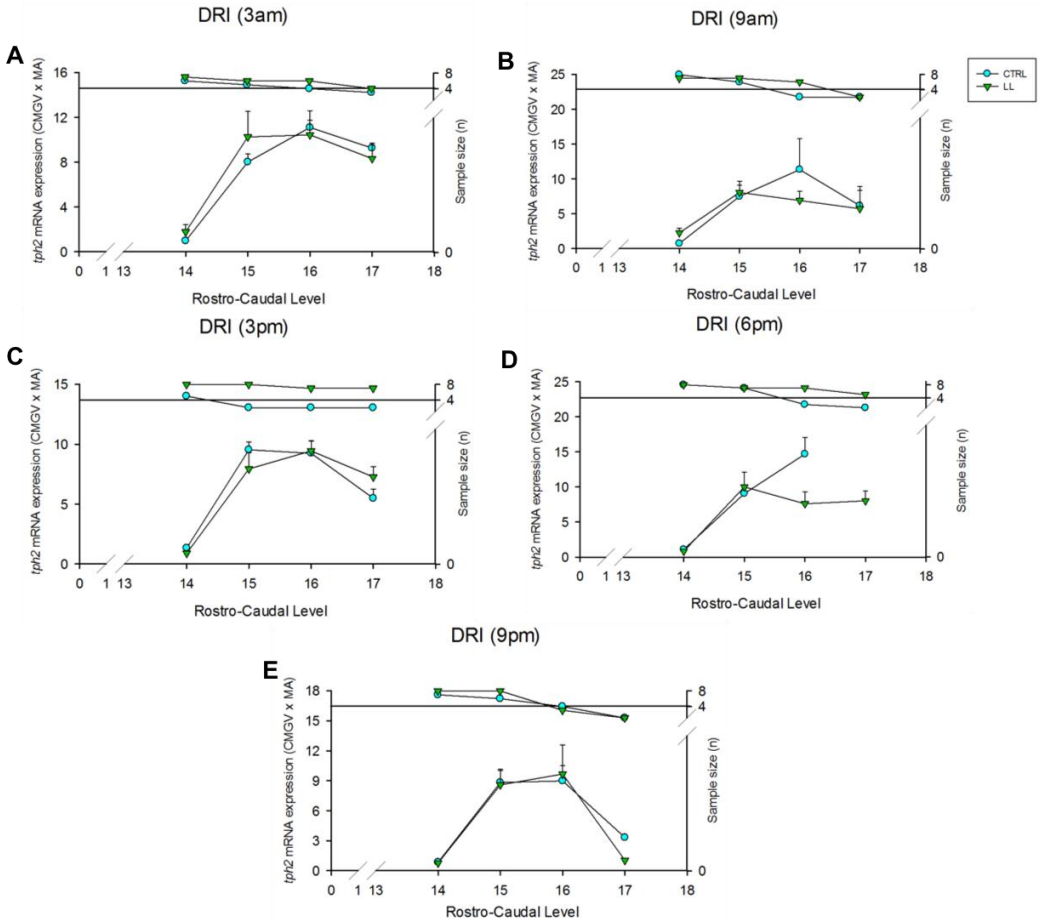

Figure 5-21: Circadian changes in tph2 mRNA expression at each rostro-caudal level in the DRI of Controls versus LL treated animals. Tph2 mRNA expression in the DRI was measured in four different rostro-caudal levels presented in the x axis (-8.420 to -8.672mm bregma) at five different time points; (A) 3am, (B) 9 am, (C) 3 pm, (D) 6 pm and (E) 9 pm. Tph2 mRNA quantification is expressed as Calibrated Mean Grey Value multiplied by its own Measured Area. Top data points are associated to the right y-axis which represent the after Grubb's test sample size at each rostro-caudal level. Bottom data points are linked to the left y-axis which correspond to the MEAN ± SEM of tph2 mRNA expression for each group (CTRL or LL [n≤ 8/each group]) at each of the four rostro-caudal level of the DRI. Fisher's Least Significant

*Difference post hoc test showed the following significant differences; (B) *p< 0.05 for CTRL vs LL in level 14 at 9 am.*

5.3.4.3 Dorsal Raphe nucleus, dorsal part (DRD).

Now, considering the subregional secondary LMM analysis performed for the DRD the resulting significant differences were revealed; a timepoint * rostro-caudal level interaction ($F_{(44,32.025)}$= 3.360, p< 0.000), a main effect in time point ($F_{(4, 34.643)}$= 4.007, p <0.009) and a main effect of rostro-caudal level ($F_{(11,30.222)}$= 316.301p<0.000). Additionally, post-tests revealed various statistically significant differences, confirming a strong circadian variation in *tph2* mRNA expression after five weeks of constant light within the DRD (Figure 5-22). Significant differences throughout the rostro-caudal levels within each time point are not shown in the Figure. However, when looking at the effect in *tph2* mRNA expression over time, six different levels of the DRD reached statistical significance. Interestingly, a strong effect of LL is observed in the caudal levels of the DRD (9 to 12) where the 3am peak becomes significantly different when compared to 3pm and 6pm time points, which is consistent with the averaged analyses of the DRD caudal levels in the section above. This condition is observed even in the rostral level 5 and 7, where 6 pm. In general, a clear trend in the data can be seen where the 6 pm nadir is different from the 3 am and 9 am peak, however statistical differences are only reached in specific levels.

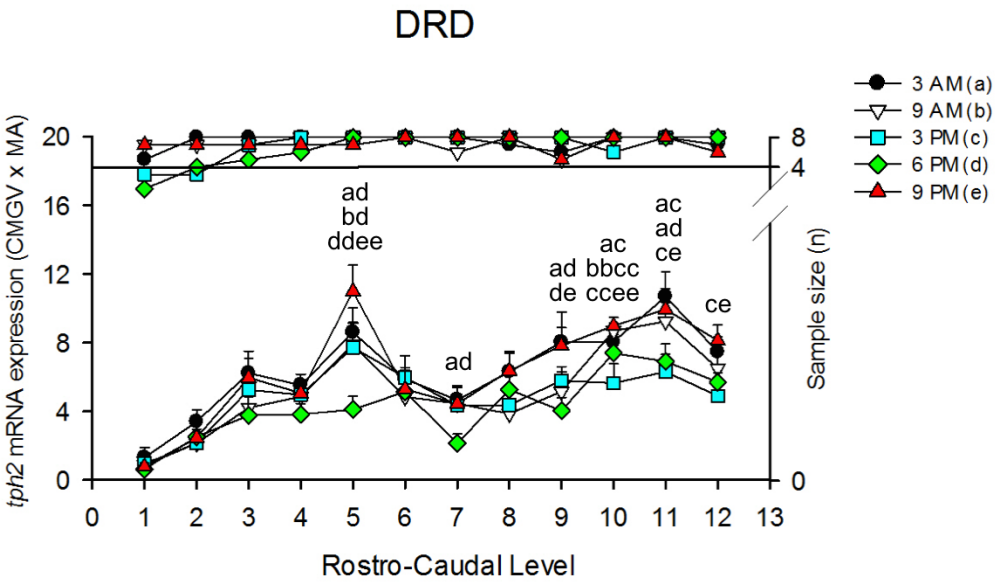

Figure 5-22: Rostro-caudal level variation of tph2 mRNA expression profile in the DRD of LL treated animals. Tph2 mRNA expression in the DRD was measured in twelve different rostro-caudal levels presented in the x axis (-7.328 to -8.252 mm bregma). Five different timepoints; 3 am, 9 am, 3 pm, 6 pm and 9 pm are shown for each rostro-caudal level (time course). Tph2 mRNA quantification is expressed as Calibrated Mean Grey Value multiplied by its own Measured Area. Top data points are associated to the right y-axis which represent the after Grubb's test sample size at each rostro-caudal level. Bottom data points are linked to the left y-axis which correspond to the MEAN value ± SEM of tph2 mRNA expression for each group/timepoint (n≤ 8/group) for each rostro-caudal level. Performed Fisher's Least Significant difference test showed the following significant differences: (bbcc) p< 0.01 for 9 am vs 3pm, (ccee) p< 0.01 for 3 pm vs 9 pm, (ddee) p< 0.01 for 6 pm vs 9 pm, (ac) p< 0.05 for 3 am vs 3 pm, (ad) p< 0.05 for 3 am vs 6 pm, (bd) p< 0.05 for 9 am vs 6 pm, (ce) p< 0.05 for 3 pm vs 9 pm, (de) p< 0.05 6 pm vs 9 pm.

To evaluate changes in the circadian rhythm of *tph2* mRNA expression after five weeks of LL when compared to controls, a secondary LMM analysis was performed for the DRD. This analysis revealed a treatment * timepoint interaction ($F_{(4, 67.790)}$= 5.899, p< 0.000), a treatment * rostro-caudal level interaction ($F_{(11, 128.787)}$= 5.701, p <0.000), a treatment *timepoint * rostro-caudal level interaction ($F_{(44, 140.805)}$= 1.803, p< 0.005) and a main effect of rostro-caudal level ($F_{(11, 128.787)}$= 100.357, p<0.000). Multiple comparisons showed an interesting pattern within the DRD (Figure 5-23) which strongly coincided with the simpler DRD analysis (section above) as higher expression of *tph2* mRNA after LL treatment was seen at 3 am (Figure 5-23A), 9am (Figure 5-23B) and 9pm (Figure 5-23E) and lower expression was observed in the 3pm (Figure 5-23C) and 6 pm (Figure 5-23D) timepoints when

compared to controls. Fascinatingly, higher *tph2* mRNA expression was mainly specific to the caudal levels (10-12), whereas lower expression was seen in the rostral levels at least in the 6 pm timepoint, because at 3 pm, even when a trend in lower levels after LL treatment was observed in almost all the levels, no statistical difference was reached.

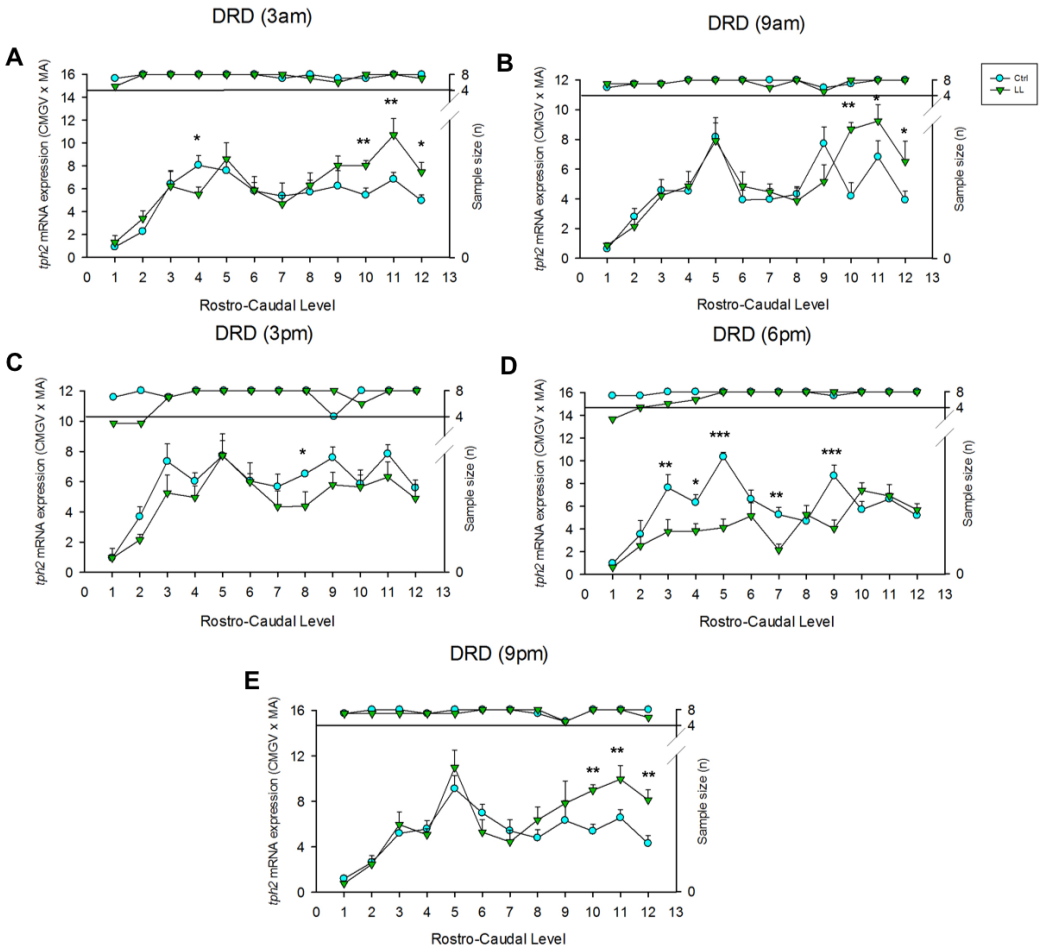

*Figure 5-23: Circadian changes in tph2 mRNA expression at each rostro-caudal level in the DRD of Controls vs LL treated animals. Tph2 mRNA expression in the DRD was measured in twelve different rostro-caudal levels presented in the x axis (-7.328 to -8.252 mm bregma) at five different time point: (A) 3am, (B) 9 am, (C) 3 pm, (D) 6 pm and (E) 9 pm. Tph2 mRNA quantification is expressed as Calibrated Mean Grey Value multiplied by its own Measured Area. Top data points are associated to the right y-axis which represent the after Grubb's test sample size at each rostro-caudal level. Bottom data points are linked to the left y-axis which correspond to the MEAN ± SEM of tph2 mRNA expression for each group (CTRL or LL [n≤ 8/each group]) at each of the twelve rostro-caudal level of the DRD. Fisher's Least Significant Difference post hoc test showed the following significant differences; (A) **p< 0.01 for CTRL vs LL in level 10 and 11, and *p< 0.05 in level 4 and 12 at 3 am; (B) **p< 0.01 for CTRL vs LL in level 10 and *p< 0.05 L in level 101 and 12 at 9 am; (C) *p< 0.05 for CTRL vs LL in level 8 at 3 pm; (D) ***p< 0.001 for CTRL vs LL in level 5 and 9, **p< 0.01 in level 3 and 11, and *p< 0.05 in level 4 at 6 pm; (E) **p< 0.01 for CTRL vs LL in level10, 11 and 12 at 9 pm.*

Accordingly, it appears that the DRD displayed a strong circadian variation across its 12 rostro-caudal levels after LL treatment, which seems to have a strong effect when compared to the natural rhythm of *tph2* mRNA expression across the 24-hour period within this specific subregion.

5.3.4.4 Dorsal Raphe nucleus, ventral part (DRV).

For the DRV, the secondary LMM analysis which assessed only the circadian variation after LL, revealed a time point *rostro-caudal interaction ($F_{(52, 69.091)}$= 1.634, p<0.028) and a main effect in rostro-caudal level ($F_{(13, 66.808)}$= 48.956, p< 0.000) (Table 5-11). Fisher's LL tests revealed various significant differences in *tph2* mRNA expression throughout the rostro-caudal gradient within each time point, nonetheless, they are not shown in the Figure. However, post-tests also revealed differences over time at each rostro-caudal level which seemed to correspond almost entirely to the differences between the 3 am and 9 pm peak and the 3 pm and 6 pm nadir (Figure 5-24). Again, similar to the DRD subregion, these changes were primarily specific to the caudal levels of the DRV (10-14), which again agrees with the simpler subregion analysis.

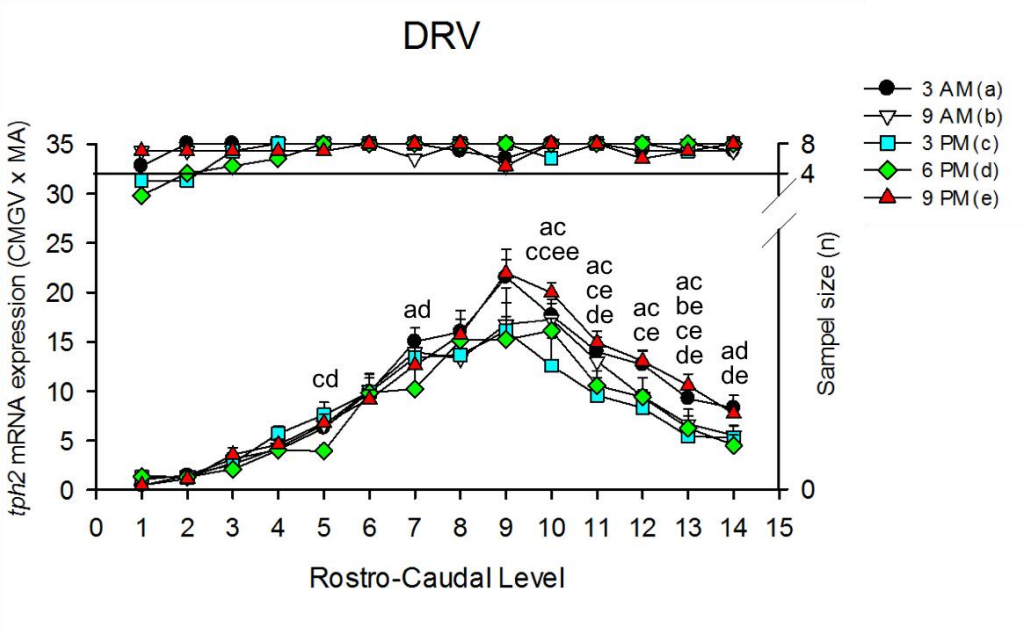

Figure 5-24: Rostro-caudal level variation of tph2 mRNA expression profile in the DRV of LL treated animals. Tph2 mRNA expression in the DRV was measured in fourteen different rostro-caudal levels presented in the x axis (-7.328 to -8.420 mm bregma). Five different timepoints; 3 am, 9 am, 3 pm, 6 pm and 9 pm are shown for each rostro-caudal level (time course). Tph2 mRNA quantification is expressed as Calibrated Mean Grey Value multiplied by its own Measured Area. Top data points are associated to the right y-axis which represent the after Grubb's test sample size at each rostro-caudal level. Bottom data points are linked to the left y-axis which correspond to the MEAN value ± SEM of tph2 mRNA expression for each group/timepoint (n≤ 8/group) for each rostro-caudal level. Performed Fisher's Least Significant difference test showed the following significant differences: (ccee) p< 0.01 for 3 pm vs 9 pm, (ac) p< 0.05 for 3 am vs 3 pm, (ad) p< 0.05 for 3 am vs 6 pm, (be) p< 0.05 for 9 am vs 9 pm, (cd) p< 0.05 for 3 pm vs 6 pm, (ce) p< 0.05 for 3 pm vs 9 pm, (de) p< 0.05 6 pm vs 9 pm.

The second subregional LMM analysis was performed for the DRV to additionally evaluate the effect of LL treatment in comparison to the 'normal' controls, and it revealed a treatment * timepoint interaction ($F_{(4,\ 87.766)}$= 3.109, p< 0.019), a timepoint * rostro-caudal level interaction ($F_{(52,\ 127.943)}$= 1.503, p< 0.034), a treatment * timepoint * rostro-caudal level interaction ($F_{(52,\ 127.943)}$= 1.750, p< 0.006) and a main effect in rostro-caudal level ($F_{(13,\ 124.997)}$= 121.636, p<0.000) (Table 5-2). Post-multiple comparisons showed a treatment effect in all time points assessed within the DRV (Figure 5-25). However, even when statistical significance was reached only at specific rostro-caudal levels (with 3 pm as an exception) a robust trend was seen in the data from 3 am (Figure 5-25A) and 9 pm (Figure 5-25E) which showed higher expression levels after LL treatment.

Moreover, these high levels contrasted with the decreased expression observed in the caudal levels of the DRV at 3 pm (Figure 5-25C).

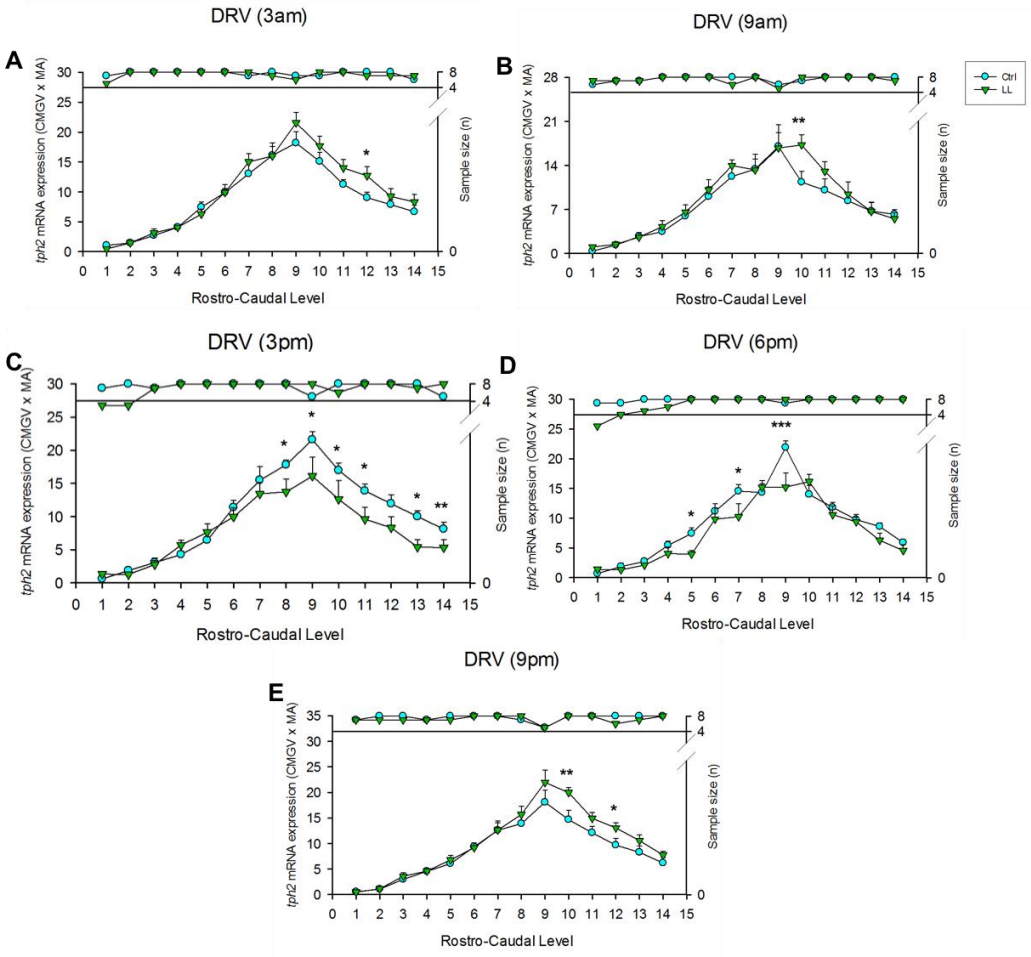

*Figure 5-25: Circadian changes in tph2 mRNA expression at each rostro-caudal level expression in the DRV of Controls vs LL treated animals. Tph2 mRNA expression in the DRV was measured in fourteen different rostro-caudal levels presented in the x axis (-7.328 to -8.420 mm bregma) at five different time point: (A) 3am, (B) 9 am, (C) 3 pm, (D) 6 pm and (E) 9 pm. Tph2 mRNA quantification is expressed as Calibrated Mean Value multiplied by its own Measured Area. Top data points are associated to the right y-axis which represent the after Grubb's test sample size at each rostro-caudal level. Bottom data points are linked to the left y-axis which correspond to the MEAN ± SEM of tph2 mRNA expression for each group (CTRL or LL [n≤8/each group]) at each of the fourteen rostro-caudal level of the DRV. Fisher's Least Significant Difference post hoc test showed the following significant differences; (A) *p< 0.05 for CTRL vs LL in level 12 at 3 am; (B) **p< 0.01 for CTRL vs LL in level 10 at 9 am; (C) **p< 0.01 for CTRL vs LL in level 13 and *p< 0.05 in level 8, 9, 10, 11, 14 at 3 pm; (D) ***p<0.01 for CTRL vs LL in level 9 at 6 pm; *p< 0.05 in level 5 and 7 at 6pm; (E) **p< 0.01 for CTRL vs LL in level 10 and *p< 0.05 in level 12.*

Once again, it looks like after LL treatment, the DRV displayed a strong circadian variation in *tph2* mRNA expression across its extent of 14 rostro-caudal levels.

Furthermore, the five weeks of LL treatment seemed to have substantially changed *tph2* mRNA expression across the 24-hour period when compared to controls within this specific DR subregion, this changed was predominantly observed in its caudal levels.

5.3.4.5 Dorsal Raphe nucleus, ventrolateral part/ventrolateral periaqueductal grey (DRVL/VLPAG).

For the DRVL/VLPAG, the secondary LMM analysis which assessed *tph2* mRNA expression after LL treatment, revealed a time point *rostro-caudal interaction ($F_{(28, 70.977)}$= 1.787, p<0.026), a main effect in timepoint ($F_{(4, 37.547)}$= 3.984, p<0.009) and a main effect in rostro-caudal level ($F_{(7, 69.588)}$= 69.599, p< 0.000). Interestingly, LSD post-tests in the DRVL.VLPAG (Figure 5-26) showed a decreased *tph2* mRNA expression at 6pm and 3pm in almost all the caudal levels when compared to the 3am and 9 pm peak in expression. All these changes however, only reached statistical significance at level 11 (with other few statistical differences in level 9,10 and 13), but a strong trend was observed from level 9 to 13.

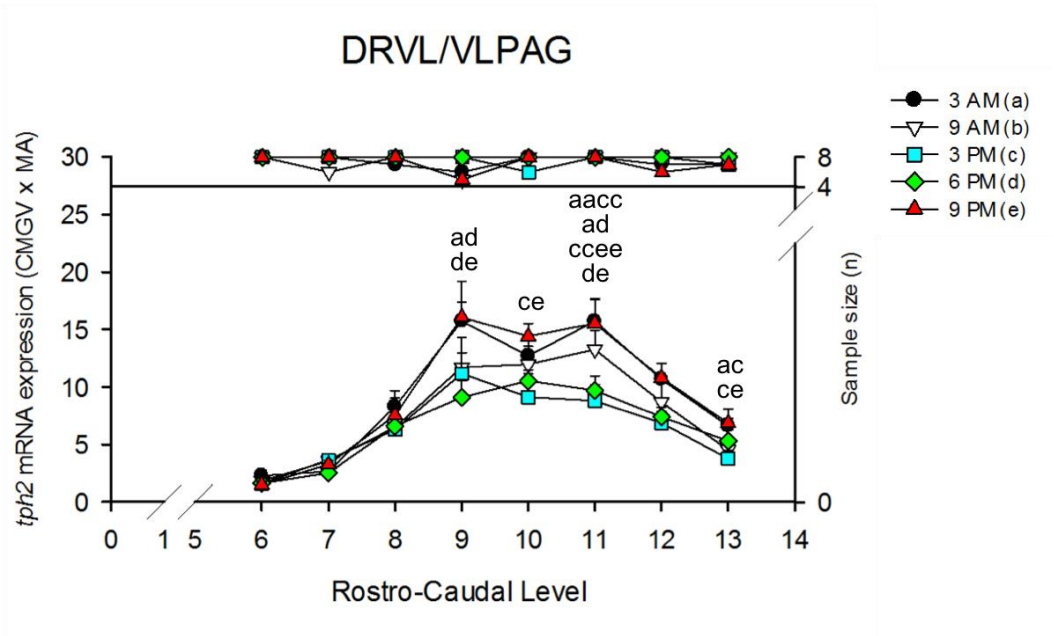

Figure 5-26: Rostro-caudal level variation of tph2 mRNA expression profile in the DRVL/VLPAG of LL treated animals. Tph2 mRNA expression in the DRVL/VLPAG was measured in eight different rostro-caudal levels presented in the x axis (-7.748 to -8.336 mm bregma). Five different timepoints; 3 am, 9 am, 3 pm, 6 pm and 9 pm are shown for each rostro-

caudal level (time course). Tph2 mRNA quantification is expressed as Calibrated Mean Grey Value multiplied by its own Measured Area. Top data points are associated to the right y-axis which represent the after Grubb's test sample size at each rostro-caudal level. Bottom data points are linked to the left y-axis which correspond to the MEAN value ± SEM of tph2 mRNA expression for each group/timepoint (n≤ 8/group) for each rostro-caudal level. Performed Fisher's Least Significant difference test showed the following significant differences: (aacc) p< 0.01 for 3 am vs 3 pm, (ccee) p< 0.01 for 3 pm vs 9 pm, (ac) p< 0.05 for 3 am vs 3 pm, (ad) p< 0.05 for 3 am vs 6 pm, (ce) p< 0.05 for 3 pm vs 9 pm, (de) p< 0.05 for 6 pm vs 9 pm.

Furthermore, the second subregional LMM analysis for DRVL/VLPAG was performed to further assess the effect of LL treatment compared to normal controls. Analysis revealed a treatment * time point interaction ($F_{(4, 76.570)}$= 6.226, p<0.000), a treatment * rostro-caudal interaction ($F_{(7, 114.074)=}$ 7.358, p<0.000), a treatment * time point * rostro-caudal level interaction ($F_{(28, 114.112)}$ = 1.624, p< 0.040) and a main effect in rostro-caudal level ($F_{(7, 114.074)=}$ 116.452, p< 0.000). Furthermore, as observed in Figure 5-27, multiple comparisons showed a very fascinating pattern which concurred with the simpler subregion analysis shown in the section above for the DRVL/VLPAG. Interestingly, even when not all rostro-caudal levels were found statistically different, for the 3 am (Figure 5-27A), 9 am (Figure 5-27B) and 9 pm (Figure 5-27E) a trend of very high *tph2* mRNA expression after LL treatment was observed in the caudal levels, relative to controls and in contrast, low expression was shown in all the almost all the rostro-caudal levels at 3 pm (Figure 5-27C) and just in specific levels at 6 pm (Figure 5-27D).

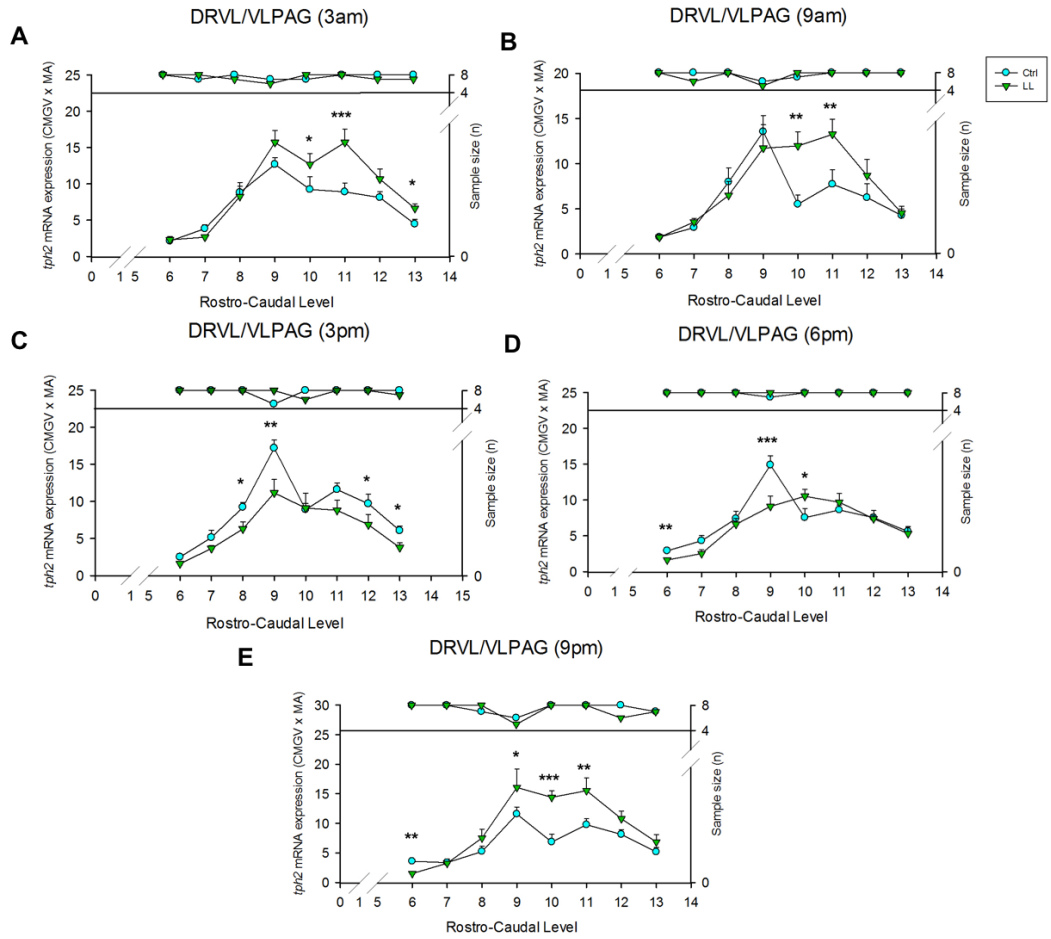

*Figure 5-27: Circadian changes in tph2 mRNA expression at each rostro-caudal level expression in the DRVL/VLPAG of Controls vs LL treated animals. Tph2 mRNA expression in the DRVL/VLPAG was measured in eight different rostro-caudal levels presented in the x axis (-7.748 to -8.336 mm bregma) at five different time point: (A) 3am, (B) 9 am, (C) 3 pm, (D) 6 pm and (E) 9 pm. Tph2 mRNA quantification is expressed as Calibrated Mean Grey Value multiplied by its own Measured Area. Top data points are associated to the right y-axis which represent the after Grubb's test sample size at each rostro-caudal level. Bottom data points are linked to the left y-axis which correspond to the MEAN ± SEM of tph2 mRNA expression for each group (CTRL or LL [n≤ 8/each group]) at each of the eight rostro-caudal level of the DRVL/VLPAG. Fisher's Least Significant Difference post hoc test showed the following significant differences; (A)***p< 0.001 for CTRL vs LL in level 11 and *p< 0.05 in level 10 and 13 at 3 am; (B) **p< 0.01 for CTRL vs LL in level 10 and 11 at 9 am; (C) **p< 0.01 for CTRL vs LL in level 9 and *p< 0.05 in level 8, 12 and 13 at 3 pm; (D) ***p< 0.001 for CTRL vs LL in level 9, **p<0.01 in level 6 and *p< 0.05 in level 10 at 6 pm; (E) ***p< 0.001 for CTRL vs LL in level 10, **p<0.01 in level 6 and 11 and *p< 0.05 in level 9 at 9 pm.*

Consistent to the other DR subregions, it looked like the DRVL/VLPAG exhibited a strong circadian variation across its rostro-caudal gradient after five weeks of LL treatment, however, in this subregion, this pattern did not seem to be specific to the caudal levels. Additionally, the five weeks of LL treatment seem to have a strong

effect in *tph2* mRNA expression across the 24-hour period when compared to normal conditions. This changed pattern, seemed to be more pronounced in the 3 am and 9 pm time point, which was consistent with the described in previous sections.

5.3.4.6 Median Raphe nucleus (MnR).

Last, to complete this particular study two final subregional LMM analyses were performed for the MnR; the first aimed to assess how the *tph2* mRNA expression changed over a 24-hour period after five weeks LL and the second to assess whether there was an additional effect of treatment (LL vs 'normal' controls) at any of the designated timepoints.

The first analysis revealed a time point * rostro-caudal level interaction ($F_{(56, 1586.409)} = 6.723$, $p < 0.000$) and a main effect in rostro-caudal level ($F_{(14, 10.452)} = 25.909$, $p < 0.000$) (Table 5-1). Post-tests within the MnR revealed many numerous differences (Figure 5-28), however, the most noticeable condition to mention is that most of the statistically significant differences were seen between level 9 to level 14, these differences seemed to depend fundamentally on the fact that in these levels, the 9 pm group exhibited the highest *tph2* mRNA expression while the 6 pm groups presented the lowest expression with the exception of level 13 which displayed its lowest expression at 3 pm. Moreover, in levels 13 to 14 more differences were shown when compared to 3 pm, given that this time point also had a high expression of *tph2* mRNA. Throughout the rostro-caudal gradient of this particular subregion, statistical significances went from strong to weak differences, demonstrating a particular circadian variation of *tph2* mRNA expression across the span of the MnR.

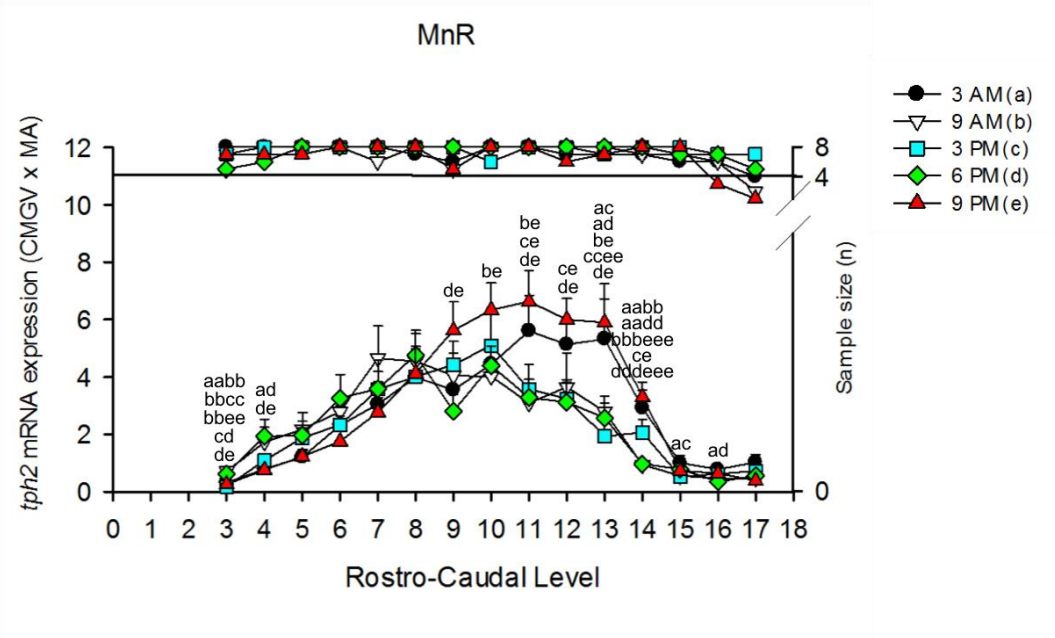

Figure 5-28: Rostro-caudal level variation of tph2 mRNA expression profile in the MnR of LL treated animals. Tph2 mRNA expression in the MnR was measured in fifteen different rostro-caudal levels presented in the x axis (-7.496 to -8.672 mm bregma). Five different timepoints; 3 am, 9 am, 3 pm, 6 pm and 9 pm are shown for each rostro-caudal level (time course). Tph2 mRNA quantification is expressed as Corrected Mean Grey Value multiplied by its own Measured Area. Top data points are associated to the right y-axis which represent the after Grubb's test sample size at each rostro-caudal level. Bottom data points are linked to the left y-axis which correspond to the MEAN value ± SEM of tph2 mRNA expression for each group/timepoint (n≤ 8/group) for each rostro-caudal level. Performed Fisher's Least Significant difference test showed the following significant differences: (bbbeee) p< 0.001 for 9 am vs 9 pm, (dddeee) p< 0.001 for 6 pm vs 9 pm, (aabb) p< 0.01 for 3 am vs 9 am, (aadd) p< 0.01 for 3 am vs 6 pm, (bbcc) p< 0.01 for 9 am vs 3 pm, (bbee) p< 0.01 for 9 am vs 9 pm (ccee) p< 0.01 for 3 pm vs 9 pm, (ac) p< 0.05 for 3 am vs 3 pm, (ad) p< 0.05 for 3 am vs 6 pm, (be) p< 0.05 for 9 am vs 9 pm, (cd) p< 0.05 for 3 pm vs 6 pm, (ce) p< 0.05 for 3 pm vs 9 pm, (de) p< 0.05 for 6 pm vs 9 pm.

Finally, the concluding secondary LMM analysis performed for the MnR revealed a treatment * time point interaction ($F_{(4,\ 118.402)}$= 2.539, p<0.043), a treatment * rostro-caudal level interaction ($F_{(13,\ 152.320)}$= 4.234, p<0.000), a time point * rostro-caudal level interaction ($F_{(52,\ 164.365)}$= 2.772, p<0.000), a treatment * time point * rostro-caudal level interaction ($F_{(51,\ 154.449)}$ = 3.667) and a main effect in rostro-caudal level ($F_{(13,\ 155.194)}$= 56.143, p< 0.000) (Table; 5-2). Multiple comparisons with Fisher's LSD tests revealed many significant differences in *tph2* mRNA expression throughout the rostro-caudal levels within each time point but these were not shown in the corresponding Figure. However, when considering differences between treatment groups in the MnR (Figure 5-29), multiple

comparisons showed that; 1) no differences whatsoever were observed at 3 am (Figure 5-29A) 2) at 9 am (Figure 5-29-B) higher *tph2* mRNA expression was found from rostro-caudal level 3 to 10, but were only statistically significant for level 4,5 and 7; 3) higher *tph2* mRNA expression was observed from level 9 to 13 at 9 pm (Figure 5-29E) in the LL treatment group and 4) low *tph2* mRNA expression appeared in levels 11 to 14 at 3 pm (Figure 5-29C) and 6 pm (Figure 5-29D). All these findings again correspond to what was observed in the simpler subregion analysis which showed a peak in expression at 9 pm, and the 9 am to 6 pm nadir.

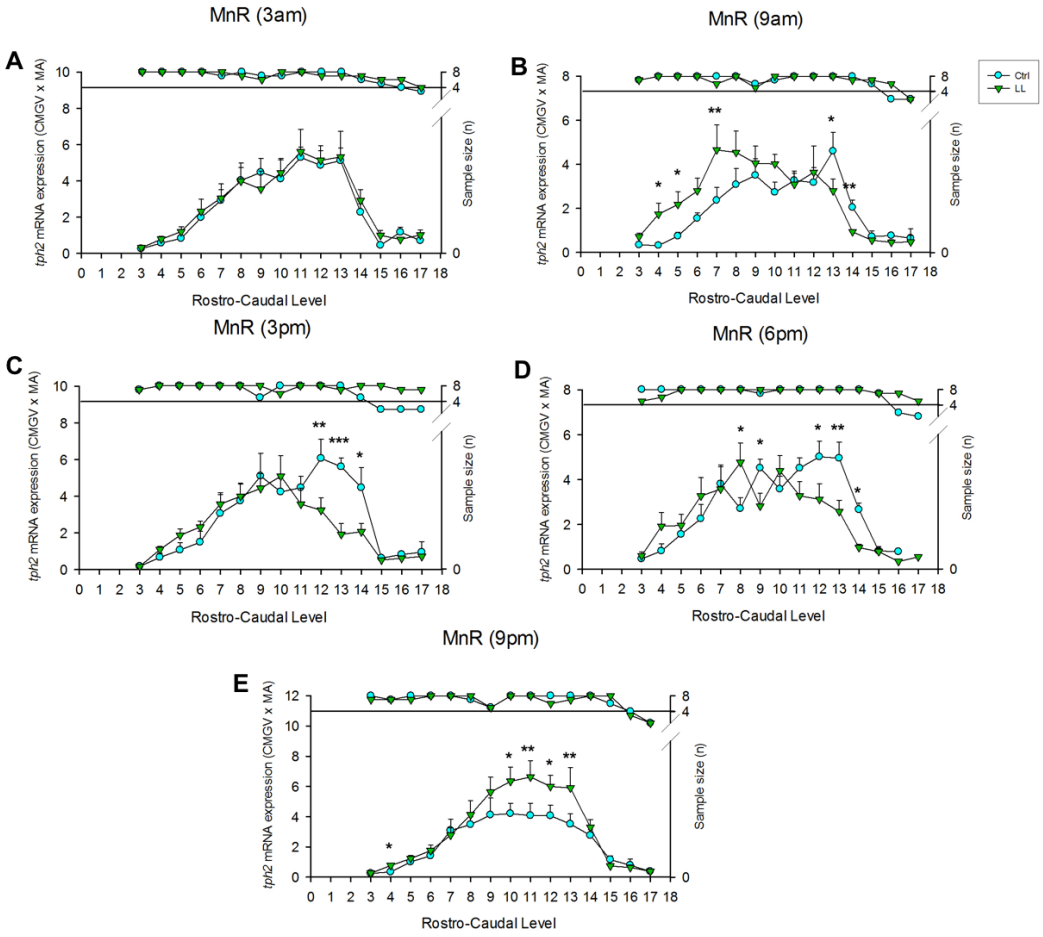

Figure 5-29: Circadian changes in tph2 mRNA expression at each rostro-caudal level expression in the MnR of Controls vs LL treated animals. Tph2 mRNA expression in the MnR was measured in fifteen different rostro-caudal levels presented in the x axis (-7.496 to -8.672 mm bregma) at five different time point: (A) 3am, (B) 9 am, (C) 3 pm, (D) 6 pm and (E) 9 pm. Tph2 mRNA quantification is expressed as Calibrated Mean Grey Value multiplied by its own Measured Area. Top data points are associated to the right y-axis which represent the after Grubb's test sample size at each rostro-caudal level. Bottom data points are linked to the left y-axis which correspond to the MEAN ± SEM of tph2 mRNA expression for each group (CTRL or LL [n≤8/each group]) at each of the fifteen rostro-caudal level of the MnR. Fisher's Least

*Significant Difference post hoc test showed the following significant differences; (A) ns at 3 am; (B) **p< 0.01 for CTRL vs LL in level 7 and 14, and *p< 0.05 in level 4, 5, and 13 at 9 am; (C) ***p< 0.001 for CTRL vs LL in level 13, **p< 0.01 level 12 and *p< 0.05 in level 14 at 3 pm; (D) ***p< 0.001 for CTRL vs LL in level 14, **p< 0.01 in level 13 and *p< 0.05 in level 8, 9 and 12 at 6 pm; (E) **p< 0.01 for CTRL vs LL in level 11 and 13 and *p< 0.05 in level 4, 10, 12 at 9 pm.*

All these changes observed in the MnR nucleus denotate a robust variation in *tph2* mRNA expression throughout its rostro-caudal levels and across a 24-hour period. Consistent to several subregions of the DR nucleus, the *tph2* mRNA circadian activity also seemed to depend mainly in the caudal levels of the MnR. Moreover, a solid effect of five weeks of LL in this pattern of expression is observed in the complete time period, however, more changes can be appreciated principally at the late time points (6 pm and 9 pm).

5.3.5 Summary of Results

The following table is a summary of the key findings on this chap

Table 5-3: Key findings of the circadian expression of tph2 mRNA after MPL treatment. Data shown by subdivision of the Raphe complex and by bregma level. Differences found by statistical analysis form ANOVA's and Linear Mixed Model analysis.

	Nadir after LL tx	Peak after LL tx	Complete Subdivisions after LL tx	LMM analysis after LL tx	Figures
Raphe complex	↓ expression from 9 am to 6 pm	↑ expression from 9 pm to 3 am	↑ expression at 3 am 9 am and 9 pm and ↓ expression at 3 pm and 6 pm when compared to ctrls	NA	(Figure 5-5)
DRC	↓ expression from 9 am to 6 pm	↑ expression from 9 pm to 3 am	Changes appeared in the rhythm of expression, but no siginificant differences found when compared to ctrls.	No changes detected	(Figure 5-7) (Figure 5-19)
DRI	No significant changes				(Figure 5-9) (Figure 5-21)
DRD	↓ expression from 9 am to 6 pm	↑ expression from 9 pm to 3 am	↑ expression at 3 am and 9 pm with ↓ expression at 3 pm when compared to controls	Changes at level 3, 4, 5, 8, 9, 10, 11 and 12. Most differences detected were found at 6 pm.	(Figure 5-5) (Figure 5-23)
DRV	↓ expression from 9 am to 6 pm	↑ expression from 9 pm to 3 am	↑ expression at 3 am, 9 am and 9 pm with ↓ expression at 3 pm specific to caudal bregma levels when compared to ctrls.	Changes at level; 8, 9, 10, 11, 12, 13, and 14 when compared to Ctrls. Most changes at 3 pm.	(Figure 5-5) (figure 5-25)
DRVL/VLPAG	↓ expression from 9 am to 6 pm	↑ expression from 9 pm to 3 am	↑ expression at 9 am and ↓ expression at 3 am and 3 pm when compared to ctrls.	Changes at level 6, 8, 9, 10, 11, 12 and 13when compared to Ctrls. Most changes were found at 3 pm and 9 pm.	(Figure 5-15) (figure 5-27)
MnR	flattened expression from 3 am to 6 pm	9:00 PM	↓ expression at 3 pm and 6 pm with ↑ expression at 9 pm specific to caudal bregma levels when compared to ctrls.	Changes at level 4, 5, 7, 8, and from 9 to 14 when compared to Ctrls. Changes appeared in all time points except 3 am.	(Figure 5-17) (Figure 5-29)

5.4 Discussion

According to the results described in this chapter we can conclude that CORT levels in our experimental group (five weeks of LL) (Figure 5-3) correspond to a disrupted circadian activity in CORT, displaying high levels of secretion across the 24-hour period. This was expected as it was shown before by various research groups (Claustrat, Valatx, Harth, et al., 2008; Waite et al., 2012). Nevertheless, we can confirm that all our animals that were submitted to our LL model had a disruption in their circadian rhythmicity.

Considering the results of tph2 mRNA expression in the whole Raphe complex after five weeks of LL treatment, the data showed high levels of tph2 mRNA expression in the active phase but a flattened expression during the inactive phase (Figure 5-4). However, and as mentioned before, exposing rodents to constant light leads to disruption of the sleep–wake temporal patterns, and a loss of circadian rhythmicity (De La Iglesia *et al.*, 2004; Salgado-Delgado *et al.*, 2008). Moreover, Malek's group has shown that locomotor activity can also modulate tph2 mRNA expression(Malek *et al.*, 2007). Therefore, is hard to talk about an active and inactive phase under this experimental model and to hypothesize if the changes in tph2 mRNA expression are given by GC changes or by the altered locomotor activity.

Moreover, when compared to the pattern of activity under natural conditions, *tph2* mRNA expression after LL treatment (Figure 5-5) seemed to have changed considerably across the 24-hour period, displaying an almost inverted rhythm, with exception of the 9 am time point. This changed pattern included higher levels of expression at 3 am, 9 am and 9 pm, and decreased levels of *tph2* mRNA expression at 3 pm and 6 pm. Thus, the overall effect of the circadian disruption in the HPA axis appeared to trigger high levels of *tph2* mRNA expression at specific times (Figure 5-30).

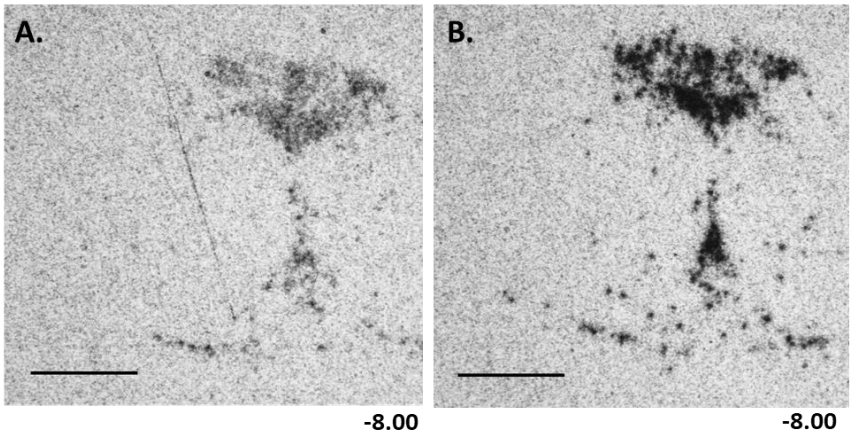

Figure 5-30: Representative image of tph2 mRNA expression of Ctrl (left) vs LL (right). Image of bregma level 10 (-8.00 bregma level) of a single brain section from a A) Control animal vs a single brain section of a B) LL treated animal from the 9 pm time point (peak expression after LL tx). Scale bar 1 mm.

Regarding the evaluation of the DR subregions and the MnR nucleus, there was an important presence of a circadian rhythm in thp2 mRNA expression the DRC (Figure 5-6), the whole, rostral and caudal DRD (Figure 5-10), the caudal DRV (Figure 5-12), the whole and caudal DRVL/VLPAG (Figure 5-14) and the whole and caudal MnR (Figure 5-16). This rhythm seemed to be specific to the caudal subpopulations of the DRV, DRVL/VLPAG and MnR, but not for the DRD. The presence of a circadian rhythm in almost all the areas of the Raphe complex might mean that the circadian disruption in the HPA axis activity was not strong enough to lose a circadian rhythm in *tph2* mRNA expression, although it might modify it.

However, and continuing with the DR subregions and the MnR nucleus analysis, when compared to the natural circadian activity changes in *tph2* mRNA expression were found in all the DRD (Figure 5-11), DRV (Figure 5-13), DRVL.VLPAG (Figure 5-15) and MnR (Figure 5-17), yet nothing was found for the DRC (Figure 5-7) or DRI (Figure 5-9). As thought previously, *tph2* mRNA expression changed considerably after LL treatment. In the DRD changes were observed, almost displaying an inverted rhythm in the caudal DRD. With the highest peak of *tph2* mRNA changing from 3 pm in controls, to 3 am after LL. Moreover, higher levels of *tph2* mRNA expression were found at almost all time points. The DRV, only displayed changes in the caudal area, where the peak of expression seemed to be shifted from 3 pm to

9 pm and continued to be high until 3 am. The changes in DRVL/VLPAG and MnR seemed to be specific of the caudal part too, where again the peak of expression shifted from 3 pm to 9 pm and maintained to be high until 3 am.

Moreover, at 9 am the whole and rostral DRD showed a strong increase in expression, which was maintained in the caudal DRD at 9 am and 6 pm. The caudal DRV suddenly showed a change when compared to control conditions; increasing *tph2* mRNA expression at 9 am and significantly reducing it at 3 pm, nothing happened when comparing whole or rostral DRV. Changes were found in the whole, rostral and caudal DRVL/VLPAG, where the biggest changes occurred in the rostral part, with MPL treatment reducing *tph2* mRNA expression across all time points but being significant only at 3 am and 3 pm. Furthermore, higher *tph2* mRNA expression profiles in MPL groups were found at 9 am in the whole and caudal DRVL/VLPAG. Finally, a decrease in *tph2* mRNA expression at 3 pm for the whole and caudal MnR were seen when compared to the natural activity pattern, additionally, a decrease was also found at 3 am in the caudal MnR.

Considering the rostro-caudal gradient of each of the subregions of the DR and the MnR nucleus after five weeks of LL, LMM analyses showed that *tph2* mRNA expression profile changed across this gradient in all of the areas of the Raphe complex, which was expected as anatomical variances (anatomical extent/size) are natural through the whole Raphe complex. Moreover, the LL analyses indicated changes across time for the all the subregions of the DR and the MnR nucleus. After LL treatment we saw changes across time but only in specific levels of all subregions, nevertheless, when looking at the DRD (Figure 5-22), DRV (Figure 5-24) and MnR (Figure 5-28) these changes were more specific of the caudal levels. Furthermore, these changes were not particularly consistent to a specific time point for all the areas or all the levels, so further discussion will be given in chapter 6 when specific anatomical characteristics will be examined.

Additionally, when considering the rostro-caudal gradient and the comparison between the natural *tph2* mRNA activity and the changed pattern after LL treatment the overall LMM analyses and secondary LMM analysis revealed that *tph2* mRNA

expression profile changed across this gradient in all of the areas of the Raphe complex (anatomical natural changes are confirmed). More interestingly, the LMM detected an effect of treatment and time point across the rostro-caudal level in the DRD(Figure 5-23), DRV (Figure 5-25), DRVL/VLPAG (Figure 5-27) and MnR(Figure 5-29) which again, seemed to be more significant for the caudal levels of each area but not particular of time, indicating that these changes might be an overall effect of treatment across the 24-hour cycle.

Finally, these data confirm the existence of a changed circadian pattern of *tph2* mRNA expression in a 24-hour period after the disruption of the circadian rhythm of the HPA axis. Moreover, this modified circadian variation seems to be different to the circadian rhythm under natural conditions, which again supports our premise that there is a relationship between disrupted rhythm of circulating CORT and the activity *tph2* mRNA expression. This again indicates that *tph2* mRNA rhythm dysregulation may be a possible mechanism underpinning high risk of, or vulnerability to, depression in patients with disrupted circadian HPA-axis activity.

Chapter 6 General Discussion

6.1 Introduction

My PhD is based on the hypothesis that the serotonergic system's activity, at the level of *tph2* mRNA expression, has a strong temporal relationship with the circadian activity of the HPA axis, and that this specific link between them could be the underlying mechanism of stress-related psychiatric disorders, such as depression and anxiety.

Many studies have shown that the brain serotonergic system has a strong relationship with HPA axis activity (Tsigos and Chrousos, 2002; Pompili *et al.*, 2010; Mahar *et al.*, 2014; Checkley, SL and WS, 2015). Moreover, many studies have focused on the relationship between *tph2* mRNA expression and HPA axis activity (Malek *et al.*, 2007; Waider *et al.*, 2011; Donner, Montoya, *et al.*, 2012; Lukkes *et al.*, 2013; Donner *et al.*, 2018). However, none of these studies fully characterized the link between the HPA axis circadian rhythm and the daily activity of *tph2* mRNA in the five recognized subregions of the DR and MnR nuclei (Pollak Dorocic *et al.*, 2014). Therefore, the importance of my PhD was set on this basis.

But why study *tph2* gene expression to assess the relationship between HPA-axis activity and the serotonergic system? Studies have shown that stressed-triggered induction of *tph* mRNA is related to the induction in TPH protein levels (F.M. *et al.*, 2004; Helene Bach-Mizrachi *et al.*, 2006) and to serotonin brain levels, as KO of *tph2* show a substantial decrease of 5-HT (Brommage *et al.*, 2015). Moreover, studies have shown that *tph2* gene expression is induced by antidepressant drugs (Matthes *et al.*, 2010) and that it contributes to the antidepressant effects (Hanson, Owens and Nemeroff, 2011), thus, *tph2* has become of great relevance for the understanding and development of strategies for psychiatric disorders and our interest was to describe its rhythmic activity under natural conditions and pathophysiological conditions.

With the mentioned above, I consider that my PhD project provides strong evidence to support the premise that *tph2* mRNA rhythmic expression, is linked to the HPA axis rhythm, therefore, suggesting that this relationship could be the molecular foundation of stress-related psychiatric disorders (Figure 6.1).

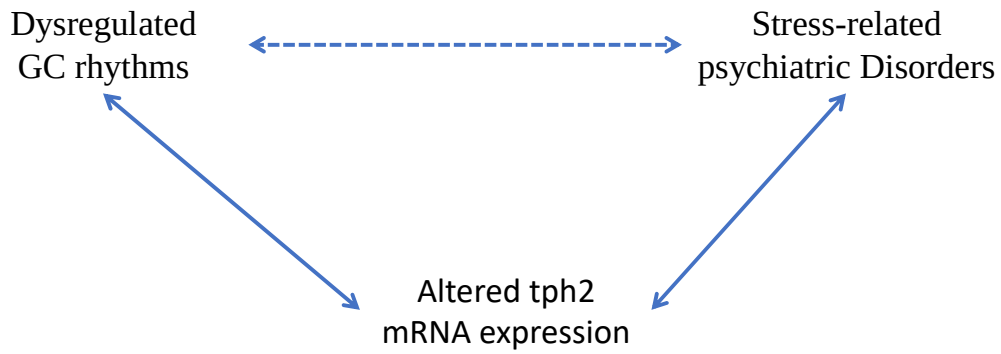

Figure 6-1: Schematic representation of the proposed relationships involved in stress-related psychiatric disorders. This model suggests that abnormal GC activity induces altered serotonergic system activity which can in turn be the underlying mechanism of psychiatric disorders.

Ultimately, the evidence found in this project could lead to the expansion of therapeutic methods of treatment of psychiatric conditions with more consideration given to the timing of drug delivery. Additionally, it could set the basis for the development of new strategies for the control of specific subpopulations of serotonergic neurons which could result in the reduction of side effects of pharmacological therapies used nowadays. Based upon the data presented in this thesis, chronotherapy (drug administration at a time of day that works optimally with the body's natural rhythms) appears to be extremely important when targeting the serotonergic system in the treatment of neuropsychiatric disorders.

6.2 Natural rhythm of tp2 mRNA Expression

According to my findings presented in chapter 3, *tph2* mRNA expression exhibits a significant natural circadian variation when assessed in the complete raphe complex (Figure 3-4); and more specifically, in three distinct subregions of the DR (DRD, DRV and DRVL/VLPAG) (Figure 3-7 to Figure 3-9) and MnR nucleus (Figure 3-10). Importantly for my research question, my data shows that the natural circadian variation in *tph2* mRNA expression exhibits a temporal relationship with

the natural circadian CORT rhythm (Figure 3-2), this had also been shown by other research groups (Malek *et al.*, 2007; Donner, Montoya, *et al.*, 2012), however, the neuroanatomical and circadian detail had not been assessed. The nadir in *tph2* mRNA expression matches the nadir of CORT at 9 am, while the peak in *tph2* mRNA expression is reached at 3 pm, therefore closely following the initial rise of CORT that precedes the onset of the active phase. Hence, the dynamics that I have found indicate a rapid and transient induction of *tph2* mRNA in many of the subregions of the Raphe complex, such as the DRV, DRVL/VLPAG and MnR nucleus. The one exception to this transient induction is the DRD, where the peak in *tph2* mRNA expression is more prolonged, with elevated expression at both 3pm and 6pm, before reducing at 9pm.

Overall, the results obtained in the DRD, DRV, DRVL/VLPAG and the MnR suggest that the circadian variation in *tph2* mRNA expression is quite similar in most of the subregions of the Raphe complex, characterised by the 9 am nadir and 3 pm peak in expression. The circadian *tph2* mRNA nadir of 9 am that I found was consistent with, what is to my knowledge, the only previous study of the full circadian *tph2* mRNA profile (Malek *et al.*, 2007). However the peak in *tph2* mRNA expression that I found was different to the one reported by this group, where they observed the circadian *tph2* mRNA peak at 5 pm (Malek *et al.*, 2007). Nonetheless, despite not having the same time-matched data points in analysis, both studies do agree that the peak *tph2* mRNA expression is reached prior to 'lights off', which is the start of the active phase for these nocturnal rodents. The data I present in this dissertation are novel as no study has ever assessed the *tph2* mRNA circadian rhythm with the topographically organized details that I have used.

Notably, I have found that the circadian variation in *tph2* mRNA expression was predominantly localized to the caudal bregma levels of each subregion, with the exception of the DRD (Figure 3-7). This caudal-dependent circadian variation in the DRV (Figure 3-8), DRVL/VLPAG (Figure 3-9) and MnR (Figure 3-10) is consistent with previous reports showing that serotonergic neurons in the mid-rostral caudal and caudal parts of the DR and the MnR nucleus are more responsive to stress and anxiety-related states (Singewald and Sharp, 2000). This suggests that the caudal

levels might also be more responsive to GCs. Consistent with this, I found that *tph2* mRNA expression increased with the early CORT rise that occurs prior to the onset of the active phase.

I believe that with the exception of the DRD mentioned above, this also makes sense based upon previous studies, which showed that differential rostral or caudal activation in the DRD was dependent on the type of stress-related stimuli (Amat *et al.*, 2005; Gardner *et al.*, 2005), suggesting that the DRD can be differentially activated across its rostro-caudal extent, therefore displaying a robust circadian variation only in its rostral levels.

As serotonergic neurons in these Raphe subregions are sensitive to regulation by stress-induced elevated GCs (Lowry *et al.*, 2009) and they also express GC receptors (Morimoto *et al.*, 1996) , then it also seems reasonable that they might be sensitive to regulation by rising and falling GC levels over the circadian phase. My data, showing circadian regulation of *tph2* mRNA in defined caudal parts of the DR and the MnR, supports the prevailing hypothesis (proposed by Malek et al., 2007 and Donner et al., 2012) for regulation of serotonergic neurons by GC-dependent transcriptional regulation of *tph2* mRNA.

Similar to how the circadian pattern of circulating GCs is known to be important for the maintenance and resetting of the circadian timing system in slave oscillators throughout the brain and the body (Lamont *et al.*, 2005; Hood *et al.*, 2010), I can now also hypothesise that *tph2* mRNA is under circadian regulation and that its circadian rhythm is at least partially dependent upon the natural circadian variation in GC levels.

Furthermore, the serotonergic neurons that project to the hippocampus are located in the most caudal regions of the DR and the MnR (Steinbusch, 1981; Köhler and Steinbusch, 1982a; Abrams *et al.*, 2005). Therefore, the GC dependent regulation of *tph2* mRNA expression in these distinct populations could have important functional implications, for example by exerting serotonergic inhibitory influence on the HPA axis mediated via these raphe hippocampus interactions. Further, GC-dependent regulation of *tph2* mRNA expression in these distinct populations may

play an important role in the regulation of emotional responses to stress, as it is known that the hippocampus innervates the central autonomic and emotional control systems (Jacobson and Sapolsky, 1991).

To look in more depth, I evaluated the complete rostral-caudal gradient of each subregion. Many experts in the Raphe field purport that *tph2* mRNA expression changes in specific bregma levels across the raphe complex have specific and differential functional output (Price *et al.*, 1998; Lowry *et al.*, 2000). Many studies have shown that there is a robust difference in *tph2* mRNA expression levels across the rostro-caudal gradient, and that these changes are largely defined by the anatomical structure of the subregion (J. K. Abrams *et al.*, 2004; Lowry *et al.*, 2008a; Katherine L. Gardner *et al.*, 2009). For example, the further rostral levels of the DRV are structurally smaller than the -8.000 mm caudal bregma level; therefore, more *tph2* mRNA will be expressed in this particular level than in the rostral levels. However, no studies have shown if there is a circadian variation of *tph2* mRNA expression within this full rostro-caudal gradient for each subregion of the DR and the MnR.

Moreover, when studying the Raphe complex is important to take under consideration that the different subregions not only have anatomical (structure) differences, but also different afferent/efferent connections, differences in circuitry and differences in cells. For example; 1) in the DR different cell types can be identified, including small round neurones, medium-sized and fusiform or bipolar neurons, multipolar neurons, but until now, no functional properties have been based on morphology (Köhler and Steinbusch, 1982a), 2) differences in firing rates during periods of activity or inactivity can be observed in different populations of serotonergic neurons localised in specific regions of the raphe complex (Peyron *et al.*, 1997a) and 3) different serotonergic neurons respond differently in vivo (Price *et al.*, 1998) and in vitro (Lowry *et al.*, 2000). Hence, there are too many variables that must be considered when studying the serotonergic system.

However, in this study, when considering the full rostro-caudal gradient of each subregion, we can visualise exactly where the time dependent changes in *tph2*

mRNA expression are localised within the DRD (Figure 3-13), DRV (Figure 3-14), DRVL/VLPAG (Figure 3-15) subregions and the MnR nucleus (Figure 3-16). These changes correspond well to previous reports, with significant changes seen in the rostral levels of the DRD, and the caudal levels of the DRV and MnR. Fascinatingly, in the DRVL/VLPAG, changes were seen across all the rostro-caudal extent of the subregion. Additionally, a common temporal theme of 9 am nadir and 3pm peak was noted in all of the regions where significant circadian variation was detected. Therefore, I feel confident in concluding that *tph2* mRNA has a clear circadian rhythm localised to specific levels within the rostro-caudal extent of the DRD, DRV, DRVL/VLPAG and the MnR nucleus.

What might be the functional significance of this particular timing in *tph2* mRNA expression? It seems logical that the circadian expression profile of *tph2* mRNA - with its sharp and transient increase prior to the onset of the active phase, then reaching a nadir before the inactive phase - must exist for a biologically important reason. Circadian rhythms have been found to be important in many biological systems (Moore MD, 1997; Wilsbacher and Takahashi, 1998; Brown and Schibler, 2001) and based on my results the serotonin system is clearly no exception. Furthermore, many circadian biological functions have been shown to be under the control of the serotonergic system, including but not limited to the sleep-wake cycle (Beersma and Gordijn, 2007), feeding behaviour (Voigt and Fink, 2015) and locomotor activity (Geyer, 1995). Therefore, the timing of serotonin synthesis will also potentially impact on these systems.

Moreover, previous studies have shown that serotonin is involved in the synchronization of the SCN (Pickard *et al.*, 1999; Glass, Dinardo and Ehlen, 2000; Malek, Pévet and Raison, 2004). As the SCN regulates many biological rhythms, including HPA axis activity (Buijs *et al.*, 1993a) which in turn is involved in the rhythmic expression of *tph2* mRNA (Malek *et al.*, 2007), these systems are highly interdependent. In light of all this, it is unsurprising that disruption in the timing of any of these systems (circadian, HPA axis, or serotonergic) can lead to the development of affective disorders in susceptible individuals.

6.3 Effect of the long-acting synthetic GC MPL on rhythmic *tph2* mRNA expression

Synthetic glucocorticoids (sGCs) are widely used in clinic as a therapeutic treatment of inflammatory and immune diseases (Van Staa, Leufkens and Cooper, 2002). Their mechanism of action in general, is to activate GRs and promote their activity, and thereby exert their corresponding anti-inflammatory functions (Van Der Velden, 1998). However, the importance of chapter four was not only set to address the idea that MPL treatment effectively and significantly alters the temporal dynamics of circulating GCs, but also by the fact that sGCs have well-documented adverse side effects (Buchman, 2001). Whilst the metabolic side-effects of sGCs have been extensively studied, neuropsychiatric symptoms associated with GC therapy (Brown and Chandler, 2001) have yet to be explained at the mechanistic level. Therefore, my data showing how MPL treatment significantly dysregulates *tph2* mRNA expression in the Raphe complex now potentially provides a direct mechanism for how sGC treatment can impact the brain serotonergic system, leading to psychiatric disorders in susceptible individuals.

The MPL dysregulation of circadian *tph2* mRNA expression was characterised primarily by elevated expression at the 9am time point, and loss of the peak at 3pm. While significant variation over time was still found in many subregions of the DR and the MnR, the pattern exhibited an unusual bi-phasic expression profile, with two peaks in expression at 9am and 6pm. This altered pattern was observed in the complete raphe complex (Figure 4-5), in several subregions of the DR, and the MnR nucleus, and could be visualised at specific levels within the rostro-caudal gradient.

How might MPL treatment be inducing this change in *tph2* mRNA expression rhythm? As indicated by the RIA results, MPL suppressed endogenous CORT (Figure 4-3). Therefore, the normal circadian endogenous adrenal GC rhythm had been effectively replaced with the long-acting sGC MPL. The impact of this on the circadian CORT rhythm may be expected to be twofold. First, the 'anticipatory' surge in rising CORT levels that occurs prior to the onset of the active phase will be ablated when endogenous adrenal CORT is suppressed by MPL (Spiga, Waite,

et al., 2011). As the MPL is delivered in drinking water in my experiments, thus modelling oral dosing in patients, the rise in circulating GC will be delayed until the onset of drinking behaviour at the early part of the dark phase (Kowanko *et al.*, 1982; Arvidson *et al.*, 1997; Straub and Cutolo, 2007). Therefore, a phase shift in peak GC levels of approximately 4 hours would be expected with this type of oral dosing. In support of this, Stamper *et al* (Stamper *et al.*, 2015) have shown, using a frequent blood sampling protocol, that CORT delivered in drinking water indeed does result in a 4 hour phase shift in the first peak in circulating CORT. In addition, Stamper et al reported that the phase delay in circulating CORT levels persisted throughout the dark phase, explaining that this was due to continued drinking throughout the active phase. Adrenal CORT secretion in contrast is known to be reduced during the late active phase (Spiga, Waite, *et al.*, 2011).To further exaggerate the temporal dysregulation, MPL remains in the circulation (Uhl *et al.*, 2002)for far longer than the CORT used in the experiments of Stamper et al.

Additionally, MPL has been shown to activate GRs for a prolonged period of time, replacing the normal circadian (Kitchener *et al.*, 2004) and ultradian (Lightman *et al.*, 2008; Conway-Campbell *et al.*, 2010, 2012) GR activity with prolonged activation (Earl *et al.*, 2017). While MPL has been demonstrated to induce prolonged GR activation (Earl *et al.*, 2017), by definition, this can only apply to brain regions where GR is expressed. As GRs are highly expressed in the DR and MnR nuclei (Harfstrand *et al.*, 1986; Morimoto *et al.*, 1996), it is also possible that serotonergic neurons within the Raphe complex are subjected to this prolonged effect.

Therefore, it seems likely that the observed alteration in *tph2* mRNA expression pattern from the ‘normal’ 9am nadir and 3pm peak, to the highly dysregulated twin peak pattern (9am and 6pm) is due to this phase shift in circulating GCs over the 24-hour period. The phase shift in the *tph2* mRNA expression peak from 3pm to 6pm represents a 3-hour shift rather than the hypothesised 4 hour shift, but this may be due to the (lack of) finer temporal resolution in my dataset as there were no time points assessed between 6pm and 9pm. The elevated *tph2* mRNA expression at 9am is consistent with the prolonged duration of MPL in the circulation, as *tph2* mRNA

levels decrease by 3pm. However, this simplistic view of prolonged MPL-dependent increase in *tph2* mRNA expression does not explain how or why the expression levels dip again at 9pm and 3am, rather than remaining constantly high from 6pm through to 9am. A potential explanation for this biphasic rhythm might lie in the transient nature of *tph2* mRNA induction. In fact, *tph2* mRNA expression peaked at 3 pm then decreased at 6pm throughout the majority of the Raphe subregions, even though CORT levels continued to rise from 3pm to 6pm in the natural circadian profile. Therefore, it seems likely that there is complexity in the transcriptional dynamics (Coulon *et al.*, 2013) and/or mRNA stability (Higgins, 1991) over time, although the exact nature of these dynamics is not currently known for *tph2* mRNA.

With the mentioned above, it would be very interesting to assess this complexity of transcriptional dynamics" of *tph2*. Therefore, further experiments to investigate *tph2* transcription ie nascent RNA production, mRNA half-life and stability, and translation rate would need to be conducted. The relative contribution of glucocorticoids versus time of day, for example would need to be assessed in adrenalectomized (ADX) rats to decrease the circulating endogenous glucocorticoids. Injection of corticosterone at a dose that matches the physiological circadian peak would be performed, alongside vehicle injections (to control for time of day). Rats would be killed, and brains would be taken over a time course of 1, 3 and 6 hours. ISHH analysis of *tph2* mRNA and nascent transcript in the DR and MnR would be performed. For detection of the nascent transcript, probes for heteronuclear RNA (hnRNA) would need to be designed to cross the boundary between an Intron and an Exon, such that dynamic increases and decreases in the nascent transcript can be assessed. Furthermore, when the transcript is spliced to form the mature transcript (mRNA), the hnRNA probe will not be able to bind. A time course of this type could also provide valuable information about the half-life of the mRNA. It would be also important to assess whether there is a difference in nascent transcript production and mRNA accumulation at different times of the day.

It would also be extremely interesting to assess the time course of protein increase and decrease, using immunohistochemistry for *tph2* in the DR and MnR, in both the circadian context (as reported in my thesis) and in the ADX CORT injected time course model. Of course, total protein levels do not indicate protein activity, so *TPH* activity would need to be further assessed by *TPH* enzyme assay, which would need to be performed on lysates obtained from micro-punched tissue, although the spatial resolution would be absent. To address the mechanisms whereby CORT regulates *tph2* transcription, we would need to perform Chromatin Immunoprecipitation (ChIP) assays on micro-punched tissue to assess GR binding to potential regulatory sites in and near the tph2 promoter.

Finally, in order to show whether GR is required for tph2 mRNA inductions over the time course, rats could be co-treated with a GR antagonist such as RU486 (Mifeprestone). If transcription is significantly decreased by the GR antagonist, then this provides good support for a mechanism of GR mediated transcriptional regulation of the tph2 gene.

Continuing with the results, it should be noted that while a unusual 'biphasic' pattern was detected in the analysis of the whole raphe complex (Figure 4-4), the whole and caudal DRD (Figure 4-10), whole, rostral and caudal DRVL/VLPAG (Figure 4-14), and the caudal MnR (Figure 4-16), the DRV was the exception (Figure 4-12). Interestingly, the caudal DRV had a significant circadian rhythm in the control rats, yet no significant variation detected over the 24 hours during MPL treatment, indicating that MPL treatment resulted in a 'flattening' of *tph2* mRNA expression profile in this region. Studies have shown that the DRV has widespread projections to the caudate putamen and cortical fields (Waterhouse *et al.*, 1986; Kirifides *et al.*, 2001; H. H. S. Lee *et al.*, 2003) which could implicate a role in motor function and complex cognitive tasks, suggesting that an altered activity of *tph2* mRNA expression in the DRV could be related to the reported impairment of declarative memory after sGC therapy (Brown and Chandler, 2001).

MPL treatment had a significant overall effect on *tph2* mRNA expression in the DRD (Figure 4-11). These changes were mainly observed in the caudal levels of

this subregion but could also be seen in the rostral part. Interestingly, the DRD receives inputs from brain structures which control anxiety states (Peyron *et al.*, 1997a) and also sends projections to areas related to anxiety-related behavioural responses (Lowry *et al.*, 2005). Moreover, many studies have shown that the DRD is activated by different stressful stimuli (Commons, Connolley and Valentino, 2003; Amat *et al.*, 2005; Gardner *et al.*, 2005) and that it can also be activated by anxiogenic drugs (Abrams *et al.*, 2005). Therefore, this subregion has been proposed to play a role in the regulation of anxiety-related behavioural responses and in affective disorders (Commons, Connolley and Valentino, 2003), suggesting that the DRD may also be affected in patients who report anxiety and negative mood during chronic sGCs treatment.

The DRVL/VLPAG (Figure 4-15) subregion had a strong response to MPL treatment showing a robust change in *tph2* mRNA circadian activity, which was maintained through the whole, rostral and caudal divisions. Moreover, when looking to the rostro-caudal extent of the subregion, MPL treatment had a strong effect across all the time points assessed. Hence, I can say with confidence that the DRVL/VLPAG subregion was considerably affected by MPL. Because of its afferent and efferent connections (Watts, Swanson and Sanchez-Watts, 1987; Hurley *et al.*, 1991; H. H. S. Lee *et al.*, 2003) this specific subregion of the DR has been associated with emotional behaviours that involve changes in muscle tone. Moreover, it is activated by panic-inducing stimuli (Bandler *et al.*, 2000) and dysregulated activity of serotonergic neurons in this area increases panic-like symptoms (Zangrossi and Graeff, 2014). Interesting, the DRVL/VLPAG project to the DRV (Peyron *et al.*, 1997a) and various studies have suggested that this area provides a tonic inhibitory input to the DRV (Hollis *et al.*, 2006; Bouwknecht *et al.*, 2007b; Johnson *et al.*, 2008),. Therefore, dysregulation of *tph2* mRNA expression in the DRVL/VLPAG may underlie problems with verbal and declarative memory found in patients during sGCs therapy as well as panic-like symptoms of psychiatric disorders.

With regards to the MnR (Figure 4-17), an unusual pattern appeared after MPL treatment. It seemed that the nadir in the rostral MnR had not changed from the

natural nadir. However, the pattern changed quite dramatically in the caudal levels, again showing the twin peak feature described for the DRD (Figure 4-11) and DRVL/VLPAG (Figure 4-15). The pattern observed in the whole MnR after MPL treatment was significantly different from the natural rhythm of *tph2* mRNA expression. Moreover, when assessing the rostro-caudal extent of the nucleus, an overall effect of MPL treatment can be seen for the MnR. This nucleus has extensive efferent and afferent projections, however, for the interest of my study, I will focus on the fact that the MnR projects to forebrain structures involved in the inhibitory regulation of the HPA axis, mediating its inhibition by a serotonergic mechanism (Vertes, Fortin and Crane, 1999; Lowry, 2002). This nucleus has been linked to many physiological and behavioural functions, most notably to chronic psychosocial stress (Graeff *et al.*, 1996), resistance and tolerance (Deakin, 1996), control of rhythmicity (Morin, 1999) and anxiety-related behaviours (Mansur *et al.*, 2011).

I believe that the results observed in this particular study can contribute to the knowledge of why sGCs have neuropsychiatric side effects. I suggest that there is an altered serotonergic activity within the dorsal and median raphe nuclei, which is the underlying mechanism connecting abnormal HPA axis activity and the stress-related psychiatric disorders, such as depression and anxiety (Figure 6-2).

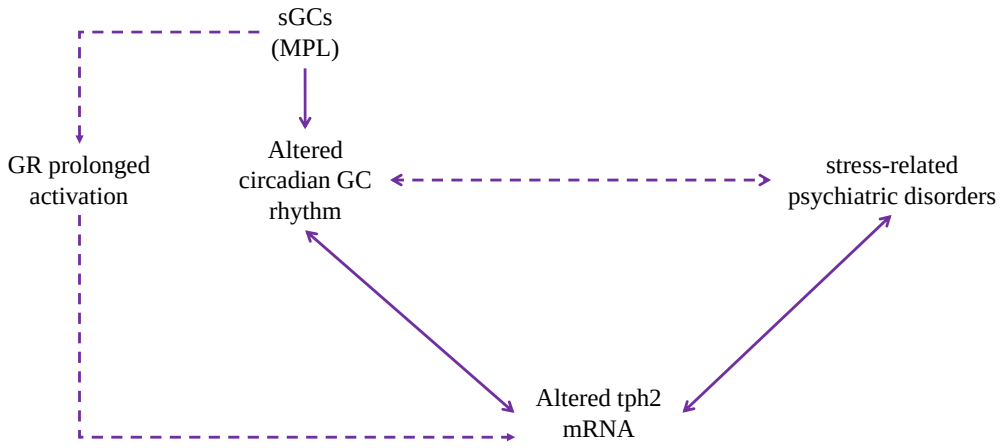

Figure 6-2: Schematic representation of the mechanism involved in the neuropsychiatric side effects of sGC therapy. The model shows the effects that long-acting sGCs might have on the development of neuropsychiatric disorders via altering the circadian tph2 mRNA expression pattern. The abnormal GC profile and abnormal tph2 mRNA expression profile in turn might

trigger altered serotonergic system activity which could be the underlying mechanism of psychiatric disorders.

6.4 Effect of chronodisruption on the circadian GC profile and *tph2* mRNA expression

In this modern world, exposure to light at night is more prevalent than ever before. Evidence has indicated that long periods of light mixed with activity can disturb our internal circadian timing system (Navara and Nelson, 2007; Fonken *et al.*, 2013) and trigger psychiatric symptoms (Gorwood, 2010). Furthermore, both chronic stress and neuropsychiatric disorders such as mayor depressive disorder (MDD) often lead to sleep problems (Drake *et al.*, 2004; Tsuno, Besset and Ritchie, 2005; Germain and Kupfer, 2008; Chrousos, 2009) and hence circadian disturbance (Czeisler and Gooley, 2007; Rahman, 2010; Zhu and Zee, 2012). In fact, there is a recognised bidirectional relationship between chronic stress and sleep problems (Basta *et al.*, 2007). Therefore, these three things – circadian timing, HPA axis, and affective state – are inextricably linked in the pathophysiology of neuropsychiatric disease. My findings in chapter 5 potentially provide an insight into how the three components may be interlinked; namely, via dysregulation of the *tph2* mRNA expression profile in the LL protocol.

The mechanisms through which light affects our internal timing system are still being investigated. However, the suprachiasmatic nucleus (SCN) has been of great interest as it is the "master clock" and is entrained by light. Additionally, the SCN has also been related to the regulation of the HPA axis activity (Buijs *et al.*, 1993a) as lesions in the SCN produce an abnormal HPA axis activity (Son *et al.*, 2008; Son, Chung and Kim, 2011) which has also been associated with affective disorders (Pompili *et al.*, 2010). The experimental model of five weeks constant light exposure, described in chapter 5, has been established to both 1) disrupt normal HPA axis activity leading to high amplitude CORT pulses throughout both the active and inactive phases of the day (Waite *et al.*, 2012) and 2) lead to anxiety and depressive-like symptoms (Fonken *et al.*, 2013). Here, I have shown that the 'normal' circadian *tph2* mRNA expression profile is also dysregulated as a result of five weeks constant light exposure, providing a mechanistic basis for the

depressive and anxious phenotype of the animals subjected to this experimental paradigm.

As expected given previous studies (Claustrat, Valatx, Harthe, *et al.*, 2008; Waite *et al.*, 2012; Park *et al.*, 2013), I observed a clear disrupted circadian rhythm in circulating CORT was found after five weeks of constant light (Figure 5-3). This model was also related to a modified *tph2* mRNA expression over the 24-hour period. However, because of the scientific knowledge it cannot be established whether this modification in expression was solely due to the disrupted HPA axis activity. An alternative hypothesis of why the LL model disrupts the serotonergic system is given by the fact that there is a direct relationship between the SCN and the serotonergic system established by the following findings: 1) the MnR is the only source of serotonergic input to the SCN (Meyer-Bernstein and Morin, 1996; Hay-Schmidt *et al.*, 2003); 2) *tph2* mRNA is found in the rat retina (Liang *et al.*, 2004) which has a direct projection to the SCN, via the retrino-hypothalamic tract (RHT) (Moore and Lenn, 1972); 3) the DR has an indirect influence on the SCN via an interaction with the MnR; and 4) an indirect projection from the DR to the SCN via the intergeniculate leaflet (IGL) has a strong input to the SCN (Glass *et al.*, 2003). Therefore, the effect of constant light on *tph2* mRNA expression most likely involves multiple mechanisms which have become dysregulated with the removal of normal light-dark cues. The striking LL-induced dysregulation of *tph2* mRNA expression throughout the Raphe complex provides an underlying mechanism which may explain the depressive and anxious behavioural phenotype reported with this model (Fonken *et al.*, 2009).

Furthermore, it has been shown that the LL model induces a disrupted locomotor activity (Cassone, 1992), and this altered locomotor activity was observed in the experimental groups submitted to 5 weeks of LL. These observations were only done “by eye” so no data is shown in regard to this. But why is this important? Studies have shown that at least voluntary exercise has an influence in serotonergic transmission. For example, rodents housed for 6 weeks with a running wheel, have modified levels of 5-HT transporter, 5-HT1A receptor mRNA levels (Greenwood *et al.*, 2005b)and an increase in tph2 mRNA levels in the DR and MnR (Malek *et*

al., 2007). Therefore, I can hypothesize that the changes found on *tph2* mRNA expression after 5 weeks of constant light could also be influenced by the altered locomotor activity observed in the animals exposed to 5 weeks of constant light and not solely by the GCs altered rhythm. However, this is only speculative and would have to be specifically studied in future behavioural experiments.

A particularly interesting aspect of the LL model is how both the central clock and the HPA axis are dysregulated. This is relevant because neuropsychiatric disease can often involve altered sleep patterns (Baglioni *et al.*, 2010; Staner, 2010; Palagini *et al.*, 2013), and hence circadian disruption. Therefore, my study represents a complex system where multiple factors may work together to dysregulate *tph2* mRNA expression. To test the relative contribution of GC hypersecretion in the system, we could infuse high dose pulses to recreate the hyperactive HPA axis that we see in the LL treated rats, while maintaining them in a normal LD cycle. This would allow us to assess the direct role that GCs play in *tph2* mRNA expression changes and depressive behaviour, without the additional factor of central clock (SCN) dysregulation.

A well-defined modification in both circulating GCs and *tph2* mRNA expression, was found after five weeks of constant light. Therefore, and due to the described link between the HPA-axis and the serotonergic system, I can speculate that the abnormal activity of circulating GCs has an association with altered *tph2* mRNA expression. Whilst my data cannot answer whether the effect is direct or indirect, it does support a functional interaction between circadian disruption, hyperactive HPA axis and *tph2* mRNA dysregulation, with the potential for development of neuropsychiatric symptoms.

Subsequently, with the described above, the results from the averaged analysis for each area, and throughout their rostro-caudal extent, suggest that LL could be evoking a chronic stress-like state as the caudal part of these DR subregions and the MnR nucleus are reportedly more responsive to stressful stimuli (Singewald and Sharp, 2000). These findings could indicate that if LL is evoking a chronic stress-like state, then GCs may very well be the main driver of the dysregulated *tph2*

pattern. However, other studies would need to be performed to test this hypothesis; for example, triggering a hyperactive CORT profile in normal LD conditions, or ablating endogenous CORT (adrenalectomy) in LL condition, and assessing the effects on *tph2* mRNA.

The constant light model used in this study had an overall effect in the whole DRC (Figure 5-6) where a circadian pattern was evident due to very high levels of *tph2* mRNA expression from 9pm to 3am, and very low levels across all other timepoints, in contrast to the lack of circadian *tph2* mRNA expression in the DRC of the control rats. This change may indicate a compensatory mechanism, as the DRC has been related to stress-coping behaviour (Bale *et al.*, 2000) via mechanisms involving projections to the ventral hippocampus, amygdala and locus coeruleus (Imai *et al.*, 1986), and interactions with the DRD (Hale and Lowry, 2011). The DRC receives innervation from the preoptic, arcuate and hypothalamic nuclei (H. H. S. Lee *et al.*, 2003); therefore it is possible that the observed effect might be due to the neural effects of constant light stimulation.

The DRD is involved in anxiety and stress-related behavioural responses (Commons, Connolley and Valentino, 2003). The overall effect seen in *tph2* mRNA expression after LL in the DRD is not specific to its caudal levels (Figure 5-10, Figure 5-23). However, studies have shown that depending on the type of stressful stimuli, the rostral or caudal levels of the DRD could be more reactive. For example, the open-field anxiety effect is more restricted to the rostral DRD (Bouwknecht *et al.*, 2007b) whereas the effect of uncontrollable stress is more restricted to the caudal DRD (Grahn *et al.*, 1999). Thus, the fact that effects were seen in both the rostral and caudal regions of the DRD indicate that constant light exposure induces both anxiety and chronic stress, consistent with the anxious and depressive-like behaviours reported for rats in this experimental model (Fonken *et al.*, 2009).

The DRV (Figure 5-13, figure 5-25) also showed an altered pattern in *tph2* mRNA expression after five weeks of constant light. However, it is difficult to interpret as only a few changes are seen, which are quite specific to the 3 pm time point, when/where a strong reduction in expression was observed when compared to its

natural expression. Moreover, because the DRV subdivision has extensive projections, few studies have investigated its functional output. However, it has been related to motor function and cognitive tasks (Greenwood *et al.*, 2005a), which is particularly interesting based on the plethora of evidence for cognitive impairments associated with chronic stress and chronic high level GC exposure.

The DRVL/VLPAG (Figure 5-15, Figure 5-27) subregion seemed to be very reactive as *tph2* mRNA expression in this subregion was markedly modified after exposure to constant light. However, in contrast to the reactivity after MPL treatment, only the caudal levels were subject to change, supporting the idea that constant light induces a stress-related state. Furthermore, as mentioned before, this area has been associated with panic-like behaviours where motor functions are involved (fight-or-flight, freezing) (Bandler *et al.*, 2000). Moreover, and of particular relevance for this specific model, the DRVL/VLPAG receives afferents from the retina (Fite *et al.*, 1999) and also projects to it (Villar *et al.*, 1988), which might indicate a direct neural modulation during LL exposure. These projections have furthermore been hypothesised (Shen and Semba, 1994) to play a role in regulation of circadian rhythms as well as sleep and wakefulness.

Finally, regarding the MnR (Figure 5-17, Figure 5-29), an important overall effect was observed in *tph2* mRNA expression after constant light, which is also caudal level dependent and found in almost all the time points assessed. In this specific study, the MnR is of great relevance as this nucleus is the unique serotonergic input of the SCN (Morin, 1999). Moreover, the interconnection between the MnR and DR (Tischler and Morin, 2003) also seems to exert a strong indirect influence on the SCN (Morin, 2013). Therefore, when speculating that our model of constant light is affecting circulating GCs and *tph2* mRNA expression via the SCN, the MnR becomes an obvious target of research. Importantly, the MnR has been implicated in inhibition of the HPA axis (Lowry, 2002) and to resistance and tolerance of stress (Deakin, 1996). Hence, as *tph2* mRNA expression reached extremely high levels in the MnR at the 9pm and 3am timepoints, it is tempting to speculate that this may be a mechanism attempting to reduce the negative effects of LL in the HPA axis. Furthermore, the MnR has also been related to the control of circadian rhythmicity

as lesions in the MnR cause premature onset and delayed offset in activity during normal LD conditions (Meyer-Bernstein and Morin, 1996). Therefore, again, there appears to be a functional association between altered *tph2* mRNA expression in the MnR and altered activity of the HPA axis.

Now, with all the aforementioned, I believe that my results indicate that constant light affects *tph2* mRNA expression throughout the Raphe complex by a combination of neural and humoral regulation, hypothesis which is consistent with previous reports (Morin and Blanchard, 1991; Azmitia, Liao and Chen, 1993; Meyer-Bernstein and Morin, 1996; Clark *et al.*, 2005). Projections directly from the retina to the DRVL/VLPAG, from the MnR to the SCN, and from hypothalamic regions to the DR and MnR (Peyron *et al.*, 1997a; H. H. S. Lee *et al.*, 2003) can all modulate serotonergic neuron activity as a result of the LL stimuli. Additionally, stress-responsive regions such as the DRD, DRVL/VLPAG and MnR appear to also be responsive to the fluctuating GC levels over the circadian period, strongly suggesting a humoral (GC-dependent transcriptional regulation of *tph2* mRNA) response. These combined actions, throughout the DR and the MnR, in turn appear to be dysregulating *tph2* mRNA expression, thus predisposing the rats to the depressive and anxiety-related behaviours described previously (Lowry *et al.*, 2008b; Katherine L. Gardner *et al.*, 2009; Donner, Johnson, *et al.*, 2012)(Figure 6-3).

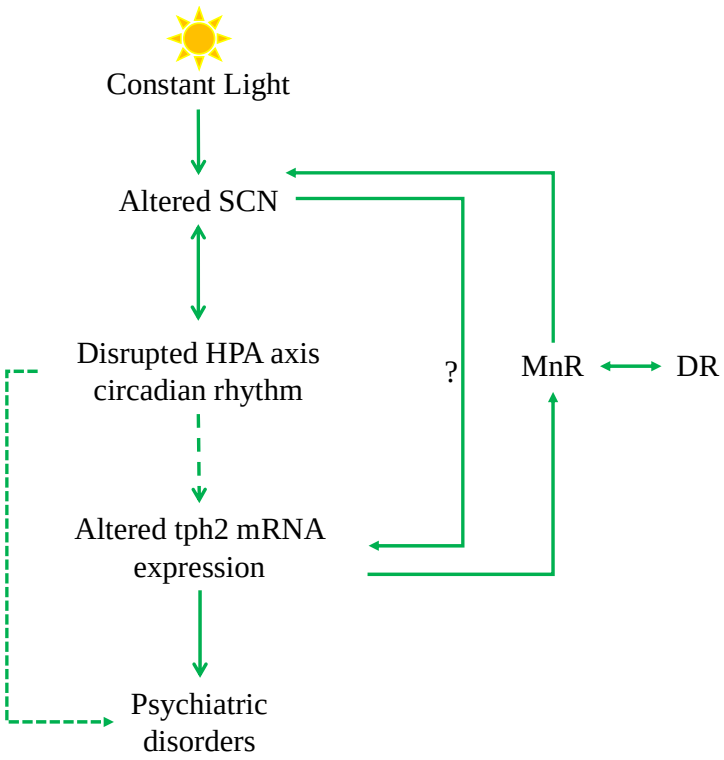

Figure 6-3: Schematic representation of the mechanisms involved in the development of psychiatric disorders. This model suggests that exposure to constant light will alter SCN activity, inducing an altered circadian rhythmicity, which in turn will cause an abnormal GC circadian rhythm and therefore, dysregulate the serotonergic system activity; this could be an underlying mechanism in the development of psychiatric disorders. However, an alternative mechanism of the consequences of exposure to constant light might be given by a direct connection between the SCN and the serotonergic system.

Many other experiments need to be performed to establish if the effect on *tph2* mRNA expression is given by the altered HPA axis activity or via the SCN. Moreover, assessing the unique characteristics of each subregion of the DR and MnR nucleus could provide a better understanding of this relationship. Hence, some of these experiments will be discussed in the "future directions" section.

6.5 Summary table of changes found after treatments.

As mentioned before, no comparison between the three treatments was made because the experimental models clearly disrupt *tph2* mRNA expression by different pathways and no consistency and relationship between them could be observed. However, the following table shows differences between the three experiments done for my PhD.

Table 6-1: Key findings of complete study. Changes in tph2 mRNA expression after MPL tx and LL tx. DRC and DRI do not appear as no change were detected.

	Nadir	**Peak**	**Nadir MPL tx**	**Peak MPL tx**	**Nadir LL tx**	**Peak LL tx**	**LMM analysis CTRL vs MPL tx**	**LMM analysis CTRL vs LL tx**
DRD	9:00 AM	6:00 PM	3:00 AM	6:00 PM	↓ mRNA expression from 9 am to 6 pm	↑ mRNA expression from 9 pm to 3 am	Changes in levels 4, 8 and 9 had mRNA expression at 3 am and 3 pm after MPL tx. Level 9, 10 11 and 12 had ↑ mRNA expression at 9 am and 6 pm. No changes at 9 pm.	Changes on levels 3 to 9 showed a ↓ mRNA expression after LL tx at 3 am, 3 pm and particularly at 6pm. ↑ mRNA expression from level 10 to 12 was detected at 9 am and 9 pm.
DRV	9:00 AM	3:00 PM	No differences detected		↓ mRNA expression	↑ mRNA expression	Changes in levels 8 and 11 had ↓ mRNA expression at 3 pm. Level 10 had ↑ mRNA expression at 9 am and	Changes at 3 pm and 6 pm in level 8 to 14 showed ↓ mRNA expression. In levels 10 and 12 ↑

					from 9 am to 6 pm	from 9 pm to 3 am	6 pm. No changes found at 3 am or 9pm after MPL tx.	mRNA expression was detected after LL tx.
DRVL/VLPAG	9:00 AM	3:00 PM	3:00 AM	6:00 PM	↓ mRNA expression from 9 am to 6 pm	↑ mRNA expression from 9 pm to 3 am	Changes in levels 6 to 9 showed ↓ mRNA expression after MPL tx at 3 am, 3 pm and 6 pm. Changes in levels 10 to 12 showed ↑ mRNA expression after MPL tx at 9 am, 6 pm and 9 pm.	All changes at 3 pm (levels 8,9,12 and 13) and at level 6 and 9 at 6 pm showed ↓ mRNA expression after LL tx. Changes observed in levels 9 to 13 at 3 am, 9 am and 9 pm showed ↑ mRNA expression.
MnR	9:00 AM	3:00 PM	3:00 AM/ 09:00 AM	6:00 PM	flattened mRNA expression from 3 am to 6 pm	9:00 PM	Changes in level 9 to 13 showed ↓ mRNA expression at 3 am, 3 pm and 6 pm after MPL tx. ↑ mRNA expression was detected in level 5 and 8 at 3 am and 6 pm, respectively. No changes detected at 9 pm.	Changesat 3 pm and 6 pm in levels 8 9, and 12 to 13 showed ↓ mRNA expression after LL tx. Changes at 9 am and 9 pm in levels 4 to 7 and 10 to 13, respectively, showed ↑ mRNA expression.

6.6 Clinical relevance

There is an extensive list of factors that have all been related to psychiatric disorders, many of which are related to the general themes of current research. These include but are not limited to: altered circadian rhythms (Bunney and Potkin, 2008); altered activity of the HPA axis (Swaab, Bao and Lucassen, 2005); high dosing of synthetic GCs (Brown and Chandler, 2001); high levels of GCs (Skórzewska *et al.*, 2014); hyperactive GRs (Modell *et al.*, 1997; Holsboer, 2000); exposure to extended periods of light (Tapia-Osorio *et al.*, 2013); abnormal serotonergic system (Arango, Underwood and Mann, 2002); abnormal *tph2* mRNA expression (Donner, Johnson, *et al.*, 2012b); polymorphisms in serotonergic receptors or the *tph2* gene itself (Tsai *et al.*, 2009); and finally, high (or confoundingly low) levels of serotonin (Cowen, 2008). However, the molecular mechanisms underpinning these 'suggestions' are still quite poorly understood.

The relationship between HPA axis activity, GCs and psychiatric disorders has long been purported. Moreover, the relationship between the brain serotonergic system and these types of disorders has been known since the mid-1960s (Dahlström and Kjell Fuxe, 1964). However, the relevance of my study was to assess whether the relationship observed between the altered HPA axis rhythms and the psychiatric disorders is established by a serotonergic mechanism. Therefore, I postulate that these three elements form a common triad in the aetiology of affective state diseases.

The reason I have assess this hypothesis based on *tph2* mRNA expression was firstly because *tph2* is responsible for the synthesis of neuronal 5-HT (Walther *et al.*, 2003), therefore targeting this enzyme would mean specific effects on brain serotonin. Moreover, tph2 expression does corelate to TPH protein activity and 5-HT levels as shown by different experimental models such as KO mice (Domínguez-López, Howell and Gobbi, 2012; Brommage *et al.*, 2015). Furthermore, tph2 expression or activity has been linked to a number of stress-related neuronal correlates (K. L. Gardner *et al.*, 2009), behavioural traits (Sadkowski *et al.*, 2013) and psychiatric disorders (Strüber, Strüber and Roth,

2014), hence, understanding tph2 rhythmic expression seemed to be the perfect target to understand HPA-axis activity, serotonergic activity and psychiatric disorders.

Because my initial interest was on the HPA axis rhythms, two different models of manipulation of its activity were used. However, both models have a clinical relevance, which implicates understanding how sGCs exert their effects producing psychiatric symptoms, and how exposure to long periods of light induce these types of symptoms. This becomes very important when one firstly considers that the use of sGCs is very common clinically with many patients suffering from side effects following long-term use, and secondly when considering why shift workers, frequent travellers, and even teenagers (who tend to use smartphones, TVs, tablets and computers at night) are at risk of developing depression or anxiety disorders. This topic is particularly relevant, because as previously mentioned in this dissertation, depression or anxiety disorders have become a huge and widespread problem in the modern world. Therefore, my aim was to investigate how *tph2* mRNA expression becomes dysregulated during chronic sGC treatment, and with the chronic stress of circadian disruption of five weeks LL exposure, as a potential underlying mechanism for the development of these types of stress-related psychiatric disorders to ultimately inform about interventions (pharmacological or lifestyle) that could help patients.

I believe that the anatomical detail in my PhD work can set the basis to identify novel therapeutic approaches or at least understand how these organized subpopulations of serotonergic neurons function, so if treatments for psychiatric disorders target specific serotonergic neurons a reduction of adverse side effects could be given.

With the above paragraph it is reasonable to think that if we wanted to use tph2 as a therapeutic strategy for psychiatric disorders we would also have to assess or at least think in the possible side effects that manipulating *tph2* could cause. Studies have shown that *tph2* Knock out mice have reduced 5-HT in the brain by 90% (Savelieva *et al.*, 2008), these mice are born in normal mendelian ratios, but they

have severe growth defects that are sustained for the first few postnatal weeks, with a recovery by 4 months of age (Alenina *et al.*, 2009). They have impaired thermoregulation, altered sleep patterns and decreased blood pressure (Migliarini *et al.*, 2013). Moreover, tph2 -/- mice have behavioural abnormalities as adults, such as anxiety-like behaviour, depression-like behaviour altered nurturing behaviour (Savelieva *et al.*, 2008; Alenina *et al.*, 2009; Migliarini *et al.*, 2013). Therefore, important changes can be seen by manipulating *tph2*, hence a careful study must be made before considering *tph2* as a therapeutic target. However, there is an important advantage of using *tph2* which is that because *tph2* is specific for brain serotonin this would not have any peripheral effect, hence, less side-effects when compared to re-uptake blocker (SSRIs) and degradation inhibitors (MAOs) (Peters *et al.*, 2004; Cowen, 2008; Andrade *et al.*, 2010).

6.7 Limitations of the study

During my PhD studies many limitations where found along the process. These limitations involved methodological and technical problems. I believe that given the novelty of what I was investigating and the fact that the project was also new to the research group I belonged to, beginning and finding the correct pathway to approach my research question was the most challenging aspect of the project.

Since the beginning, I was attempting an ambitious project, which implicated not only assessing *tph2* mRNA, but other two rate-limiting enzymes involved in different brain systems; tyrosine hydroxylase (TH) and histidine decarboxylase (HDC). It took us a while to understand that this was impossible to do in the time frame I had, so we decided to focus on *tph2* mRNA expression in the DR and MnR nucleus.

I encountered several problems at the animal experimental stage. The model design had to be carefully considered because of the need to adapt the animal experiments to the animal facility and the equipment (specialised light boxes). It was physically impossible to have a control group in parallel to the experimental groups, due not only to the limited time we had to run the experiments at our specific time points but also to the space in the light boxes. Therefore, I did not run a group of control

animals in parallel to the MPL or LL experiments. Nevertheless, the control group used in the analysis were from the same genetic breeding stock (Harlen, UK), age matched, and maintained in our 'state of the art' environmentally controlled ASU animal facility at the DHB in Bristol. We are therefore confident that the 'normal' control circadian group serves as a representative control group for both the MPL treated group, which were run simultaneously, and the LL group which was run at a different time. The advantage of using only one control group in the comparison is that the ISHH design (recommended by Dr Chris Lowry and described in detail in Chapter 2 General methods) involved batch processing so that all the ISHH results from control, MPL and LL could be directly compared. All confounding factors were carefully considered, with habituation and CORT profiling performed for all rats in the study. Most importantly, any individual control group rats that exhibited a stress response or abnormally high plasma CORT level in the RIA were excluded from the analysis.

Next, a couple of issues in the brain sectioning stage were found. Again, because of the novelty of this project in general and in our research group, there was a lack of available protocols, methods and data to carry out the correct sectioning at the first attempt. Therefore, it took me a while to get to the point of being able to collect 126 sections of tissue of 12 mm per brain in a short period of time. And even when I thought the "correct" brain sectioning and collection of tissue was obtained, the ISHH showed different, as I believe that the lack of results in the DRC and DRI was given by not having all the bregma levels of the subregions since the lack of circadian variation contradicts what other experts in the area have found (Donner *et al.*, 2012; Hale & Lowry, 2011; Abrams *et al.*, 2004a).

Thereafter, and which I believe was the biggest limitation of my PhD, was the time it took me to make the ISHH experiments work. Nobody in our research group had done this type of ISHH nor used such a large number of slides in each ISHH. Therefore, between assessing the correct protocol, using the accurate *tph2* probe, finding the correct hybridization and washing temperatures, doing the correct washes, finding the optimal exposure time, etc, optimizations of the ISHH took me approximately two years.

Then, and again because of the novelty of what I was doing, analysing the images and doing the statistical analysis, became another problem in my PhD. I used three different methods that did not work. Later, I contacted Dr Chris Lowry, an expert in the field, who kindly shared his image analysis protocol. Nonetheless, obtaining the values for 2 thousand images took me a while. Then, because the statistical analysis used by our group was not appropriate for the type of data I had, I undertook a brief internship at the University of Boulder, Colorado in Dr Chris Lowry's lab to learn the basis of the Linear Mixed Model analysis. However, I only learned the basics, so I spent some time understanding in depth how this had to be done. Moreover, the image analysis also took me a lot of time because each model took approximately 5 days to run in SPSS.

Finally, further behavioural experiments would have been very interesting to perform if time had permitted, as they would have confirmed that the modifications found in the circadian activity of *tph2* mRNA expression after manipulating HPA axis activity have a behavioural functional outcome related to psychiatric symptoms.

6.8 Future directions

As mentioned above, many other experiments were planned for my research project. Moreover, there are many possibilities of continuing this work which I think could give a better understanding of the relationship described here.

Firstly, as observed throughout the dissertation, no behavioural tests were performed because of the lack of time. However, we manage to start doing them, but did not finish. We assessed depressive-like behaviour (test for anhedonia; sucrose preference test) and anxiety-like behaviours (elevated plus maze) which could confirm that the altered HPA axis activity and the changes in *tph2* mRNA expression are actually related to psychiatric symptoms. We also thought on doing a Novelty Supressed Feeding test (NSFt) for anxiety-like behaviour. These experiments will be performed in the near future.

Moreover, doing behavioural tests specific to each of the functional subregions of the DR and MnR nucleus would be very exciting. For example, as the DRD is related to anxiety-like behaviours, therefore an open-field test would be help us understand the nature and extent of the disturbance in this region. The MnR is related to resistance and tolerance to stress, so the social defeat test would give us a better understanding of the impact of *tph2* mRNA dysregulation in this region. The DRVL/VLPAG is related to panic-like behaviours, so a foot shock test could be used to assess the impact of the disturbance in this region. These experiments would include other experiments (e.g. ISHH again, TPH immunoreactivity, electrophysiology, immunohistochemical detection of protein products) to confirm that the specific subregion can be related to the behavioural outcome, however, inter-connections between subregions might make this specific-subregion analysis difficult to study. These are only a few examples of many other experiments this project could motivate.

Next, as mention before, the need to assess *tph2* activity is also important, as the need to understand tph2 transcriptional-translational dynamics can give us a better insight of what is happening at this level. Moreover, assessing different level of the brain serotonin system, for example serotonin release in specific brain areas through micro-dialysis, would be of great relevance to understand the complete mechanism of how the serotonin system relates to the HPA axis activity. Moreover, western blotting (WB) of protein lysates prepared from DR and MnR could be done to assess rhythmic changes in protein expression of *tph2*.

Finally, there was always a plan to conduct a series of converse experiments, where we manipulate the serotonin system using specific agonists/antagonists infused into the DR and then assess the effect on glucocorticoid secretion, this would possibly give a great insight into the mechanism which relates the HPA axis and the serotonergic system.

6.9 Conclusions

I believe that this study has given two strong contributions to the knowledge in this area of research. First, it has provided a complete characterization of the circadian

variation of *tph2* mRNA expression in the subregions of the DR and in the MnR nucleus, which nobody had done before, not under this strict protocol. And secondly, and what I think is more important, it has increased our understanding of the underlying mechanism through which the HPA axis and the serotonergic systems relate to the development of psychiatric disorders.

References

Abe, K. *et al.* (1979) 'Effects of Destruction of the Suprachiasmatic Nuclei on the Circadian Rhythms in Plasma Corticosterone, Body Temperature, Feeding and Plasma Thyrotropin', *Neuroendocrinology*, pp. 119–131. doi: 10.1007/s13398-014-0173-7.2.

Abrahamson, E. E. and Moore, R. Y. (2001) 'Suprachiasmatic nucleus in the mouse: Retinal innervation, intrinsic organization and efferent projections', *Brain Research*, 916(1–2), pp. 172–191. doi: 10.1016/S0006-8993(01)02890-6.

Abrams, J. *et al.* (2004) 'Anatomical and functional topography of the dorsal raphe nucleus', *Annals of the New York Academy of Sciences*, 1018(0), pp. 46–57. doi: 10.1196/annals.1296.OOS.

Abrams, J. K. *et al.* (2004) 'Anatomic and functional topography of the dorsal raphe nucleus', in *Annals of the New York Academy of Sciences*. doi: 10.1196/annals.1296.005.

Abrams, J. K. *et al.* (2005) 'Serotonergic systems associated with arousal and vigilance behaviors following administration of anxiogenic drugs', *Neuroscience*. doi: 10.1016/j.neuroscience.2005.03.025.

Abumaria, N. *et al.* (2008) 'Stress upregulates TPH1 but not TPH2 mRNA in the rat dorsal raphe nucleus: Identification of two TPH2 mRNA splice variants', *Cellular and Molecular Neurobiology*. doi: 10.1007/s10571-007-9259-5.

Adams, W., Kusljic, S. and van den Buuse, M. (2008) 'Serotonin depletion in the dorsal and ventral hippocampus: Effects on locomotor hyperactivity, prepulse inhibition and learning and memory', *Neuropharmacology*. doi: 10.1016/j.neuropharm.2008.06.035.

Aguilera, G. (1994) 'Regulation of pituitary ACTH secretion during chronic stress', *Frontiers in Neuroendocrinology*. doi: 10.1006/frne.1994.1013.

Van Aken, M. O. *et al.* (2005) 'Irregular and frequent cortisol secretory episodes with preserved diurnal rhythmicity in primary adrenal cushing's syndrome', *Journal of Clinical Endocrinology and Metabolism*. doi: 10.1210/jc.2004-1281.

Alenina, N. *et al.* (2009) 'Growth retardation and altered autonomic control in mice lacking brain serotonin', *Proceedings of the National Academy of Sciences*. doi: 10.1073/pnas.0810793106.

Almawi, W. Y. and Melemedjian, O. K. (2002) 'Molecular mechanisms of glucocorticoid antiproliferative effects: antagonism of transcription factor activity by glucocorticoid receptor.', *Journal of leukocyte biology*.

Amaral, D. G. and Cowan, W. M. (1980) 'Subcortical afferents to the hippocampal formation in the monkey', *Journal of Comparative Neurology*. doi: 10.1002/cne.901890402.

Amat, J. *et al.* (2005) 'Medial prefrontal cortex determines how stressor controllability affects behavior and dorsal raphe nucleus', *Nature Neuroscience*. doi: 10.1038/nn1399.

Anagnostis, P. *et al.* (2009) 'The pathogenetic role of cortisol in the metabolic syndrome: A hypothesis', *Journal of Clinical Endocrinology and Metabolism*, pp. 2692–2701. doi: 10.1210/jc.2009-0370.

Andrade, C. *et al.* (2010) 'Serotonin reuptake inhibitor antidepressants and abnormal bleeding: A review for clinicians and a reconsideration of mechanisms', *Journal of Clinical Psychiatry*. doi: 10.4088/JCP.09r05786blu.

Antoni, F. A. *et al.* (1984) 'Evidence that the effects of arginine-8-vasopressin (AVP) on pituitary corticotropin (ACTH) release are mediated by a novel type of receptor', *Peptides*. doi: 10.1016/0196-9781(84)90080-9.

Arango, V. *et al.* (2003) 'Genetics of the serotonergic system in suicidal behavior', *Journal of Psychiatric Research*, 37(5), pp. 375–386. doi: 10.1016/S0022-3956(03)00048-7.

Arango, V., Underwood, M. D. and Mann, J. J. (2002) 'Serotonin brain circuits involved in major depression and suicide', in *Progress in Brain Research*. doi: 10.1016/S0079-6123(02)36037-0.

Arborelius, L. *et al.* (1999) 'The role of corticotropin-releasing factor in depression and anxiety disorders.', *The Journal of endocrinology*. doi: 10.1677/joe.0.1600001.

Archer, S. N. *et al.* (2014) 'Mistimed sleep disrupts circadian regulation of the human transcriptome', *Proceedings of the National Academy of Sciences*. doi: 10.1073/pnas.1316335111.

Arlt, W. and Allolio, B. (2003) 'Adrenal insufficiency', in *Lancet*. doi: 10.1016/S0140-6736(03)13492-7.

Arlt, W. and Stewart, P. M. (2005) 'Adrenal corticosteroid biosynthesis, metabolism, and action', *Endocrinology and Metabolism Clinics of North America*. doi: 10.1016/j.ecl.2005.01.002.

Arriza, J. L. *et al.* (1988) 'The neuronal mineralocorticoid receptor as a mediator of glucocorticoid response', *Neuron*. doi: 10.1016/0896-6273(88)90136-5.

Arvidson, N. G. *et al.* (1997) 'The timing of glucocorticoid administration in rheumatoid arthritis', *Annals of the Rheumatic Diseases*. doi: 10.1136/ard.56.1.27.

Aschoff, J. (1965) 'Circadian rhythms in man', *Science*. doi: 10.1126/science.148.3676.1427.

Aston-Jones, G. *et al.* (2001) 'A neural circuit for circadian regulation of arousal', *Nature Neuroscience*. doi: 10.1038/89522.

Atkinson, H. C. *et al.* (2008) 'Corticosteroids mediate fast feedback of the rat hypothalamic-pituitary-adrenal axis via the mineralocorticoid receptor', *American Journal of Physiology - Endocrinology And Metabolism*. doi: 10.1152/ajpendo.00721.2007.

Axelrod, L. (1976) *Glucocorticoid therapy, Medicine (Baltimore)*. doi:

10.1016/B978-0-323-18907-1.00100-1.

Axelson, D. A. *et al.* (1993) 'Hypercortisolemia and hippocampal changes in depression', *Psychiatry Research*, 47(2), pp. 163–173. doi: 10.1016/0165-1781(93)90046-J.

Aziz, N. A. *et al.* (2009) 'Increased hypothalamic-pituitary-adrenal axis activity in Huntington's disease.', *The Journal of clinical endocrinology and metabolism*. doi: 10.1210/jc.2008-2543.

Azmitia, E. C., Liao, B. and Chen, Y. S. (1993) 'Increase of tryptophan hydroxylase enzyme protein by dexamethasone in adrenalectomized rat midbrain.', *The Journal of neuroscience : the official journal of the Society for Neuroscience*.

Azmitia, E. C. and Segal, M. (1978a) 'An autoradiographic analysis of the differential ascending projections of the dorsal and median raphe nuclei in the rat.', *The Journal of comparative neurology*, 179(3), pp. 641–667. doi: 10.1002/cne.901790311.

Azmitia, E. C. and Segal, M. (1978b) 'An autoradiographic analysis of the differential ascending projections of the dorsal and median raphe nuclei in the rat.', *J Comp Neurol*. doi: 10.1002/cne.901790311.

Bach-Mizrachi, Helene *et al.* (2006) 'Neuronal tryptophan hydroxylase mRNA expression in the human dorsal and median raphe nuclei: major depression and suicide.', *Neuropsychopharmacology : official publication of the American College of Neuropsychopharmacology*. doi: 10.1038/sj.npp.1300897.

Bach-Mizrachi, H *et al.* (2006) 'Neuronal tryptophan hydroxylase mRNA expression in the human dorsal and median raphe nuclei: major depression and suicide', *Neuropsychopharmacology*. doi: 1300897 [pii] 10.1038/sj.npp.1300897.

Baglioni, C. *et al.* (2010) 'Sleep and emotions: A focus on insomnia', *Sleep Medicine Reviews*. doi: 10.1016/j.smrv.2009.10.007.

Bago, M., Marson, L. and Dean, C. (2002) 'Serotonergic projections to the

rostroventrolateral medulla from midbrain and raphe nuclei', *Brain Research*. doi: 10.1016/S0006-8993(02)02811-1.

Bailey, M. and Silver, R. (2014) 'Sex differences in circadian timing systems: implications for disease', *Front Neuroendocrinol.*

Bailly, D. *et al.* (1993) 'Platelet serotonin levels in alcoholic patients: changes related to physiological and pathological factors.', *Psychiatry research*. doi: 10.1016/0165-1781(93)90055-L.

Baker, K. G., Halliday, G. M. and Tork, I. (1990) 'Cytoarchitecture of the human dorsal raphe nucleus', *J Comp Neurol*. doi: 10.1002/cne.903010202.

Baker, K. G., Halliday, G. M. and Törk, I. (1990) 'Cytoarchitecture of the human dorsal raphe nucleus', *The Journal of comparative neurology*. doi: 10.1002/cne.903010202.

Bale, T. L. *et al.* (2000) 'Mice deficient for corticotropin-releasing hormone receptor-2 display anxiety-like behaviour and are hypersensitive to stress', *Nature Genetics*. doi: 10.1038/74263.

Balsalobre, A. *et al.* (2000) 'Resetting of circadian time in peripheral tissues by glucocorticoid signaling', *Science*. doi: 10.1126/science.289.5488.2344.

Bandler, R. *et al.* (2000) 'Central circuits mediating patterned autonomic activity during active vs. passive emotional coping', *Brain Research Bulletin*. doi: 10.1016/S0361-9230(00)00313-0.

Barassin, S. *et al.* (2002) 'Circadian tryptophan hydroxylase levels and serotonin release in the suprachiasmatic nucleus of the rat', *European Journal of Neuroscience*, 15(5), pp. 833–840. doi: 10.1046/j.1460-9568.2002.01928.x.

Baratta, M. V. *et al.* (2009) 'Selective activation of dorsal raphe nucleus-projecting neurons in the ventral medial prefrontal cortex by controllable stress', *European Journal of Neuroscience*. doi: 10.1111/j.1460-9568.2009.06867.x.

Barton, D. A. *et al.* (2008) 'Elevated brain serotonin turnover in patients with depression: Effect of genotype and therapy', *Archives of General Psychiatry*. doi: 10.1001/archgenpsychiatry.2007.11.

Basta, M. *et al.* (2007) 'Chronic Insomnia and the Stress System', *Sleep Medicine Clinics*. doi: 10.1016/j.jsmc.2007.04.002.

Beersma, D. G. M. and Gordijn, M. C. M. (2007) 'Circadian control of the sleep-wake cycle', *Physiology and Behavior*. doi: 10.1016/j.physbeh.2006.09.010.

Benca, R. *et al.* (2009) 'Biological rhythms, higher brain function, and behavior: Gaps, opportunities, and challenges', *Brain Research Reviews*. doi: 10.1016/j.brainresrev.2009.09.005.

Bendotti, C. and Samanin, R. (1986) '8-Hydroxy-2-(Di-n-propylamino)tetralin (8-OH-DPAT) elicits eating in free-feeding rats by acting on central serotonin neurons', *European Journal of Pharmacology*. doi: 10.1016/0014-2999(86)90405-X.

Benstaali, C. *et al.* (2001) 'Circadian rhythms of body temperature and motor activity in rodents - Their relationships with the light-dark cycle', *Life Sciences*. doi: 10.1016/S0024-3205(01)01081-5.

Berger, M., Gray, J. A. and Roth, B. L. (2009) 'The Expanded Biology of Serotonin', *Annual Review of Medicine*. doi: 10.1146/annurev.med.60.042307.110802.

Beyer, C. E. and Cremers, T. I. F. H. (2008) 'Do selective serotonin reuptake inhibitors acutely increase frontal cortex levels of serotonin?', *European Journal of Pharmacology*. doi: 10.1016/j.ejphar.2007.11.028.

Bockaert, J. *et al.* (2006) 'Neuronal 5-HT metabotropic receptors: Fine-tuning of their structure, signaling, and roles in synaptic modulation', *Cell and Tissue Research*. doi: 10.1007/s00441-006-0286-1.

Van Bockstaele, E. J., Biswas, A. and Pickel, V. M. (1993) 'Topography of

serotonin neurons in the dorsal raphe nucleus that send axon collaterals to the rat prefrontal cortex and nucleus accumbens', *Brain Research*. doi: 10.1016/0006-8993(93)90077-Z.

Van Den Bogaert, A. *et al.* (2006) 'Association of Brain-Specific Tryptophan Hydroxylase, TPH2,With Unipolar and Bipolar Disorder in a Northern Swedish, Isolated Population', *Archives of general psychiatry*.

Bolanos, S. H. *et al.* (2004) 'Assessment of mood states in patients receiving long-term corticosteroid therapy and in controls with patient-rated and clinician-rated scales', *Annals of Allergy, Asthma and Immunology*. doi: 10.1016/S1081-1206(10)61756-5.

Bonaventure, P. *et al.* (2004) 'Radioligand binding analysis of knockout mice reveals 5-hydroxytryptamine(7) receptor distribution and uncovers 8-hydroxy-2-(di-n-propylamino)tetralin interaction with alpha(2) adrenergic receptors.', *Neuroscience*. doi: 10.1016/j.neuroscience.2004.01.014.

Boularand, S., Darmon, M. C. and Mallet, J. (1995) 'The human tryptophan hydroxylase gene. An unusual splicing complexity in the 5'-untranslated region', *Journal of Biological Chemistry*. doi: 10.1074/jbc.270.8.3748.

Bouwknecht, J. A. *et al.* (2007a) 'Differential effects of exposure to low-light or high-light open-field on anxiety-related behaviors: Relationship to c-Fos expression in serotonergic and non-serotonergic neurons in the dorsal raphe nucleus', *Brain Research Bulletin*. doi: 10.1016/j.brainresbull.2006.12.009.

Bouwknecht, J. A. *et al.* (2007b) 'Differential effects of exposure to low-light or high-light open-field on anxiety-related behaviors: Relationship to c-Fos expression in serotonergic and non-serotonergic neurons in the dorsal raphe nucleus', *Brain Research Bulletin*. doi: 10.1016/j.brainresbull.2006.12.009.

Bräunig, P., Bleistein, J. and Rao, M. L. (1989) 'Suicidality and corticosteroid-induced psychosis', *Biological Psychiatry*. doi: 10.1016/0006-3223(89)90026-7.

Brodal, A., Walberg, F. and Taber, E. (1960) ‘The raphe nuclei of the brain stem in the cat. III. Afferent connections’, *Journal of Comparative Neurology*. doi: 10.1002/cne.901140305.

Brody, S. (1952) ‘Psychiatric observations in patients treated with cortisone and ACTH.’, *Psychosomatic medicine*. doi: 10.1097/00006842-195203000-00004.

Brommage, R. *et al.* (2015) ‘Adult Tph2 knockout mice without brain serotonin have moderately elevated spine trabecular bone but moderately low cortical bone thickness’, *BoneKEy Reports*. doi: 10.1038/bonekey.2015.87.

Brown, E. S. and Chandler, P. A. (2001) ‘Mood and Cognitive Changes During Systemic Corticosteroid Therapy.’, *Primary care companion to the Journal of clinical psychiatry*, 3(1), pp. 17–21. doi: 10.4088/PCC.v03n0104.

Brown, H. J., Henderson, L. A. and Keay, K. A. (2006) ‘Hypotensive but not normotensive haemorrhage increases tryptophan hydroxylase-2 mRNA in caudal midline medulla’, *Neuroscience Letters*. doi: 10.1016/j.neulet.2006.01.019.

Brown, S. A. *et al.* (2002) ‘Rhythms of mammalian body temperature can sustain peripheral circadian clocks’, *Current Biology*. doi: 10.1016/S0960-9822(02)01145-4.

Brown, S. A. and Schibler, U. (2001) ‘Circadian rhythms: Mop up the clock!’, *Current Biology*, 11(7), pp. 268–270. doi: 10.1016/S0960-9822(01)00135-X.

Buchman, A. L. (2001) ‘Side effects of corticosteroid therapy’, *Journal of Clinical Gastroenterology*. doi: 10.1097/00004836-200110000-00006.

Buckingham, J. C. (2006) ‘Glucocorticoids: Exemplars of multi-tasking’, *British Journal of Pharmacology*. doi: 10.1038/sj.bjp.0706456.

Buijs, R. M. *et al.* (1993a) ‘Suprachiasmatic nucleus lesion increases corticosterone secretion.’, *The American journal of physiology*, 264(6 Pt 2), pp. R1186-92. Available at: http://www.ncbi.nlm.nih.gov/pubmed/8322972.

Buijs, R. M. *et al.* (1993b) 'Suprachiasmatic nucleus lesion increases corticosterone secretion.', *The American journal of physiology*. doi: 10.1152/ajpregu.1993.264.6.R1186.

Buijs, R. M. (1999) 'Anatomical and functional demonstration of a multisynaptic suprachiasmatic nucleus adrenal (cortex) pathway', *European Journal of Neuroscience*. doi: 10.1046/j.1460-9568.1999.00575.x.

Buijs, R. M. *et al.* (2003) 'The biological clock tunes the organs of the body: Timing by hormones and the autonomic nervous system', *Journal of Endocrinology*. doi: 10.1677/joe.0.1770017.

Buijs, R. M. and Kalsbeek, A. (2001) 'Hypothalamic integration of central and peripheral clocks', *Nature Reviews Neuroscience*. doi: 10.1038/35081582.

Bunger, M. K. *et al.* (2000) 'Mop3 is an essential component of the master circadian pacemaker in mammals', *Cell*. doi: 10.1016/S0092-8674(00)00205-1.

Bunney, J. N. and Potkin, S. G. (2008) 'Circadian abnormalities, molecular clock genes and chronobiological treatments in depression', *British Medical Bulletin*, pp. 23–32. doi: 10.1093/bmb/ldn019.

Buttgereit, F. and Scheffold, A. (2002) 'Rapid glucocorticoid effects on immune cells', *Steroids*. doi: 10.1016/S0039-128X(01)00171-4.

Cannon, W. (1929) 'Organization for physiological homeostasis', *Physiological Reviews*, IX(3), pp. 399–431. doi: 10.1111/j.1468-229X.1929.tb00576.x.

Canteras, N. S. *et al.* (1990) 'Afferent connections of the subthalamic nucleus: a combined retrograde and anterograde horseradish peroxidase study in the rat', *Brain Research*. doi: 10.1016/0006-8993(90)91087-W.

Card, J. P. and Moore, R. Y. (1989) 'Organization of lateral geniculate-hypothalamic connections in the rat', *Journal of Comparative Neurology*. doi: 10.1002/cne.902840110.

Carey, R. M. (2010) ‘Aldosterone and cardiovascular disease’, *Curr Opin Endocrinol Diabetes Obes*, 17(3), pp. 194–198. doi: 10.1097/MED.0b013e3283390fa4.

Carkaci-Salli, N. *et al.* (2011) ‘TPH2 in the ventral tegmental area of the male rat brain’, *Brain Research Bulletin*. doi: 10.1016/j.brainresbull.2011.01.006.

de Carvalho Tofoli, S. M. *et al.* (2011) ‘Early life stress, HPA axis, and depression.’, *Psychology & Neuroscience*. doi: 10.3922/j.psns.2011.2.008.

Cascio, C. S., Shinsako, J. and Dallman, M. F. (1987) ‘The suprachiasmatic nuclei stimulate evening ACTH secretion in the rat’, *Brain Research*. doi: 10.1016/0006-8993(87)90837-7.

Cassone, V. M. (1992) ‘The Pineal Gland Influences Rat Circadian Activity Rhythms in Constant Light’, *Journal of Biological Rhythms*. doi: 10.1177/074873049200700103.

Cermakian, N. and Boivin, D. B. (2003) ‘A molecular perspective of human circadian rhythm disorders.’, *Brain research. Brain research reviews*, 42(3), pp. 204–20. doi: 10.1016/S0165-0173(03)00171-1.

Chalmers, D. T., Lovenberg, T. W. and De Souza, E. B. (1995) ‘Localization of novel corticotropin-releasing factor receptor (CRF2) mRNA expression to specific subcortical nuclei in rat brain: comparison with CRF1 receptor mRNA expression.’, *The Journal of neuroscience : the official journal of the Society for Neuroscience*.

Chaouloff, F. (1993) ‘Physiopharmacological interactions between stress hormones and central serotonergic systems’, *Brain Research Reviews*, 18(1), pp. 1–32. doi: 10.1016/0165-0173(93)90005-K.

Charmandari, E., Tsigos, C. and Chrousos, G. (2005) ‘Endocrinology of the Stress Response (1)’, *Annu Rev Physiol*.

Checkley, S., SL, L. and WS, Y. IL (2015) ‘The neuroendocrinology of depression and chronic stress’, *British Medical bulletin*, 52(3), pp. 597–617.

Chen, G. L. and Miller, G. M. (2008) 'Rhesus monkey tryptophan hydroxylase-2 coding region haplotypes affect mRNA stability', *Neuroscience*. doi: 10.1016/j.neuroscience.2008.05.050.

Chen, G. L. and Miller, G. M. (2012) 'Advances in tryptophan hydroxylase-2 gene expression regulation: New insights into serotonin-stress interaction and clinical implications', *American Journal of Medical Genetics, Part B: Neuropsychiatric Genetics*. doi: 10.1002/ajmg.b.32023.

Chen, J. *et al.* (1992) 'Serotonergic projections from the midbrain periaqueductal gray and nucleus raphe dorsalis to the nucleus parafasccicularis of the thalamus', *Brain Research*. doi: 10.1016/0006-8993(92)90908-R.

Cherrington, A. D. (1999) 'Banting Lecture 1997. Control of Glucose Uptake and Release by the Liver In Vivo', *Diabetes*. doi: 10.2337/diabetes.48.5.1198.

Chikanza, I. C. (2002) 'Mechanisms of corticosteroid resistance in rheumatoid arthritis: A putative role for the corticosteroid receptor β isoform', in *Annals of the New York Academy of Sciences*. doi: 10.1111/j.1749-6632.2002.tb04200.x.

Childs, G. V (1992) 'Structure-function correlates in the corticotropes of the anterior pituitary.', *Frontiers in neuroendocrinology*.

Chrousos, G. P. (2009) 'Stress and disorders of the stress system', *Nature Reviews Endocrinology*. Nature Publishing Group, 5(7), pp. 374–381. doi: 10.1038/nrendo.2009.106.

Chrousos, G. P. and Gold, P. W. (1992) 'The Concepts of Stress and Stress System Disorders: Overview of Physical and Behavioral Homeostasis', *JAMA: The Journal of the American Medical Association*. doi: 10.1001/jama.1992.03480090092034.

Chrousos, G. P., Loriaux, D. L. and Gold, P. W. (1988) 'Mechanisms of Physical and Emotional Stress', in *Springer Science & Business Media, New York*. doi: 10.1017/CBO9781107415324.004.

Chrousos, G., Pavlaki, A. N. and Magiakou, M. A. (2000) 'Glucocorticoid Therapy

and Adrenal Suppression', *Endotext*, (2), pp. 1–27. Available at: http://www.ncbi.nlm.nih.gov/pubmed/25905379.

Chung, S., Son, G. H. and Kim, K. (2011a) 'Adrenal peripheral oscillator in generating the circadian glucocorticoid rhythm', *Annals of the New York Academy of Sciences*, 1220(1), pp. 71–81. doi: 10.1111/j.1749-6632.2010.05923.x.

Chung, S., Son, G. H. and Kim, K. (2011b) 'Circadian rhythm of adrenal glucocorticoid: Its regulation and clinical implications', *Biochimica et Biophysica Acta - Molecular Basis of Disease*, pp. 581–591. doi: 10.1016/j.bbadis.2011.02.003.

Clark, J. A. *et al.* (2005) 'Differential hormonal regulation of tryptophan hydroxylase-2 mRNA in the murine dorsal raphe nucleus', *Biological Psychiatry*. doi: 10.1016/j.biopsych.2005.01.013.

Clark, J. A. *et al.* (2008) 'Glucocorticoid modulation of tryptophan hydroxylase-2 protein in raphe nuclei and 5-hydroxytryptophan concentrations in frontal cortex of C57/Bl6 mice', *Molecular Psychiatry*. doi: 10.1038/sj.mp.4002041.

Clark, M. S., McDevitt, R. A. and Neumaier, J. F. (2006) 'Quantitative mapping of tryptophan hydroxylase-2, 5-HT1A, 5-HT1B, and serotonin transporter expression across the anteroposterior axis of the rat dorsal and median raphe nuclei', *Journal of Comparative Neurology*. doi: 10.1002/cne.21073.

Clark, M. S. and Russo, A. F. (1997) 'Tissue-specific glucocorticoid regulation of tryptophan hydroxylase mRNA levels', *Molecular Brain Research*. doi: 10.1016/S0169-328X(97)00106-X.

Clarke, B. A. *et al.* (2007) 'The E3 Ligase MuRF1 Degrades Myosin Heavy Chain Protein in Dexamethasone-Treated Skeletal Muscle', *Cell Metabolism*. doi: 10.1016/j.cmet.2007.09.009.

Claustrat, B., Valatx, J. L., Harth, C., *et al.* (2008) 'Effect of constant light on prolactin and corticosterone rhythms evaluated using a noninvasive urine sampling

protocol in the rat', *Hormone and Metabolic Research*, 40(6), pp. 398–403. doi: 10.1055/s-2008-1065330.

Claustrat, B., Valatx, J. L., Harth??, C., *et al.* (2008) 'Effect of constant light on prolactin and corticosterone rhythms evaluated using a noninvasive urine sampling protocol in the rat', *Hormone and Metabolic Research*. doi: 10.1055/s-2008-1065330.

Coffield, J. A., Bowen, K. K. and Miletic, V. (1992) 'Retrograde tracing of projections between the nucleus submedius, the ventrolateral orbital cortex, and the midbrain in the rat', *Journal of Comparative Neurology*. doi: 10.1002/cne.903210314.

Commons, K. G., Connolley, K. R. and Valentino, R. J. (2003) 'A neurochemically distinct dorsal raphe-limbic circuit with a potential role in affective disorders', *Neuropsychopharmacology*. doi: 10.1038/sj.npp.1300045.

Conway-Campbell, B. L. *et al.* (2007) 'Proteasome-dependent down-regulation of activated nuclear hippocampal glucocorticoid receptors determines dynamic responses to corticosterone', *Endocrinology*. doi: 10.1210/en.2007-0585.

Conway-Campbell, B. L. *et al.* (2010) 'Glucocorticoid ultradian rhythmicity directs cyclical gene pulsing of the clock gene period 1 in rat hippocampus', *Journal of Neuroendocrinology*, 22(10), pp. 1093–1100. doi: 10.1111/j.1365-2826.2010.02051.x.

Conway-Campbell, B. L. *et al.* (2012) 'Molecular dynamics of ultradian glucocorticoid receptor action', *Molecular and Cellular Endocrinology*, pp. 383–393. doi: 10.1016/j.mce.2011.08.014.

Cook Jr., E. H. *et al.* (1994) 'Primary structure of the human platelet serotonin 5-HT2A receptor: identify with frontal cortex serotonin 5-HT2A receptor', *J Neurochem*.

Coulon, A. *et al.* (2013) 'Eukaryotic transcriptional dynamics: From single

molecules to cell populations', *Nature Reviews Genetics*. doi: 10.1038/nrg3484.

Cowen, P. J. (2002) 'Cortisol, serotonin and depression: All stressed out?', *British Journal of Psychiatry*, 180(02), pp. 99–100. doi: 10.1192/bjp.180.2.99.

Cowen, P. J. (2008) 'Serotonin and depression: pathophysiological mechanism or marketing myth?', *Trends in Pharmacological Sciences*. doi: 10.1016/j.tips.2008.05.004.

Crawford, L. K., Craige, C. P. and Beck, S. G. (2010) 'Increased Intrinsic Excitability of Lateral Wing Serotonin Neurons of the Dorsal Raphe: A Mechanism for Selective Activation in Stress Circuits', *Journal of Neurophysiology*. doi: 10.1152/jn.01132.2009.

Crosio, C. *et al.* (2000) 'Light induces chromatin modification in cells of the mammalian circadian clock', *Nature Neuroscience*. doi: 10.1038/81767.

Czeisler, C. A. and Gooley, J. J. (2007) 'Sleep and circadian rhythms in humans', *Cold Spring Harb Symp Quant Biol*. doi: 10.1101/sqb.2007.72.064.

Daban, C. *et al.* (2005) 'Hypothalamic-pituitary-adrenal axis and bipolar disorder', *Psychiatric Clinics of North America*, pp. 469–480. doi: 10.1016/j.psc.2005.01.005.

Dahlström, A. and Fuxe, Kjell (1964) 'EVIDENCE FOR THE EXISTENCE OF MONOAMINE-CONTAINING NEURONS IN THE CENTRAL NERVOUS SYSTEM. I. DEMONSTRATION OF MONOAMINES IN THE CELL BODIES OF BRAIN STEM NEURONS.', *Acta Physiologica Scandinavica*. doi: 10.1007/BF00160582.

Dahlström, A. and Fuxe, K. (1964) 'Localization of monoamines in the lower brain stem', *Experientia*. doi: 10.1007/BF02147990.

DALLMAN, M. F. *et al.* (1987) 'Regulation of ACTH Secretion: Variations on a Theme of B', in *Proceedings of the 1986 Laurentian Hormone Conference*. doi: 10.1016/B978-0-12-571143-2.50010-1.

Damiola, F. *et al.* (2000) 'Restricted feeding uncouples circadian oscillators in peripheral tissues from the central pacemaker in the suprachiasmatic nucleus', *Genes and Development*. doi: 10.1101/gad.183500.

Darmon, M. C. *et al.* (1988) 'Sequence of Two mRNAs Encoding Active Rat Tryptophan Hydroxylase', *Journal of Neurochemistry*. doi: 10.1111/j.1471-4159.1988.tb04871.x.

Day, H. E. W. *et al.* (2004) 'Differential expression of 5HT-1A, α1b adrenergic, CRF-R1, and CRF-R2 receptor mRNA in serotonergic, γ-aminobutyric acidergic, and catecholaminergic cells of the rat dorsal raphe nucleus', *Journal of Comparative Neurology*. doi: 10.1002/cne.20138.

Deakin, J. F. W. (1996) '5-HT, antidepressant drugs and the psychosocial origins of depression', *Journal of Psychopharmacology*. doi: 10.1177/026988119601000106.

Deboer, T., Ruijgrok, G. and Meijer, J. H. (2007) 'Short light-dark cycles affect sleep in mice', *European Journal of Neuroscience*. doi: 10.1111/j.1460-9568.2007.05964.x.

Desan, P. H. *et al.* (2000) 'Genetic polymorphism at the CLOCK gene locus and major depression', *Am J Med Genet*.

Deuschle, M., Schweiger, U., Weber, B., Gotthardt, U., Körner, A., *et al.* (1997) 'Diurnal activity and pulsatility of the hypothalamus-pituitary-adrenal system in male depressed patients and healthy controls', *Journal of Clinical Endocrinology and Metabolism*. doi: 10.1210/jcem.82.1.3689.

Deuschle, M., Schweiger, U., Weber, B., Gotthardt, U., K??rner, A., *et al.* (1997) 'Diurnal activity and pulsatility of the hypothalamus-pituitary-adrenal system in male depressed patients and healthy controls', *Journal of Clinical Endocrinology and Metabolism*, 82(1), pp. 234–238. doi: 10.1210/jc.82.1.234.

Dibner, C., Schibler, U. and Albrecht, U. (2010) *The mammalian circadian timing*

system: organization and coordination of central and peripheral clocks., *Annual review of physiology*. doi: 10.1146/annurev-physiol-021909-135821.

Dickmeis, T. (2009) 'Glucocorticoids and the circadian clock', *Journal of Endocrinology*, pp. 3–22. doi: 10.1677/JOE-08-0415.

Ding, Y. Q. *et al.* (2003) 'Lmx1b is essential for the development of serotonergic neurons', *Nature Neuroscience*, 6(9), pp. 933–938. doi: 10.1038/nn1104.

Domínguez-López, S., Howell, R. and Gobbi, G. (2012) 'Characterization of serotonin neurotransmission in knockout mice: Implications for major depression', *Reviews in the Neurosciences*. doi: 10.1515/revneuro-2012-0044.

Donner, N. C., Montoya, C. D., *et al.* (2012) 'Chronic non-invasive corticosterone administration abolishes the diurnal pattern of tph2 expression', *Psychoneuroendocrinology*. doi: 10.1016/j.psyneuen.2011.08.008.

Donner, N. C., Johnson, P. L., *et al.* (2012a) 'Elevated tph2 mRNA expression in a rat model of chronic anxiety', *Depression and Anxiety*, 29(4), pp. 307–319. doi: 10.1002/da.21925.

Donner, N. C., Johnson, P. L., *et al.* (2012b) 'Elevated tph2 mRNA expression in a rat model of chronic anxiety', in *Depression and Anxiety*, pp. 307–319. doi: 10.1002/da.21925.

Donner, N. C. *et al.* (2018) 'Two models of inescapable stress increase tph2 mRNA expression in the anxiety-related dorsomedial part of the dorsal raphe nucleus', *Neurobiology of Stress*. Elsevier, 8(September 2017), pp. 68–81. doi: 10.1016/j.ynstr.2018.01.003.

Donner, N. and Handa, R. J. (2009) 'Estrogen receptor beta regulates the expression of tryptophan-hydroxylase 2 mRNA within serotonergic neurons of the rat dorsal raphe nuclei', *Neuroscience*. doi: 10.1016/j.neuroscience.2009.06.046.

Drake, C. *et al.* (2004) 'Vulnerability to stress-related sleep disturbance and hyperarousal', *Sleep*. doi: 10.1093/sleep/27.2.285.

Dudley, T. E., DiNardo, L. a and Glass, J. D. (1998) 'Endogenous regulation of serotonin release in the hamster suprachiasmatic nucleus.', *The Journal of neuroscience : the official journal of the Society for Neuroscience*. doi: 10.1523/JNEUROSCI.18-13-05045.1998.

Duricki, D. A., Soleman, S. and Moon, L. D. F. (2016a) 'Analysis of longitudinal data from animals with missing values using SPSS', *Nature Protocols*. Nature Publishing Group, 11(6), pp. 1112–1129. doi: 10.1038/nprot.2016.048.

Duricki, D. A., Soleman, S. and Moon, L. D. F. (2016b) 'Analysis of longitudinal data from animals with missing values using SPSS', *Nature Protocols*, 11(6), pp. 1112–1129. doi: 10.1038/nprot.2016.048.

Earl, E. *et al.* (2017) 'Synthetic glucocorticoid treatment causes dysregulated activation dynamics of glucocorticoid receptors in brain and pituitary', in *Brain and Neuroscience Advances: BNA 2017 Festival of Neuroscience: Abstract Book*.

Edgar, R. S. *et al.* (2012) 'Peroxiredoxins are conserved markers of circadian rhythms', *Nature*. doi: 10.1038/nature11088.

Edmunds, L. N. (1988) 'Cellular and molecular bases of biological clocks. Models and mechanisms for circadian timekeeping', *Cell*. doi: 10.1016/0092-8674(88)90563-6.

Edwards, C. R. W. *et al.* (1988) 'LOCALISATION OF 11β-HYDROXYSTEROID DEHYDROGENASE-TISSUE SPECIFIC PROTECTOR OF THE MINERALOCORTICOID RECEPTOR', *The Lancet*. doi: 10.1016/S0140-6736(88)90742-8.

Engeland, W. C. and Arnhold, M. M. (2005) 'Neural circuitry in the regulation of adrenal corticosterone rhythmicity', *Endocrine*. doi: 10.1385/ENDO:28:3:325.

Erickson, J. D. *et al.* (1996) 'Distinct pharmacological properties and distribution in neurons and endocrine cells of two isoforms of the human vesicular monoamine transporter.', *Proceedings of the National Academy of Sciences of the United States*

of America. doi: 10.1073/pnas.93.10.5166.

Esler, M. *et al.* (2007) 'Increased brain serotonin turnover in panic disorder patients in the absence of a panic attack: reduction by a selective serotonin reuptake inhibitor.', *Stress (Amsterdam, Netherlands)*. doi: 10.1080/10253890701300904.

Evans, A. K., Heerkens, J. L. T. and Lowry, C. A. (2009) 'Acoustic stimulation in vivo and corticotropin-releasing factor in vitro increase tryptophan hydroxylase activity in the rat caudal dorsal raphe nucleus', *Neuroscience Letters*. doi: 10.1016/j.neulet.2009.03.025.

F.M., C. *et al.* (2004) 'Immobilization stress elevates tryptophan hydroxylase mRNA and protein in the rat raphe nuclei', *Biological Psychiatry*. doi: 10.1016/S0006-3223(03)00788-1.

Fairchild, G., Leitch, M. M. and Ingram, C. D. (2003) 'Acute and chronic effects of corticosterone on 5-HT1A receptor-mediated autoinhibition in the rat dorsal raphe nucleus', *Neuropharmacology*. doi: 10.1016/S0028-3908(03)00269-7.

Faravelli, C. *et al.* (2012) 'The Role of Life Events and HPA Axis in Anxiety Disorders: A Review', *Current Pharmaceutical Design*. doi: 10.2174/138161212803530907.

Ferrari, E. *et al.* (2001) 'Age-related changes of the adrenal secretory pattern: Possible role in pathological brain aging', *Brain Research Reviews*. doi: 10.1016/S0165-0173(01)00133-3.

Finocchiaro, L. M. *et al.* (1988) 'Serotonin and melatonin synthesis in peripheral blood mononuclear cells: stimulation by interferon-gamma as part of an immunomodulatory pathway.', *Journal of interferon research*. doi: 10.1089/jir.1988.8.705.

Fiorica-Howells, E., Maroteaux, L. and Gershon, M. D. (2000) 'Serotonin and the 5-HT(2B) receptor in the development of enteric neurons.', *The Journal of neuroscience : the official journal of the Society for Neuroscience*. doi:

10.1523/JNEUROSCI.20-01-00294.2000.

Fite, K. V *et al.* (1999) 'Retinal afferents to the dorsal raphe nucleus in rats and Mongolian gerbils.', *The Journal of comparative neurology*.

Fitzpatrick, P. F. (1999) 'Tetrahydropterin-Dependent Amino Acid Hydroxylases', *Annual Review of Biochemistry*. doi: 10.1146/annurev.biochem.68.1.355.

Fonken, L. K. *et al.* (2009) 'Influence of light at night on murine anxiety- and depressive-like responses', *Behavioural Brain Research*. doi: 10.1016/j.bbr.2009.07.001.

Fonken, L. K. *et al.* (2010) 'Light at night increases body mass by shifting the time of food intake', *Proceedings of the National Academy of Sciences*. doi: 10.1073/pnas.1008734107.

Fonken, L. K. *et al.* (2013) 'Dim light at night disrupts molecular circadian rhythms and increases body weight', *Journal of Biological Rhythms*. doi: 10.1177/0748730413493862.

Fonken, L. K. and Nelson, R. J. (2011) 'Illuminating the deleterious effects of light at night', *F1000 Medicine Reports*. doi: 10.3410/M3-18.

Fornal, C. A. *et al.* (1996) 'A subgroup of dorsal raphe serotonergic neurons in the cat is strongly activated during oral-buccal movements', *Brain Research*. doi: 10.1016/0006-8993(96)00006-6.

Forster, G. L. *et al.* (2008) 'Corticotropin-releasing factor in the dorsal raphe nucleus increases medial prefrontal cortical serotonin via type 2 receptors and median raphe nucleus activity', *European Journal of Neuroscience*. doi: 10.1111/j.1460-9568.2008.06333.x.

Le François, B. *et al.* (2008) 'Transcriptional regulation at a HTR1A polymorphism associated with mental illness', *Neuropharmacology*, 55(6), pp. 977–985. doi: 10.1016/j.neuropharm.2008.06.046.

Freedman, L. P. *et al.* (1988) 'The function and structure of the metal coordination sites within the glucocorticoid receptor DNA binding domain', *Nature*. doi: 10.1038/334543a0.

Frodl, T. and O'Keane, V. (2013) 'How does the brain deal with cumulative stress? A review with focus on developmental stress, HPA axis function and hippocampal structure in humans', *Neurobiology of Disease*. Elsevier Inc., 52, pp. 24–37. doi: 10.1016/j.nbd.2012.03.012.

FULLER, R. W. and WONG, D. T. (1990) 'Serotonin Uptake and Serotonin Uptake Inhibition', *Annals of the New York Academy of Sciences*. doi: 10.1111/j.1749-6632.1990.tb16873.x.

Gachon, F. *et al.* (2004) 'The mammalian circadian timing system: from gene expression to physiology.', *Chromosoma*. doi: 10.1007/s00412-004-0296-2.

Gametchu, B., Watson, C. S. and Wu, S. (1993) 'Use of receptor antibodies to demonstrate membrane glucocorticoid receptor in cells from human leukemic patients.', *The FASEB journal : official publication of the Federation of American Societies for Experimental Biology*.

Gao, J. *et al.* (2012) 'TPH2 gene polymorphisms and major depression - a meta-analysis', *PLoS ONE*, 7(5), pp. 3–7. doi: 10.1371/journal.pone.0036721.

Garaulet, M. and Madrid, J. A. (2010) 'Chronobiological aspects of nutrition, metabolic syndrome and obesity', *Advanced Drug Delivery Reviews*. doi: 10.1016/j.addr.2010.05.005.

Gardner, K. L. *et al.* (2005) 'Early life experience alters behavior during social defeat: Focus on serotonergic systems', *Neuroscience*. doi: 10.1016/j.neuroscience.2005.07.042.

Gardner, Katherine L. *et al.* (2009a) 'Adverse early life experience and social stress during adulthood interact to increase serotonin transporter mRNA expression', *Brain Research*. doi: 10.1016/j.brainres.2009.09.065.

Gardner, Katherine L. *et al.* (2009b) 'Adverse early life experience and social stress during adulthood interact to increase serotonin transporter mRNA expression', *Brain Research*. Elsevier B.V., 1305, pp. 47–63. doi: 10.1016/j.brainres.2009.09.065.

Gardner, K. L. *et al.* (2009) 'Adverse experience during early life and adulthood interact to elevate tph2 mRNA expression in serotonergic neurons within the dorsal raphe nucleus', *Neuroscience*. Elsevier Inc., 163(4), pp. 991–1001. doi: 10.1016/j.neuroscience.2009.07.055.

Gekakis, N. *et al.* (1998) 'Role of the CLOCK Protein in the Mammalian Circadian Mechanism', *SCIENCE*. doi: 10.1126/science.280.5369.1564.

Germain, A. and Kupfer, D. J. (2008) 'Circadian rhythm and sleep disturbances in depression', *Hum Psychopharmalcol.* doi: 10.1002/hup.964.

Gershon, M. D. (2004) 'Review article: serotonin receptors and transporters - roles in normal and abnormal gastrointestinal motility', *Alimentary Pharmacology and Therapeutics*. doi: 10.1111/j.1365-2036.2004.02180.x.

Gershon, M. D. and Tack, J. (2007) 'The Serotonin Signaling System: From Basic Understanding To Drug Development for Functional GI Disorders', *Gastroenterology*, 132(1), pp. 397–414. doi: 10.1053/j.gastro.2006.11.002.

Geyer, M. A. (1995) 'Serotonergic functions in arousal and motor activity', *Behavioural Brain Research*. doi: 10.1016/0166-4328(96)00065-4.

Gillette, M. U. and Prosser, R. A. (1988) 'Circadian rhythm of the rat suprachiasmatic brain slice is rapidly reset by daytime application of cAMP analogs', *Brain Research*, 474(2), pp. 348–352. doi: 10.1016/0006-8993(88)90449-0.

Glass, J. D. *et al.* (2003) 'Midbrain raphe modulation of nonphotic circadian clock resetting and 5-HT release in the mammalian suprachiasmatic nucleus', *J. Neurosci.* doi: citeulike-article-id:12006428.

Glass, J. D., Dinardo, L. A. and Ehlen, J. C. (2000) 'Dorsal raphe nuclear stimulation of SCN serotonin release and circadian phase-resetting', *Brain Research*. doi: 10.1016/S0006-8993(00)01963-6.

Goodman, M. *et al.* (2005) 'Psychotherapy and combined treatment in bpd: possible effects', *158th.Annual Meeting of the American Psychiatric Association; 2005.May.21 26.; Atlanta., GA.*

Goodwin, G. M. *et al.* (2009) 'Agomelatine prevents relapse in patients with major depressive disorder without evidence of a discontinuation syndrome: A 24-week randomized, double-blind, placebo-controlled trial', *Journal of Clinical Psychiatry*. doi: 10.4088/JCP.08m04548.

Gorwood, P. *et al.* (2007) 'Gene-environment interactions in addictive disorders: epidemiological and methodological aspects', *Comptes Rendus - Biologies*. doi: 10.1016/j.crvi.2007.02.017.

Gorwood, P. (2010) 'Review: Restoring circadian rhythms: a new way to successfully manage depression', *Journal of Psychopharmacology*. doi: 10.1177/1359786810372981.

Graeff, F. G. *et al.* (1996) 'Role of 5-HT in stress, anxiety, and depression', in *Pharmacology Biochemistry and Behavior*. doi: 10.1016/0091-3057(95)02135-3.

Graeff, F. G. (2007) 'Anxiety, panic and the hypothalamic-pituitary-adrenal axis', *Revista Brasileira de Psiquiatria*. doi: S1516-44462007000500002 [pii].

Grahn, R. E. *et al.* (1999) 'Activation of serotonin-immunoreactive cells in the dorsal raphe nucleus in rats exposed to an uncontrollable stressor', *Brain Research*. doi: 10.1016/S0006-8993(99)01208-1.

Gray, T. S. and Magnuson, D. J. (1992) 'Peptide immunoreactive neurons in the amygdala and the bed nucleus of the stria terminalis project to the midbrain central gray in the rat', *Peptides*. doi: 10.1016/0196-9781(92)90074-D.

Greenwood, B. N. *et al.* (2005a) 'Wheel running alters serotonin (5-HT)

transporter, 5-HT1A, 5-HT1B, and alpha1b-adrenergic receptor mRNA in the rat raphe nuclei', *Biological Psychiatry*. doi: 10.1016/j.biopsych.2004.11.025.

Greenwood, B. N. *et al.* (2005b) 'Wheel running alters serotonin (5-HT) transporter, 5-HT1A, 5-HT1B, and alpha1b-adrenergic receptor mRNA in the rat raphe nuclei', *Biological Psychiatry*. doi: 10.1016/j.biopsych.2004.11.025.

Grenett, H. *et al.* (1987) 'Full-length cDNA for rabbit tryptophan hydroxylase : Functional domains and evolution of aromatic amino acid hydroxylases Identification of TrpOHase Immunoreactive Protein and', *Biochemistry*.

Groenewegen, H. J. (1988) 'Organization of the afferent connections of the mediodorsal thalamic nucleus in the rat, related to the mediodorsal-prefrontal topography', *Neuroscience*. doi: 10.1016/0306-4522(88)90339-9.

Grohmann, M. *et al.* (2010) 'Alternative splicing and extensive RNA editing of human TPH2 transcripts', *PLoS ONE*. doi: 10.1371/journal.pone.0008956.

Grove, E. A. (1988) 'Neural associations of the substantia innominata in the rat: Afferent connections', *Journal of Comparative Neurology*. doi: 10.1002/cne.902770302.

Grubss, F. E. (1969) 'Procedures for Detecting Outlying Observations in Samples', *American Statistical Association*, 11(1), pp. 1–21.

Guillaumond, F. *et al.* (2005) 'Differential control of Bmal1 circadian transcription by REV-ERB and ROR nuclear receptors', *Journal of Biological Rhythms*. doi: 10.1177/0748730405277232.

Gupta, P. and Bhatia, V. (2008) 'Corticosteroid physiology and principles of therapy', in *Indian Journal of Pediatrics*. doi: 10.1007/s12098-008-0208-1.

Gyermek, L. (1995) '5-HT3 receptors: pharmacologic and therapeutic aspects.', *Journal of clinical pharmacology*.

Haghighi, F. *et al.* (2008) 'Genetic architecture of the human tryptophan

hydroxylase 2 Gene: Existence of neural isoforms and relevance for major depression', *Molecular Psychiatry*. doi: 10.1038/sj.mp.4002127.

Hale, M. W. *et al.* (2008) 'Exposure to an open-field arena increases c-Fos expression in a subpopulation of neurons in the dorsal raphe nucleus, including neurons projecting to the basolateral amygdaloid complex', *Neuroscience*, 157(4), pp. 733–748. doi: 10.1016/j.neuroscience.2008.09.050.

Hale, M. W. *et al.* (2010) 'Urocortin 2 increases c-Fos expression in serotonergic neurons projecting to the ventricular/periventricular system', *Experimental Neurology*. doi: 10.1016/j.expneurol.2010.04.002.

Hale, M. W. and Lowry, C. A. (2011) 'Functional topography of midbrain and pontine serotonergic systems: Implications for synaptic regulation of serotonergic circuits', *Psychopharmacology*, 213(2–3), pp. 243–264. doi: 10.1007/s00213-010-2089-z.

Hale, M. W., Shekhar, A. and Lowry, C. A. (2011) 'Development by environment interactions controlling tryptophan hydroxylase expression', *Journal of Chemical Neuroanatomy*. Elsevier B.V., 41(4), pp. 219–226. doi: 10.1016/j.jchemneu.2011.05.002.

Hale, M. W., Shekhar, A. and Lowry, C. A. (2012) 'Stress-related serotonergic systems: Implications for symptomatology of anxiety and affective disorders', *Cellular and Molecular Neurobiology*. doi: 10.1007/s10571-012-9827-1.

Haller, J., Mikics, É. and Makara, G. B. (2008) 'The effects of non-genomic glucocorticoid mechanisms on bodily functions and the central neural system. A critical evaluation of findings', *Frontiers in Neuroendocrinology*. doi: 10.1016/j.yfrne.2007.10.004.

Hammack, S. E. *et al.* (2002) 'The role of corticotropin-releasing hormone in the dorsal raphe nucleus in mediating the behavioral consequences of uncontrollable stress.', *The Journal of neuroscience : the official journal of the Society for Neuroscience*.

Hamon M., Bourgom S., Artaud F, and N. D. (1981) 'Regulatory properties of neuronal tryptophan hydroxylase.', *Adv. Exp. Med. Bzol*. doi: 10.1036/ommbid.97.

Hannon, J. and Hoyer, D. (2002) 'Serotonin receptors and systems: Endless diversity?', *Acta Biologica Szegediensis*.

Hannon, J. and Hoyer, D. (2008) 'Molecular biology of 5-HT receptors', *Behavioural Brain Research*. doi: 10.1016/j.bbr.2008.03.020.

Hanson, N. D., Owens, M. J. and Nemeroff, C. B. (2011) 'Depression, antidepressants, and neurogenesis: A critical reappraisal', *Neuropsychopharmacology*. doi: 10.1038/npp.2011.220.

Hardin, P. E., Hall, J. C. and Rosbash, M. (1990) 'Feedback of the Drosophila period gene product on circadian cycling of its messenger RNA levels', *Nature*. doi: 10.1038/343536a0.

Harfstrand, A. *et al.* (1986) 'Glucocorticoid receptor immunoreactivity in monoaminergic neurons of rat brain', *Proc Natl Acad Sci U S A*.

Hartmann, A. *et al.* (1997) 'Twenty-four hour cortisol release profiles in patients with Alzheimer's and Parkinson's disease compared to normal controls: ultradian secretory pulsatility and diurnal variation', *Neurobiol Aging*. doi: 10.1016/S0197-4580(97)80309-0.

Harvey, A. G., Mullin, B. C. and Hinshaw, S. P. (2006) 'Sleep and circadian rhythms in children and adolescents with bipolar disorder', *Development and Psychopathology*. doi: 10.1017/S095457940606055X.

Hasegawa, H. *et al.* (1995) 'Rapid turnover of tryptophan hydroxylase in serotonin producing cells: demonstration of ATP-dependent proteolytic degradation', *FEBS Letters*. doi: 10.1016/0014-5793(95)00629-N.

Hastings, M. H. *et al.* (1998) 'Non-photic signalling in the suprachiasmatic nucleus. [Review] [43 refs]', *Biology.of the Cell*.

Haus, E. and Smolensky, M. (2006) 'Biological clocks and shift work: Circadian dysregulation and potential long-term effects', *Cancer Causes and Control*. doi: 10.1007/s10552-005-9015-4.

Hay-Schmidt, A. *et al.* (2003) 'Projections from the raphe nuclei to the suprachiasmatic nucleus of the rat', *Journal of Chemical Neuroanatomy*, 25(4), pp. 293–310. doi: 10.1016/S0891-0618(03)00042-5.

Haycock, J. W. *et al.* (2002) 'A monoclonal antibody to tryptophan hydroxylase: Applications and identification of the epitope', *Journal of Neuroscience Methods*. doi: 10.1016/S0165-0270(01)00530-1.

Heim, C. *et al.* (1997) 'The role of early adverse life events in the etiology of depression and posttraumatic stress disorder', in *Annals of the New York Academy of Sciences*. doi: 10.1111/j.1749-6632.1997.tb48279.x.

Hench, P. S. and Kendall, E. C. (1949) 'The effect of a hormone of the adrenal cortex (17-hydroxy-11-dehydrocorticosterone; compound E) and of pituitary adrenocorticotropic hormone on rheumatoid arthritis.', *Proceedings of the staff meetings. Mayo Clinic*. doi: 12/18/2013.

Hendrickson, A. E., Wagoner, N. and Cowan, W. M. (1972) 'An autoradiographic and electron microscopic study of retino-hypothalamic connections', *Zeitschrift f??r Zellforschung und mikroskopische Anatomie*, 135(1), pp. 1–26. doi: 10.1007/BF00307084.

Henley, D. E. *et al.* (2009) 'Hypothalamic-pituitary-adrenal axis activation in obstructive sleep apnea: the effect of continuous positive airway pressure therapy.', *The Journal of clinical endocrinology and metabolism*. doi: 10.1210/jc.2009-1174.

Herbert, H. (1992) 'Evidence for projections from medullary nuclei onto serotonergic and dopaminergic neurons in the midbrain dorsal raphe nucleus of the rat', *Cell and Tissue Research*. doi: 10.1007/BF00381889.

Herbert, H. and Saper, C. B. (1992) 'Organization of medullary adrenergic and

noradrenergic projections to the periaqueductal gray matter in the rat', *Journal of Comparative Neurology*. doi: 10.1002/cne.903150104.

Herbert, J. *et al.* (2006) 'Do corticosteroids damage the brain?', *Journal of Neuroendocrinology*, pp. 393–411. doi: 10.1111/j.1365-2826.2006.01429.x.

Herman, J. P. *et al.* (2003) 'Central mechanisms of stress integration: Hierarchical circuitry controlling hypothalamo-pituitary-adrenocortical responsiveness', *Frontiers in Neuroendocrinology*, 24(3), pp. 151–180. doi: 10.1016/j.yfrne.2003.07.001.

Herman, J. P. *et al.* (2016) 'Regulation of the hypothalamic-pituitary-adrenocortical stress response', *Comprehensive Physiology*. doi: 10.1002/cphy.c150015.

Higgins, C. F. (1991) 'Stability and degradation of mRNA', *Current Opinion in Cell Biology*. doi: 10.1016/0955-0674(91)90122-F.

Hiroi, R. *et al.* (2011) 'Overexpression or knockdown of rat tryptophan hyroxylase-2 has opposing effects on anxiety behavior in an estrogen-dependent manner', *Neuroscience*. doi: 10.1016/j.neuroscience.2010.12.019.

Hollenberg, S. M. *et al.* (1987) 'Colocalization of DNA-binding and transcriptional activation functions in the human glucocorticoid receptor.', *Cell*. doi: 0092-8674(87)90753-7 [pii].

Hollis, J. H. *et al.* (2006) 'Lipopolysaccharide has indomethacin-sensitive actions on Fos expression in topographically organized subpopulations of serotonergic neurons', *Brain, Behavior, and Immunity*. doi: 10.1016/j.bbi.2006.01.006.

Holsboer, F. (2000a) 'The corticosteroid receptor hypothesis of depression', *Neuropsychopharmacology*. doi: 10.1016/S0893-133X(00)00159-7.

Holsboer, F. (2000b) 'The corticosteroid receptor hypothesis of depression', *Neuropsychopharmacology*, 23(5), pp. 477–501. doi: 10.1016/S0893-133X(00)00159-7.

Holstege, G. G., Mouton, L. J. and Gerrits, N. M. (2003) 'Emotional Motor System', in *The Human Nervous System: Second Edition*. doi: 10.1016/B978-012547626-3/50037-5.

Holstege, G., Meiners, L. and Tan, K. (1985) 'Projections of the bed nucleus of the stria terminalis to the mesencephalon, pons, and medulla oblongata in the cat', *Experimental Brain Research*. doi: 10.1007/BF00235319.

Honda, M. *et al.* (2000) 'Expression of glucocorticoid receptor beta in lymphocytes of patients with glucocorticoid-resistant ulcerative colitis', *Gastroenterology*.

Honma, K. I. and Hiroshige, T. (1978) 'Endogenous ultradian rhythms in rats exposed to prolonged continuous light.', *The American journal of physiology*, 235(5), pp. R250-6. Available at: http://www.ncbi.nlm.nih.gov/pubmed/727287.

Hood, S. *et al.* (2010) 'Endogenous Dopamine Regulates the Rhythm of Expression of the Clock Protein PER2 in the Rat Dorsal Striatum via Daily Activation of D2 Dopamine Receptors', *Journal of Neuroscience*. doi: 10.1523/JNEUROSCI.2128-10.2010.

Horikawa, K. *et al.* (2000) 'Nonphotic entrainment by 5-HT1A/7 receptor agonists accompanied by reduced Per1 and Per2 mRNA levels in the suprachiasmatic nuclei.', *The Journal of neuroscience : the official journal of the Society for Neuroscience*. doi: 20/15/5867 [pii].

Hornung, J. P. (2003) 'The human raphe nuclei and the serotonergic system', *Journal of Chemical Neuroanatomy*, 26(4), pp. 331–343. doi: 10.1016/j.jchemneu.2003.10.002.

Hoyer, D., Hannon, J. P. and Martin, G. R. (2002) 'Molecular, pharmacological and functional diversity of 5-HT receptors', *Pharmacology Biochemistry and Behavior*. doi: 10.1016/S0091-3057(01)00746-8.

Hoyer, D. and Martin, G. (1997) '5-HT receptor classification and nomenclature: Towards a harmonization with the human genome', *Neuropharmacology*. doi:

10.1016/S0028-3908(97)00036-1.

Huang, W. *et al.* (2011) 'Circadian rhythms, sleep, and metabolism', *Journal of Clinical Investigation*. doi: 10.1172/JCI46043.

Huang, Z. *et al.* (2008) 'Posttranslational regulation of TPH1 is responsible for the nightly surge of 5-HT output in the rat pineal gland', *Journal of Pineal Research*. doi: 10.1111/j.1600-079X.2008.00627.x.

Hufton, S. E., Jennings, I. G. and Cotton, R. G. (1995) 'Structure and function of the aromatic amino acid hydroxylases.', *Biochemical Journal*.

Hurley, K. M. *et al.* (1991) 'Efferent projections of the infralimbic cortex of the rat', *Journal of Comparative Neurology*. doi: 10.1002/cne.903080210.

Huscher, D. *et al.* (2009) 'Dose-related patterns of glucocorticoid-induced side effects', *Annals of the Rheumatic Diseases*. doi: 10.1136/ard.2008.092163.

Hutchison, K. A. *et al.* (1993) 'FK506 Binding to the 56-Kilodalton Immunophilin (Hsp56) in the Glucocorticoid Receptor Heterocomplex Has No Effect on Receptor Folding or Function', *Biochemistry*. doi: 10.1021/bi00066a015.

Imai, H. *et al.* (1986) 'The morphology and divergent axonal organization of midbrain raphe projection neurons in the rat', *Brain and Development*. doi: 10.1016/S0387-7604(86)80054-7.

Imai, H., Steindler, D. A. and Kitai, S. T. (1986) 'The organization of divergent axonal projections from the midbrain raphe nuclei in the rat', *Journal of Comparative Neurology*. doi: 10.1002/cne.902430307.

Inouye, S. T. and Kawamura, H. (1979) 'Persistence of circadian rhythmicity in a mammalian hypothalamic "island" containing the suprachiasmatic nucleus', *Proceedings of the National Academy of Sciences*, 76(11), pp. 5962–5966. doi: 10.1073/pnas.76.11.5962.

Ishida, A. *et al.* (2005) 'Light activates the adrenal gland: Timing of gene

expression and glucocorticoid release', *Cell Metabolism*, 2(5), pp. 297–307. doi: 10.1016/j.cmet.2005.09.009.

Iwamoto, J., Takeda, T. and Ichimura, S. (2002) 'Forearm bone mineral density in postmenopausal women with rheumatoid arthritis', *Calcified Tissue International*. doi: 10.1007/s00223-001-1054-6.

Jacobs, B. L. and Azmitia, E. C. (1992) 'Structure and function of the brain serotonin system', *Physiological Reviews*. doi: 10.1152/physrev.1992.72.1.165.

Jacobs, B. L. and Fornal, C. A. (1991) 'Activity of brain serotonergic neurons in the behaving animal', *Pharmacological Reviews*.

Jacobson, L. and Sapolsky, R. (1991) 'The role of the hippocampus in feedback regulation of the hypothalamic- pituitary-adrenocortical axis', *Endocr Rev*. doi: 10.1210/edrv-12-2-118.

Jahanshahi, A. *et al.* (2011) 'Altered expression of neuronal tryptophan hydroxylase-2 mRNA in the dorsal and median raphe nuclei of three genetically modified mouse models relevant to depression and anxiety', *Journal of Chemical Neuroanatomy*. doi: 10.1016/j.jchemneu.2011.05.015.

Jin, H. *et al.* (1992) 'Characterization of the human 5-hydroxytryptamine(1B) receptor', *Journal of Biological Chemistry*. doi: 10.1161/01.CIR.100.5.483.

Joëls, M. *et al.* (2008) 'The coming out of the brain mineralocorticoid receptor', *Trends in Neurosciences*. doi: 10.1016/j.tins.2007.10.005.

Johnson, P. L. *et al.* (2005) 'Acute hypercarbic gas exposure reveals functionally distinct subpopulations of serotonergic neurons in rats', *Journal of Psychopharmacology*. doi: 10.1177/0269881105053281.

Johnson, P. L. *et al.* (2008) 'Disruption of GABAergic tone in the dorsomedial hypothalamus attenuates responses in a subset of serotonergic neurons in the dorsal raphe nucleus following lactate-induced panic', *Journal of Psychopharmacology*. doi: 10.1177/0269881107082900.

Jones, M. T., Hillhouse, E. W. and Burden, J. L. (1977) 'Dynamics and mechanics of corticosteroid feedback at the hypothalamus and anterior pituitary gland', *Journal of Endocrinology*. doi: 10.1677/joe.0.0730405.

Judge, S. J., Ingram, C. D. and Gartside, S. E. (2004) 'Moderate differences in circulating corticosterone alter receptor-mediated regulation of 5-hydroxytryptamine neuronal activity', *Journal of Psychopharmacology*. doi: 10.1177/0269881104047274.

Juruena, M. F. (2014) 'Early-life stress and HPA axis trigger recurrent adulthood depression', *Epilepsy and Behavior*. Elsevier Inc., 38, pp. 148–159. doi: 10.1016/j.yebeh.2013.10.020.

Kamphuis, W. *et al.* (2005) 'Circadian expression of clock genes and clock-controlled genes in the rat retina', *Biochem Biophys Res Commun*. doi: S0006-291X(05)00394-3 [pii]\r10.1016/j.bbrc.2005.02.118.

Kamphuis, W. *et al.* (2009) 'Resetting of circadian time in peripheral tissues by glucocorticoid signaling', *Journal of cell science*. doi: 10.1242/jcs.208223.

Kaper, T. J., Kramer, M. A. and Rotstein, H. G. (2013) 'Introduction to focus issue: Rhythms and dynamic transitions in neurological disease: Modeling, computation, and experiment', *Chaos*. doi: 10.1063/1.4856276.

Kawano, H., Decker, K. and Reuss, S. (1996a) 'Is there a direct retina-raphe-suprachiasmatic nucleus pathway in the rat?', *Neuroscience Letters*. doi: 10.1016/0304-3940(96)12795-6.

Kawano, H., Decker, K. and Reuss, S. (1996b) 'Is there a direct retina-raphe-suprachiasmatic nucleus pathway in the rat?', *Neuroscience Letters*, 212(2), pp. 143–146. doi: 10.1016/0304-3940(96)12795-6.

Kazakov, V. N. *et al.* (1992) 'Sources of cortical, hypothalamic and spinal serotonergic projections: Topical organization in the dorsal raphe nucleus', *Neurophysiology*. doi: 10.1007/BF01053485.

Keller-Wood, M. E. and Dallman, M. F. (1984) ‘Corticosteroid inhibition of ACTH secretion’, *Endocrine Reviews*. doi: 10.1210/edrv-5-1-1.

Kepser, L. J. and Homberg, J. R. (2015) ‘The neurodevelopmental effects of serotonin: A behavioural perspective’, *Behavioural Brain Research*, pp. 3–13. doi: 10.1016/j.bbr.2014.05.022.

Kim, M. A. *et al.* (2004) ‘Reciprocal connections between subdivisions of the dorsal raphe and the nuclear core of the locus coeruleus in the rat’, *Brain Research*. doi: 10.1016/j.brainres.2004.08.022.

King, D. P. and Takahashi, J. S. (2000) ‘Molecular Genetics of Circadian Rhythms in Mammals’, *Annual Review of Neuroscience*. doi: 10.1146/annurev.neuro.23.1.713.

Kirby, L. G., Rice, K. C. and Valentino, R. J. (2000) ‘Effects of corticotropin-releasing factor on neuronal activity in the serotonergic dorsal raphe nucleus’, *Neuropsychopharmacology*. doi: 10.1016/S0893-133X(99)00093-7.

Kirifides, M. L. *et al.* (2001) ‘Topographic organization and neurochemical identity of dorsal raphe neurons that project to the trigeminal somatosensory pathway in the rat’, *Journal of Comparative Neurology*. doi: 10.1002/cne.1033.

Kiser, D. *et al.* (2012) ‘The reciprocal interaction between serotonin and social behaviour’, *Neuroscience and Biobehavioral Reviews*. doi: 10.1016/j.neubiorev.2011.12.009.

Kitchener, P. *et al.* (2004) ‘Differences between brain structures in nuclear translocation and DNA binding of the glucocorticoid receptor during stress and the circadian cycle’, *European Journal of Neuroscience*. doi: 10.1111/j.1460-9568.2004.03267.x.

Kjellman, B. F. *et al.* (1985) ‘Effect of TRH on TSH and prolactin levels in affective disorders’, *Psychiatry Research*. doi: 10.1016/0165-1781(85)90103-9.

Klein, D. ., Moore, R. Y. and S.M., R. (1991) ‘SCN electrophysiology in vitro:

rhythmic activity and endogenous clock properties', *Suprachiasmatic Nucleus: The Mind's Clock*.

Klemenhagen, K. C. *et al.* (2006) 'Increased fear response to contextual cues in mice lacking the 5-HT1A receptor', *Neuropsychopharmacology*. doi: 10.1038/sj.npp.1300774.

de Kloet, E. R. (1991) 'Brain corticosteroid receptor balance and homeostatic control', *Frontiers in Neuroendocrinology*. doi: 10.1080/09614520701469617.

De Kloet, E. R. (2004) 'Hormones and the stressed brain', in *Annals of the New York Academy of Sciences*. doi: 10.1196/annals.1296.001.

De Kloet, E. R. and Reul, J. M. H. M. (1987) 'Feedback action and tonic influence of corticosteroids on brain function: A concept arising from the heterogeneity of brain receptor systems', *Psychoneuroendocrinology*. doi: 10.1016/0306-4530(87)90040-0.

de Kloet, E. R. and Sarabdjitsingh, R. A. (2008) 'Everything Has Rhythm: Focus on Glucocorticoid Pulsatility', *Endocrinology*, 149(7), pp. 3241–3243. doi: 10.1210/en.2008-0471.

Knight, J. C. (2005) 'Regulatory polymorphisms underlying complex disease traits', *Journal of Molecular Medicine*. doi: 10.1007/s00109-004-0603-7.

Ko, C. H. and Takahashi, J. S. (2006) 'Molecular components of the mammalian circadian clock', *Human Molecular Genetics*. doi: 10.1093/hmg/ddl207.

Kohen, R. *et al.* (1996) 'Cloning, characterization, and chromosomal localization of a human 5-HT6 serotonin receptor.', *Journal of neurochemistry*. doi: 10.1046/j.1471-4159.1996.66010047.x.

Köhler, C., Chan-Palay, V. and Steinbusch, H. (1982) 'The distribution and origin of serotonin-containing fibers in the septal area: A combined immunohistochemical and fluorescent retrograde tracing study in the rat', *Journal of Comparative Neurology*. doi: 10.1002/cne.902090109.

Köhler, C. and Steinbusch, H. (1982a) 'Identification of serotonin and non-serotonin-containing neurons of the mid-brain raphe projecting to the entorhinal area and the hippocampal formation. A combined immunohistochemical and fluorescent retrograde tracing study in the rat brain', *Neuroscience*. doi: 10.1016/0306-4522(82)90054-9.

Köhler, C. and Steinbusch, H. (1982b) 'Identification of serotonin and non-serotonin-containing neurons of the mid-brain raphe projecting to the entorhinal area and the hippocampal formation. A combined immunohistochemical and fluorescent retrograde tracing study in the rat brain', *Neuroscience*. doi: 10.1016/0306-4522(82)90054-9.

Konopka, R. J. and Benzer, S. (1971) 'Clock mutants of Drosophila melanogaster.', *Proceedings of the National Academy of Sciences of the United States of America*. doi: 10.1073/pnas.68.9.2112.

Kornhauser, J. M. *et al.* (1990) 'Photic and Circadian Regulation of ~40s Gene Expression in the Hamster Suprachiasmatic Nucleus', *Neuron*.

Kornmann, B. *et al.* (2007) 'System-driven and oscillator-dependent circadian transcription in mice with a conditionally active liver clock', *PLoS Biology*. doi: 10.1371/journal.pbio.0050034.

Kowanko, I. C. *et al.* (1982) 'Time of day of prednisolone administration in rheumatoid arthritis', *Annals of the Rheumatic Diseases*. doi: 10.1136/ard.41.5.447.

Krasner, A. S. (1999) 'Glucocorticoid-induced adrenal insufficiency', *Journal of the American Medical Association*. doi: 10.1001/jama.282.7.671.

Krout, K. E. *et al.* (2002) 'CNS inputs to the suprachiasmatic nucleus of the rat', *Neuroscience*. doi: 10.1016/S0306-4522(01)00551-6.

Krout, K. E., Belzer, R. E. and Loewy, A. D. (2002) 'Brainstem projections to midline and intralaminar thalamic nuclei of the rat', *Journal of Comparative Neurology*. doi: 10.1002/cne.10236.

Krystal, A. D., Benca, R. M. and Kilduff, T. S. (2013) 'Understanding the sleep-wake cycle: Sleep, insomnia, and the orexin system', in *Journal of Clinical Psychiatry*. doi: 10.4088/JCP.13011su1c.

Kumar, R. and Thompson, E. B. (1999) 'The structure of the nuclear hormone receptors', *Steroids*. doi: 10.1016/S0039-128X(99)00014-8.

De La Iglesia, H. O. *et al.* (2004) 'Forced desynchronization of dual circadian oscillators within the rat suprachiasmatic nucleus', *Current Biology*. doi: 10.1016/j.cub.2004.04.034.

Laaris, N. *et al.* (1999) 'Differential effects of stress on presynaptic and postsynaptic 5- hydroxytryptamine-1A receptors in the rat brain: An in vitro electrophysiological study', *Neuroscience*. doi: 10.1016/S0306-4522(98)00674-5.

Lamia, K. A., Storch, K.-F. and Weitz, C. J. (2008) 'Physiological significance of a peripheral tissue circadian clock.', *Proceedings of the National Academy of Sciences of the United States of America*. doi: 10.1073/pnas.0806717105.

Lamont, E. W. *et al.* (2005) 'The central and basolateral nuclei of the amygdala exhibit opposite diurnal rhythms of expression of the clock protein Period2', *Proceedings of the National Academy of Sciences*. doi: 10.1073/pnas.0500901102.

Lanfumey, L. *et al.* (1999) '5-HT(1A) autoreceptor desensitization by chronic ultramild stress in mice', *NeuroReport*. doi: 10.1097/00001756-199911080-00021.

Lanfumey, L. *et al.* (2008) 'Corticosteroid-serotonin interactions in the neurobiological mechanisms of stress-related disorders', *Neuroscience and Biobehavioral Reviews*. doi: 10.1016/j.neubiorev.2008.04.006.

Lee, H. H. S. *et al.* (2003) 'Glutamatergic afferent projections to the dorsal raphe nucleus of the rat', *Brain research*. doi: 10.1016/S0006-8993(02)03841-6.

Lee, H. S. *et al.* (2003) 'Glutamatergic afferent projections to the dorsal raphe nucleus of the rat', *Brain Research*. doi: 10.1016/S0006-8993(02)03841-6.

Lemonde, S. *et al.* (2003) 'Impaired repression at a 5-hydroxytryptamine 1A receptor gene polymorphism associated with major depression and suicide.', *The Journal of neuroscience : the official journal of the Society for Neuroscience*. doi: 23/25/8788 [pii].

Lesch, K. P. *et al.* (2012) 'Targeting brain serotonin synthesis: Insights into neurodevelopmental disorders with long-term outcomes related to negative emotionality, aggression and antisocial behaviour', *Philosophical Transactions of the Royal Society B: Biological Sciences*. doi: 10.1098/rstb.2012.0039.

Liang, J. *et al.* (2004) 'Diurnal rhythms of tryptophan hydroxylase 1 and 2 mRNA expression in the rat retina', *NeuroReport*. doi: 10.1097/01.wnr.0000131007.59315.66.

Lightman, S. L. *et al.* (2000) 'Significance of pulsatility in the HPA axis', *Novartis Foundation Symposium*, 227, pp. 244–260. doi: 10.1002/0470870796.ch14.

Lightman, S. L. (2008) 'The neuroendocrinology of stress: A never ending story', *Journal of Neuroendocrinology*, 20(6), pp. 880–884. doi: 10.1111/j.1365-2826.2008.01711.x.

Lightman, S. L. *et al.* (2008) 'The significance of glucocorticoid pulsatility', *European Journal of Pharmacology*, pp. 255–262. doi: 10.1016/j.ejphar.2007.11.073.

Lightman, S. L. and Conway-Campbell, B. L. (2010) 'The crucial role of pulsatile activity of the HPA axis for continuous dynamic equilibration', *Nat Rev Neurosci*, 11(10), pp. 710–718. doi: nrn2914 [pii]\r10.1038/nrn2914.

Lind, R. W. (1986) 'Bi-directional, chemically specified neural connections between the subfornical organ and the midbrain raphe system', *Brain Research*. doi: 10.1016/0006-8993(86)91161-3.

Litinski, M., Scheer, F. A. J. L. and Shea, S. A. (2009) 'Influence of the Circadian System on Disease Severity', *Sleep Medicine Clinics*. doi:

10.1016/j.jsmc.2009.02.005.

Liu, A. C. *et al.* (2007) 'Intercellular Coupling Confers Robustness against Mutations in the SCN Circadian Clock Network', *Cell*. doi: 10.1016/j.cell.2007.02.047.

Liu, J. *et al.* (2006) 'The circadian clock Period 2 gene regulates gamma interferon production of NK cells in host response to lipopolysaccharide-induced endotoxic shock', *Infection and Immunity*. doi: 10.1128/IAI.00287-06.

Ljubic-Thibal, V. *et al.* (1999) 'Origin of the serotonergic innervation to the rat dorsolateral hypothalamus: Retrograde transport of cholera toxin and upregulation of tryptophan hydroxylase mRNA expression following selective nerve terminals lesion', *Synapse*. doi: 10.1002/(SICI)1098-2396(19990601)32:3<177::AID-SYN4>3.0.CO;2-D.

López-Narváez, M. L. *et al.* (2015) 'Association analysis of TPH-1 and TPH-2 genes with suicidal behavior in patients with attempted suicide in Mexican population', *Comprehensive Psychiatry*. The Authors, 61, pp. 72–77. doi: 10.1016/j.comppsych.2015.05.002.

Lowry, C. A. *et al.* (2000) 'Corticotropin-releasing factor increases in vitro firing rates of serotonergic neurons in the rat dorsal raphe nucleus: evidence for activation of a topographically organized mesolimbocortical serotonergic system.', *The Journal of neuroscience : the official journal of the Society for Neuroscience*. doi: 20/20/7728 [pii].

Lowry, C. A. (2002) 'Functional subsets of serotonergic neurones: Implications for control of the hypothalamic-pituitary-adrenal axis', *Journal of Neuroendocrinology*, 14(11), pp. 911–923. doi: 10.1046/j.1365-2826.2002.00861.x.

Lowry, C. A. *et al.* (2005a) 'Modulation of anxiety circuits by serotonergic systems', *Stress*, 8(4), pp. 233–246. doi: 10.1080/10253890500492787.

Lowry, C. A. *et al.* (2005b) 'Modulation of anxiety circuits by serotonergic systems', *Stress*. doi: 10.1080/10253890500492787.

Lowry, C. A. *et al.* (2007) 'Identification of an immune-responsive mesolimbocortical serotonergic system: Potential role in regulation of emotional behavior', *Neuroscience*. doi: 10.1016/j.neuroscience.2007.01.067.

Lowry, C. A. *et al.* (2008a) 'Serotonergic systems, anxiety, and affective disorder: Focus on the dorsomedial part of the dorsal raphe nucleus', in *Annals of the New York Academy of Sciences*. doi: 10.1196/annals.1410.004.

Lowry, C. A. *et al.* (2008b) 'Serotonergic systems, anxiety, and affective disorder: Focus on the dorsomedial part of the dorsal raphe nucleus', in *Annals of the New York Academy of Sciences*. doi: 10.1196/annals.1410.004.

Lowry, C. A. *et al.* (2008c) 'Serotonergic systems, anxiety, and affective disorder: Focus on the dorsomedial part of the dorsal raphe nucleus', *Annals of the New York Academy of Sciences*, 1148, pp. 86–94. doi: 10.1196/annals.1410.004.

Lowry, C. A. *et al.* (2009) 'Serotonergic Systems, Anxiety, and Affective Disorder', *Annals of the New York Academy of Sciences*. doi: 10.1196/annals.1410.004.

Lu, N. Z. and Cidlowski, J. A. (2005) 'Translational regulatory mechanisms generate N-terminal glucocorticoid receptor isoforms with unique transcriptional target genes', *Molecular Cell*. doi: 10.1016/j.molcel.2005.03.025.

Lukkes, J. L. *et al.* (2013) 'Development×environment interactions control tph2 mRNA expression', *Neuroscience*, 237, pp. 139–150. doi: 10.1016/j.neuroscience.2013.01.070.

Ma, W. P. *et al.* (2007) 'Exposure to chronic constant light impairs spatial memory and influences long-term depression in rats', *Neuroscience Research*. doi: 10.1016/j.neures.2007.06.1474.

Macfarlane, D. P., Forbes, S. and Walker, B. R. (2008) 'Glucocorticoids and fatty

acid metabolism in humans: Fuelling fat redistribution in the metabolic syndrome', *Journal of Endocrinology*. doi: 10.1677/JOE-08-0054.

Mahar, I. *et al.* (2014) 'Stress, serotonin, and hippocampal neurogenesis in relation to depression and antidepressant effects', *Neuroscience and Biobehavioral Reviews*. Elsevier Ltd, 38, pp. 173–192. doi: 10.1016/j.neubiorev.2013.11.009.

De Mairan, J. J. . (1729) 'Observation Botanique', *Histoire de l'Academie Royale des Sciences*, p. 35. doi: 10.1002/embj.201386357.

Malek, Z. S. *et al.* (2005) 'Tissue-specific expression of tryptophan hydroxylase mRNAs in the rat midbrain: Anatomical evidence and daily profiles', *European Journal of Neuroscience*, 22(4), pp. 895–901. doi: 10.1111/j.1460-9568.2005.04264.x.

Malek, Z. S. *et al.* (2007) 'Daily rhythm of tryptophan hydroxylase-2 messenger ribonucleic acid within raphe neurons is induced by corticoid daily surge and modulated by enhanced locomotor activity', *Endocrinology*, 148(11), pp. 5165–5172. doi: 10.1210/en.2007-0526.

Malek, Z. S. (2007) 'Daily rhythm of tryptophan hydroxylase-2 messenger ribonucleic acid within raphe neurons is induced by corticoid daily surge and modulated by enhanced locomotor activity', *Endocrinology*, 148(11), pp. 5165–5172. doi: 10.1210/en.2007-0526.

Malek, Z. S., Pévet, P. and Raison, S. (2004) 'Circadian change in tryptophan hydroxylase protein levels within the rat intergeniculate leaflets and raphe nuclei', *Neuroscience*, 125(3), pp. 749–758. doi: 10.1016/j.neuroscience.2004.01.031.

Man, M. S., Young, A. H. and McAllister-Williams, R. H. (2002) 'Corticosterone modulation of somatodendritic 5-HT1Areceptor function in mice', *Journal of Psychopharmacology*. doi: 10.1177/026988110201600310.

Mangelsdorf, D. J. *et al.* (1995) 'The nuclear receptor superfamily: the second decade.', *Cell*, 83, pp. 835–839. doi: 10.1016/0092-8674(95)90199-X.

Mann, J. J. *et al.* (1989) 'Evidence for the 5-HT hypothesis of suicide: A review of post-mortem studies', in *British Journal of Psychiatry*, pp. 7–14.

Mansur, S. S. *et al.* (2011) 'Phenylephrine into the median raphe nucleus evokes an anxiolytic-like effect in free-feeding rats but does not alter food intake in free feeding rats', *Behavioural Brain Research*. doi: 10.1016/j.bbr.2010.10.003.

Mason, P. (1999) 'Central mechanisms of pain modulation', *Curr Opin Neurobiol*. doi: 10.1016/S0959-4388(99)80065-8.

Matthes, S. *et al.* (2010) 'Tryptophan hydroxylase as novel target for the treatment of depressive disorders', *Pharmacology*, 85(2), pp. 95–109. doi: 10.1159/000279322.

Mazziotti, G., Gazzaruso, C. and Giustina, A. (2011) 'Diabetes in Cushing syndrome: Basic and clinical aspects', *Trends in Endocrinology and Metabolism*. doi: 10.1016/j.tem.2011.09.001.

McClung, C. A. (2007) 'Circadian genes, rhythms and the biology of mood disorders', *Pharmacology and Therapeutics*. doi: 10.1016/j.pharmthera.2007.02.003.

Mcelroy, S. L. *et al.* (2006) 'Antidepressants and suicidal behavior in bipolar disorder', *Bipolar Disorders*. doi: 10.1111/j.1399-5618.2006.00348.x.

McEWEN, B. S. (1998) 'Stress, Adaptation, and Disease: Allostasis and Allostatic Load', *Annals of the New York Academy of Sciences*, 840(1), pp. 33–44. doi: 10.1111/j.1749-6632.1998.tb09546.x.

McNamara, P. *et al.* (2001) 'Regulation of CLOCK and MOP4 by nuclear hormone receptors in the vasculature: A humoral mechanism to reset a peripheral clock', *Cell*. doi: 10.1016/S0092-8674(01)00401-9.

Meaney, M. J. *et al.* (1989) 'Neonatal handling alters adrenocortical negative feedback sensitivity and hippocampal type II glucocorticoid receptor binding in the rat.', *Neuroendocrinology*, 50(5), pp. 597–604. doi: 10.1159/000125287.

Meijer, O. C. *et al.* (1997) 'Regulation of hippocampal 5-HT(1A) receptor mRNA and binding in transgenic mice with a targeted disruption of the glucocorticoid receptor', *Molecular Brain Research*. doi: 10.1016/S0169-328X(97)00002-8.

Meijer, O. C. and de Kloet, E. R. (1994) 'Corticosterone suppresses the expression of 5-HT1A receptor mRNA in rat dentate gyrus', *European Journal of Pharmacology: Molecular Pharmacology*. doi: 10.1016/0922-4106(94)90134-1.

Meijer, R. T. *et al.* (2001) 'OKT3 versus methylprednisolone for primary treatment of rejection: A retrospective evaluation', *Transplantation Proceedings*. doi: 10.1016/S0041-1345(01)01940-6.

Mendelson, S. D. and McEwen, B. S. (1991) 'Autoradiographic analyses of the effects of restraint-induced stress on 5-ht<inf>1a</inf>, 5-ht<inf>1c</inf> and 5-ht<inf>2</inf> receptors in the dorsal hippocampus of male and female rats', *Neuroendocrinology*. doi: 10.1159/000125951.

Mendelson, S. D. and McEwen, B. S. (1992) 'Autoradiographic analyses of the effects of adrenalectomy and corticosterone on 5-HT<inf>1A</inf> and 5-HT<inf>1B</inf> receptors in the dorsal hippocampus and cortex of the rat', *Neuroendocrinology*. doi: 10.1159/000126160.

el Mestikawy, S. *et al.* (1991) 'The 5-HT1A receptor: an overview of recent advances.', *Neurochemical research*. doi: 10.1007/BF00965820.

Meyer-Bernstein, E. L. and Morin, L. P. (1996) 'Differential serotonergic innervation of the suprachiasmatic nucleus and the intergeniculate leaflet and its role in circadian rhythm modulation', *The Journal of neuroscience : the official journal of the Society for Neuroscience*, 16(6), pp. 2097–2111. Available at: papers2://publication/uuid/719B7D9B-67A5-4861-BFE7-2F540AAEBBCC.

Meyer, J. H. (2007) 'Imaging the serotonin transporter during major depressive disorder and antidepressant treatment ', *J Psychiatry Neurosci* .

Mifsud, K. R. and Reul, J. M. H. M. (2016) 'Acute stress enhances

heterodimerization and binding of corticosteroid receptors at glucocorticoid target genes in the hippocampus', *Proceedings of the National Academy of Sciences*. doi: 10.1073/pnas.1605246113.

Migliarini, S. *et al.* (2013) 'Lack of brain serotonin affects postnatal development and serotonergic neuronal circuitry formation', *Molecular Psychiatry*. doi: 10.1038/mp.2012.128.

Mikkelsen, J. D., Hay-Schmidt, A. and Larsen, P. J. (1997) 'Central innervation of the rat ependyma and subcommissural organ with special reference to ascending serotoninergic projections from the raphe nuclei', *Journal of Comparative Neurology*. doi: 10.1002/(SICI)1096-9861(19970811)384:4<556::AID-CNE5>3.0.CO;2-1.

Miller, W. L. and Auchus, R. J. (2011) 'The molecular biology, biochemistry, and physiology of human steroidogenesis and its disorders', *Endocr Rev*. doi: er.2010-0013 [pii]\r10.1210/er.2010-0013.

Le Minh, N. *et al.* (2001) 'Glucocorticoid hormones inhibit food-induced phase-shifting of peripheral circadian oscillators', *EMBO Journal*, 20(24), pp. 7128–7136. doi: 10.1093/emboj/20.24.7128.

Mitchell, J. M., Lowe, D. and Fields, H. L. (1998) 'The contribution of the rostral ventromedial medulla to the antinociceptive effects of systemic morphine in restrained and unrestrained rats', *Neuroscience*. doi: 10.1016/S0306-4522(98)00119-5.

Modell, S. *et al.* (1997) 'Corticosteroid receptor function is decreased in depressed patients', *Neuroendocrinology*. doi: 10.1159/000127275.

Moffitt, T. E. *et al.* (1998) 'Whole Blood Serotonin Relates to Violence in an Epidemiological Study', *Biological Psychiatry*. doi: 10.1016/S0006-3223(97)00340-5.

Moga, M. M. and Moore, R. Y. (1997) 'Organization of neural inputs to the

suprachiasmatic nucleus in the rat', *Journal of Comparative Neurology*. doi: 10.1002/(SICI)1096-9861(19971222)389:3<508::AID-CNE11>3.0.CO;2-H.

Monteleone, F. *et al.* (2011) 'Duloxetine in the treatment of depression: An overview', *Central Nervous System Agents in Medicinal Chemistry*.

Moore-Ede, M. C. M. (1986) 'Physiology of the circadian timing system: Predictive versus reactive homeostasis', *The American Journal of Physiology*. doi: 10.1152/ajpregu.1986.250.5.R737.

Moore MD, R. Y. (1997) 'CIRCADIAN RHYTHMS: Basic Neurobiology and Clinical Applications', *Annual Review of Medicine*. doi: 10.1146/annurev.med.48.1.253.

Moore, R. Y. and Eichler, V. B. (1972a) 'Loss of a circadian adrenal corticosterone rhythm following suprachiasmatic lesions in the rat', *Brain Research*, 42(1), pp. 201–206. doi: 10.1016/0006-8993(72)90054-6.

Moore, R. Y. and Eichler, V. B. (1972b) 'Loss of a circadian adrenal corticosterone rhythm following suprachiasmatic lesions in the rat', *Brain Research*. doi: 10.1016/0006-8993(72)90054-6.

Moore, R. Y. and Lenn, N. J. (1972) 'A retinohypothalamic projection in the rat', *Journal of Comparative Neurology*. doi: 10.1002/cne.901460102.

Moore, R. Y. and Speh, J. C. (1993) 'GABA is the principal neurotransmitter of the circadian system', *Neuroscience Letters*, 150(1), pp. 112–116. doi: 10.1016/0304-3940(93)90120-A.

Moore, R. Y., Speh, J. C. and Leak, R. K. (2002) 'Suprachiasmatic nucleus organization', *Cell and Tissue Research*. doi: 10.1007/s00441-002-0575-2.

Morimoto, M. *et al.* (1996) 'Distribution of glucocorticoid receptor immunoreactivity and mRNA in the rat brain: An immunohistochemical and in situ hybridization study', *Neuroscience Research*. doi: 10.1016/S0168-0102(96)01105-4.

Morin, L. P. *et al.* (1994) 'Projections of the suprachiasmatic nuclei, subparaventricular zone and retrochiasmatic area in the golden hamster', *Neuroscience*. doi: 10.1016/0306-4522(94)90240-2.

Morin, L. P. (1999) 'Serotonin and the regulation of mammalian circadian rhythmicity.', *Annals of medicine*. doi: 10219711.

Morin, L. P. (2013) 'Neuroanatomy of the extended circadian rhythm system', *Experimental Neurology*. Elsevier Inc., 243, pp. 4–20. doi: 10.1016/j.expneurol.2012.06.026.

Morin, L. P. and Blanchard, J. (1991) 'Depletion of brain serotonin by 5,7-DHT modifies hamster circadian rhythm response to light', *Brain Research*. doi: 10.1016/0006-8993(91)91696-X.

Mukherjee, S. *et al.* (2010) 'Knockdown of clock in the ventral tegmental area through RNA interference results in a mixed state of mania and depression-like behavior', *Biological Psychiatry*. doi: 10.1016/j.biopsych.2010.04.031.

Murphy, D. L. *et al.* (1998) 'Brain serotonin neurotransmission: An overview and update with an emphasis on serotonin subsystem heterogeneity, multiple receptors, interactions with other neurotransmitter systems, and consequent implications for understanding the actions of serotonergi', *Journal of Clinical Psychiatry*, pp. 4–12.

Naber, D., Sand, P. and Heigl, B. (1996) 'Psychopathological and neuropsychological effects of 8-days' corticosteroid treatment. A prospective study.', *Psychoneuroendocrinology*. doi: 10.1016/0306-4530(95)00031-3.

Nagpal, S. *et al.* (1993) 'RARs and RXRs: evidence for two autonomous transactivation functions (AF-1 and AF-2) and heterodimerization in vivo.', *The EMBO journal*.

Naughton, M., Mulrooney, J. B. and Leonard, B. E. (2000a) 'A review of the role of serotonin receptors in psychiatric disorders ', *Human Psychopharmacology: Clinical and Experimental* . doi: 10.1002/1099-1077(200008)15:6<397::AID-

HUP212>3.0.CO;2-L.

Naughton, M., Mulrooney, J. B. and Leonard, B. E. (2000b) ‘A review of the role of serotonin receptors in psychiatric disorders ’, *Human Psychopharmacology: Clinical and Experimental* , 15(6), pp. 397–415. doi: 10.1002/1099-1077(200008)15:6<397::AID-HUP212>3.0.CO;2-L.

Navara, K. J. and Nelson, R. J. (2007) ‘The dark side of light at night: Physiological, epidemiological, and ecological consequences’, *Journal of Pineal Research*. doi: 10.1111/j.1600-079X.2007.00473.x.

Naylor, E. *et al.* (2000) ‘The circadian clock mutation alters sleep homeostasis in the mouse.’, *The Journal of neuroscience : the official journal of the Society for Neuroscience*. doi: 20/21/8138 [pii].

Neumeister, A. (2004) ‘Reduced Serotonin Type 1A Receptor Binding in Panic Disorder’, *Journal of Neuroscience*. doi: 10.1523/JNEUROSCI.4921-03.2004.

Nexon, L. *et al.* (2009) ‘Complex regional influence of photoperiod on the nycthemeral functioning of the dorsal and median raphé serotoninergic system in the Syrian hamster’, *European Journal of Neuroscience*. doi: 10.1111/j.1460-9568.2009.06986.x.

Oishi, K. *et al.* (1998) ‘Humoral signals mediate the circadian expression of rat period homologue (rPer2) mRNA in peripheral tissues’, *Neuroscience Letters*. doi: 10.1016/S0304-3940(98)00765-4.

Oishi, K. *et al.* (2005) ‘Genome-wide expression analysis reveals 100 adrenal gland-dependent circadian genes in the mouse liver’, *DNA Research*. doi: 10.1093/dnares/dsi003.

Oquendo, M. A. *et al.* (2007) ‘Brain serotonin transporter binding in depressed patients with bipolar disorder using positron emission tomography.’, *Archives of general psychiatry*, 64(2), pp. 201–8. doi: 10.1001/archpsyc.64.2.201.

Orchinik, M. (1998) ‘Glucocorticoids, stress, and behavior: Shifting the

timeframe', *Hormones and Behavior*. doi: 10.1006/hbeh.1998.1488.

Oster, H. *et al.* (2006) 'The circadian rhythm of glucocorticoids is regulated by a gating mechanism residing in the adrenal cortical clock', *Cell Metabolism*, 4(2), pp. 163–173. doi: 10.1016/j.cmet.2006.07.002.

Ottenhof, K. W. *et al.* (2018) 'TPH2 polymorphisms across the spectrum of psychiatric morbidity: A systematic review and meta-analysis', *Neuroscience and Biobehavioral Reviews*. Elsevier, 92(February), pp. 29–42. doi: 10.1016/j.neubiorev.2018.05.018.

Owens, M. J. and Nemeroff, C. B. (1994) 'Role of serotonin in the pathophysiology of depression: Focus on the serotonin transporter', in *Clinical Chemistry*, pp. 288–295. doi: 10.1371/clinchem.2009.123752.

Owens, M. J. and Nemeroff, C. B. (1998) 'The serotonin transporter and depression', *Depression and Anxiety*. doi: 10.1002/(SICI)1520-6394(1998)8:1+<5::AID-DA2>3.0.CO;2-I.

Palagini, L. *et al.* (2013) 'REM sleep dysregulation in depression: State of the art', *Sleep Medicine Reviews*. doi: 10.1016/j.smrv.2012.11.001.

Paragliola, R. M. *et al.* (2017) 'Treatment with synthetic glucocorticoids and the hypothalamus-pituitary-adrenal axis', *International Journal of Molecular Sciences*, 18(10). doi: 10.3390/ijms18102201.

Pariante, C. M., Nemeroff, C. B. and Miller, A. H. (1995) 'Glucocorticoid receptors in depression.', *Israel journal of medical sciences*. doi: 10.1136/bmj.292.6531.1334-d.

Park, S. Y. *et al.* (2013a) 'Constant light disrupts the circadian rhythm of steroidogenic proteins in the rat adrenal gland', *Molecular and Cellular Endocrinology*. Elsevier Ireland Ltd, 371(1–2), pp. 114–123. doi: 10.1016/j.mce.2012.11.010.

Park, S. Y. *et al.* (2013b) 'Constant light disrupts the circadian rhythm of

steroidogenic proteins in the rat adrenal gland', *Molecular and Cellular Endocrinology*. doi: 10.1016/j.mce.2012.11.010.

Partch, C. L., Green, C. B. and Takahashi, J. S. (2014) 'Molecular architecture of the mammalian circadian clock', *Trends in Cell Biology*. doi: 10.1016/j.tcb.2013.07.002.

Pastinen, T., Ge, B. and Hudson, T. J. (2006) 'Influence of human genome polymorphism on gene expression.', *Human molecular genetics*. doi: 10.1093/hmg/ddl044.

Patel, P. D., Pontrello, C. and Burke, S. (2004) 'Robust and tissue-specific expression of TPH2 versus TPH1 in rat raphe and pineal gland', *Biological Psychiatry*, 55(4), pp. 428–433. doi: 10.1016/j.biopsych.2003.09.002.

Paxinos, G. and Watson, C. (1998) 'The Rat Brain in Stereotaxic Coordinates', *Academic Press*. doi: 10.1007/s13398-014-0173-7.2.

Paxinos, G. and Watson, C. (2005) 'The Rat Brain in Stereotaxic Coordinates', *English*. doi: 10.1017/CBO9781107415324.004.

Peckett, A. J., Wright, D. C. and Riddell, M. C. (2011) 'The effects of glucocorticoids on adipose tissue lipid metabolism', *Metabolism: Clinical and Experimental*. doi: 10.1016/j.metabol.2011.06.012.

Peeters, B. *et al.* (2015) 'The HPA axis response to critical illness: New study results with diagnostic and therapeutic implications', *Molecular and Cellular Endocrinology*. Elsevier Ireland Ltd, 408, pp. 235–240. doi: 10.1016/j.mce.2014.11.012.

Perroud, N. *et al.* (2010) 'Simultaneous analysis of serotonin transporter, tryptophan hydroxylase 1 and 2 gene expression in the ventral prefrontal cortex of suicide victims', *American Journal of Medical Genetics, Part B: Neuropsychiatric Genetics*. doi: 10.1002/ajmg.b.31059.

Peters, E. J. *et al.* (2004) 'Investigation of serotonin-related genes in antidepressant

response', *Molecular Psychiatry*. doi: 10.1038/sj.mp.4001502.

Peyron, C. *et al.* (1997a) 'Forebrain afferents to the rat dorsal raphe nucleus demonstrated by retrograde and anterograde tracing methods', *Neuroscience*. doi: 10.1016/S0306-4522(97)00268-6.

Peyron, C. *et al.* (1997b) 'Forebrain afferents to the rat dorsal raphe nucleus demonstrated by retrograde and anterograde tracing methods', *Neuroscience*. doi: 10.1016/S0306-4522(97)00268-6.

Pickard, G. E. *et al.* (1999) '5-HT1B Receptor-mediated presynaptic inhibition of retinal input to the suprachiasmatic nucleus', *J. Neurosci.*

Pittendrigh, C. S. and Caldarola, P. C. (1973) 'General homeostasis of the frequency of circadian oscillations.', *Proceedings of the National Academy of Sciences of the United States of America*. doi: 10.1073/pnas.70.9.2697.

Plotsky, P. M., Owens, M. J. and Nemeroff, C. B. (1998) 'Psychoneuroendocrinology of depression: Hypothalamic-pituitary-adrenal axis', *Psychiatric Clinics of North America*. doi: 10.1016/S0193-953X(05)70006-X.

Pollak Dorocic, I. *et al.* (2014) 'A Whole-Brain Atlas of Inputs to Serotonergic Neurons of the Dorsal and Median Raphe Nuclei', *Neuron*, 83(3), pp. 663–678. doi: 10.1016/j.neuron.2014.07.002.

Pompili, M. *et al.* (2010) 'The hypothalamic-pituitary-adrenal axis and serotonin abnormalities: A selective overview for the implications of suicide prevention', *European Archives of Psychiatry and Clinical Neuroscience*, 260(8), pp. 583–600. doi: 10.1007/s00406-010-0108-z.

Porrino, L. J. and Goldman-Rakic, P. S. (1982) 'Brainstem innervation of prefrontal and anterior cingulate cortex in the rhesus monkey revealed by retrograde transport of HRP', *Journal of Comparative Neurology*. doi: 10.1002/cne.902050107.

Portas, C. M., Bjorvatn, B. and Ursin, R. (2000) 'Serotonin and the sleep/wake cycle: Special emphasis on microdialysis studies', *Progress in Neurobiology*. doi:

10.1016/S0301-0082(98)00097-5.

Pozzoli, G. *et al.* (1996) 'Corticotropin-releasing factor (CRF) and glucocorticoids modulate the expression of type 1 CRF receptor messenger ribonucleic acid in rat anterior pituitary cell cultures.', *Endocrinology*. doi: 10.1210/endo.137.1.8536643.

Pratt, W. B. *et al.* (2006) 'Chaperoning of glucocorticoid receptors', *Handbook of Experimental Pharmacology*. doi: 10.1007/3-540-29717-0-5.

Prendergast, B. J. and Kay, L. M. (2008) 'Affective and adrenocorticotrophic responses to photoperiod in wistar rats', *Journal of Neuroendocrinology*. doi: 10.1111/j.1365-2826.2007.01633.x.

Price, J. L. and Drevets, W. C. (2012) 'Neural circuits underlying the pathophysiology of mood disorders', *Trends in Cognitive Sciences*, 16(1), pp. 61–71. doi: 10.1016/j.tics.2011.12.011.

Price, M. L. *et al.* (1998) 'Effects of corticotropin-releasing factor on brain serotonergic activity', *Neuropsychopharmacology*. doi: 10.1016/S0893-133X(97)00197-8.

Pringle, A. *et al.* (2013) 'Antidepressant treatment and emotional processing: Can we dissociate the roles of serotonin and noradrenaline?', *Journal of Psychopharmacology*. doi: 10.1177/0269881112474523.

Pullar, I. a *et al.* (2004) 'The role of the 5-HT1D receptor as a presynaptic autoreceptor in the guinea pig.', *European journal of pharmacology*. doi: 10.1016/j.ejphar.2004.04.029.

Radhakutty, A. *et al.* (2016) 'Effect of acute and chronic glucocorticoid therapy on insulin sensitivity and postprandial vascular function', *Clinical Endocrinology*. doi: 10.1111/cen.12966.

Rahman, S. A. (2010) *Attenuation of circadian dysfunction improves sleep, mood and neuropsychometric performance*, *ProQuest Dissertations and Theses*.

Ramamoorthy, S. and Cidlowski, J. A. (2016) ‘Corticosteroids. Mechanisms of Action in Health and Disease’, *Rheumatic Disease Clinics of North America*. doi: 10.1016/j.rdc.2015.08.002.

Ratman, D. *et al.* (2013) ‘How glucocorticoid receptors modulate the activity of other transcription factors: A scope beyond tethering’, *Molecular and Cellular Endocrinology*. doi: 10.1016/j.mce.2012.12.014.

Reichardt, H. M. and Schütz, G. (1998) ‘Glucocorticoid signalling—multiple variations of a common theme’, *Molecular and Cellular Endocrinology*. doi: 10.1016/S0303-7207(98)00208-1.

Reick, M. *et al.* (2001) ‘NPAS2: An analog of clock operative in the mammalian forebrain’, *Science*. doi: 10.1126/science.1060699.

Reiter, R. J. *et al.* (2012) ‘Obesity and metabolic syndrome: Association with chronodisruption, sleep deprivation, and melatonin suppression’, *Annals of Medicine*. doi: 10.3109/07853890.2011.586365.

Reul, J M H M and De Kloet, E. R. (1985) ‘2 Receptor Systems for Corticosterone in Rat-Brain - Microdistribution and Differential Occupation’, *Endocrinology*. doi: 10.1210/endo-117-6-2505.

Reul, J. M.H.M. and De Kloet, E. R. (1985) ‘Two receptor systems for corticosterone in rat brain: Microdistribution and differential occupation’, *Endocrinology*. doi: 10.1210/endo-117-6-2505.

Reynolds, G. P. *et al.* (1995) ‘5-Hydroxytryptamine (5-HT)4 receptors in post mortem human brain tissue: distribution, pharmacology and effects of neurodegenerative diseases.’, *British journal of pharmacology*. doi: 10.1111/j.1476-5381.1995.tb13303.x.

Rhen, T. and Cidlowski, J. a (2005) ‘Antiinflammatory action of glucocorticoids--new mechanisms for old drugs.’, *The New England journal of medicine*. doi: 10.1056/NEJMra050541.

Rivier, C. and Vale, W. (1983) ‘Interaction of corticotropin-releasing factor and arginine vasopressin on adrenocorticotropin secretion in Vivo’, *Endocrinology*. doi: 10.1210/endo-113-3-939.

Rosenberg, D. *et al.* (2002) ‘Role of the PKA-regulated transcription factor CREB in development and tumorigenesis of endocrine tissues’, *Annals of the New York Academy of Sciences*, 968, pp. 65–74. doi: 10.1111/j.1749-6632.2002.tb04327.x.

Ruddick, J. P. *et al.* (2006) ‘Tryptophan metabolism in the central nervous system: medical implications.’, *Expert reviews in molecular medicine*, 8(20), pp. 1–27. doi: 10.1017/S1462399406000068.

Sadkowski, M. *et al.* (2013) ‘The role of the serotonergic system in suicidal behavior’, *Neuropsychiatric Disease and Treatment*, 9, pp. 1699–1716. doi: 10.2147/NDT.S50300.

Sainio, E. L., Lehtola, T. and Roininen, P. (1988) ‘Radioimmunoassay of total and free corticosterone in rat plasma: Measurement of the effect of different doses of corticosterone’, *Steroids*. doi: 10.1016/0039-128X(88)90056-6.

Sakai, K. and Crochet, S. (2001) ‘Differentiation of presumed serotonergic dorsal raphe neurons in relation to behavior and wake-sleep states’, *Neuroscience*. doi: 10.1016/S0306-4522(01)00103-8.

Salgado-Delgado, R. *et al.* (2008) ‘Internal desynchronization in a model of night-work by forced activity in rats’, *Neuroscience*. doi: 10.1016/j.neuroscience.2008.03.066.

Saper, C. B. and Loewy, A. D. (1980) ‘Efferent connections of the parabrachial nucleus in the rat’, *Brain Research*. doi: 10.1016/0006-8993(80)91117-8.

Saper, C. B., Scammell, T. E. and Lu, J. (2005) ‘Hypothalamic regulation of sleep and circadian rhythms’, *Nature*. doi: 10.1038/nature04284.

Saper, C. B., Swanson, L. W. and Cowan, W. M. (1979) ‘An autoradiographic study of the efferent connections of the lateral hypothalamic area in the rat’, *Journal of*

Comparative Neurology. doi: 10.1002/cne.901830402.

Sarabdjitsingh, R. A., Joëls, M. and de Kloet, E. R. (2012) 'Glucocorticoid pulsatility and rapid corticosteroid actions in the central stress response', *Physiology and Behavior*. Elsevier Inc., 106(1), pp. 73–80. doi: 10.1016/j.physbeh.2011.09.017.

Sato, T. K. *et al.* (2004) 'A functional genomics strategy reveals rora as a component of the mammalian circadian clock', *Neuron*. doi: 10.1016/j.neuron.2004.07.018.

Savelieva, K. V. *et al.* (2008) 'Genetic disruption of both tryptophan hydroxylase genes dramatically reduces serotonin and affects behavior in models sensitive to antidepressants', *PLoS ONE*. doi: 10.1371/journal.pone.0003301.

Savitz, J., Lucki, I. and Drevets, W. C. W. (2009) '5-HT1A Receptor Function in Major Depressive Disorder', *Prog Neurobiol*. doi: 10.1016/j.pneurobio.2009.01.009.5-HT.

Schäcke, H., Döcke, W. D. and Asadullah, K. (2002) 'Mechanisms involved in the side effects of glucocorticoids.', *Pharmacology & therapeutics*, 96(1), pp. 23–43. doi: 10.1016/S0163-7258(02)00297-8.

Schernhammer, E. S. *et al.* (2001) 'Rotating night shifts and risk of breast cancer in women participating in the nurses' health study', *Journal of the National Cancer Institute*. doi: 10.1093/jnci/93.20.1563.

Scheving, L. E. and Pauly, J. E. (1966) 'Effect of light on corticosterone levels in plasma of rats.', *The American Journal of Physiology*, 210(5), pp. 1112–1117. Available at: http://www.ncbi.nlm.nih.gov/pubmed/5947258.

Schibler, U. and Sassone-Corsi, P. (2002) 'A web of circadian pacemakers', *Cell*, pp. 919–922. doi: 10.1016/S0092-8674(02)01225-4.

Schmuck, K. *et al.* (1994) 'Cloning and functional characterization of the human 5-HT2B serotonin receptor.', *FEBS letters*.

Scott ', L. V and Dinan, T. G. (1998) 'MINIREVIEW VASOPRESSIN AND THE REGULATION OF HYPOTHALAMIC-PITUITARY-ADRENAL AXIS FUNCTION: IMPLICATIONS FOR THE PATHOPHYSIOLOGY OF DEPRESSION', *Life Sciences HPA and Depression*.

Scott, L. V and Dinan, T. G. (1998) 'Vasopressin and the regulation of hypothalamic-pituitary-adrenal axis function: implications for the pathophysiology of depression.', *Life sciences*.

Selye, H. (1936) 'A syndrome produced by diverse nocuous agents [13]', *Nature*. doi: 10.1038/138032a0.

Serretti, A. *et al.* (2011) 'Influence of TPH2 variants on diagnosis and response to treatment in patients with major depression, bipolar disorder and schizophrenia', *Psychiatry Research*. Elsevier Ltd, 189(1), pp. 26–32. doi: 10.1016/j.psychres.2011.02.001.

Shanks, N. *et al.* (2000) 'Early-life exposure to endotoxin alters hypothalamic-pituitary-adrenal function and predisposition to inflammation.', *Proceedings of the National Academy of Sciences of the United States of America*, 97(10), pp. 5645–50. doi: 10.1073/pnas.090571897.

Sharp, T. and Cowen, P. J. (2011) '5-HT and depression: is the glass half-full?', *Current Opinion in Pharmacology*, 11(1), pp. 45–51. doi: 10.1016/j.coph.2011.02.003.

Shen, H. and Semba, K. (1994) 'A direct retinal projection to the dorsal raphe nucleus in the rat', *Brain Research*. doi: 10.1016/0006-8993(94)91435-4.

Shih, J. C., Wu, J. B. and Chen, K. (2011) 'Transcriptional regulation and multiple functions of MAO genes.', *Journal of Neural Transmission (Vienna, Austria : 1996)*. doi: 10.1007/s00702-010-0562-9.

Shishkina, G. T., Kalinina, T. S. and Dygalo, N. N. (2008) 'Serotonergic changes produced by repeated exposure to forced swimming: Correlation with behavior', in

Annals of the New York Academy of Sciences. doi: 10.1196/annals.1410.074.

Silver, R. and Kriegsfeld, L. J. (2014) 'Circadian rhythms have broad implications for understanding brain and behavior', *European Journal of Neuroscience*, 39(11), pp. 1866–1880. doi: 10.1111/ejn.12593.

Silver, R. and Moore, R. Y. (1998) 'The Suprachiasmatic Nucleus and Circadian Function: An Interoduction', *Chronobiology International*. doi: 10.3109/07420529808998698.

Simerly, R. B. and Swanson, L. W. (1986) 'The organization of neural inputs to the medial preoptic nucleus of the rat', *Journal of Comparative Neurology*. doi: 10.1002/cne.902460304.

Simpson, K. L. *et al.* (1998) 'Projection patterns from the raphe nuclear complex to the ependymal wall of the ventricular system in the rat', *Journal of Comparative Neurology*. doi: 10.1002/(SICI)1096-9861(19980914)399:1<61::AID-CNE5>3.0.CO;2-8.

Singewald, N. and Sharp, T. (2000) 'Neuroanatomical targets of anxiogenic drugs in the hindbrain as revealed by Fos immunocytochemistry', *Neuroscience*. doi: 10.1016/S0306-4522(00)00177-9.

Sirois, F. (2003) 'Steroid psychosis: A review', *General Hospital Psychiatry*. doi: 10.1016/S0163-8343(02)00241-4.

Skórzewska, A. *et al.* (2014) 'The effect of chronic administration of corticosterone on anxiety- and depression-like behavior and the expression of GABA-A receptor alpha-2 subunits in brain structures of low- and high-anxiety rats', *Hormones and Behavior*, 65(1), pp. 6–13. doi: 10.1016/j.yhbeh.2013.10.011.

Solarewicz, J. Z. *et al.* (2015) 'The sleep-wake cycle and motor activity, but not temperature, are disrupted over the light-dark cycle in mice genetically depleted of serotonin', *AJP: Regulatory, Integrative and Comparative Physiology*, 308(1), pp. R10–R17. doi: 10.1152/ajpregu.00400.2014.

Somers, D. E. (1999) ‘The physiology and molecular bases of the plant circadian clock.’, *Plant physiology*, 121(1), pp. 9–20. doi: 10.1104/pp.121.1.9.

Son, G. H. *et al.* (2008) ‘Adrenal peripheral clock controls the autonomous circadian rhythm of glucocorticoid by causing rhythmic steroid production.’, *Proceedings of the National Academy of Sciences of the United States of America*, 105(52), pp. 20970–20975. doi: 10.1073/pnas.0806962106.

Son, G. H., Chung, S. and Kim, K. (2011a) ‘The adrenal peripheral clock: Glucocorticoid and the circadian timing system’, *Frontiers in Neuroendocrinology*. Elsevier Inc., 32(4), pp. 451–465. doi: 10.1016/j.yfrne.2011.07.003.

Son, G. H., Chung, S. and Kim, K. (2011b) ‘The adrenal peripheral clock: Glucocorticoid and the circadian timing system’, *Frontiers in Neuroendocrinology*, pp. 451–465. doi: 10.1016/j.yfrne.2011.07.003.

Spiga, F. *et al.* (2007) ‘Effect of the glucocorticoid receptor antagonist Org 34850 on basal and stress-induced corticosterone secretion’, *Journal of Neuroendocrinology*. doi: 10.1111/j.1365-2826.2007.01605.x.

Spiga, F., Waite, E. J., *et al.* (2011) ‘ACTH-dependent ultradian rhythm of corticosterone secretion’, *Endocrinology*, 152(4), pp. 1448–1457. doi: 10.1210/en.2010-1209.

Spiga, F., Knight, D. M., *et al.* (2011) ‘Differential effect of glucocorticoid receptor antagonists on glucocorticoid receptor nuclear translocation and DNA binding.’, *Journal of psychopharmacology (Oxford, England)*, 25(2), pp. 211–221. doi: 10.1177/0269881109348175.

Spiga, Francesca *et al.* (2017) ‘Dynamic responses of the adrenal steroidogenic regulatory network’, *Proceedings of the National Academy of Sciences*. doi: 10.1073/pnas.1703779114.

Spiga, F. *et al.* (2017) ‘Ultradian Rhythms’, in *Stress: Neuroendocrinology and Neurobiology*. doi: 10.1016/B978-0-12-802175-0.00043-7.

Van Staa, T. P. *et al.* (2001) 'Epidemiology of fractures in England and Wales', *Bone*. doi: 10.1016/S8756-3282(01)00614-7.

Van Staa, T. P., Leufkens, H. G. M. and Cooper, C. (2002) 'The epidemiology of corticosteroid-induced osteoporosis: A meta-analysis', *Osteoporosis International*. doi: 10.1007/s001980200108.

Stahl, S. M. (1998) 'Mechanism of action of serotonin selective reuptake inhibitors', *Journal of Affective Disorders*. doi: 10.1016/S0165-0327(98)00221-3.

Stamper, C. E. *et al.* (2015) 'Role of the dorsomedial hypothalamus in glucocorticoid-mediated feedback inhibition of the hypothalamic–pituitary–adrenal axis', *Stress*, 18(1), pp. 76–87. doi: 10.3109/10253890.2015.1004537.

Stamper, C. E. *et al.* (2017) 'Activation of 5-HT1Areceptors in the rat dorsomedial hypothalamus inhibits stress-induced activation of the hypothalamic–pituitary–adrenal axis', *Stress*. doi: 10.1080/10253890.2017.1301426.

Staner, L. (2010) 'Comorbidity of insomnia and depression', *Sleep Medicine Reviews*. doi: 10.1016/j.smrv.2009.09.003.

Starick, S. R. *et al.* (2015) 'ChIP-exo signal associated with DNA-binding motifs provides insight into the genomic binding of the glucocorticoid receptor and cooperating transcription factors', *Genome Research*. doi: 10.1101/gr.185157.114.

Staub, D. R., Spiga, F. and Lowry, C. A. (2005) 'Urocortin 2 increases c-Fos expression in topographically organized subpopulations of serotonergic neurons in the rat dorsal raphe nucleus', *Brain Research*. doi: 10.1016/j.brainres.2005.02.080.

Stavreva, D. a *et al.* (2009) 'Ultradian hormone stimulation induces glucocorticoid receptor-mediated pulses of gene transcription.', *Nat Cell Biol*, 11(9), pp. 1093–1102. doi: 10.1038/ncb1922.

Steinbusch, H. W. M. *et al.* (1980) 'Serotonergic and non-serotonergic projections from the nucleus raphe dorsalis to the caudate-putamen complex in the rat, studied by a combined immunofluorescence and fluorescent retrograde axonal labeling

technique', *Neuroscience Letters*. doi: 10.1016/0304-3940(80)90184-6.

Steinbusch, H. W. M. (1981) 'Distribution of serotonin-immunoreactivity in the central nervous system of the rat-Cell bodies and terminals', *Neuroscience*. doi: 10.1016/0306-4522(81)90146-9.

Stephan, F. K. and Zucker, I. (1972) 'Circadian rhythms in drinking behavior and locomotor activity of rats are eliminated by hypothalamic lesions', *Proc Natl Acad Sci U S A*.

Stetler, C., Dickerson, S. S. and Miller, G. E. (2004) 'Uncoupling of social zeitgebers and diurnal cortisol secretion in clinical depression', *Psychoneuroendocrinology*. doi: 10.1016/j.psyneuen.2004.03.003.

Stezhka, V. V. and Lovick, T. A. (1997) 'Projections from dorsal raphe nucleus to the periaqueductal grey matter: Studies in slices of rat midbrain maintained in vitro', *Neuroscience Letters*. doi: 10.1016/S0304-3940(97)00464-3.

Stoll, J., Kozak, C. A. and Goldman, D. (1990) 'Characterization and chromosomal mapping of a cDNA encoding tryptophan hydroxylase from a mouse mastocytoma cell line', *Genomics*. doi: 10.1016/0888-7543(90)90522-V.

Stratmann, M. and Schibler, U. (2006) 'Properties, entrainment, and physiological functions of mammalian peripheral oscillators', *Journal of Biological Rhythms*. doi: 10.1177/0748730406293889.

Straub, R. H. and Cutolo, M. (2007) 'Circadian rhythms in rheumatoid arthritis: Implications for pathophysiology and therapeutic management', *Arthritis and Rheumatism*. doi: 10.1002/art.22368.

Strömstedt, P. E. *et al.* (1991) 'The glucocorticoid receptor binds to a sequence overlapping the TATA box of the human osteocalcin promoter: a potential mechanism for negative regulation.', *Molecular and Cellular Biology*. doi: 10.1128/MCB.11.6.3379.

Strüber, N., Strüber, D. and Roth, G. (2014) 'Impact of early adversity on

glucocorticoid regulation and later mental disorders', *Neuroscience and Biobehavioral Reviews*. Elsevier Ltd, 38(1), pp. 17–37. doi: 10.1016/j.neubiorev.2013.10.015.

Stubbs, F. E. *et al.* (2018) 'SKOV3 cells containing a truncated ARID1a protein have a restricted genome-wide response to glucocorticoids', *Molecular and Cellular Endocrinology*. doi: 10.1016/j.mce.2017.09.018.

Swaab, D. F., Bao, A. M. and Lucassen, P. J. (2005) 'The stress system in the human brain in depression and neurodegeneration', *Ageing Research Reviews*, 4(2), pp. 141–194. doi: 10.1016/j.arr.2005.03.003.

Swaab, D. F., Fliers, E. and Partiman, T. S. (1985) 'The suprachiasmatic nucleus of the human brain in relation to sex, age and senile dementia', *Brain Research*. doi: 10.1016/0006-8993(85)91350-2.

SWEENEY, B. M. (1987) *Rhythmic Phenomena in Plants*, *Rhythmic Phenomena in Plants*. doi: 10.1016/B978-0-12-679052-8.50015-3.

Szabó, S. (2014) 'HANS SELYE 70 YEARS LATER: STEROIDS, STRESS ULCERS & H. PYLORI.', *Ideggyógyászati szemle*, 67(3–4), pp. 91–4. Available at: http://www.ncbi.nlm.nih.gov/pubmed/26118247.

Taber, E., Brodal, A. and Walberg, F. (1960) 'The raphe nuclei of the brain stem in the cat. I. Normal topography and cytoarchitecture and general discussion', *Journal of Comparative Neurology*. doi: 10.1002/cne.901140205.

Tannenbaum, G. S. and Martin, J. B. (1976) 'Evidence for an endogenous ultradian rhythm governing growth hormone secretion in the rat', *Endocrinology*. doi: 10.1210/endo-98-3-562.

Tapia-Osorio, A. *et al.* (2013) 'Disruption of circadian rhythms due to chronic constant light leads to depressive and anxiety-like behaviors in the rat', *Behavioural Brain Research*. Elsevier B.V., 252, pp. 1–9. doi: 10.1016/j.bbr.2013.05.028.

Tasker, J. G. and Herman, J. P. (2011) 'Mechanisms of rapid glucocorticoid

feedback inhibition of the hypothalamic-pituitary-adrenal axis', *Stress*. doi: 10.3109/10253890.2011.586446.

Teclemariam-mesbah, R. *et al.* (1999) 'Anatomical Demonstration of the Suprachiasmatic Nucleus–Pineal Pathway', *J. Comp. Neurol*. doi: 10.1002/(SICI)1096-9861(19990405)406:2<171::AID-CNE3>3.0.CO;2-U [pii].

Thomas, D. R. (2006) '5-ht5A receptors as a therapeutic target', *Pharmacology and Therapeutics*. doi: 10.1016/j.pharmthera.2005.12.006.

Thomas, D. R. and Hagan, J. J. (2004) '5-HT7 receptors.', *Current drug targets. CNS and neurological disorders*. doi: 10.2174/1568007043482633.

Thompson, A. J. and Lummis, S. C. R. (2006) '5-HT3 receptors.', *Current pharmaceutical design*. doi: 10.2174/138161206778522029.

Tidemand, K. D. *et al.* (2017) 'Isoform-Specific Substrate Inhibition Mechanism of Human Tryptophan Hydroxylase', *Biochemistry*, 56(46), pp. 6155–6164. doi: 10.1021/acs.biochem.7b00763.

Tischler, R. C. and Morin, L. P. (2003) 'Reciprocal serotonergic connections between the hamster median and dorsal raphe nuclei', *Brain Research*. doi: 10.1016/S0006-8993(03)02994-9.

Truss, M. and Beato, M. (1993) 'Steroid hormone receptors: interaction with deoxyribonucleic acid and transcription factors.', *Endocrine reviews*. doi: 10.1210/edrv-14-4-459.

Tsai, S. J. *et al.* (2009) 'Tryptophan hydroxylase 2 gene is associated with major depression and antidepressant treatment response', *Progress in Neuro-Psychopharmacology and Biological Psychiatry*. Elsevier Inc., 33(4), pp. 637–641. doi: 10.1016/j.pnpbp.2009.02.020.

Tsang, A. H., Barclay, J. L. and Oster, H. (2013) 'Interactions between endocrine and circadian systems', *Journal of Molecular Endocrinology*. doi: 10.1530/JME-13-0118.

Tsigos, C. and Chrousos, G. P. (2002) 'Hypothalamic – pituitary – adrenal axis , neuroendocrine factors and stress', 53, pp. 865–871. doi: 10.1016/S0022-3999(02)00429-4.

Tsuno, N., Besset, A. and Ritchie, K. (2005) 'Sleep and depression', *Journal of Clinical Psychiatry*. doi: 10.4088/JCP.v66n1008.

Turek, F. W. *et al.* (2005) 'Obesity and Metabolic Syndrome in Circadian Clock Mutant Mice', *Science*. doi: 10.1126/science.1108750.

Uhl, A. *et al.* (2002) 'Pharmacokinetics and pharmacodynamics of methylprednisolone after one bolus dose compared with two dose fractions', *Journal of Clinical Pharmacy and Therapeutics*, 27(4), pp. 281–287. doi: 10.1046/j.1365-2710.2002.00422.x.

Ulrich-Lai, Y. M. and Herman, J. P. (2009) 'Neural regulation of endocrine and autonomic stress responses', *Nature Reviews Neuroscience*. doi: 10.1038/nrn2647.

Ursin, R. (2002) 'Serotonin and sleep.', *Sleep medicine reviews*, 6(1), pp. 55–69. doi: 10.1053/smrv.2001.0174.

Vandewalle, J. *et al.* (2018) 'Therapeutic Mechanisms of Glucocorticoids', *Trends in Endocrinology and Metabolism*. Elsevier Ltd, 29(1), pp. 42–54. doi: 10.1016/j.tem.2017.10.010.

Van Der Velden, V. H. J. (1998) 'Glucocorticoids: Mechanisms of action and anti-inflammatory potential in asthma', *Mediators of Inflammation*. doi: 10.1080/09629359890910.

Veldhuis, J. D. *et al.* (1989) 'Amplitude modulation of a burstlike mode of cortisol secretion subserves the circadian glucocorticoid rhythm.', *The American journal of physiology*. doi: 10.1152/ajpendo.1989.257.1.E6.

Verhagen, L. A. W. *et al.* (2004) 'Temporal organization of the 24-h corticosterone rhythm in the diurnal murid rodent Arvicanthis ansorgei Thomas 1910', *Brain Research*. doi: 10.1016/j.brainres.2003.10.003.

Vertes, R. P. *et al.* (1994) 'Pharmacological suppression of the median raphe\rnucleus with serotonin1A agonists, 8-OH-DPAT and\rbuspirone, produces hippocampal theta rhythm in the\rrat.', *Neuroscience*.

Vertes, R. P., Fortin, W. J. and Crane, A. M. (1999a) 'Projections of the median raphe nucleus in the rat', *The Journal of Comparative Neurology*, 407(4), pp. 555–582. doi: 10.1002/(SICI)1096-9861(19990517)407:4<555::AID-CNE7>3.3.CO;2-5.

Vertes, R. P., Fortin, W. J. and Crane, A. M. (1999b) 'Projections of the median raphe nucleus in the rat', *Journal of Comparative Neurology*. doi: 10.1002/(SICI)1096-9861(19990517)407:4<555::AID-CNE7>3.0.CO;2-E.

Vertes, R. P. and Linley, S. B. (2008) 'Efferent and afferent connections of the dorsal and median raphe nuclei in the rat', in *Serotonin and Sleep: Molecular, Functional and Clinical Aspects*. doi: 10.1007/978-3-7643-8561-3_3.

Villar, M. J. *et al.* (1988) 'Dorsal raphe serotoninergic branching neurons projecting both to the lateral geniculate body and superior colliculus: A combined retrograde tracing–immunohistochemical study in the rat', *Journal of Comparative Neurology*. doi: 10.1002/cne.902770109.

Villar, M. J., Vitale, M. L. and Parisi, M. N. (1987) 'Dorsal raphe serotonergic projection to the retina. A combined peroxidase tracing-neurochemical/high-performance liquid chromatography study in the rat', *Neuroscience*. doi: 10.1016/0306-4522(87)90364-2.

Vincent, M. Y. *et al.* (2013) 'Sensitivity of depression-like behavior to glucocorticoids and antidepressants is independent of forebrain glucocorticoid receptors', *Brain Research*. doi: 10.1016/j.brainres.2013.05.031.

Voigt, J. P. and Fink, H. (2015) 'Serotonin controlling feeding and satiety', *Behavioural Brain Research*. doi: 10.1016/j.bbr.2014.08.065.

Waddell, D. S. *et al.* (2008) 'The glucocorticoid receptor and FOXO1

synergistically activate the skeletal muscle atrophy-associated MuRF1 gene', *AJP: Endocrinology and Metabolism*. doi: 10.1152/ajpendo.00646.2007.

Waider, J. *et al.* (2011) 'Tryptophan hydroxylase-2 (TPH2) in disorders of cognitive control and emotion regulation: A perspective', *Psychoneuroendocrinology*. Elsevier Ltd, 36(3), pp. 393–405. doi: 10.1016/j.psyneuen.2010.12.012.

Waite, E. J. *et al.* (2012) 'Ultradian corticosterone secretion is maintained in the absence of circadian cues', *European Journal of Neuroscience*, 36(8), pp. 3142–3150. doi: 10.1111/j.1460-9568.2012.08213.x.

Walker, J. J. *et al.* (2012a) 'The origin of glucocorticoid hormone oscillations', *PLoS Biology*, 10(6). doi: 10.1371/journal.pbio.1001341.

Walker, J. J. *et al.* (2012b) 'The origin of glucocorticoid hormone oscillations', *PLoS Biology*. doi: 10.1371/journal.pbio.1001341.

Walker, Jamie J, Terry, J. R. and Lightman, S. L. (2010) 'Origin of ultradian pulsatility in the hypothalamic-pituitary-adrenal axis.', *Proceedings. Biological sciences / The Royal Society*, 277(1688), pp. 1627–33. doi: 10.1098/rspb.2009.2148.

Walker, Jamie J., Terry, J. R. and Lightman, S. L. (2010) 'Origin of ultradian pulsatility in the hypothalamic-pituitary-adrenal axis', in *Proceedings of the Royal Society B: Biological Sciences*. doi: 10.1098/rspb.2009.2148.

Walker, L. C. and Lawrence, A. J. (2017) 'The Role of Orexins/Hypocretins in alcohol use and abuse', in *Current Topics in Behavioral Neurosciences*. doi: 10.1007/7854_2016_55.

Walther, D. J. *et al.* (2003) 'Synthesis of serotonin by a second tryptophan hydroxylase isoform.', *Science (New York, N.Y.)*, 299(5603), p. 76. doi: 10.1126/science.1078197.

Walther, D. J. and Bader, M. (2003) 'A unique central tryptophan hydroxylase

isoform', *Biochemical Pharmacology*, 66(9), pp. 1673–1680. doi: 10.1016/S0006-2952(03)00556-2.

Wang, X. *et al.* (2005) 'Single nucleotide polymorphism in transcriptional regulatory regions and expression of environmentally responsive genes', in *Toxicology and Applied Pharmacology*. doi: 10.1016/j.taap.2004.09.024.

Waselus, M., Valentino, R. J. and Van Bockstaele, E. J. (2011) 'Collateralized dorsal raphe nucleus projections: A mechanism for the integration of diverse functions during stress', *Journal of Chemical Neuroanatomy*. Elsevier B.V., 41(4), pp. 266–280. doi: 10.1016/j.jchemneu.2011.05.011.

Waterhouse, B. D. *et al.* (1986) 'Topographical distribution of dorsal and median raphe neurons projecting to motor, sensorimotor, and visual cortical areas in the rat', *Journal of Comparative Neurology*. doi: 10.1002/cne.902490403.

Waterhouse, B. D. *et al.* (1993) 'Topographic organization of rat locus coeruleus and dorsal raphe nuclei: Distribution of cells projecting to visual system structures', *Journal of Comparative Neurology*. doi: 10.1002/cne.903360304.

Watson, L. C. *et al.* (2013) 'The glucocorticoid receptor dimer interface allosterically transmits sequence-specific DNA signals', *Nature Structural and Molecular Biology*. doi: 10.1038/nsmb.2595.

Watts, A. G. and Swanson, L. W. (1987) 'Efferent projections of the suprachiasmatic nucleus: II. Studies using retrograde transport of fluorescent dyes and simultaneous peptide immunohistochemistry in the rat', *Journal of Comparative Neurology*. doi: 10.1002/cne.902580205.

Watts, A. G., Swanson, L. W. and Sanchez-Watts, G. (1987) 'Efferent projections of the suprachiasmatic nucleus: I. Studies using anterograde transport ofPhaseolus vulgaris leucoagglutinin in the rat', *The Journal of Comparative Neurology*, 258(2), pp. 204–229. doi: 10.1002/cne.902580204.

Watts, A. G., Tanimura, S. and Sanchez-Watts, G. (2004) 'Corticotropin-Releasing

Hormone and Arginine Vasopressin Gene Transcription in the Hypothalamic Paraventricular Nucleus of Unstressed Rats: Daily Rhythms and Their Interactions with Corticosterone', *Endocrinology*. doi: 10.1210/en.2003-0394.

Weitzman, E. D. *et al.* (1971) 'Twenty-four hour pattern of the episodic secretion of cortisol in normal subjects', *Journal of Clinical Endocrinology and Metabolism*. doi: 10.1210/jcem-33-1-14.

Welsh, D. K., Takahashi, J. S. and Kay, S. A. (2010) 'Suprachiasmatic nucleus: cell autonomy and network properties.', *Annual review of physiology*, 72(4), pp. 551–77. doi: 10.1146/annurev-physiol-021909-135919.

Whitnall, M. H., Mezey, E. and Gainer, H. (1985) 'Co-localization of corticotropin-releasing factor and vasopressin in median eminence neurosecretory vesicles', *Nature*. doi: 10.1038/317248a0.

Wikström, A. C. (2003) 'Glucocorticoid action and novel mechanisms of steroid resistance: Role of glucocorticoid receptor-interacting proteins for glucocorticoid responsiveness', *Journal of Endocrinology*. doi: 10.1677/joe.0.1780331.

Wilsbacher, L. D. and Takahashi, J. S. (1998) 'Circadian rhythms: Molecular basis of the clock', *Current Opinion in Genetics and Development*. doi: 10.1016/S0959-437X(98)80017-8.

Windle, R. J. *et al.* (1998) 'The pulsatile characteristics of hypothalamo-pituitary-adrenal activity in female Lewis and Fischer 344 rats and its relationship to differential stress responses', *Endocrinology*, 139(10), pp. 4044–4052. doi: 10.1210/endo.139.10.6238.

Windle, R. J. *et al.* (2001) 'Increased corticosterone pulse frequency during adjuvant-induced arthritis and its relationship to alterations in stress responsiveness', *Journal of Neuroendocrinology*, 13(10), pp. 905–911. doi: 10.1046/j.1365-2826.2001.00715.x.

Winter, B. (2015) 'Linear models and linear mixed effects models in R: Tutorial 1',

Archives of environmental contamination and toxicology.

Wirtshafter, D. and Krebs, J. C. (1990) 'Control of food intake by kainate/quisqualate receptors in the median raphe nucleus', *Psychopharmacology*. doi: 10.1007/BF02253731.

World Health Organisation (2013) 'Guidelines for the Management of Conditions Specifically Related to Stress', *Assessment and Management of Conditions Specifically Related to Stress: mhGAP Intervention Guide Module (version 1.0)*.

World Health Organization (2017) 'Depression and other common mental disorders: global health estimates', *World Health Organization*. doi: CC BY-NC-SA 3.0 IGO.

Wurtman, R. J. and Axelrod, J. (1965) 'Adrenaline synthesis: Control by the pituitary gland and adrenal glucocorticoids', *Science*. doi: 10.1126/science.150.3702.1464.

Yamakawa, G. R. and Antle, M. C. (2010) 'Phenotype and function of raphe projections to the suprachiasmatic nucleus', *European Journal of Neuroscience*. doi: 10.1111/j.1460-9568.2010.07228.x.

Yosipovitch, G. *et al.* (2004) 'Circadian and ultradian (12 h) variations of skin blood flow and barrier function in non-irritated and irritated skin - Effect of topical corticosteroids', *Journal of Investigative Dermatology*. doi: 10.1111/j.0022-202X.2004.22313.x.

You, J. S. *et al.* (2005) 'Serotonin transporter and tryptophan hydroxylase gene polymorphisms in Chinese patients with generalized anxiety disorder', *Psychiatric genetics*, 15(1), pp. 7–11. doi: 10.1097/00041444-200503000-00002.

Young, E. A., Abelson, J. and Lightman, S. L. (2004) 'Cortisol pulsatility and its role in stress regulation and health', *Frontiers in Neuroendocrinology*, pp. 69–76. doi: 10.1016/j.yfrne.2004.07.001.

Young, E. A., Carlson, N. E. and Brown, M. B. (2001) 'Twenty-four-hour ACTH

and cortisol pulsatility in depressed women', *Neuropsychopharmacology*. doi: 10.1016/S0893-133X(00)00236-0.

Yu, P. L. *et al.* (1999) 'Immunohistochemical localization of tryptophan hydroxylase in the human and rat gastrointestinal tracts', *Journal of Comparative Neurology*. doi: 10.1002/(SICI)1096-9861(19990906)411:4<654::AID-CNE9>3.0.CO;2-H.

Zangrossi, H. and Graeff, F. G. (2014) 'Serotonin in anxiety and panic: Contributions of the elevated T-maze', *Neuroscience and Biobehavioral Reviews*. doi: 10.1016/j.neubiorev.2014.03.007.

Zhang, E. E. and Kay, S. A. (2010) 'Clocks not winding down: Unravelling circadian networks', *Nature Reviews Molecular Cell Biology*. doi: 10.1038/nrm2995.

Zhang, X. *et al.* (2004) 'Tryptophan hydroxylase-2 controls brain serotonin synthesis.', *Science (New York, N.Y.)*, 305(July), p. 217. doi: 10.1126/science.1097540.

Zhu, L. and Zee, P. C. (2012) 'Circadian Rhythm Sleep Disorders', *Neurologic Clinics*, pp. 1167–1191. doi: 10.1016/j.ncl.2012.08.011.

Zill, Peter *et al.* (2004) 'Regional mRNA expression of a second tryptophan hydroxylase isoform in postmortem tissue samples of two human brains', *European Neuropsychopharmacology*, 14(4), pp. 282–284. doi: 10.1016/j.euroneuro.2003.10.002.

Zill, P *et al.* (2004) 'SNP and haplotype analysis of a novel tryptophan hydroxylase isoform (TPH2) gene provide evidence for association with major depression.', *Molecular psychiatry*, 9, pp. 1030–1036. doi: 10.1038/sj.mp.4001525.

Zill, P. *et al.* (2007) 'Analysis of tryptophan hydroxylase I and II mRNA expression in the human brain: A post-mortem study', *Journal of Psychiatric Research*, 41(1–2), pp. 168–173. doi: 10.1016/j.jpsychires.2005.05.004.

Zylka, M. J. *et al.* (1998) ‘Three period homologs in mammals: Differential light responses in the suprachiasmatic circadian clock and oscillating transcripts outside of brain’, *Neuron*. doi: 10.1016/S0896-6273(00)80492-4.

Appendix A: Linear Mixed Models

Statistical analysis with Linear Mixed Models. Taken from Duricki's protocol (Duricki, Soleman and Moon, 2016a).

Linear mixed models, also called "multilevel models" or "hierarchical models", are a type of regression model that take into account both (1) variation that *is* explained by the independent variables of interest (fixed effects), and (2) variation that is *not* explained by the independent variables of interest (random effects). Since the model includes a mixture of fixed and random effects, it's called a mixed model. These random effects essentially give structure to the error term (Winter, 2015).

For analysis of all in situ hybridization histochemistry data I used a linear mixed effect model (LMM), modelling of *tph2*mRNA expression (CMGVxMA) by experiment (CTRL, MPL or LL) or treatment (CTRL vs MPL or CTRL vs LL) in five different time point (3am, 9 am, 3 pm, 6 pm and 9 pm) within 5 different subregions of the DR (DRC, DRI, DRD, DRV, DRVL/VLPAG) and the MnR nuclei at each rostro-caudal bregma level (mm from bregma: −7.328, −7.412, −7.496, −7.580, −7.664, −7.748, −7.832, −7.916, −8.000, −8.084, −8.168, −8.252, −8.336, −8.420, −8.588, −8.672).

Additionally, this models were run with 16 covariate structures, including ARMA (1,1), Compound Symmetry, Correlation Compound Symmetry, Diagonal, First-order Analytic, First-order Ante-dependence, First-order Autoregressive, First-order Factor Analytic, Heterogeneous Compound Symmetry, Heterogeneous First-order Autoregressive, Heterogeneous Toeplitz, Huynh-Feldt, Identity, Toeplitz, Unstructured, and Unstructured Correlations.

The following steps were done for all LMM analyses.

1) Diagnostics

These models included a series of diagnostics to confirm that the assumptions made for each fitted model were not violated. These diagnostics included; descriptives,

normality test, error variances and a file of analysis of predicted and residual values of the fitted model. The SPSS syntax for the descriptives was as follows;

> EXAMINE VARIABLES (*tph2* or AREA)* BY Timepoint Treatment ROSTROCAUDAL, /PLOT BOXPLOT HISTOGRAM NPPLOT, /COMPARE GROUPS, /STATISTICS DESCRIPTIVES, /CINTERVAL 95, /MISSING LISTWISE, /NOTOTAL.

All analyses (overall or secondaries) would include these files. In this case, if we were testing the overall model, then the thp2 variable would appear, in secondary models **AREA*** could mean DRC, DRI, DRD, DRV, DRVL/VLPAG or MnR.

The SPSS syntax for the normality test, the error variances and the predicted and residual values analysis for each model was as follows;

> GGRAPH, /GRAPHDATASET NAME="graphdataset" VARIABLES= **(one COVARIATE TYPE from the sixteen possible)*** _RESID MISSING=LISTWISE REPORTMISSING=NO, /GRAPHSPEC SOURCE=INLINE. BEGIN GPL, SOURCE: s=userSource(id("graphdataset")), DATA: **(one COVARIATE TYPE from the sixteen possible)*** _RESID=col(source(s), name("**(one COVARIATE TYPE from the sixteen possible)*** _RESID")), GUIDE: axis(dim(1), label("Residuals")), GUIDE: axis(dim(2), label("Frequency")), ELEMENT: interval(position(summary.count(bin.rect((**one COVARIATE TYPE from the sixteen possible)*** _RESID))), shape.interior(shape.square)), ELEMENT: line(position(density.normal(**(one COVARIATE TYPE from the sixteen possible)*** _RESID)), color("Normal")), END GPL.
>
> * Chart Builder. GGRAPH, /GRAPHDATASET NAME="graphdataset" VARIABLES=**(one COVARIATE TYPE from the sixteen possible)*** _RESID **(AREA)** MISSING=LISTWISE REPORTMISSING=NO
>
> /GRAPHSPEC SOURCE=INLINE, BEGIN GPL, SOURCE: s=userSource(id("graphdataset")), DATA: **(one COVARIATE TYPE from the sixteen possible)*** _RESID=col(source(s), name("**(one COVARIATE TYPE from the sixteen possible)*** _RESID")), DATA: **(AREA)** =col(source(s), name("**(AREA)** ")), GUIDE: axis(dim(1), label("Predicted Values")), GUIDE: axis(dim(2), label("**(AREA)** ")), ELEMENT: point(position ((**one COVARIATE TYPE from the sixteen possible)*** _RESID***(AREA)**))), END GPL.
>
> GGRAPH, /GRAPHDATASET NAME="graphdataset" VARIABLES=**(one COVARIATE TYPE from the sixteen possible)*** _PRED **(one COVARIATE TYPE from the sixteen possible)*** _RESID, MISSING=LISTWISE REPORTMISSING=NO, /GRAPHSPEC SOURCE=INLINE. BEGIN GPL, SOURCE: s=userSource(id("graphdataset")), DATA: **(one COVARIATE TYPE from the sixteen possible)*,** _PRED=col(source(s), name("**(one COVARIATE**

TYPE from the sixteen possible)* _PRED")), DATA: **(one COVARIATE TYPE from the sixteen possible)*** _RESID=col(source(s), name("**(one COVARIATE TYPE from the sixteen possible)*** _RESID")), GUIDE: axis(dim(1), label("Predicted Values")), GUIDE: axis(dim(2), label("Residuals")), ELEMENT: point(position(**(one COVARIATE TYPE from the sixteen possible)*** _PRED***(one COVARIATE TYPE from the sixteen possible)*** _RESID)) END GPL.

NPAR TEST, /K-S(NORMAL)= **(one COVARIATE TYPE from the sixteen possible)*** _RESID, /MISSING ANALYSIS

PPLOT, /VARIABLES=**(one COVARIATE TYPE from the sixteen possible)*** _RESID, /NOLOG, /NOSTANDARDIZE, /TYPE=P-P, /FRACTION=BLOM, /TIES=MEAN, /DIST=NORMAL.

PPLOT, /VARIABLES=**(one COVARIATE TYPE from the sixteen possible)*** _RESID, /NOLOG, /NOSTANDARDIZE, /TYPE=Q-Q, /FRACTION=BLOM, /TIES=MEAN, /DIST=NORMAL.

All analyses (overall or secondaries) included these files. Therefore, **AREA*** could mean DRC, DRI, DRD, DRV, DRVL/VLPAG or MnR and **(one COVARIATE TYPE from the sixteen possible) *** implicated the fitted model for the particular analysis.

The following tables and plots are an example of the SPSS output for the descriptive files for MnR in the Ctrls data base;

Case Processing Summary

		Cases					
		Valid		Missing		Total	
	TimePoint	N	Percent	N	Percent	N	Percent
MNR	3am	103	75.7%	33	24.3%	136	100.0%
	9am	98	72.1%	38	27.9%	136	100.0%
	3pm	92	67.6%	44	32.4%	136	100.0%
	6pm	104	76.5%	32	23.5%	136	100.0%
	9pm	101	74.3%	35	25.7%	136	100.0%

Tests of Normality

		Kolmogorov-Smirnov[a]			Shapiro-Wilk		
	TimePoint	Statistic	df	Sig.	Statistic	df	Sig.
MNR	3am	.122	103	.001	.905	103	.000
	9am	.132	98	.000	.900	98	.000
	3pm	.170	92	.000	.905	92	.000
	6pm	.108	104	.004	.944	104	.000
	9pm	.123	101	.001	.911	101	.000

a. Lilliefors Significance Correction

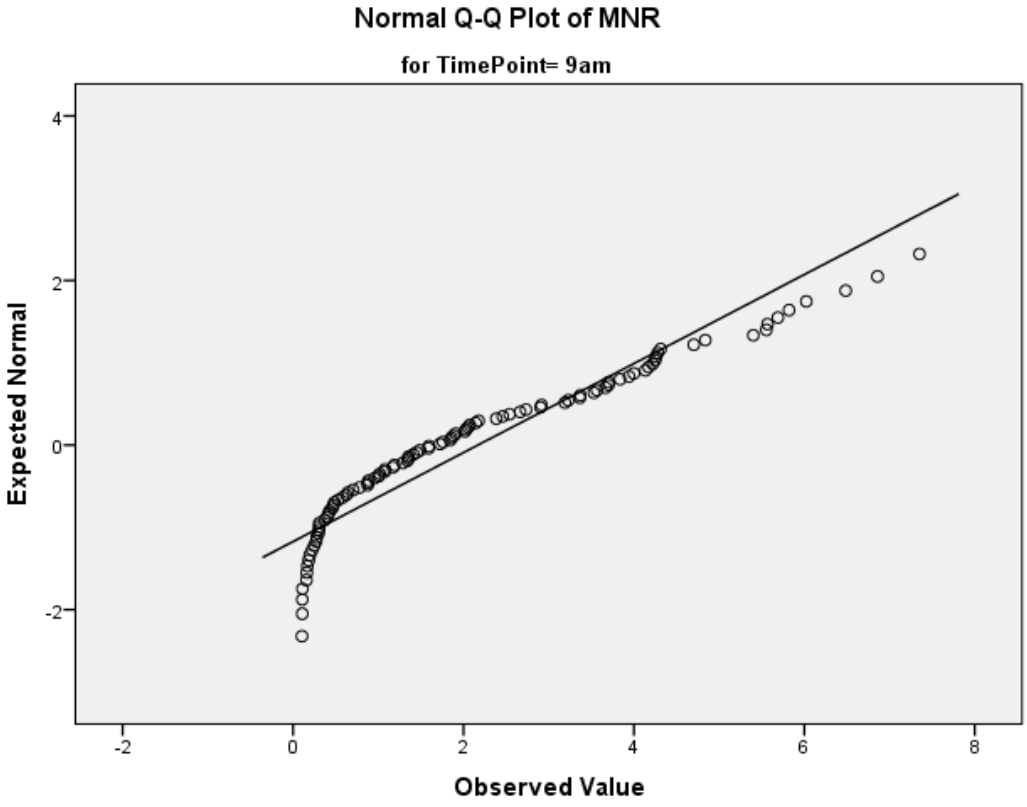

Case Processing Summary

		Cases					
		Valid		Missing		Total	
	ROSTROCAUDAL	N	Percent	N	Percent	N	Percent
MNR	3	36	90.0%	4	10.0%	40	100.0%
	4	38	95.0%	2	5.0%	40	100.0%
	5	38	95.0%	2	5.0%	40	100.0%
	6	40	100.0%	0	0.0%	40	100.0%
	7	39	97.5%	1	2.5%	40	100.0%
	8	39	97.5%	1	2.5%	40	100.0%
	9	29	72.5%	11	27.5%	40	100.0%
	10	38	95.0%	2	5.0%	40	100.0%
	11	39	97.5%	1	2.5%	40	100.0%
	12	40	100.0%	0	0.0%	40	100.0%
	13	40	100.0%	0	0.0%	40	100.0%
	14	34	85.0%	6	15.0%	40	100.0%
	15	26	65.0%	14	35.0%	40	100.0%
	16	14	35.0%	26	65.0%	40	100.0%
	17	8	20.0%	32	80.0%	40	100.0%

Tests of Normality[a]

		Kolmogorov-Smirnov[b]			Shapiro-Wilk		
	ROSTROCAUDAL	Statistic	df	Sig.	Statistic	df	Sig.
MNR	3	.187	36	.003	.846	36	.000
	4	.210	38	.000	.779	38	.000
	5	.165	38	.011	.806	38	.000
	6	.140	40	.048	.915	40	.006
	7	.127	39	.113	.947	39	.063
	8	.097	39	.200*	.968	39	.318
	9	.108	29	.200*	.978	29	.793
	10	.124	38	.146	.966	38	.299
	11	.066	39	.200*	.993	39	.998
	12	.109	40	.200*	.965	40	.256
	13	.093	40	.200*	.981	40	.738
	14	.113	34	.200*	.917	34	.014
	15	.154	26	.117	.886	26	.008
	16	.214	14	.081	.945	14	.482
	17	.213	8	.200*	.919	8	.419

*. This is a lower bound of the true significance.

a. There are no valid cases for MNR when ROSTROCAUDAL = 1.000. Statistics cannot be computed for this level.

b. Lilliefors Significance Correction

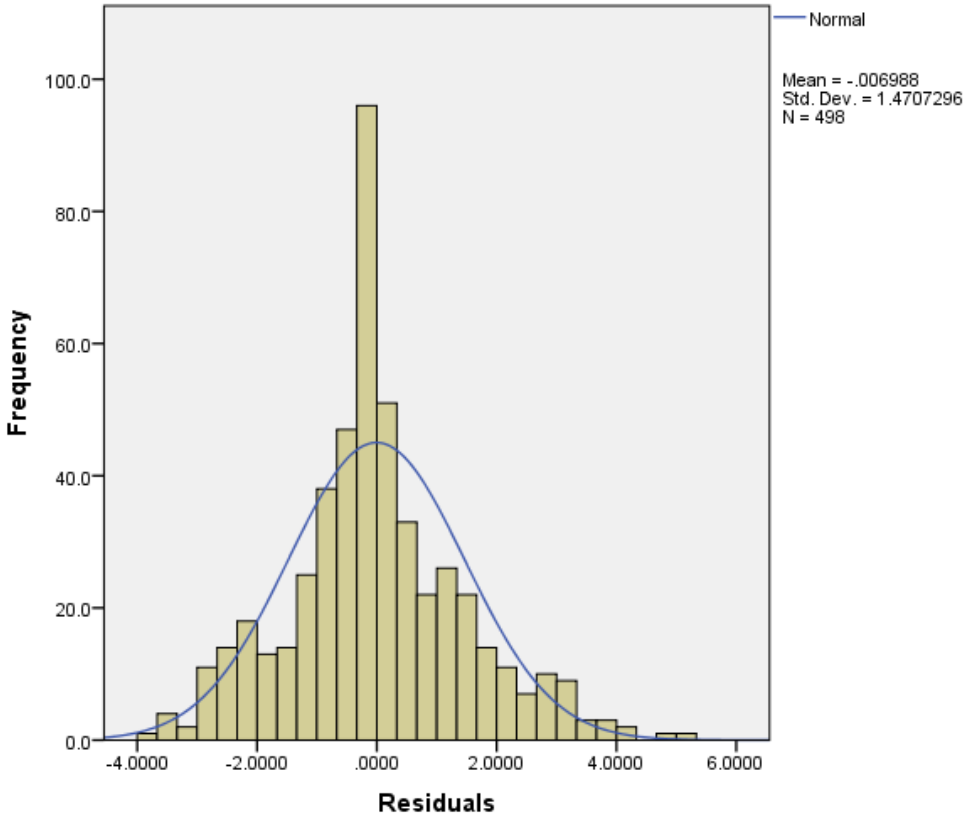
Normal
Mean = -.006988
Std. Dev. = 1.4707296
N = 498
Frequency
100.0
80.0
60.0
40.0
20.0
0.0
-4.0000
-2.0000
.0000
2.0000
4.0000
6.0000
Residuals

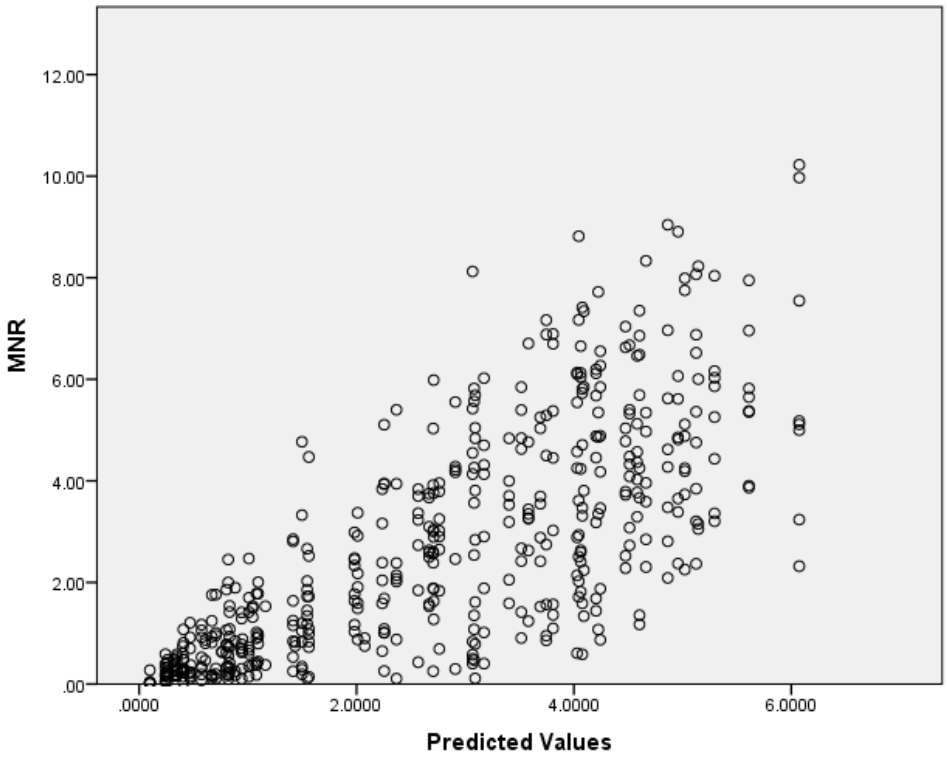
MNR
12.00
10.00
8.00
6.00
4.00
2.00
.00
.0000
2.0000
4.0000
6.0000
Predicted Values

One-Sample Kolmogorov-Smirnov Test

		Residuals
N		498
Normal Parameters[a,b]	Mean	-.006988
	Std. Deviation	1.4707296
Most Extreme Differences	Absolute	.085
	Positive	.085
	Negative	-.056
Test Statistic		.085
Asymp. Sig. (2-tailed)		.000[c]

a. Test distribution is Normal.

b. Calculated from data.

c. Lilliefors Significance Correction.

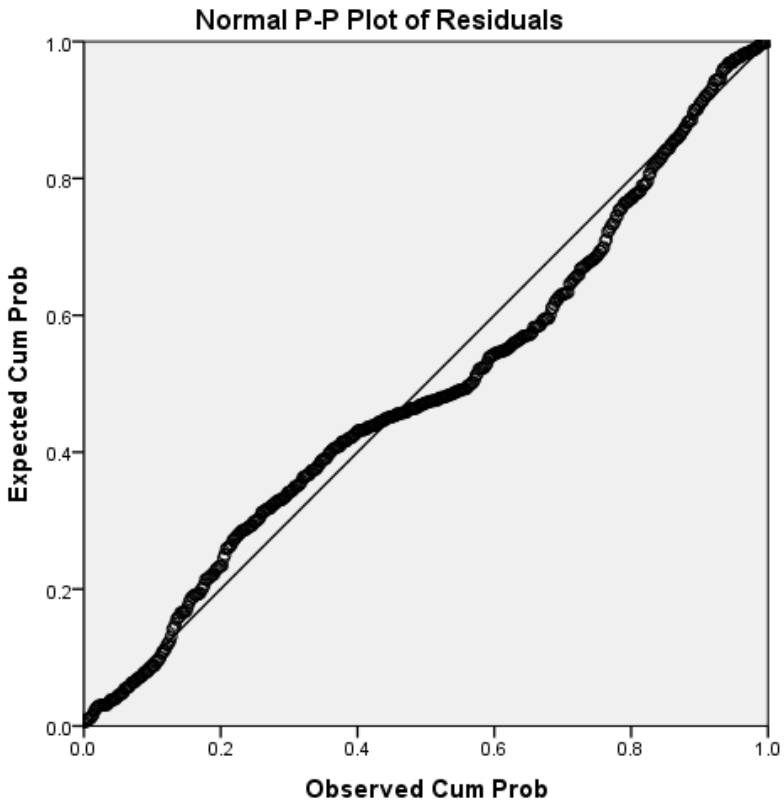

2) Overall models

After diagnostics, two overall models (higher level models) were run for two different conditions; 1) to assess the overall effect of time in *tph2* mRNA expression, for the CTRL, MPL and LL experiments, within each subregion of the DR and MnR nucleus throughout all their rostro-caudal extent across the 5 different time points measured and 2) to assess the effect of time and treatment, for CTRL vs MPL and CTRL vs LL comparisons, within each subregion of the DR and MnR nucleus throughout all their rostro-caudal extent across the 5 different time points measured.

The SPSS syntax for the first condition i.e., 3 higher levels models (CTRL, MPL and LL) which assessed the effect of time, was as follows;

MIXED *Tph2* BY Subdivision Rostro-caudalL Timepoint, /CRITERIA=CIN(95) MXITER(100) MXSTEP(10), SCORING(1) SINGULAR(0.000000000001) HCONVERGE(0, ABSOLUTE) LCONVERGE(0, ABSOLUTE) PCONVERGE(0.000001, ABSOLUTE), /FIXED=ROSTROCAUDAL Subdivision Timepoint Timepoint*ROSTROCAUDAL Timepoint*Subdivision, ROSTROCAUDAL(Subdivision), Timepoint*ROSTROCAUDAL(Subdivision) | SSTYPE(3), /METHOD=REML, /PRINT=DESCRIPTIVES /REPEATED=ROSTROCAUDAL | SUBJECT(AnimalID*Subdivision) COVTYPE(**(one from the sixteen possible)***), /SAVE=PRED RESID.

The following tables are an example of the SPSS output for the first condition of the higher-level model for *tph2* of Ctrls:

Model Dimension[a]

		Number of Levels	Covariance Structure	Number of Parameters	Subject Variables	Number of Subjects
Fixed Effects	Intercept	1		1		
	ROSTROCAUDAL	17		16		
	Subdivision	6		5		
	TimePoint	5		4		
	ROSTROCAUDAL * TimePoint	84		63		
	Subdivision * TimePoint	30		20		
	ROSTROCAUDAL (Subdivision)	58		36		
	ROSTROCAUDAL * TimePoint(Subdivision)	287		142		
Repeated Effects	ROSTROCAUDAL	17	First-Order Ante-Dependence	33	AnimalID * Subdivision	234
Total		505		320		

a. Dependent Variable: Tph2.

Information Criteria[a]

-2 Restricted Log Likelihood	7878.574
Akaike's Information Criterion (AIC)	7944.574
Hurvich and Tsai's Criterion (AICC)	7945.922
Bozdogan's Criterion (CAIC)	8157.002
Schwarz's Bayesian Criterion (BIC)	8124.002

The information criteria are displayed in smaller-is-better form.

a. Dependent Variable: Tph2.

Type III Tests of Fixed Effects[a]

Source	Numerator df	Denominator df	F	Sig.
Intercept	1	220.865	6203.323	.000
ROSTROCAUDAL	16	111.562	205.278	.000
Subdivision	5	127.176	254.618	.000
TimePoint	4	247.606	10.793	.000
ROSTROCAUDAL * TimePoint	63	140.564	1.577	.014
Subdivision * TimePoint	20	139.185	1.102	.354
ROSTROCAUDAL (Subdivision)	36	134.754	40.036	.000
ROSTROCAUDAL * TimePoint(Subdivision)	142	185.681	.736	.972

a. Dependent Variable: Tph2.

The SPSS syntax for the second condition i.e., 2 higher level models (CTRL vs MPL and CTRL vs LL) was as follows;

MIXED *Tph2* BY TREATMENT TIMEPOINT Rostrocaudal Subdivision, /CRITERIA=CIN(95) MXITER(100) MXSTEP(10) SCORING(1) SINGULAR(0.000000000001) HCONVERGE(0, ABSOLUTE) LCONVERGE(0, ABSOLUTE) PCONVERGE(0.000001, ABSOLUTE), /FIXED=TREATMENT TIMEPOINT Rostrocaudal Subdivision TREATMENT*TIMEPOINT TREATMENT*Subdivision, TREATMENT*Rostrocaudal TIMEPOINT*Rostrocaudal TIMEPOINT*Subdivision Rostrocaudal*Subdivision, TREATMENT*TIMEPOINT*Subdivision TREATMENT*TIMEPOINT*Rostrocaudal, TREATMENT*Rostrocaudal(Subdivision) TIMEPOINT*Rostrocaudal(Subdivision), TREATMENT*TIMEPOINT*Rostrocaudal(Subdivision) | SSTYPE(3), /METHOD=REML, /PRINT=DESCRIPTIVES, /REPEATED=Rostrocaudal | SUBJECT(ANIMALID*Subdivision) COVTYPE(**(one from the sixteen possible)***), /SAVE=PRED RESID.

The following tables are an example of the SPSS output for the second condition of the higher-level model for *tph2* of Ctrls vs MPL;

Information Criteria[a]

-2 Restricted Log Likelihood	16002.671
Akaike's Information Criterion (AIC)	16068.671
Hurvich and Tsai's Criterion (AICC)	16069.352
Bozdogan's Criterion (CAIC)	16303.315
Schwarz's Bayesian Criterion (BIC)	16270.315

The information criteria are displayed in smaller-is-better form.

a. Dependent Variable: Tph2.

Model Dimension[a]

		Number of Levels	Covariance Structure	Number of Parameters	Subject Variables	Number of Subjects
Fixed Effects	Intercept	1		1		
	TREATMENT	2		1		
	TIMEPOINT	5		4		
	Rostrocaudal	17		16		
	Subdivision	6		5		
	TREATMENT * TIMEPOINT	10		4		
	TREATMENT * Subdivision	12		5		
	TREATMENT * Rostrocaudal	34		16		
	TIMEPOINT * Rostrocaudal	85		64		
	TIMEPOINT * Subdivision	30		20		
	Rostrocaudal * Subdivision	58		36		
	TREATMENT * TIMEPOINT * Subdivision	60		20		
	TREATMENT * TIMEPOINT * Rostrocaudal	168		62		
	TREATMENT * Rostrocaudal (Subdivision)	116		36		
	TIMEPOINT * Rostrocaudal (Subdivision)	290		144		
	TREATMENT * TIMEPOINT * Rostrocaudal (Subdivision)	574		140		
Repeated Effects	Rostrocaudal	17	First-Order Ante-Dependence	33	ANIMALID * Subdivision	464
Total		1485		607		

a. Dependent Variable: Tph2.

Type III Tests of Fixed Effects[a]

Source	Numerator df	Denominator df	F	Sig.
Intercept	1	344.824	6888.318	.000
TREATMENT	1	351.113	.537	.464
TIMEPOINT	4	356.439	6.124	.000
Rostrocaudal	16	283.275	215.876	.000
Subdivision	5	232.201	302.652	.000
TREATMENT * TIMEPOINT	4	409.745	4.732	.001
TREATMENT * Subdivision	5	232.913	.651	.661
TREATMENT * Rostrocaudal	16	300.823	5.733	.000
TIMEPOINT * Rostrocaudal	64	290.087	2.022	.000
TIMEPOINT * Subdivision	20	238.828	.506	.963
Rostrocaudal * Subdivision	36	338.936	55.640	.000
TREATMENT * TIMEPOINT * Subdivision	20	255.376	.597	.913
TREATMENT * TIMEPOINT * Rostrocaudal	62	321.711	1.618	.004
TREATMENT * Rostrocaudal (Subdivision)	36	341.576	1.653	.013
TIMEPOINT * Rostrocaudal (Subdivision)	144	349.080	1.082	.280
TREATMENT * TIMEPOINT * Rostrocaudal (Subdivision)	140	394.304	.863	.847

a. Dependent Variable: Tph2.

To determine the best fitted model, the 16 different (with different covariance structures) output models were compared with their specific Akaike information criterion (AIC) score and the one which had the lowest, was the best fitted model for the data. Following these overall analyses, if a main effect or interaction between a main effect and any other factor reached $p < 0.05$, secondary LMM were run for each individual subregion of the DR and the MnR nucleus.

3) Secondary Liner Mixed Models

Secondary models (lower level models) were run again with 16 different covariates structures and included all the diagnostic files.

These models intended to assess 2 different conditions; 1) the effect of time, for the CTRL, MPL and LL experiments, in each DR subregion and MnR nucleus separately, throughout all their rostro-caudal extent across the 5 different time points measured and 2) the effect of time and treatment, for CTRL vs MPL and CTRL vs LL comparisons in each DR subregion and MnR nucleus separately throughout all their rostro-caudal extent across the 5 different time points measured. The SPSS syntax for the first condition, i.e., six different lower level models one for each subregion) was as follows:

MIXED **SUBREGION*** BY Timepoint ROSTROCAUDAL, /CRITERIA=CIN(95) MXITER(100) MXSTEP(10) SCORING(1) SINGULAR(0.000000000001) HCONVERGE(0,ABSOLUTE) LCONVERGE(0, ABSOLUTE) PCONVERGE(0.000001, ABSOLUTE), /FIXED=Timepoint ROSTROCAUDAL Timepoint*ROSTROCAUDAL SSTYPE(3), /METHOD=REML, /PRINT=DESCRIPTIVES, /REPEATED=ROSTROCAUDAL | SUBJECT(AnimalID) COVTYPE(**(one from the sixteen possible)***), /SAVE=PRED RESID.

The following tables are an example of the SPSS output for the secondary model for the first condition for MnR;

Model Dimension[a]

		Number of Levels	Covariance Structure	Number of Parameters	Subject Variables	Number of Subjects
Fixed Effects	Intercept	1		1		
	TimePoint	5		4		
	ROSTROCAUDAL	15		14		
	TimePoint * ROSTROCAUDAL	74		55		
Repeated Effects	ROSTROCAUDAL	15	Unstructured	120	AnimalID	40
Total		110		194		

a. Dependent Variable: MNR.

Information Criteria[a]

-2 Restricted Log Likelihood	1187.028
Akaike's Information Criterion (AIC)	1427.028
Hurvich and Tsai's Criterion (AICC)	1522.870
Bozdogan's Criterion (CAIC)	2032.996
Schwarz's Bayesian Criterion (BIC)	1912.996

The information criteria are displayed in smaller-is-better form.

a. Dependent Variable: MNR.

Type III Tests of Fixed Effects[a]

Source	Numerator df	Denominator df	F	Sig.
Intercept	1	1098153.768	713.611	.000
TimePoint	4	950445.357	3.081	.015
ROSTROCAUDAL	14	2489.673	64.654	.000
TimePoint * ROSTROCAUDAL	55	52.645	3.463	.000

a. Dependent Variable: MNR.

Additionally, the secondary lower level models for the second condition were done assessing each timepoint separately, hence, for example CTRL vs MPL in the DRC, at 3 am in one LMM analysis, CTRL vs MPL in the DRC at 9 am in another LMM CTRL vs MPL in the DRC at 3 pm in a third model, and so on for the 5 time points were assessed. However, these analyses only corresponded to the DRC, so the same number of LMM analysis for the DRI, DRD, DRV, DRVL/VLPAG and MnR were performed. Therefore, for this secondary lower level models 30 different models were completed. The SPSS syntax for the first condition, i.e., 30 different lower level models (one for each subregion at each time point) was as follows:

MIXED **SUBREGION*** BY ROSTROCAUDAL Treatment, /CRITERIA=CIN(95) MXITER(100) MXSTEP(10) SCORING(1) SINGULAR(0.000000000001) HCONVERGE(0,ABSOLUTE) LCONVERGE(0, ABSOLUTE) PCONVERGE(0.000001, ABSOLUTE), /FIXED=ROSTROCAUDAL Treatment ROSTROCAUDAL*Treatment SSTYPE(3), /METHOD=REML, /PRINT=DESCRIPTIVES,

/REPEATED=ROSTROCAUDAL | SUBJECT(AnimalID) COVTYPE(AD1), /SAVE=PRED RESID.

The following tables are an example of the SPSS output for the secondary lower level model for the second condition for MnR;

Model Dimension[a]

		Number of Levels	Covariance Structure	Number of Parameters	Subject Variables	Number of Subjects
Fixed Effects	Intercept	1		1		
	ROSTROCAUDAL	15		14		
	Treatment	2		1		
	ROSTROCAUDAL * Treatment	30		14		
Repeated Effects	ROSTROCAUDAL	15	First-Order Ante-Dependence	29	AnimalID	16
Total		63		59		

a. Dependent Variable: MNR.

Type III Tests of Fixed Effects[a]

Source	Numerator df	Denominator df	F	Sig.
Intercept	1	21.667	282.273	.000
ROSTROCAUDAL	14	24.586	21.032	.000
Treatment	1	21.667	1.453	.241
ROSTROCAUDAL * Treatment	14	24.586	2.223	.040

a. Dependent Variable: MNR.

Information Criteria[a]

-2 Restricted Log Likelihood	533.271
Akaike's Information Criterion (AIC)	591.271
Hurvich and Tsai's Criterion (AICC)	602.719
Bozdogan's Criterion (CAIC)	713.188
Schwarz's Bayesian Criterion (BIC)	684.188

The information criteria are displayed in smaller-is-better form.

a. Dependent Variable: MNR.

For the last stage of this analysis, to determine the best fitted model the covariance structures were compared to the AIC score. The model with the lowest score was the best fitted model. Following these secondary analyses, if a main effect or interaction between a main effect and any other factor reached $p < 0.05$, post hoc pairwise comparisons were made with Fisher's LSD test. The SPSS syntax for the post hoc analysis was as follows;

```
UNIANOVA SUBREGION*BY Groups, /METHOD=SSTYPE(3),
/INTERCEPT=INCLUDE, /POSTHOC=Groups(TUKEY LSD
BONFERRONI SIDAK), /EMMEANS=TABLES(OVERALL),
/PRINT=DESCRIPTIVE HOMOGENEITY, /CRITERIA=ALPHA(.05)
/DESIGN=Groups.
```

The following tables are an example of the SPSS output for the pairwise comparisons with Fisher's LSD test for the MnR comparing Ctrls vs LL at 3 am.

Tests of Between-Subjects Effects

Dependent Variable: MNR

Source	Type III Sum of Squares	df	Mean Square	F	Sig.
Corrected Model	693.733[a]	29	23.922	7.174	.000
Intercept	1418.111	1	1418.111	425.265	.000
Groups	693.733	29	23.922	7.174	.000
Error	596.903	179	3.335		
Total	2936.803	209			
Corrected Total	1290.636	208			

a. R Squared = .538 (Adjusted R Squared = .463)

Between-Subjects Factors

		Value Label	N
Groups	3.00	ctrls 3	8
	4.00	ctrls 4	8
	5.00	ctrls 5	8
	6.00	ctrl6	8
	7.00	ctrls7	7
	8.00	ctrls8	8
	9.00	ctrls9	7
	10.00	ctrls10	7
	11.00	ctrls11	8
	12.00	ctrls12	8
	13.00	ctrls13	8
	14.00	ctrls14	6
	15.00	ctrls15	5
	16.00	ctrls16	4
	17.00	ctrsl17	3
	20.00	LL3	8
	21.00	LL4	8
	22.00	LL5	8
	23.00	LL6	8
	24.00	LL7	8
	25.00	LL8	7
	26.00	LL9	6
	27.00	LL10	8
	28.00	LL11	8
	29.00	LL12	7
	30.00	LL13	7
	31.00	LL14	7
	32.00	LL15	6
	33.00	LL16	6
	34.00	LL17	4

Finally, important to clarify three different conditions had to be accomplished in order to performed post hoc analyses; 1) if a main effect or interaction between a main effect and any other factor reached $p < 0.05$, 2) if both the overall and secondary LMM reach significance in interaction or a main effect and 3) if the sample sizes was not below 50% of the full sample size.